2013

Transport and adsorption-desorption of heavy metals in different soils

Tamer A. Elbana
Louisiana State University and Agricultural and Mechanical College

TRANSPORT AND ADSORPTION-DESORPTION OF HEAVY METALS IN DIFFERENT SOILS

A Dissertation

Submitted to the Graduate Faculty of the
Louisiana State University and
Agricultural and Mechanical College
in partial fulfillment of the
requirements for the degree of
Doctor of Philosophy

in

The School of Plant, Environmental, and Soil Sciences

by
Tamer A. Elbana
B.S., Alexandria University, Egypt, 1999
M.S., Alexandria University, Egypt, 2003
May 2013

ACKNOWLEDGMENTS

I am grateful to Dr. H.M Selim for serving as chairman of my dissertation research. I appreciate your continued guidance and professional support throughout my study. I would also like to thank members of my doctoral committee: Dr. Donald L. Sparks, Dr. Donald D. Adrian, Dr. Robert P. Gambrell, Dr. Lewis Gaston, and the dean's representative, Dr. Van L. Cox. Thank you for your continuous interest and valuable insight.

My deep appreciation to faculty and staff in the School of Plant, Environmental and Soil Sciences, Louisiana State University Agricultural Center for the financial support and offered me a fabulous opportunity to serve as teaching assistant, also for financial support to attend 2012 Kirkham Conference, Palmerston North, New Zealand. Also, thanks to Dr. Syam Dodla for his technical help on using the ICP. I extend my gratitude to all my friends for their continued support: Dr. Chang Y. Jeong, Dr. Lixia Liao, Dr. Keli Zhao, Mr. Eric Fergusson, and all my friends in our research group.

I would also like to acknowledge the National Research Center (NRC), Egypt, and the Egyptian government for their financial support from 2008 to 2010. Thanks to Dr. Malak A. Ramadan and staff in the department of Soil and Water Use, NRC, Egypt for their guidance through the research done in Egypt. Also, I would like to thank Dr. Ahmed S. Elneklawy who passed away in 2011 and Dr. Faiz Assad for introducing me to Dr. Selim asking the opportunity of achieving a research under his supervision in the US.

My gratitude also extends to my former advisors; Dr. Fawzy M. Kishk and Dr. Hesham M. Gaber, Faculty of Agriculture, Alexandria University, Egypt for their guidance through the research part that done in Egypt as well as their continued encouragement. Also, I am thankful to Dr. Mohamed Bahnassy, Vice Dean, Faculty of Agriculture, Alexandria University, Egypt for offering satellite images and his help in GIS work.

I would like to express my deepest gratitude to my friend Mohamed Ali for his continuous encouragement and his help in the field work that done in Egypt. Thanks to my friend, Shady Selim, for being supportive and open to bouncing ideas back and forth. Also thanks to Rasha Badr, Hiba Bawadi and Hashem Stietiya for their continued concern and advice and their warm friendship.

Despite being far away from my big family in Egypt, they always take care of me and provide support throughout my life. Special thanks to my parents and my brothers and sisters.

Very special thanks go to my beloved wife, Noura Bakr, and my children, Yehia and Janna. You are the best people I know, and my best friends. Noura, you are the inspiration and motivation for pursuing this work. Also, thanks for your continuous assistance in GIS work, without your support and understanding this work would not have been achieved.

This dissertation is dedicated to my big love….Egypt.

TABLE OF CONTENTS

ACKNOWLEDGMENTS..... ii

LIST OF TABLES..... vii

LIST OF FIGURES..... ix

ABSTRACT..... xv

CHAPTER 1. INTRODUCTION/LITERATURE REVIEW..... 1
1.1 Heavy Metals..... 1
1.2 Heavy Metals in Agroecosystem..... 2
1.2.1 Cadmium..... 3
1.2.2 Copper..... 5
1.2.3 Lead..... 7
1.2.4 Tin..... 9
1.3 Heavy Metals Sequential Extraction..... 11
1.4 Heavy Metals Transport in Soils..... 16
1.4.1 Modeling Heavy Metals Retention..... 17
1.4.2 Modeling heavy Metals Transport..... 22
1.5 Statement of Problems..... 26
1.6 Objectives..... 27
1.7 References..... 28

CHAPTER 2. CADMIUM TRANSPORT IN ALKALINE AND ACIDIC SOILS: MISCIBLE DISPLACEMENT EXPERIMENTS..... 41
2.1 Introduction..... 41
2.2 Modeling..... 43
2.2.1 Nonlinear Model..... 43
2.2.2 Linear Model..... 45
2.3 Materials and Methods..... 46
2.3.1 Adsorption-desorption..... 47
2.3.2 Miscible Displacement Experiments..... 48
2.4 Results and Discussion..... 49
2.4.1 Retention and Release..... 49
2.4.2 Retention Kinetics and Sequential Extractions..... 53
2.4.3 Transport..... 57
2.5 Conclusions..... 67
2.6 References..... 67

CHAPTER 3. COPPER MOBILITY IN ACIDIC AND ALKALINE SOILS: MISCIBLE DISPLACEMENT EXPERIMENTS..... 71
3.1 Introduction..... 71
3.2 Multireaction Model..... 73
3.3 Materials and Methods..... 75
3.3.1 Adsorption Isotherms..... 76

3.3.2 Miscible Displacement..... 76
3.4 Results and Discussion..... 78
3.4.1 Sorption Isotherms..... 78
3.4.2 Tracer Transport..... 80
3.4.3 Copper Transport..... 82
3.5 References..... 94

CHAPTER 4. COPPER TRANSPORT IN CALCAREOUS SOILS: SECOND-ORDER MODELING..... 98
4.1 Introduction..... 98
4.2 Second-Order Two Sites Model..... 100
4.3 Materials and Methods..... 104
4.3.1 Sorption..... 104
4.3.2 Miscible Displacement Experiments..... 105
4.4 Results and Discussion..... 106
4.4.1 Sorption Isotherms..... 106
4.4.2 Copper Transport..... 108
4.4.3 Copper Distribution with Depth..... 115
4.5 Conclusions..... 118
4.6 References..... 118

CHAPTER 5. LEAD MOBILITY IN ALKALINE SOILS: INFLUENCE OF CADMIUM AND COPPER..... 121
5.1 Introduction..... 121
5.2 Materials and Methods..... 123
5.3 Results and Discussion..... 126
5.3.1 Transport in Surface Soil..... 126
5.3.2 Transport in Subsurface Soil..... 132
5.3.3 Transport in Reference Sand..... 136
5.4 Conclusions..... 140
5.5 References..... 140

CHAPTER 6. REACTIVITY OF LEAD AND TIN IN SOILS: SORPTION-DESORPTION EXPERIMENTS..... 144
6.1 Introduction..... 144
6.2 Materials and Methods..... 147
6.2.1 Sorption and Release..... 147
6.2.2 Sorption Isotherms and Kinetic Modeling..... 149
6.3 Results and Discussion..... 151
6.3.1 Sorption Isotherm..... 151
6.3.2 Hysteresis and Retention Kinetics..... 158
6.3.3 SOTS Modeling..... 161
6.3.4 Lead and Tin Influence on Release of Al, Fe, and Mn..... 165
6.3.5 Lead and Tin Sequential Extractions..... 168
6.4 Conclusions..... 172
6.5 References..... 173

CHAPTER 7. INFLUENCE OF TIN ON LEAD MOBILITY IN SOILS 175
7.1 Introduction 175
7.2 Materials and Methods 178
7.2.1 Sorption 178
7.2.2 Miscible Displacement Experiments 179
7.2.3 Modeling with Second-Order Two-Site Model 181
7.3 Results and Discussion 184
7.3.1 Sorption Isotherms 184
7.3.2 Tracer Transport 186
7.3.3 Tin and Pb Transport in Reference Sand 188
7.3.4 Tin and Pb Transport in Windsor Soil 193
7.3.5 Tin and Pb Transport in Olivier Soil 200
7.3.6 Tin and Lead Distribution with Depth 204
7.4 Conclusions 208
7.5 References 209

CHAPTER 8. HEAVY METALS ACCUMULATION AND SPATIAL DISTRIBUTION IN LONG TERM WASTEWATER IRRIGATED SOILS 212
8.1 Introduction 212
8.2 Materials and Methods 214
8.2.1 Study Area 214
8.2.2 Sampling and Laboratory Analyses 215
8.2.3 Spatial Analyses 216
8.3 Results and Discussion 217
8.3.1 Irrigation Water Characteristics 217
8.3.2 Spatial Variability of Soil Properties 219
8.3.3 Spatial Variability of Pb, Cd, Cu, and Ni Cationic Metals 222
8.3.4 Distribution with Soil Depth 227
8.4 Conclusions 230
8.5 References 231

CHAPTER 9. CONCLUSIONS 235

APPENDIX. PERMISSION TO REPRINT 239

VITA 248

LIST OF TABLES

Table 2.1. Selected physical and chemical properties of the studied soils……..... 46

Table 2.2. Soil physical and experimental conditions of the miscible displacement columns experiments……...……..... 49

Table 2.3. Estimated Freundlich distribution coefficient (K_F) and reaction order (b) for Cd retention by the different soils (standard errors in parentheses) and coefficients of determination (r^2)…..... 50

Table 2.4. Goodness of several model versions for Cd retention by the Bustan surface and subsurface and the Windsor soils. Estimates of reaction rates for (standard errors in parentheses), root mean square error (RMSE), and coefficient of determination (r^2) values. 52

Table 2.5. Total extracted Cd and fractions from soil batch kinetic experiments for different initial Cd concentrations……..... 56

Table 2.6. Multireaction transport model parameter estimates for Cd transport in different soil columns: model parameters estimates (standard error in parentheses), root mean square error (RMSE), and coefficient of determination (r^2) values..... 61

Table 2.7. Total extracted (or sorbed) Cd and the different fractions from sectioned soil columns…… 65

Table 3.1. Selected physiochemical properties of the studied soil and its soil classification. 76

Table 3.2. Soil physical and experimental conditions of the miscible displacement columns experiments…….. 77

Table 3.3. Estimated Freundlich parameters and their standard errors (SE) for Cu retention by the different soils……. 79

Table 3.4. Multireaction transport model parameter estimates for Cu transport in Bustan surface soil (long pulse): model parameter estimated standard error (SE), root mean square error (RMSE), and coefficient of determination (r^2) values……. 87

Table 3.5. Multireaction transport model parameter estimates for Cu transport in Bustan-subsurface and Windsor soils columns: model parameter estimated standard error (SE), root mean square error (RMSE), and coefficient of determination (r^2) values……... 92

Table 4.1. Selected physiochemical properties of the soils used in this study……. 104

Table 4.2. Soil physical and experimental conditions of the miscible displacement columns experiments…….. 105

Table 4.3. Estimated Freundlich and Langmuir parameters and their standard errors (SE) for Cu retention by the different soils..... 107

Table 4.4. Second-order two-site (SOTS) model parameter estimates for Cu transport in surface soil, subsurface soil, and surface soil after carbonate removal: estimates of adsorption maximum (S_{max}) and reaction rates (K_e, k_1, k_2, k_3, and k_{irr}) $\pm$ their standard errors, with root mean square error (RMSE), and coefficient of determination (r^2)..... 113

Table 4.5. Total extracted Cu and the different fractions from sectioned soil column..... 116

Table 5.1. Selected physiochemical properties of the studied soils and reference sand material..... 124

Table 5.2. Soil physical and experimental conditions of the miscible displacement columns experiments..... 125

Table 6.1. Selected physical and chemical properties of the studied soils..... 147

Table 6.2 Estimated Freundlich and Langmuir parameters $\pm$ their standard errors (SE) for single Pb, single Sn, and Pb retention in the presence of different Sn concentrations by Windsor and Olivier soils for one and seven days-sorption experiments..... 153

Table 6.3 Second-order, two-site (SOTS) model parameter estimates for Pb retention by Windsor and Olivier soils reaction rates (K_e, k_1, k_2, k_3, and k_{irr}) ± their standard errors, with root mean square error (RMSE) and coefficient of determination (r^2)..... 164

Table 6.4 Total extracted and fractions of Sn and Pb from Windsor soil batch kinetic experiments for different initial concentrations..... 169

Table 6.5 Total extracted and fractions of Sn and Pb from Olivier soil batch kinetic experiments for different initial concentrations..... 170

Table 7.1. Selected physical and chemical properties of the studied soils..... 179

Table 7.2. Soil physical and experimental conditions of the miscible displacement columns experiments..... 180

Table 7.3 Estimated Langmuir parameters and their standard errors (SE) for Pb retention in the presence of different Sn concentrations by Windsor and Olivier soils after 1day-sorption experiments..... 185

Table 7.4. Second-order two-site (SOTS) model parameter estimates for Sn and Pb transport in Reference sand, Windsor, Olivier soil columns: Estimates of adsorption maximum (S_{max}) and reaction rates for root mean square error (*RMSE*), coefficient of determination (r^2) values and (standard error in parentheses)..... 189

Table 8.1. The mean characteristics of irrigation water sources in *Elgabal Elasfar* farm for north (*Fondi*), middle (*Bahari*), and south (*Kablia*) sections..... 218

Table 8.2. The main statistical parameters for physiochemical characteristics of surface and subsurface soil samples for 15 sampling locations..... 221

Table 8.3. Soil analyses of samples from sampling locations 2, 8, 10, and 13 in the study area shown in Fig. 8.1. 229

LIST OF FIGURES

Fig. 2.1. A schematic diagram of the multireaction and transport model, where C is concentration in solution, S_e represents the amount retained on equilibrium sites, S_1 and S_2 represent the amount retained on reversible kinetic sites, S_{irr} and S_s represent the amounts irreversibly retained, and K_e, k_1, k_2, k_3, k_4, k_5, and k_{irr} are the respective reaction rates..... 44

Fig. 2.2. Adsorption and desorption of Cd for the Bustan surface and subsurface and Windsor soils. The solid and dashed curves are the multireaction and transport model simulations for sorption and desorption, respectively..... 51

Fig. 2.3. Cadmium sorbed vs. time during release for the Bustan surface and subsurface and Windsor soils. Symbols are for different initial concentrations (C_o); solid curves are multireaction and transport model simulations..... 54

Fig. 2.4. Tritium breakthrough curves from the reference sand, Bustan surface and subsurface soil, and Windsor soil columns. Solid curves are simulations using the CXTFIT model..... 58

Fig. 2.5. Breakthrough results of Ca and Cd from the Bustan surface soil column. The multireaction and transport model (MRTM) and CXTFIT model simulations are denoted by the solid and dashed curves, respectively; arrows indicate when flow interruption occurred..... 59

Fig. 2.6. Breakthrough results of Ca and Cd from the Bustan subsurface soil column. The multireaction and transport model (MRTM) and CXTFIT model simulations are denoted by the solid and dashed curves, respectively; the arrow indicates when flow interruption occurred..... 60

Fig. 2.7. Breakthrough results of Ca and Cd from the Windsor soil column. The multireaction and transport model (MRTM) and CXTFIT model simulations are denoted by the solid and dashed curves, respectively; the arrow indicates when flow interruption occurred..... 63

Fig. 2.8. Cadmium breakthrough results from the reference sand column. The multireaction and transport model (MRTM) and CXTFIT model simulations are denoted by the solid and dashed curves, respectively; the arrow indicates when flow interruption occurred..... 64

Fig. 2.9. Cadmium sorbed vs. column depth based on soil extractions. Solid and dashed curves represent the multireaction and transport model (MRTM) and CXTFIT model predictions, respectively; closed and open symbols are experimental measurements and represent different replications..... 66

Fig. 3.1. Schematic of the multireaction and transport model (MRTM)..... 74

Fig. 3.2. Cu adsorption isotherms for Windsor, Bustan-surface, and Bustan-subsurface soils. Solid curves are Freundlich model calculations..... 79

Fig. 3.3. Tritium breakthrough curves (BTCs) from the reference sand, Bustan-surface, Bustan-subsurface, and Windsor soil columns. Circle symbols for measured data. Solid curves are simulations using the CXTFIT model..... 81

Fig. 3.4. Copper breakthrough curve (BTC) for the reference sand. Solid curve is multireaction and transport model (MRTM) simulation..... 82

Fig. 3.5. Breakthrough results of Ca and Cu from the Bustan surface (top) and Bustan subsurface (bottom) soil columns. Solid curve is multireaction and transport model (MRTM) simulation..... 84

Fig. 3.6. Breakthrough results of Ca and Cu from the Bustan surface soil column with a Cu pulse of 59.0 pore volumes. Solid and dashed curves represent multireaction and transport model (MRTM) model simulation using different n values..... 85

Fig.3.7. Breakthrough results of Cu from the Bustan surface soil column with a Cu pulse of 59.0 pore volumes..... 88

Fig. 3.8. Breakthrough results of Ca and Cu from the Bustan subsurface soil column with a Cu pulse of 59.0 pore volumes. Solid and dashed curves represent multireaction and transport model (MRTM) and ion exchange model simulations, respectively..... 90

Fig.3.9. Breakthrough results of Ca and Cu from the Windsor soil column with a Cu pulse of 8.6 pore volumes. The multireaction transport model (MRTM) and ion exchange model simulations denoted by solid and dashed curves, respectively..... 91

Fig.3.10. Breakthrough results of Ca and Cu from the Windsor soil column with a Cu pulse of 49.6 pore volumes. The multireaction transport model (MRTM) and ion exchange model simulations denoted by solid and dashed curves, respectively..... 93

Fig. 4.1. A schematic of the second-order, two-site (SOTS) model for retention of reactive chemicals in soils, where C is the solute in the solution phase, S_e is the amount retained on equilibrium-type sites, S_k is the amount retained on kinetic-type sites, S_s is the amount retained irreversibly by consecutive reaction, S_{irr} is the amount retained irreversibly by concurrent type of reaction, and K_e, k_1, k_2, k_3, and k_{irr} are reaction rates..... 102

Fig. 4.2. Copper adsorption isotherms for Bustan surface soil, subsurface soil, and surface soil after removal of carbonate. The solid curves are Freundlich model calculations..... 107

Fig. 4.3. Breakthrough results of Cu and Ca from surface soil (top) and subsurface soil (bottom). Solid curves are simulations using the second-order, two-site (SOTS) model version V1 (full model)..... 109

Fig. 4.4. Breakthrough results of Cu from surface soil (top) and subsurface soil (bottom). Solid curves are simulations using the consecutive version (V2 using the amount retained on equilibrium-type sites, S_e, the amount retained on kinetic-type sites, S_k, and the amount retained irreversibly by consecutive reaction, S_s) of the second-order, two-site (SOTS) model. Dashed curves represent CXTFIT simulations..... 111

Fig. 4.5. Breakthrough results of Cu and Ca from the surface soil after removal of carbonate. Solid curves are simulations using the full version (V1) and consecutive version (V2, disregarding the amount retained irreversibly by concurrent type of reaction) of the second order, two-site (SOTS) model. The dashed curve represents CXTFIT simulations. 114

Fig. 4.6. Copper sorbed vs. column depth based on soil extractions. Solid and dashed curves represent the second-order, two-site (SOTS) model and CXTFIT predictions, respectively. Symbols are experimental measurements and represent different replications. 117

Fig.5.1. Breakthrough results of Pb, Cd, and Cu from the Bustan surface soil column; vertical dashed lines indicate the starting of Cd and Cu pulses; vertical solid arrows indicate when the flow interruption occurred..... 127

Fig. 5.2. Breakthrough results of Pb from the Bustan surface soil column; solid and dashed horizontal arrows indicate pore volumes of different elements or leaching solutions..... 128

Fig. 5.3. Breakthrough results of Ca from the Bustan surface soil column; dashed horizontal lines indicate starting of Cd and Pb pulses; vertical solid arrows indicate when the flow interruption occurred. The pH measurements were represented on secondary Y axis..... 130

Fig. 5.4. Different Pb, Cd, and Cu fractions from sectioned soil columns for Bustan surface soil..... 131

Fig. 5.5. Breakthrough results of Pb, Cd, and Cu from the Bustan subsurface soil column; vertical dashed lines indicate the starting of Cd and Cu pulses; vertical solid arrows indicate when the flow interruption occurred..... 133

Fig. 5.6. Breakthrough results of Pb from the Bustan subsurface soil column; solid and dashed horizontal arrows indicate pore volumes of different elements or leaching solutions..... 134

Fig. 5.7. Breakthrough results of Ca from the Bustan surface soil column; dashed horizontal lines indicate starting of Cd and Pb pulses; vertical solid arrows indicate when the flow interruption occurred. The pH measurements were represented on secondary Y axis..... 134

Fig. 5.8. Different Pb, Cd, and Cu fractions from sectioned soil columns for Bustan subsurface soil..... 135

Fig. 5.9. Breakthrough results of Pb (top) and Ca (bottom) from the reference sand column when pulse of 0.483 mmol L^{-1} of Pb was introduced; the arrow indicates when flow interruption occurred..... 137

Fig. 5.10. Breakthrough results of Pb from the reference sand column when pulse of 2.413 mmol L^{-1} was introduced; the arrow indicates when flow interruption occurred..... 138

Fig 5.11. Lead sorbed vs. reference sand columns depth based on XRF scanning when a pulse of 0.483 mmol L^{-1} (top) and 2.413 mmol L^{-1} (bottom) of Pb were introduced..... 139

Fig. 6.1. A schematic of the second-order, two-site (SOTS) model for retention of reactive chemicals in soils, where C is the solute in the solution phase, S_e is the amount retained on equilibrium-type sites, S_k is the amount retained on kinetic-type sites, S_s is the amount retained irreversibly by consecutive reaction, S_{irr} is the amount retained irreversibly by concurrent type of reaction, and K_e, k_1, k_2, k_3, and k_{irr} are reaction rates..... 151

Fig. 6.2. Sn sorption isotherms for Windsor (top) and Oliver (bottom) soils for 1d and 7d sorption experiments, symbols are experimental measurements and represent different replications..... 152

Fig. 6.3. Lead sorption isotherms for Windsor and Oliver soils for 1d and 7d sorption experiments, symbols are experimental measurements and represent different replications. Solid and dashed curves are Freundlich calculations..... 154

Fig. 6.4. Lead sorption isotherms for Windsor (top) and Olivier (bottom) soils. Different symbols represent the experimental results in the presence of different Sn levels added (0, 200, and 400 ppm) in the soil solution. Solid and dashed curves represent calculations using the Freundlich model equestion (6.1)..... 156

Fig. 6.5. Effect of different Pb levels added (0, 200, and 400 ppm) into the background solutions on the sorption amount of Sn after 1d sorption experiment..... 157

Fig 6.6. Sorption and desorption of Pb for the Windsor soil in the presence of different Sn levels (0, 1.685, and 3.370 mmol L^{-1}) in soil solutions. The solid and dashed curves are the second-order two-site model simulations for sorption and desorption, respectively..... 159

Fig. 6.7. Sorption and desorption of Pb for the Olivier soil in the presence of different Sn levels (0, 1.685, and 3.370 mmol L^{-1}) in soil solutions. The solid and dashed curves are the second-order two-site model simulations for sorption and desorption, respectively..... 160

Fig. 6.8. Lead sorbed vs. time during release for Windsor soil. Symbols are for different initial concentrations (C_o); the solid curves are the second-order two-site model simulations..... 162

Fig. 6.9. Lead sorbed vs. time during release for Olivier soil. Symbols are for different initial concentrations (C_o); the solid curves are the second-order two-site model simulations..... 163

Fig. 6.10. Induced releases of Al, Fe, and Mn versus the sorbed amount of Pb after 1d sorption for Windsor and Olivier soils. The measured pH in the solution is shown in secondary Y axis..... 166

Fig. 6.11. Induced releases of Al, Fe, and Mn versus the sorbed amount of Sn after 1d sorption for Windsor and Olivier soils. The measured pH in the solution is shown in secondary Y axis..... 168

Fig. 7.1. A schematic of the second-order, two-site (SOTS) model for retention of reactive chemicals in soils, where C is the solute in the solution phase, Se is the amount retained on equilibrium-type sites, S_k is the amount retained on kinetic-type sites, S_s is the amount

retained irreversibly by consecutive reaction, S_{irr} is the amount retained irreversibly by concurrent type of reaction, and K_e, k_1, k_2, k_3, and k_{irr} are reaction rates..... 183

Fig. 7.2. Langmuir sorption isotherm for Pb retention in the presence of different Sn concentrations by Windsor and Olivier soils after 1 day-sorption experiments..... 186

Fig.7.3. Tritium breakthrough curves (BTCs) from the reference sand, Windsor soil, and Olivier soil columns. Circles represent experimental data. Solid curves are simulations using the CXTFIT model..... 187

Fig.7.4. Breakthrough results of Sn from the reference sand. Solid curve is the SOTS model simulation..... 190

Fig. 7.5. Breakthrough results of Pb from the reference sand; the arrow indicates when flow interruption occurred. The solid curve is the SOTS model simulation..... 191

Fig. 7.6. Release of different elements (K, Mg, Fe, and Al) from reference sand and pH change due to application of 11.04 pore volumes of Pb pulse (right) and 18.91 pore volumes of Sn pulse (left); the arrow indicates when flow interruption occurred..... 192

Fig. 7.7. Tin breackthrough curve (top) and release of different elements (K, Mg, Fe, Al, and Mn) from Windsor soil and pH change due to application of 170 pore volumes of Sn pulse..... 194

Fig. 7.8. Breakthrough results of Pb from Windsor soil where Pb - Sn (top) and Sn - Pb (bottom) pulses sequence were applied. The solid curve is the SOTS model simulation; the arrow indicates the introduction of the second pulse..... 196

Fig. 7.9. Breakthrough results of Pb from Windsor soil where mixed Sn and Pb pulses were applied. The solid curve is the SOTS model simulation; the arrow indicates when flow interruption occurred..... 197

Fig. 7.10. Release of different elements (K, Mg, Fe, Al, and Mn) from Windsor soil and pH change due to application of Pb-Sn, Sn-Pb, and mixed Pb & Sn pulses from right to left, respectively; the arrow indicates when flow interruption occurred..... 199

Fig. 7.11. Release of different elements (K, Mg, Fe, Al, and Mn) from Olivier soil and pH change due to application of 176 pore volumes of Sn pulse..... 200

Fig. 7.12. Breakthrough results of Pb from Olivier soil where Pb-Sn (top) and Sn - Pb (bottom) pulses sequence were applied. The solid curve is the SOTS model simulation; the arrow indicates the introduction of the second pulse..... 202

Fig. 7.13. Breakthrough results of Pb from Olivier soil where mixed Sn and Pb pulses were applied. The solid curve is the SOTS model simulation; the arrow indicates when flow interruption occurred..... 203

Fig. 7.14. Release of different elements (K, Mg, Fe, Al, and Mn) from Olivier soil and pH change due to application of Pb-Sn, Sn-Pb, and mixed Pb&Sn pulses from right to left, respectively; the arrow indicates when flow interruption occurred..... 205

Fig. 7.15 . Tin (top) and Lead (bottom) sorbed vs. column depth based on XRF measurements for Windsor soil columns (mixed Sn+Pb; sequential Pb-Sn; sequential Sn-Pb; long Sn pulse, respectively from right to left)..... 206

Fig. 7.16 . Tin (top) and Lead (bottom) sorbed vs. column depth based on XRF measurements for Olivier soil columns (mixed Sn+Pb; sequential Pb-Sn; sequential Sn-Pb; long Sn pulse, respectively from right to left)..... 207

Fig. 7.17. Tin (left) and Lead (right) sorbed vs. column depth based on XRF measurements for reference sand columns..... 208

Fig. 8.1 Geo-spatial distribution of soil profiles in the study area; a) spaceborne thermal emission and reflection radiometer (ASTER) image for the study area, and b) unsupervised classified image with sampling locations among *Fondi*, *Bahari*, and *Kabli* sections..... 215

Fig. 8.2. Geo-spatial distribution of soil properties; a) calinity classes, b) pH, c) organic matter (OM), and d) cation exchange capacity (CEC)..... 220

Fig. 8.3. Geo-spatial distribution of (a) total and (b) available Pb (mg kg^{-1})..... 223

Fig. 8.4. Geo-spatial distribution of (a) total and (b) available Cd (mg kg^{-1})..... 224

Fig. 8.5. Geo-spatial distribution of (a) total and (b) available Cu (mg kg^{-1})..... 225

Fig. 8.6. Geo-spatial distribution of (a) total and (b) available Ni (mg kg^{-1})..... 226

Fig. 8.7. Distribution of Pb, Cd, Cu, and Ni versus soil profiles depth (cm) for location 5.... 228

Fig. 8.8. Distribution of Pb, Cd, Cu, and Ni versus soil profiles depth (cm) for the buried profile, location 8..... 230

ABSTRACT

Understanding the reactivity and mobility of heavy metals in soils is indispensable for assessing their potential risk to the environment. In this study, column transport and batch kinetic experiments were performed to assess the sorption-desorption and mobility of Cd, Cu, Pb, and Sn in alkaline and acidic soils. Furthermore, sequential extractions were accomplished to examine their behavior in soils. Also, the competitive reactivity of Sn and Pb in two acidic soils was quantified. Additionally, the effect of introducing Cd and Cu after a Pb pulse in calcareous soil was presented. Modeling of these heavy metals retention and transport was carried out using different models; multireaction and transport model, CXTFIT model, kinetic ion exchange formulation, and second-order two-site model. The results revealed that: 1) the studied heavy metals exhibited strong nonlinear and kinetic retention behavior; 2) Cd was nearly immobile in alkaline soil with 2.8% $CaCO_3$, whereas 20 and 30% of the applied Cd was mobile in the acidic soil and the subsurface layer of the alkaline soil with 1.2% $CaCO_3$, respectively; 3) for a short Cu pulse, the recoveries were <1 and 11% for alkaline and acidic soils, respectively, whereas, for the long Cu pulse, the recoveries ranged from 27 to 85% for the studied soils; 4) tin was highly sorbed in acidic soils where more than 99% of applied Sn was retained in the acidic soils columns; 5) the presence of Sn in solution reduced Pb retention in soils since the Pb recovery in the effluent solution ranged from 37.4 to 96.4%; and 6) the multireaction approach was capable of describing heavy metals retention and transport in soil columns.

Moreover, a field study of the spatial distributions and the accumulation of Pb, Cd, Cu, and Ni among soil depth as consequence of irrigation with domestic wastewater were studied. The results of this research showed that Pb, Cu, and Ni had high affinity for retention in the surface soil layer whereas Cd results showed homogeneous distribution within soil depth. The

impact of time scale effect on accumulation and spatial distribution of heavy metals indicated the urgent need for remediation and rational management.

CHAPTER 1. INTRODUCTION/LITERATURE REVIEW

1.1 Heavy Metals

The term "heavy metals" has been used in environmental legislation publications related to chemical hazards and the safe use of chemicals (Duffus, 2002). This term is universally used by soil scientists (Alloway, 1995; 2013; Selim and Sparks, 2001; Sherameti and Varma, 2010; Selim, 2012). There are a number of definitions for heavy metals, some definitions based on the specific gravity. The oldest scientific use of the term in the English literature was reported in the Oxford English Dictionary (Bjerrum, 1936), since Bjerrum classified the metals in two groups based on their specific gravity, the light metals with densities below 4 g cm^{-3} and the heavy metals with densities above 7 g cm^{-3}. Thornton (1995) defined heavy metals as elements with a density exceeding 6 g cm^{-3}. Recently, Berkowitz et al. (2008) defined the term "heavy metal" as any metallic chemical element that has specific density of more than 5 g cm^{-3} and is toxic or poisonous at low concentrations.

Other scientists defined heavy metals based on their atomic weight. Bennet (1986) defined them as metals of atomic weight greater than sodium. According to Harrison and Waites (1998), heavy metals were defined as a collective term for metals of high atomic mass, particularly those transition metals that are toxic and cannot be processed by living organisms, such as Pb, Hg, and Cd. However, there are some definitions based on the atomic number such as any metal with an atomic number beyond calcium (Venugopal and Luckey, 1975). Lyman, 1995 defined them as metals with an atomic number between 21 (scandium) and 92 (uranium). In addition there are some definitions based on the toxicity such as elements commonly used in industry and generally toxic to animals (Scott and Smith, 1981).

Duffus (2002) reviewed the usage that has developed for the term "heavy metals" and he concluded that a classification of metals and their compounds based on their chemical properties

is needed. Such a classification would permit interpretation of the biochemical basis for toxicity. It would also provide a rational basis for determining which metal ionic species or compounds are likely to be most toxic. As a general conclusion he reported that even if the term "heavy metal" should become obsolete because it has no coherent scientific basis, there will still be a problem with the common use of the term "metal" to refer to a metal and all its compounds. This usage implies that the pure metal and all its compounds have the same physicochemical, biological, and toxicological properties. Recently, Appenroth (2010) recommended that the term "heavy metals" should not be avoided but defined in a better way. He suggested that this term should be defined in relation to the position of the element in the period table and there are three groups in the periodic table should be considered heavy metals: (1) transition elements, (2) rare earth elements, (3) some elements from the p-group that are either metals or metalloids/borderline elements.

In general, the term "heavy metals" is used to deal with the elements that have a high density and belong largely to the transition group of the periodic table. Most of these metals are called trace elements, stressing their relatively low abundance in soils (De Vries et al., 2002). The considered elements generally include; As, Cd, Co, Cr, Cu, Hg, Ni, Pb, Se, V and Zn (De Haan and Zwerman, 1978). One aspect of sustainability is the accumulation of heavy metals in soil which causes problems if certain levels are exceeded (Alloway 1990). The aim of sustainable metal management in agroecosystems is to ensure that the soil continues to fulfill its functions in agricultural production, by not restricting nutrient cycling or limiting soil biodiversity.

1.2 Heavy Metals in Agroecosystem

Heavy metals enter an agroecosystem through both natural and anthropogenic processes. Most heavy-metal inputs to agricultural soils originate from atmospheric deposition and from

different soil amendments such as sewage sludge, fertilizers, liming materials, pesticides, manures, and compost (Raven and Loeppert, 1996). Agricultural practices are frequently a source of heavy metals contamination (Kabata-Pendias, 1995), usually as a result of impurities in the fertilizers used. Other sources include sewage sludge, when used as an organic amendment, manure, and compost as well as airborne particulate transport (Alloway, 1995; Forstner, 1995).

Heavy metals are naturally circulated by biogeochemical processes, and metallic elements play a variety of roles in all living organisms. Some metals are essential elements, and their deficiency results in impairment of biological functions. When present in excess, essential metals may also become toxic. Other metals are not known to have any essential function, and they may give rise to toxic manifestations even when intakes are only moderately in excess of the "natural" intake (Friberg and Nordberg, 1986). Heavy-metal inputs need not always be as small as possible because some metals are indispensable for life. Copper (Cu) and zinc (Zn) are essential elements whose lack may give rise to deficiency problems in plants and animals. Both essential (Cu and Zn) and nonessential such as cadmium (Cd) and lead (Pb) metals become toxic when critical contents are exceeded, excessive metal input to agricultural systems can be considered a stress that potentially affects diversity, productivity, and overall functioning of agricultural systems (Ross, 1994). In this study, we will focus mainly on Cd, Cu, Pb, and Sn.

1.2.1 Cadmium

Cadmium is of potential concern as an environmental contaminant. It exhibits adverse effects on biological processes in humans, animals, and plants (Kabata-Pendias and Mukherjee, 2007). In aquatic systems, Cd exists as Cd^{2+}, $Cd(OH)_2(aq)$, $Cd(OH)_3^-$, $Cd(OH)_4^{2-}$, and $CdCO_3$ and in a various other organic and inorganic complexes (Moore, 1991). In the soil, Cd may occur as cationic such as; $CdCl^+$, $CdOH^+$, and $CdHCO_3^+$ and as anionic species such as; $CdCl_3^-$, $Cd(OH)_4^{2-}$, and $Cd(HS)_4^{2-}$ (Kabata-Pendias and Sadurski, 2004). In the soil solution, Cd may

also occur in complexes with various organic acids (Krishnamurti et al., 1997). Cadmium adsorbed to mineral surfaces or organic materials is more easily bioaccumulated or released in a dissolved state when sediments are disturbed, such as during flooding (Berkowitz et al., 2008).

Cadmium behavior is governed by several physical and chemical processes in soils. It may be retained in soils through precipitation and adsorption reactions. For instance, Cd is associated with several mineral phases during flooding periods in the paddy soils, including carbonates, kaolinite, ferrihydrite, humic acid, and CdS (Khaokaew et al., 2011). Precipitation appears to be the predominant process in the presence of anions such as S^{2-}, CO_3^{2-}, OH^- and PO_4^{3-} and sorption of Cd at soil mineral surfaces may occur by both specific and nonspecific processes (Naidu et al., 1997). Adsorption increases with pH and sorbed Cd may become irreversible. Thus, potential mobility for Cd is greatest in acidic soil (Dijkstra et al., 2004). In smectite-rich vertisol, Cd adsorbed to siloxane cavities at pH < 6.5 and to the aluminol functional group at pH > 6.5 (Choi, 2006). Moreover, in oxidizing environments and alkaline soils, Cd is likely to precipitate to minerals such as octavite ($CdCO_3$) as well as CdO and $Cd(OH)_2$ (McBride, 1994; Holm et al., 1996).

Retention/release phenomena are governing mechanisms which influence the mobility of Cd in aqueous porous media. The retention/release mechanisms are various and often intricate. These phenomena sometimes are kinetically controlled. So that time-dependence of the sorption isotherm must be specified (Strawn and Sparks, 1999). The distribution coefficient (k_d) is the ratio of the Cd concentration in the soil to the concentration of Cd^{+2} in the solution phase. The value of the k_d indicates the potential of Cd to be sorbed in soils. Cadmium solid–solution partitioning is dependent on soil solution pH, soil organic matter (OM), and total metal content (Sauve´et al., 2000). Moreover, the k_d value increases with increasing pH (Lee, 1996). For instance, in an acidic soil with pH less than 5.0 and low cation exchange capacity (CEC), Chang

et al. (2001) reported k_d values ranged between 2.71 to 5.04 L kg^{-1}. The respective k_d values for high pH, larger than 7.4, and high CEC soils ranged between 147.5 to 1699.6 L kg^{-1} (Shaheen, 2009). Nonlinearity of Cd sorption has been demonstrated by several investigators. Buchter et al. (1989) reported strong nonlinearity of Cd sorption isotherm for a calcareous soil. Krishnamurti and Naidu (2003) reported nonlinear sorption for Palexeralf and Xerochrept soils having pH values ranging from 8.0-8.4.

Cadmium transport depends on the retention/release properties of the soil as well as environmental conditions. Transport characteristics may use the breakthrough curves (BTCs) to characterize the transport of Cd in soils (Liu et al., 2006).Cadmium concentrations were underestimated when sorption was assumed linear and of the equilibrium type. Improvements in predictions were realized when the mobile-immobile (or two-region) approach of van Genuchten and Wierenga (1976) was utilized. On the other hand, Gerritse (1996) found that BTCs of Cd from an acidic sandy soil were simulated successfully using linear sorption isotherm based on batch experiments. Over the last three decades, several models of the equilibrium and the kinetic types were proposed to describe the fate of Cd in soils. Evidence of time-dependent sorption in soils has been observed by numerous investigations (e.g., Aringhieri et al., 1985; Selim et al., 1992; Strawn and Sparks, 1999).

1.2.2 Copper

The general values for the average total copper (Cu) contents in soils of different types all over the world are reported to range between 20 and 30 mg kg^{-1} (Alloway 1995). Copper is an essential element in both plants and animals. In plants, Cu is especially important in oxidation, photosynthesis, and protein and carbohydrate metabolism. Also, copper concentrations may affect nitrogen fixation, valence changes, and cell wall metabolism (Kabata-Pendias and Pendias, 2001). However, at elevated levels Cu harmfully affects the environment (Alloway 1995).

Understanding Cu mobility in soil is necessary for plant nutrition management as well as pollution control. The toxicity of Cu depends on soil properties that control its reactivity in soil. Oorts (2013) reported that predicted no effect concentrations (PNECs), protecting 95% of all species or microbial processes, vary between 10 and 200 mg kg^{-1} soil and increase with increasing CEC, clay, and OM content. In agroecosystem, Cu is extensively used in the form of fertilizers (Holmgren et al., 1993; Mermut et al., 1996), bactericides and fungicides (Epstein and Bassein, 2001). Copper reactivity and transport in soils is often observed for extended periods of time (Pietrzak and McPhail, 2004). In soils, Cu may occur in various forms: Cu^{2+}, Cu^{+}, $CuCl_2^-$, $CuSO_4^0$, $Cu(OH)_2$, $CuCO_3^0$, and $CuCl^0$ (McBride 1981; Alloway 1995).

Copper exhibits strong affinity to various soil constituents such as OM, clay minerals, and metal hydroxides with varying strengths (Adriano, 2001; Kabata-Pendias and Sadurski, 2004; Han, 2007). Sparks (2003) stated that mobility and fate of heavy metals in soils are affected by soil properties and reflected by the partitioning between the soil and solution. Copper retention in soils was found to be significantly correlated with soil pH, OM, CEC, amorphous Fe, Al, Si, and Mn oxides, and clay content (Chen et al., 1999; Adriano, 2001; Shahen et al., 2009). Moreover, soil-solution parameters such as ionic strength and competing and counter ions have been shown to influence the adsorption of metals in soils (Harter and Naidu, 2001). In an acidic soil with pH less than 5.0 and low CEC, Chang et al. (2001) reported k_d values ranged between 5.3 to 9.6 L kg^{-1}. The respective k_d values for high pH, larger than 7.4, and elevated CEC soils ranged between 743.7 to 7502.4 L kg^{-1} (Shaheen et al., 2009). Nonlinearity of Cu sorption has been demonstrated by several investigators. Selim and Ma (2001) found that the use of multiple reaction approaches such as second order two sites (SOTS) and the multireaction model (MRM) were capable of describing the observed nonlinear kinetic behavior of Cu in soils during adsorption as well as during desorption.

Copper in a calcareous soils is found primarily in nonexchangeable form and possibly adsorbed on surface as hydroxy or hydroxycarbonate species (McBride and Bouldin, 1984). In a calcareous soil, Maftoun et al. (2002) found that Cu retained easily and rapidly on clay, OM, and calcium carbonate sites. Rodriguez-Rubio et al. (2003) suggested that Cu was preferentially retained in calcareous soils through precipitation of CuO, $Cu_2(OH)_2CO_3$ or $Cu(OH)_2$ and by adsorption on soil carbonates. Elzinga and Reeder (2002) used extended X-ray absorption fine-structure (EXAFS) spectroscopy to characterize Cu adsorption complexes at the calcite surface. They observed that Cu occupied Ca sites in the calcite structure, and formed inner-sphere Cu adsorption complexes at calcite surfaces. The EXAFS results revealed that the precipitation of malachite ($Cu_2(OH)_2CO_3$) did not take place in Cu/calcite suspensions at Cu concentration of 5.0 μM and 10.0 μM.

Appreciable leaching of Cu in soil profiles has been shown in humus-poor acidic soils (Mathur et al., 1984), and in soils which received repeated application of Cu fertilizer in alkaline soils (Wei et al., 2007). Several studies attempted to model Cu reactivities and transport in soils. For example, He et al. (2006) found that the release of Cu at short times was likely due to the exchangeable fraction. In contrast, long-term leaching experiments showed that the exchangeable and carbonate-bound fractions were the primary contributors to Cu release. Tsang and Lo (2006) showed that a first-order two-site nonequilibrium model, with one site representing instantaneous sorption and the other rate-limited sorption, provided better simulation of Cu BTCs when compared to an equilibrium transport model.

1.2.3 Lead

Lead is a naturally occurring element which can be found in all environmental media: air, soil, sediment, and water. It is not considered to be an essential element for plant growth and development. Moreover it inhibits growth, reduces photosynthesis (by inhibiting enzymes unique

to photosynthesis), interferes with cell division and respiration, reduces water absorption and transpiration, accelerates abscission or defoliation and pigmentation, and reduces chlorophyll and ATP synthesis (USEPA, 1979). Lead is also not considered an essential element for birds or mammals. According to the U.S. Environmental Protection Agency, the concentrations of Pb in soil that are protective of ecological receptors as known as ecological soil screening levels (Eco-SSLs) are 11, 56, and 120 ppm for birds, mammals, and plants respectively, (USEPA 2005). Lead abundance in sediments is a function of clay fraction content and thus argillaceous sediments contain more Pb than sands, sandstones, and limestones. Lead enters the soils through natural processes such as weathering of parent materials and/or anthropogenic sources. Many anthropogenic sources for Pb contamination were reported; Steinnes (2013) listed automobile exhausts, mining and smelting, sewage sludge, shooting ranges, and urban soils as sources for Pb pollution. Lead concentrations vary from one soil to another due to the variation in soil physiochemical characteristics and the occurrence of anthropogenic sources of Pb contamination. Lead in soil is relatively immobile, when released to soil; it is normally converted from soluble lead compounds to relatively insoluble sulfate or phosphate derivatives. It also forms complexes with OM and clay minerals which limits its mobility. Plant toxicity levels of Pb in soils are not easy to evaluate, but it is generally agreed that a soil Pb concentration ranging from 100 to 500 mg kg^{-1} is considered excessive (Kabata-Pendias and Pendias, 2001).

The study of the transfer of trace elements, especially lead, under real conditions is difficult to carry out due to the physicochemical and hydrodynamic complexity of real soil (preferential flows, conditions of unsaturation...). So, Barkouch et al. (2007) presented a study to gain a better understanding of the parameters influencing the migration processes of trace elements in simplified systems; it was based on the study of Pb transfer in laboratory columns filled with soil. Their results showed that the retention of lead in soil is strongly dependent on

feed flow rate, particulate bed tortuosity, bed height, water–soil surface contact and volume of water. Increase in bed height, water–soil surface contact and particulate bed tortuosity leads to higher contact time thus higher lead retention by soil, whereas increase in feed flow rate and volume of water leads to lower contact time thus lower lead retention by soil.

Melamed et al. (2003) conducted a pilot-scale field demonstration at a Pb-contaminated site to assess the effectiveness of Pb immobilization using P amendments. They found that a mixture of H_3PO_4 and $Ca(H_2PO_4)_2$ or phosphate rock was effective in immobilizing Pb with minimum adverse impacts associated with pH reduction. Vile et al. (1999) evaluated Pb mobility and the chemical forms in which Pb is stabilized in peat profiles by adding either soluble or particulate Pb to intact peat cores that were maintained under different water level regimes and were subjected to simulated precipitation over a five-month period. Their results indicated that added soluble Pb^{2+} was retained in the peat through physiochemical binding to OM, and as such Pb^{2+} was largely immobile in peat even under conditions of a fluctuating water table. Rouff et al. (2002) investigated the sorption of Pb with calcite in a radiotracer study. The effect of Pb concentration, calcite loading, and ionic strength on Pb sorption with time was monitored. Their results indicated a high affinity of Pb for the calcite surface under the given experimental conditions and the uptake kinetics were of a dual nature. Whereby, most of Pb was sorbed to the surface within the first few seconds of metal-mineral contact, followed by a slow continuous sorption process with time. However, re-release of metal via desorption was also possible, as experimental results indicated that only a small fraction of Pb became irreversibly bound with the calcite under the conditions specified in this study.

1.2.4 Tin

Tin (Sn) occurs in the Earth's crust at an average concentration above 2 mg kg^{-1} and has two possible oxidation states, +2 and +4 stannous and stannic, respectively (Kabata-Pendias and

Mukherjee, 2007). In contaminated soils and sediments , Sn concentration may be highly elevated up to 1000 mg kg^{-1} (Schafer and Fembert 1984; Bryan and Langston, 1992).The main Sn minerals include cassiterite (SnO_2), Stannite (Cu_2FeSnS_4), teallite ($PbZnSnS_2$), kesterite ($CuZnSnS_4$), and montesite ($PbSn_4S_3$). Tin is used in tin-plated containers, in solders, alloys, wood coloring, antifouling in marine paints, and agricultural fungicides and acaricides (Ostrakhovitch and Cherian, 2007). Various versions of Eh–pH diagrams for inorganic Sn have been constructed (Takeno, 2005) and Sn may exist in different species such as Sn^{4+}, Sn^{2+}, $Sn(OH)_2(aq)$, $Sn(OH)_2(S)$, Sn $(OH)_2^{2+}$ and others. Also, Sn is found to passivate in aqueous environments from below pH 1 to above pH 12, forming an oxide film that consists of $Sn(OH)_4$ or the more stable SnO_2 which may form either initially or transform gradually with time from the hydroxide (Lyon, 2009).

Tin exhibits high potential to be sorbed and retained on soil. Some of inorganic tin compounds dissolve in water, whereas most inorganic tin compounds bind to soil and to sediments (Ostrakhovitch and Cherian, 2007). There is a relatively small dataset concerning inorganic tin in soil, and no suggestion that levels are sufficiently high to cause toxicity (Clifford et al., 2010). The behavior of Sn in soil will depend on soil and environmental conditions. In recent marine deposits, Sterckeman et al. (2004) found that total Sn concentration in alkaline cultivated soils ranged from 0.98 to 1.02 mg $kg^{-1}$for surface soil samples and from 0.49 to 2.18 mg kg^{-1} for deeper horizon soil samples. The authors showed that Sn was associated with the fine mineral fraction of the deep horizons. Nakamaru and Uchida (2008) studied sorption behavior of Sn in Japanese agricultural soils using ^{113}Sn tracer, and reported that Sn distribution coefficient, k_d, ranged between 128 and 1590000 L kg^{-1}. Unexpectedly, the authors found that the k_d values increased with decreasing pH. Due to the high retention of Sn on soil, low and limited mobility is expected. Hou (2005) showed the low mobility of Sn after 18 months in column experiments

exposed to precipitation in a grass-covered field. Lasley et al. (2010) studied the vertical and lateral transport of Sn from biosolid at a mineral sands mine reclamation site. Their results revealed that Sn exhibited a limited vertical mobility and no Sn was detected in lateral samples. The lack of lateral movement for Sn is an evidence of the insolubility and immobility of it in biosolids.

1.3 Heavy Metals Sequential Extraction

Quantifying the proportions of metals bound to different soil constituents is important to understand heavy metals behavior and fate in soils. The mobility and bioavailability of metals in soil depend on the strength of the bond between metal and soil surface as well as the properties of soil solution (Filgueiras et al., 2002). Metal ions could associate with oxyhydroxides, carbonates, sulfides, OM, and clay minerals by different mechanisms such as outer- or inner-sphere surface complexation. Ure (1991) defined the term "speciation" as "The active process of identification and quantification of different defined species, forms or phases in which an element occurs in a material." Numerous authors used the term "fractionation" interchangeably with speciation (Chang et al., 1984; Tack and Verloo, 1995; Gleyzes et al., 2002; Hou et al. 2006). The objective of chemical partitioning of trace element in soil is to quantify metal fractions associated with various phases by instrumental methods or chemical extraction methods (Amacher, 1996).

Several chemical sequential extraction schemes were proposed for heavy metals fractionation in soil and sediments (Tessier et al., 1979; Emmerich et al., 1982; Amacher, 1996; Gomez et al., 2000). For more details, Rao et al. (2008) provided comprehensive review of the single and sequential extraction schemes for metal fractionation in environmental samples. Most of those sequential extraction methods considered the exchangeable fraction which includes weakly adsorbed metals that can be readily desorbed by ion exchange process using salt

solutions such as $MgCl_2$, $CaCl_2$, $Mg(NO_3)_2$ among others. For the reducible fraction that represents the amount of metals associated with hydrous oxides of Mn and Fe is extracted by hydroxylamine hydrochloride or oxalic acid/ammonium oxalate buffer at low pH. Whereas the oxidisable fraction which is the amount associated with the OM or sulfides, may be obtained by oxidation process. On the other hand, the carbonate fraction is extracted by mild acidic solutions such as sodium acetate. In general, the applications of sequential extraction methods were summarized by Filgueiras et al. (2002) as follows: i) characterization of pollution sources, ii) evaluation of metal mobility and bioavailability, and iii) identification of binding sites of metals for assessing metal accumulation, pollution and transport mechanisms. Although sequential extractions are time consuming, these methods provide imperative knowledge about element mobility and availability in soil. However, the measurement of total concentration of metals in soils is useful to detect any net change due to different possible phenomena. Sequential extraction procedures cannot be used as stand-alone evaluations to identify the actual form of metals in soils and should be accompanied by deeper experimental investigations (Dahlin et al., 2002).

Total cadmium concentration is not a particularly useful measure for assessing potential phyto-availability (Campos et al., 2003), however several scientists applied sequential extraction schemes to determine the extent of contamination based on partition of trace elements in soils (Ramos et al., 1994; Pueyo et al., 2003). Moral et al. (2005) reported that for non-calcareous soils, Cd was recovered in oxidizable, reducible and residual fractions. However for the calcareous soils, Cd was recovered mainly in sorbed-carbonate and residual fractions. Also, the authors explained that the partition of Cd in non-calcareous soils followed different sequences depending on the nature of the pollutant input and the soil. Biosolids application increased the concentration of Cd in exchangeable and specifically adsorbed fractions. Sukkariyah et al. (2005)

showed that the application biosolids increased Cd concentrations significantly compared with untreated soil from not detected to 1.32 mg kg^{-1} and from 0.4 mg kg^{-1} to 0.6 mg kg^{-1} in the exchangeable and specifically adsorbed fractions, respectively. Clevenger (1990) determined the total concentration and the solid phase chemical forms of the various heavy metals present in the land disposed Pb-Zn mine tailings. The author found that Cd is primarily found in the residual fraction 62-89% of total Cd 24-83 mg kg^{-1}. Also, Carapeto and Purchase (2000) evaluated a three-step Cd-extraction method using contaminated sediment samples from a constructed wetland receiving urban runoff. They reported that the highest proportion of Cd was found in the residual fraction (54-65% of the total Cd), followed by the organic fraction (26-37%) and the exchangeable fraction contained the least amount of Cd (6-18%).

Copper retained in the soil is commonly associated with various soil components including OM, clays, carbonate, and Fe and Mn oxides (Tessier et al., 1979; Emmerich et al., 1982; Baker and Senft, 1995). These components exhibit varying potential for retention as well as release of Cu in soils. He et al. (2006) suggested that based on column leaching, short-term Cu pulse was primarily due to the exchangeable Cu fraction. They also found that, based on batch extractions, carbonate-bound and exchangeable fractions contribute to long-term Cu release from sandy soils. Initial total Cu concentration and soil properties influence Cu fractionation in soils. Ho and Evans (2000) found that 4, 3, 46, and 47% of total Cu associated with acid-extractable, reducible, oxidizable, and residual fractions, respectively for alkaline soil with 8% organic carbon (OC) and initial total Cu of 875 µg g^{-1}. Whereas, the respective values for another alkaline soil with OC of 15% and initial total Cu of 4250 µg g^{-1} were 13, 14, 33, and 41%, respectively. In a study of the long term behavior of Cu added by sewage sludge in small-plot trial, Schaecke et al. (2002) found that 72.9, 15.3, and 8.7% of Cu associated with the organically bound, Fe oxides, and residual fractions, respectively after nine years of the last application of

sewage sludge. Whereas, the perspective values for the control plots were 52.2, 27.8, and 19.3%, respectively. However, the sum of the easily released Cu fractions was less than 5%, Cu had moved as far as 50 cm in depth during 9-11 years. The strong retention of Cu was attributed to that Cu retained on OM by complexation rather than by ion exchange (Balasoiu et al., 2001). Although strong organic complexes are known to form with Cu, Sukkariyah et al. (2005) results revealed that the metal-oxide fraction contained the highest concentration of Cu. Their results showed that the application of 210 Mg ha^{-1} biosolids that contained 760 kg Cu ha^{-1} increased concentrations of Cu significantly compared with untreated soil from 0.2, 2.9, 27.7, and 4.6 mg kg^{-1} to 7.4, 62.4, 125.7, and 48 mg kg^{-1} in the exchangeable, specifically adsorbed, oxide, and organic fractions, respectively. Moreover, Zemberyouva et al. (1998) distinguished the Cu fractions bound to humic compounds. They found that 16 -22% bounded to OM as exchanging for acid-base effect at pH 1 whereas 7-18% associated with the humic compounds. Recently, in semi-arid grassland, Ippolito et al. (2009) showed that Cu concentrations in a surface soil were greatest in the amorphous and crystalline Mn/Fe oxyhydroxide-bound fraction (51-53%) whereas lesser amounts of Cu were presented in the organically complexed (17–20%) and residual inorganic phases (18-26%). Moreover, the potential for downward Cu transport associated with the organically complexed phase was enhanced by the repeated biosolids application, and with time Cu was likely transformed to the less bioavailable amorphous and crystalline Mn/Fe oxyhydroxide- bound phase.

Lead speciation studies showed that Pb fractionation depends on soil properties and total amount of pollution loading. Marin et al. (1997) applied the sequential extraction scheme procedure recommended by Bureau Commun de Reference (BCR) to test its long term precision of measurements and performance. They found that Pb was essentially extracted from the Fe-Mn oxides fraction with 32% of the total (11.01 mg kg^{-1}) whereas the 5.5 and 4.5% associated with

the exchangeable and OM fractions, respectively. Also, Davidson et al. (1998) used the BCR procedure to study Pb fractionation in an industrially contaminated site. They reported that for a surface layer (2-13 cm) there were 32 and 25% of approximately 0.6 g kg^{-1} total Pb associated with the Fe-Mn oxides and OM/sulfides fractions, respectively. Whereas, less than 0.1% of Pb associated with Fe-Mn oxides in the deep layer (60-85 cm) that contained around 6 g kg^{-1} total Pb, and more than 45% associated with OM/sulfides fraction. Moreover, Maiz et al. (2000) applied two different sequential extraction procedures to evaluate Pb availability from polluted soils affected by numerous anthropogenic sources. They found that the mobile (extracted by 0.01 mol L^{-1} $CaCl_2$) and the mobilisable (extracted by 0.005 mol L^{-1} DTPA) fractions counted for 14% of total Pb. On the other hand, 15% of the total Pb bounded with exchangeable and carbonates fractions whereas 17 and 4% associated with Fe-Mn oxides and OM/sulphides fractions, respectively. Under a semi-arid environment, Illera et al. (2000) measured the distribution of Pb in soil after one year application of biowastes. They found that in the control soil 39.6 and 37.1% of Pb was present in the residual and Fe-Mn oxides fractions, respectively. Whereas, after 1 year of waste application, an increase of total lead content was noticed (from 75.2 to 87.8 mg kg^{-1}) and remarkable increase of Fe-Mn oxides fraction was observed in the amended plots (45.1%).

Tin speciation studies were carried out on reference-marine sediments contained total Sn of 1.21 mg kg^{-1} by Marin et al. (1997). They found that the high portion of Sn associated with the residual fraction (>95%) which indicated that Sn bounded to silicates of detrital origin. In a recent study on five different Japanese soils, Hou et al. (2006) showed that Sn occurred in relatively diverse fractions and the concentration of Sn in the residues were large in clay-rich soils. They reported that the average percentages of Sn bound to metal-organic complex, amorphous metal oxides, crystalline Fe oxides, H_2O_2-extractable organic and residual (extracted

by HNO_3-$HClO_4$-HF) were 25±12, 17±8, 11±5, 6.2±3.7, and 40±22%, respectively. Also in Japanese soils using a selective extraction methods, Nakamaru and Uchida (2008) showed that the major part of the soil-sorbed Sn associated with OM (18 to 72%) or Al/Fe-(hydr)oxide-bound (24 to 88%) fractions whereas, the acid soluble fraction was less than 0.2%. the literature review of Sn speciation studies indicated that Sn fractionation depended on soil properties and the total Sn concentration in soil.

1.4 Heavy Metals Transport in Soils

Understanding the reactivity of heavy metals in soil is a prerequisite for modeling its transport and fate in soil environment. Chao (1984) stated that adsorption and desorption; precipitation and solubilization; surface complex formation; ion exchange; penetration of the crystal structure of minerals; and biological mobilization and immobilization are the major process that control mobility of heavy metals in soil. Also, the mobility is affected with the association of the heavy metals with different fractions such as soluble, exchangeable, carbonate, oxide, organic, and residual. Near to the flue dust dump site, Li and Shuman (1996) found that the exchangeable fraction and soluble form of Zn migrated down to 100 cm in depth whereas Cd was observed in the subsoil from 30 to 75 cm. In contaminated soils by mine drainage and sediment, Levy et al. (1992) noticed that the greatest concentrations of total metals were found either in the surface horizons or in hydraulically deposited sand layers that were buried. Also, the authors concluded that the movement of heavy metals with ground water into public water supply might present hazards to aquatic life and humans as well. Sterckeman et al. (2000) evaluated the vertical distribution and downward mobility of Cd, Zn, and Pb in soils around smelters. They found that most of heavy metals contamination in the upper horizons (20 or 30 cm) and Pb enrichment is suspected to depth of 1.2 m whereas the respective values for Zn and Cd are 1.6 m and 2 m, respectively.

The most important factors that affect the mobility of heavy metals in soils are pH, redox reaction, and concentration of dissolved organic matter (DOM) in soil. Low heavy metals mobility is anticipated in alkaline soils compared with acidic soils. In a rice paddy contaminated soil, Chuan et al. (1996) found that Pb, Cd, and Zn solubilities increased drastically under acidic conditions. Moreover, they found that 14, 39, and 100% of total Pb, Zn, and Cd, respectively, were solublizied at the highly oxidizing state (330 mV), and soluble Pb and Zn concentrations increased from 280.8 to 678.6 mg kg^{-1} and 110.3 to 189.6 mg kg^{-1}, respectively at moderately oxidizing condition (200 mV). Whereas at redox potential of 100mV, solubility of Pb and Cd were decreased slightly, while Zn was not affected. Redox processes and the presence of organic ligands in wetlands could cause the transfer of a wide variety of trace elements from soil minerals to soil solution, and then to surface water (Olivie-Lauquet et al., 2001). The DOM has an important influence on metal solubility (Sauve´et al., 2000). Metal binding to the DOM can affect the solubility of metals to a considerable extent and increase the concentration of dissolved metals by more than 2 orders of magnitude (Weng et al., 2002).

1.4.1 Modeling Heavy Metals Retention

Retention or Sorption are interchangeably terms commonly used to describe the attachment of heavy metals (adsorbate) to soil particles (adsorbent) when no information are available regarding the bonding mechanism. Numerous equations were practically applied to predict chemical retention on soils. These equations were developed to find the relationship between the sorbed amount (*S*) on a soil and the concentration (*C)* in the surrounding soil-solution at equilibrium which well known as sorption isotherm since,

$$S = f\ (C) \qquad [1.1]$$

The simplest equation is the linear form where *S* assumed to increase linearly as *C* increase,

$$S = k_d C \qquad [1.2]$$

where k_d is the distribution coefficient ($L^3\ M^{-1}$). Here, larger k_d value implies stronger sorption on soil. The k_d is a measure of the affinity of a heavy metal to a soil and is widely reported in the literature for various heavy metals (Buchter et al., 1989). Adequate simulation of heavy metals sorption using linear empirical equation was carried out in numerous studies (Christensen, 1989; Gao 1997; Alumaa et al., 2002). Unfortunately, linear sorption does not fit under most circumstances such as sorption at high surface loadings and when heavy metals exhibit nonlinear isotherm (Covelo et al., 2007; Shaheen et al., 2009; Ramírez-Pérez et al., 2013). Accordingly, other equations were extensively applied to describe the nonlinear sorption isotherms such as Freundlich equation,

$$S = K_F\, C^b \qquad [1.3]$$

where b is a dimensionless reaction order and K_F is the Freundlich distribution coefficient where unit depends on the units of S ($M\ M^{-1}$) and C ($M\ L^{-3}$). Here, the b value indicates the shape of sorption isotherms as convex, linear, and concave with $b < 1$, $b=1$, and $b > 1$, respectively. Buchter et al. (1989) reported a range of b values from 0.57 to 0.90 for Cd in 11 soils having different properties, including calcareous and organic soils. Whereas, the respective range for Cu and Pb were of 0.50 to 1.42 and of 0.56 to 5.39, respectively. In a recent study, Shaheen et al. (2009) indicated the highest b values (b= 0.93) for adsorption of Cu on a calcareous soil whereas lowest values (b=0.19) associated with a sandy soil with low carbonates.

Also Langmuir equation was commonly used for such nonlinear isotherm,

$$S = \frac{S_{max} K_L C}{1 + K_L C} \qquad [1.4]$$

Where S_{max} is the sorption capacity ($M\ M^{-1}$) and K_L is a Langmuir coefficient ($L^3\ M^{-1}$) related to the binding strength. Accounting for the maximum sorption capacity in Langmuir equation, is a major advantage. The equation provides a reliable manner to compare different soils affinities for

certain element or to compare the sorption capacities of different elements on a specific soil. Generally, Langmuir isotherms were broadly used to simulate heavy metals retention on soils (Ho et al., 2002; Markiewicz-Patkowska et al., 2005; Chaturvedi et al., 2006; Covelo et al., 2007). However, the Langmuir isotherm is derived by assuming a finite number of uniform adsorption sites and the absence of lateral interaction between adsorbed species; both assumptions are violated in soils particularly at high solution metal concentrations (Goldberg and Criscenti, 2008). Soil exhibited higher S_{max} as a result of increasing reaction time (Zhang and Selim, 2005). This is emphasizing the importance time dependent reactions in soils. Equations 1.2, 1.3, and 1.4 are equilibrium type models and did not account for reaction time.

Frequently, the heavy metals retention on soils is strongly kinetic. In such case, the time-dependence of the sorption isotherm must be specified. The sorption reaction time varies from few seconds to many years (Sparks, 2011). The kinetic models such as first and second order reactions are commonly applied for such sorption simulation. Here, reaction time and initial concentration are significantly affect the reaction type. For instance, the half-life period ($t_{1/2}$) for a first order reaction is independent of initial concentration of reactant, whereas it is inversely proportional to the initial concentration for a second order reaction (Upadhyay, 2006). Numerous authors provided several examples of kinetic retention of heavy metals in soils (Selim, 1992; Strawn and Sparks, 1999; Bellir et al., 2005; Fonseca et al., 2009)

Lagergren's kinetics equation commonly used to describe adsorption kinetics where the pseudo-first order rate equation could be written as flow:

$$\frac{dx}{dt} = k(X - x) \qquad [1.5]$$

where X and x are adsorption capacities (M M^{-1}) at equilibrium and at time t (T), respectively. k is the rate constant (T^{-1}) of pseudo-first order reaction (Ho, 2004). The integration of equation 1.5 using boundary conditions $t = 0$ to $t = t$ and $x = 0$ to $x = x$ gives,

$$x = X\,(1 - e^{-kt}) \qquad [1.6]$$

For the fully reversible first order kinetic type, Selim (1992) stated the formula as,

$$\frac{dS}{dt} = \frac{\theta}{\rho} k_f C - k_b S \qquad [1.7]$$

where k_f and k_b are the forward and backward rates of reactions (T^{-1}), respectively. θ is the moisture content ($L^3\ L^{-3}$) and ρ is the bulk density ($M\ L^{-3}$). In this equation, the small values of k_f and k_b is indicative of slow and strong kinetic behavior (Selim, 1992).

The rate law for pseudo-second-order model can be expressed as:

$$\frac{dx}{dt} = k_2 (X - x)^2 \qquad [1.8]$$

Integrating within the boundary conditions t = 0 to t = t and x = 0 to x = x, gives

$$\frac{1}{(X-x)} = \frac{1}{X} + k_2 t \qquad [1.9]$$

where k_2 is the pseudo-second-order rate constant of sorption ($M\ M^{-1}\ T^{-1}$) . Yin et al. (1997) successfully described Hg sorption-desorption on acidic soils using second-order kinetic model when reverse reactions were ignored where, backward rates of reactions were assumed to be zero. In a study of Cd sorption data within different pH range (3-8), Gupta et al. (2009) showed that the pseudo second order kinetics model provided better simulation for the experimental than the pseudo-first order model that was found to be insufficient. Recently, Anirudhan et al. (2012) evaluated the adsorption and desorption of phosphatic clay for the removal of Hg, Cd, and Co from aqueous solutions using first and second order reaction models. They found that Pseudo-second-order model gave good correlation with the experimental data, and film diffusion process appears to be the rate-limiting step for the adsorption of the studied elements.

All simulations using the previous equations (1.2 to 1.9) are based only on single site/reaction. In order to quantify multisite or multireaction, these models were modified. For instance, two-site Langmuir to estimate *j* couples of L_i and $S_{max,i}$

$$S = \sum_{i=1}^{j} S_{max,i} \frac{L_i C}{1+L_i C} \quad [1.10]$$

Another example for accounting for two-site, Chen et al. (2006) described Cd sorption in two soils by developing a two-site model that combining a linear instantaneous model for the surface adsorption and a first-order reaction kinetic model with forward and backward reaction constants for the immobilization and precipitation of the mineral phase. Their results indicated that the forward reaction was five times faster than the backward reaction for both studied soils and the reaction rates were two times faster in the heavier textured clay soil.

The multisite/multireaction approach is a good representation for the real soil system where soil consists of many constituents such as oxides, OM, $CaCO_3$, and clay minerals among other. Each soil component could react differently with the chemical that might exist in the soil solution. Selim (1992) provided the multireaction and transport model (MRTM) that accounts for several interactions of heavy metals with soil matrix surfaces. The uniqueness of this model is that its aim is to describe the reactivity of solutes with natural systems versus time during transport in the soil profile. On the other hand, other commonly used models including linear, Freundlich, Langmuir, and Elovich, the equilibrium sorption is often assumed (see Selim and Amacher, 1997). Moreover, the use of such models yields a set of parameters that are only applicable for a specific reaction time. MRTM provides a comprehensive accounting of solute sorption-desorption processes, where a single set of parameters is sought that is applicable for an entire data set and for a wide range of initial (or input) concentrations. In this model S_e represents the amount retained on equilibrium sites; S_1 and S_2 represent the amount retained on reversible kinetic sites; S_{irr} and S_s represent the amounts irreversibly retained. The retention reactions associated with MRTM are,

$$S_e = \frac{\theta}{\rho} K_e C^N \quad [1.11]$$

$$\frac{dS_1}{dt} = k_1 \left(\frac{\theta}{\rho}\right) C^n - k_2 S_1 \quad [1.12]$$

$$\frac{dS_2}{dt} = \left[k_3 \left(\frac{\theta}{\rho}\right) C^n - k_4 S_2\right] - k_5 S_2 \qquad [1.13]$$

$$\frac{dS_s}{dt} = k_5 S_2 \qquad [1.14]$$

$$S_{irr} = k_{irr} \left(\frac{\theta}{\rho}\right) C \qquad [1.15]$$

where N and n are dimensionless reaction orders, the parameter K_e is a dimensionless equilibrium constant, and k_1, k_2, k_3, k_4, k_5, and k_{irr} (T^{-1}) are the associated rates of reactions. The MRTM was successfully used to describe retention of several heavy metals in soils such as Cd, Cr, Cu, Zn, among others (Amacher et al., 1988; Selim, 1992; Selim and Ma, 2001; Zhao and Selim, 2010).

1.4.2 Modeling Heavy Metals Transport

Environmental studies require accurate simulation of heavy metals transport in soils. The law of conservation of mass is expressed in a mass balance equation, which accounts for the flux of mass going into and out from a defined volume. The transport of heavy metals in soil involves convection (advection), hydrodynamic dispersion, and sorption/desorption processes. The advection-dispersion model considers the spreading phenomenon to be principally the result of a complex velocity distribution caused by the presence of heterogeneities (Gillham et al., 1984). The partial differential equation describing one-dimensional transport of nonreactive solute through a soil is written as,

$$\frac{\partial C}{\partial t} = -v \frac{\partial C}{\partial z} + \frac{\partial}{\partial z}\left(D \frac{\partial C}{\partial z}\right) \qquad [1.16]$$

Where $\frac{\partial C}{\partial t}$ is the net change of the concentration in time (t), $v = (q/\theta)$ is the average pore water velocity (L T^{-1}) where q is the Darcy's water flux (L T^{-1}), z is the distance (L). The term $v \frac{\partial C}{\partial z}$ is known as advection whereas $\frac{\partial}{\partial z}\left(D \frac{\partial C}{\partial z}\right)$ is known as dispersion term. And thus, equation 1.16 is well known as convection-dispersion equation (CDE), also known as advection-dispersion

equation (ADE). Under steady state flow, q and θ are constants over space and time (see Selim and Amacher, 1997). The CDE is widely used to predict solute transport in soils. Sidle and Kardos (1977) were among the earliest researchers to utilize the convection-dispersion equation (CDE) for the description of Cu, Zn, and Cd movement in a sludge treated forest soil. In soil column experiments, Vogeler (2001) described Cu concentration in the effluent based on the CDE where ion exchange for a Cu–Ca binary system was assumed as the governing retention mechanism. Measured Cu results were significantly retarded when compared to CDE simulation, however. As a result, the authors suggested that nonexchange processes are also involved in Cu transport in soils. Recently, modeling studies based on two-site nonequilibrium models are reasonable for the elements that are highly sorbed on soils such as Pb (Fonseca et al., 2011; Chotpantarat et al., 2012).

As an example of transport model based on linear sorption, CXTFIT (version 2.1, Toride et al., 1999) is widely used to describe the behavior of reactive chemicals in soils (e.g., Pang and Close, 1999 and Tsang and Lo, 2006). This analytical model was used to solve the inverse problem based upon the CDE where linear equilibrium sorption was assumed. The CDE used by CXTFIT incorporates a first-order decay coefficient (μ) as follows,

$$R\frac{\partial C}{\partial t} = \frac{\partial}{\partial z}\left(D\frac{\partial C}{\partial z}\right) - v\frac{\partial C}{\partial z} - \mu C \qquad [1.17]$$

where R is a dimensionless retardation factor ($R = 1 + \rho K_d/\theta$), and K_d is a partitioning coefficient ($L^3 M^{-1}$). The term R accounts for linear equilibrium sorption. The term μC is a sink term which captures irreversible retention (or removal) of a chemical directly from the soil solution based on first-order decay. Since heavy metals such as Cd or Cu do not undergo decay or degradation, we consider this term as that for irreversible retention, in a similar manner or equivalent to that associated with k_{irr} in equation 1.15 of MRTM.

The MRTM is an example of a transport model that accounts for kinetic sorption (Selim, 1992). Incorporation of the CDE with the reactions given in equations [1.11]-[1.15], yields

$$\rho \frac{\partial S}{\partial t} + \theta \frac{\partial C}{\partial t} = \theta D \frac{\partial^2 C}{\partial z^2} - q \frac{\partial C}{\partial z} \qquad [1.18]$$

where S is the total amount sorbed,

$$S = S_e + S_1 + S_2 + S_s + S_{irr} \qquad [1.19]$$

where D is the hydrodynamic dispersion coefficient ($L^2 T^{-1}$). To obtain model simulations of heavy metal transport in the soil columns, MRTM is utilized along with a nonlinear least-squares optimization scheme, which provided best-fit of the model to the experimental BTCs. Criteria used for estimating the goodness-of-fit of the model to the data were the coefficient of determination (r^2) and the root mean square error (*RMSE*) statistics:

$$RMSE = \sqrt{\frac{\sum (C_{ops} - C)^2}{n_o - n_p}} \qquad [1.20]$$

where C_{ops} is the observed metal concentration at time t, C is the simulated metal concentration at time t, n_o is the number of measurements, and n_p is the number of fitted parameters.

The second-order two-site (SOTS) model is another example for nonlinear kinetics model. Basic to the second-order formulation is the assumption that a limited number of sites are available for solute adsorption in soils. As a result, the reaction rate is a function of the solute concentration in the soil solution and the availability of adsorption sites on soil matrix surfaces. Specifically, retention mechanisms are assumed to depend not only on C but also the number of sites (φ) that are available for solute adsorption in soils (Selim and Amacher, 1988; Selim and Amacher 1997). The model also assumes that a fraction of the total sorption sites is rate limited, while the remaining fractions interact rapidly or instantaneously with the solute in the soil solution. The sorbed phases S_e, S_k, and S_{irr} are in direct contact with the solute in the solution phase (C) and are governed by concurrent reactions. Specifically, C is assumed to react rapidly

and reversibly with the equilibrium phase S_e. The relations between C and S_k and S_{irr} are governed by reversible nonlinear and irreversible linear kinetic reactions, respectively. A second irreversible reaction was assumed as a consecutive reaction of the S_k phase into a less accessible or strongly retained phase S_s. Therefore, the model formulation can be expressed as

$$S_e = K_e \theta\, C\, \varphi \qquad [1.21]$$

$$\frac{\partial S_k}{\partial t} = k_1 \theta\, C\, \varphi - (k_2 + k_3) S_k \qquad [1.22]$$

$$\frac{\partial S_s}{\partial t} = k_3 S_k \qquad [1.23]$$

$$\rho \frac{\partial S_{irr}}{\partial t} = k_{irr}\, \theta C \qquad [1.24]$$

Here φ is related to the sorption capacity (S_{max}) by:

$$S_{max} = \varphi + S_e + S_k + S_s + S_{irr} \qquad [1.25]$$

where φ and S_{max} (M solute M^{-1} soil) are the unoccupied (or vacant) and total sorption sites on soil surfaces, respectively. The total sorption sites S_{max} was considered as an intrinsic soil property and is time invariant. In addition, S_e is the amount retained on equilibrium-type sites (M M^{-1}), S_k is the amount retained on kinetic-type sites (M M^{-1}), S_s is the amount retained irreversibly by consecutive reaction (M M^{-1}), and S_{irr} is the amount retained irreversibly by a concurrent type of reaction (M M^{-1}). The equilibrium constant is K_e (L^3 M^{-1}). The reaction rate coefficients are k_1 (L^3 M^{-1} T^{-1}), k_2 (T^{-1}), k_3 (T^{-1}), and k_{irr} (T^{-1}), while C is the solute concentration (M L^{-3}), θ is the volumetric water content (L^3 L^{-3}), and t is the reaction time (T). At any time t, the total amount of solute sorbed by the soil matrix, S, can be expressed as

$$S = S_e + S_k + S_s + S_{irr} \qquad [1.26]$$

The above reactions were incorporated into the CDE (Eq. [1.18]). For the reactive transport of metal in soils, the second term in Eq. [1.18], $\partial S/\partial t$, was accounted for using the second-order approach described above in Eq. [1.21–1.25]. A finite difference (Crank–Nicholson forward–

backward) method was used to provide numerical solutions of the transport equation subject to a solute-free initial condition:

$$C(x, t = 0) = 0 \qquad [1.27]$$

and the boundary conditions:

$$vC - D\frac{\partial C}{\partial x}|_{(x=0,t)} = \{_{0}^{vC_o} \quad {}^{0<t\leq t_o}_{t>t_o} \qquad [1.28]$$

$$\frac{\partial C}{\partial x}(x = L, t) = 0 \qquad [1.29]$$

where C_o is the input metal concentration (M L^{-3}), t_o is the duration of the metal input pulse (T), L is the length of the soil column (L), and v is the pore water velocity (L T^{-1}). The kinetic retention processes of the SOTS model (Eq. [1.21–1.25]) were solved using the fourth-order Runge–Kutta method. The BTC data from column experiments were fitted to the models described above using the Levenberg–Marquardt nonlinear least square optimization method (Press et al., 1992). Statistical criteria used for estimating the goodness-of-fit of the models to the data were the coefficients of determination, r^2, and the root mean square error (RMSE).

1.5 Statement of Problems

The mobility of heavy metals in soils is highly depended on the physical and chemical soil characteristics as well as heavy metals' properties. Due to soil heterogeneity and the composition complexity, the heavy metals reactivity and kinetics vary from one soil to another. Quantifying the heavy metals kinetics is essential for obtaining a precise simulation of its mobility in soils. A literature search revealed that heavy metals transport such as Cd and Cu are commonly described and predicted based on linear retention where equilibrium adsorption is the dominant mechanism. Moreover, several studies have been conducted to investigate Cu mobility and release in acidic as well as alkaline soils (Sidle et al., 1977; Zhu and Alva, 1993; Chang et al., 2001; Bang and Hesterberg, 2004; Wang et al., 2009; Sayyad et al., 2010). Only a few

studies, however, have focused on modeling Cu transport in soils, especially alkaline calcareous soils. Thus, the focus of the current studies is to describe Cd and Cu transport based on multiple component or multisite approaches where adsorption is accounted for based on several nonlinear reactions of the kinetic as well as equilibrium types.

Additionally, literature review regarding Pb reactivity and transport in soils revealed that numerous studies were carried out for competitive sorption and transport for Pb with other heavy metals. However, we were not aware of a study to examine the effect of introducing Cd and Cu subsequently to Pb pulse into a soil. Also, several studies accounted for the sorption of inorganic Sn on soil whereas it appears that no studies have been carried out to explore the influence of Sn on Pb mobility in soils. In the current research, we used miscible displacement column and sequential extraction experiments to assess Pb mobility in two alkaline sandy soils and the influence of Cd and Cu on Pb release. Moreover, batch and column experiments were carried out to quantify the sorption-desorption and mobility of single and binary systems of Sn and Pb in two acid soils.

Finally, long-term accumulation of bioavailable forms of heavy metals in soils remain as particularly significant gaps in the science of sustainable wastewater irrigation (Hamilton et al., 2007). The behavior of these chemicals in the environment and the resulting risk to human health is largely unknown (O'Connor et al., 2008). For these reasons, we assessed the effects of long-term irrigation with sewage effluents on soil properties and accumulation of total and available forms of Cd, Cu, Ni, and Pb in soil. Also, we provided spatial variability maps of those heavy metals using remote sensing data and GIS to delineate areas of heavy metals contamination.

1.6 Objectives

This dissertation explores the retention-release and mobility of Cd, Cu, Pb, and Sn in acids and alkaline soils and quantifies the proportions of these heavy metals that bind to different

soil constituents. Also, the study aims to simulate reactivity and mobility of these elements using different models such as MRTM and SOTS models. The specific objectives of Cd and Cu studies were to (i) measure the transport and retention of Cd in columns of acidic and alkaline soils; (ii) quantify time-dependent sorption and release and predict the kinetics of Cd hysteresis in soils; (iii) predict the extent of Cd mobility and distribution of Cd retained with depth in the soil columns; (iv) quantify the sorption of Cu on acidic and alkaline soils; (v) quantify the kinetics of Cu retention during transport in soil columns using miscible displacement; (vi) test the predictive capability of kinetic multireaction modeling approaches to describe Cu transport and reactivity of Cu in soils; (vii) quantify the mobility and retention of Cu in calcareous soils based on miscible displacement; (viii) assess the capability of two modeling approaches (SOTS model and CXTFIT) in describing the mobility of Cu, and (ix) simulate the distribution of Cu with soil depth with and without the presence of $CaCO_3$.

For Pb and Sn studies, the objectives were to (i) study the reactivity of Sn and Pb in acidic soils and their impact on the release of other elements found in soil; (ii) study Pb mobility in alkaline sandy soils and the influence of Cd and Cu on its retention; and (iii) explore the mobility of Sn and Pb in acidic soils and the influence of each one on the other. Also, the dissertation aims to study the long-term accumulation of bioavailable forms of Cd, Cu, Ni, and Pb in contaminated soils through (i) assessing the effects of long-term irrigation with sewage effluents on soil properties and accumulation of total and available forms of these heavy metals in soil; and (ii) creating spatial variability maps of those heavy metals using remote sensing data and GIS tool to delineate areas of heavy metals contamination.

1.7 References

Adriano, D.C. 2001. Trace Elements in Terrestrial Environments: Biogeochemistry, Bioavailability and Risk of Metals. 2nd ed. Springer, New York.

Alloway, B. 2013. Heavy Metals in Soils-Trace Metals and Metalloids in Soils and their Bioavailability. Springer Dordrecht Heidelberg New York London, (613 p).

Alloway, B.J., ed. 1990. Heavy metals in soils. Blackie and John Wiley & Sons, Glasgow.

Alloway, B.J. 1995. The origins of heavy metals in soils. p. 38–57.*In*: Alloway, B.J. (ed.), Heavy Metals in Soils. Blackie Academic and Professional, London, UK.

Alumaa, P., U. Kirso, V. Petersell, and E. Steinnes. 2002. Sorption of toxic heavy metals to soils, Int. J. Hyg. Environ. Health. 204: 375-376.

Amacher, M.C., H.M. Selim, and I.K. Iskandar. 1988. Kinetics of chromium (VI) and cadmium retention in soils; a nonlinear multireaction model. Soil Soc. Soc. Am. J. 52:398-408.

Amacher, M.C. 1996. Nickel, Cadmium, and lead. p. 739-768. *In*: Sparks, D.L. (ed.) Methods of Soil Analysis: Chemical Methods. Part 3. SSSA No.5. ASA-CSSA-SSSA, Madison, WI.

Anirudhan, T.S., C.D. Bringle, and P.G. Radhakrishnan. 2012. Heavy metal interactions with phosphatic clay: Kinetic and equilibrium studies. Chem. Eng. J. 200–202:149–157.

Appenroth, K. 2010. Definition of "Heavy Metals" and Their Role in Biological Systems. p.19-29. *In*: Sherameti, A. and A. Varma, Soil Heavy Metals. Springer-Verlag Berlin Heidelberg.

Aringhieri, R., P. Carrai, and G. Petruzzelli. 1985. Kinetics of Cu^{2+} and Cd^{2+} adsorption by an Italian soil. Soil Sci. 139:197–204.

Baker, D.E., and J.P. Senft. 1995. Copper. p. 179–205. *In*: Alloway, B.J. (ed.), Heavy Metals in Soils. Blackie Academic & Professional, London, UK.

Balasoiu, C.F., G.J. Zagury, and L. Deschenes. 2001. Partitioning and speciation of chromium, copper, and arsenic in CCA-contaminated soils: influence of soil composition. Sci. Total Environ. 280:239–255.

Bang, J., and D. Hesterberg. 2004. Dissolution of trace element contaminants from two Coastal Plain soils as affected by pH. J. Environ. Qual. 33:891–901.

Barkouch, Y., A. Sedki, and A. Pineau. 2007. A new approach for understanding lead transfer in agricultural soil. Water Air Soil Pollut. 186:3–13.

Bellir, K., M. Bencheikh-Lehocine, A.-H. Meniai, and N. Gherbi. 2005. Study of the retention of heavy metals by natural material used as liners in landfills. Desalination.185:111-119.

Bennet, H. 1986. Concise Chemical and Technical Dictionary, 4^{th} enlarged (Ed.), Edward Arnold, London.

Berkowitz, B., I. Dror, and B. Yaron. 2008. Contaminant Geochemistry: Interactions and Transport. *In*: The Subsurface Environment. Springer, Heidelberg, 412 pp.

Bjerrum, N. 1936. Bjerrum's Inorganic Chemistry, 3rd Danish ed., Heinemann, London.

Bryan, G. W, and W.J. Langston. 1992. Bioavailability, accumulation and effects of heavy metals in sediments with special reference to United Kingdom estuaries: a review. Environ. Pollut. 76, 89-131.

Buchter, B., B. Davidoff, M.C. Amacher, C. Hinz, I.K. Iskander and H.M. Selim . 1989. Correlation of Freundlich *Kd* and *n* retention parameters with soils and elements. Soil Sci. 148: 370-379.

Campos, M.L., M.A.P. Pierangeli, L.R.G. Guilherme, J.J. Marques, and N. Curi. 2003. Baseline concentrations of heavy metals in Brazilian latosols. Commun. Soil Sci. Plant Anal. 34:547-557.

Carapeto, C., and D. Purchase. 2000. Use of sequential extraction procedures for the analysis of cadmium and lead in sediment samples from a constructed wetland. Bull. Environ. Contam. Toxicol. 64: 51-58.

Chang, A.C., A.L. Page, J.E. Warneke, and E. Grgurevic. 1984. Sequential extraction of soil heavy metals following a sludge application. J. Environ. Qual. 13:33-38.

Chang, C.M., Wang, M.K., Chang, T.W., Lin, C., Chen, Y.R., 2001. Transport modeling of copper and cadmium with linear and nonlinear retardation factors. Chemosphere 43, 1133-1139.

Chao, T.T. 1984. Use of partial dissolution techniques in geochemical exploration. J. Geochem. Explor. 20:101-135.

Chaturvedi, P. K., C. S. Seth, and V. Misra. 2006. Sorption kinetics and leachability of heavy metal from the contaminated soil amended with immobilizing agent (humus soil and hydroxyapatite). Chemosphere 64:1109-1114.

Chen, M., L.Q. Ma, and W.G. Harris. 1999. Baseline concentrations of 15 trace elements in Florida surface soils. J. Environ. Qual. 28: 1173-1181.

Chen, W., A. C. Chang, L. Wu, and A. L. Page. 2006. Modeling dynamic sorption of cadmium in cropland soils. Vadose Zone J. 5:1216-1221.

Choi, J. 2006. Geochemical modeling of cadmium sorption to soil as a function of soil properties. Chemosphere 63, 1824-1834.

Chotpantarat, S., S.K. Ong, C. Sutthirat, and K. Osathaphan. 2012. Competitive modeling of sorption and transport of Pb^{2+}, Ni^{2+}, Mn^{2+} and Zn^{2+} under binary and multi-metal systems in lateritic soil columns. Geoderma.189-190: 278-287.

Christensen, T.H. 1989. Cadmium soil sorption at low concentrations: VIII. correlation with soil parameters. Water Air Soil Pollut. 44: 71-82.

Chuan, M. C., G.Y. Shu , and J. C. Liu. 1996. Solubility of heavy metals in a contaminated soil: effects of redox potential and pH. Water Air Soil Pollut. 90:543-556.

Clevenger, T.E., 1990. Use of sequential extraction to evaluate the heavy metal in mining wastes. Water Air Soil Pollut., 50: 241-254.

Clifford, M.J, G.M. Hilson, and M.E Hodson**.** 2010. Tin and mercury. p.497-513. *In*: Hooda, P. (Ed.) Trace Elements in Soils. Wiley/ Blackwell.

Covelo, E.F., F.A. Vega, and M.L. Andrade. 2007. Simultaneous sorption and desorption of Cd, Cr, Cu, Ni, Pb, and Zn in acid soils: I. Selectivity sequences. J. Hazard. Mater. 147:852-861.

Dahlin, C.L., C.A. Williamson, W.K. Collins, and D.C. Dahlin. 2002 Sequential extraction versus comprehensive characterization of heavy metal species in brownfield soils. Environ. Forensics. 3: 191-201.

Davidson, C.M., A.L. Duncan, D. Littlejohn, A.M. Ure, and L.M. Garden. 1998. A critical evaluation of the three-stage BCR sequential extraction procedure to assess the potential mobility and toxicity of heavy metals in industrially-contaminated land. Anal. Chim. Acta 363:45-55.

De Haan, F.A.M and Zwerman, P.J. 1978. Pollution of soil. *In*: Bolt, G.H and Bruggenwert, M.G.M. (eds) Development in Soil Science 5A: Soil Chemistry A. Basic Element. Elsevier Science.

De Vries, W., P.F.A.M. Römkens, T. van Leeuwen, and J.J.B. Bronswijk. 2002. Heavy metals. p. 107–132. *In*: P.M. Haygarth, and Jarvis, S.C. (Ed.) Agriculture, Hydrology, and Water Quality; CAB International, Wallingford, Oxfordshire.

Dijkstra, J.J., J.C.L. Meeussen, and R.N.J. Comans. 2004. Leaching of heavy metals from contaminated soils: an experimental and modeling study. Environ. Sci. Technol. 38: 4390-4395.

Duffus, J.H. 2002. Heavy metals-a meaningless term?. Pure Appl. Chem. 74:793-807.

Elzinga, E.J. and R.J., Reeder. 2002. X-ray absorption spectroscopy study of Cu^{2+} and Zn^{2+} adsorption complexes at the calcite surface: implications for site specific metal incorporation preferences during calcite crystal growth. Geochim. Cosmochim. Acta 66: 3943-3954.

Emmerich, W.E., L.J. Lund, A.L. Page, and A.C. Chang. 1982. Solid phase forms of heavy metal in sewage sludge-treated soils. J. Environ. Qual. 11:178-181.

Epstein, L. and S. Bassein. 2001. Pesticide applications of copper on perennial crops in California, 1993 to 1998. J. Environ. Qual. 30:1844-1847.

Filgueiras, A.V., I. Lavilla, and C. Bendicho. 2002. Chemical sequential extraction for metal portioning in environmental solid samples. J. Environ. Monit. 4: 823-857.

Fonseca, B., H. Figueiredo, J. Rodrigues, A. Queiroz, and T. Tavares. 2011. Mobility of Cr, Pb, Cd, Cu and Zn in a loamy soil: a comparative study. Geoderma 164:232-237.

Fonseca, B., H. Maio, C. Quintelas, A. Teixeira, and T. Tavares. 2009. Retention of Cr(VI) and Pb(II) on a loamy sand soil: Kinetics, equilibria and breakthrough. Chem. Eng. J. 152: 212-219.

Forstner, U., 1995. Land contamination by metals: global scope and magnitude of problem. In: Allen, H.E., Huang, C.P., Bailey, G.W., Bowers, A.R. (Eds.), Metal Speciation and Contamination of Soil. Lewis Publishers and CRC Press, Boca Raton, FL.

Friberg, L. and G. F. Nordberg. 1986. Introduction. In Handbook on the toxicology of metals. Vol. I: General aspects, edited by L. Friberg, G. F. Nordberg, V. B. Vouk,. Amsterdam: Elsevier Science Publishers B.V.

Gao, S., W.J. Walker, R.A. Dahlgren, and J. Bold. 1997. Simultaneous sorption of Cd, Cu, Ni, Zn, Pb and Cr on soils treated with sewage sludge supernatant, Water Air Soil Pollut. 93:331-345.

Gerritse, R.G. 1996. Dispersion of cadmium in columns of saturated sandy soils. J. Environ. Qual. 25:1344-1349.

Gillham, R.W., E.A. Sudicky, J.A. Cherry, and E.O. Frind. 1984. An advection-diffusion concept for solute transport in heterogeneous unconsolidated geological deposits. Water Resour. Res. 20:369-378.

Gleyzes, C., S. Tellier, and M. Astruc. 2002. Fractionation studies of trace elements in contaminated soils and sediments: a review of sequential extraction procedures. Trends in Analytical Chemistry, 21: 451-467.

Goldberg, S., and L.J. Criscenti. 2008. Modeling adsorption of metals and metalloids by soil components. p. 215-264. *In* A. Violante, P.M. Huang, and G.M. Gadd (ed). Biophysico-chemical processes of heavy metals and metalloids in soil environments. John Wiley&Sons, Inc.

Gomez, A. J. L., I. Giraldez, D. Sanchez-Rodas, and E. Moralesm. 2000. Metal sequential extraction procedure optimized for heavily polluted and iron oxide rich sediments. Anal. Chimica Acta. 414: 151-164.

Gupta, M.K., A.K. Singh, and R.K. Srivastava. 2009. Kinetic Sorption Studies of Heavy Metal Contamination on Indian Expansive Soil. E-J. Chem. 6:1125-1132.

Hamilton, A.J., F. Stagnitti, X. Xiong, S.L. Kreidl, K.K. Benke, and P. Maher. 2007. Wastewater irrigation: The state of play. Vadose Zone J. 6:823-840.

Han, F.X. 2007. Binding and distribution of trace elements among solid-phase components in arid zone soils. p. 131-167. *In* B. J. Alloway, and J. K. Trevors (ed.) Biogeochemistry of trace elements in arid environments, Springer Netherlands.

Harrison, P., and G. Waites. 1998. The Cassell Dictionary of Chemistry, Cassell, London.

Harter, R.D., and R. Naidu. 2001. An assessment of environmental and solution parameter impact on trace-metal sorption by soils. Soil Sci. Soc. Am. J. 65:597-612.

He, Z.L., M. Zhang, X.E. Yang, and P.J. Stoffella. 2006. Release behavior of copper and zinc from sandy soils. Soil Sci. Soc. Am. J. 70:1699-1707.

Ho, M.D., and G.J. Evans. 2000. Sequential extraction of metal contaminated soils with radiochemical assessment of readsorption effects. Environ Sci Technol. 34:1030-1035.

Ho, Y. S., J. F. Porter, and G. Mckay. 2002. Equilibrium isotherm studies for the sorption of Divalent metal ions onto peat: copper, nickel and lead Single component systems. Water, Air, and Soil Poll. 141**:**1-33.

Ho, Y.S. 2004. Citation review of Lagergren kinetic rate equation on adsorption reactions. Scientometrics 59:171-177.

Holm, P.E., B.B.H. Andersen, and T.H. Christensen. 1996. Cadmium solubility in aerobic soils. Soil. Sci. Soc. Am. J. 60:775-780.

Holmgren, G.G.S., M.W. Meyer, R.L. Chaney, and R.B. Daniels. 1993. Cadmium, zinc, copper and nickel in agricultural soils in the United States of America. J. Environ. Qual. 22:335-348.

Hou H, T.Takamatsu , M.K. Koshikawa, and M. Hosomi. 2005. Migration of silver, indium, tin, antimony, and bismuth and variations in their chemical fractions on addition to uncontaminated soils. Soil Sci. 170:624-639.

Hou, H., T. Takamatsu, M.K. Koshikawa, and M. Hosomi. 2006. Concentrations of Ag, In, Sn, Sb and Bi, and their chemical fractionation in typical soils in Japan. European Journal of Soil Science 57: 214-227.

Illera, V., I. Walter, P. Souza, and V. Cala. 2000. Short-term effects of biosolid and municipal solid waste applications on heavy metals distribution in a degraded soil under a semi-arid environment. Sci. Total Environ. 255: 29-44.

Ippolito, J.A., k.A. Barbarick, and R.B. Brobst. 2009. Fate of biosolids Cu and Zn in a semi-arid grassland. Agricult. Ecosys. Environ. 131:325-332.

Kabata-Pendias A, and A.B. Mukherjee. 2007. Trace Elements from Soil to Human. Springer. 556 pp.

Kabata-Pendias A, and H. Pendias .2001. Trace Elements in Soils and Plants, 3rd ed., CRC Press, Boca Raton, FL.

Kabata-Pendias, A., 1995. Agricultural problems related to excessive trace metal contents of soils. p. 3-18. *In*: Salomons,W., Forstner, U., Mader, P. (Eds.), Heavy Metals Problems and Solutions. Springer- Verlag, Berlin, Germany.

Kabata-Pendias, A., and W. Sadurski. 2004. Trace elements and compounds in soil. p. 79-99. *In* E. Merian et al. (ed.) Elements and their compounds in the environment. Wiley-VCH, Weinheim, Germany.

Khaokaew, S., R.L. Chaney, G. Landrot, M. Ginder-Vogel, and D.L. Sparks. 2011. Speciation and release kinetics of cadmium in an alkaline paddy soil under various flooding periods and draining conditions. Environ. Sci. Technol. 45 (10):4249-4255.

Krishnamurti, G.S.R., and R. Naidu. 2003. Solid-solution equilibria of cadmium in soils. *Geoderma* 113: 17-30.

Krishnamurti, G.S.R., P.M. Huang, and K.C.J. van Rees. 1997. Kinetics of cadmium release from soils as influenced by organic acids: Implication in cadmium availability. J. Environ. Qual. 26:271-277.

Lasley, K.K., G.K. Evanylo, K.I. Kostyanovsky, C. Shang, M. Eick, and W.L. Daniels. 2010. Chemistry and transport of metals from entrenched biosolids at a reclaimed mineral sands mining site. J. Environ. Qual. 39:1467-1477.

Lee, S.Z., H.E. Allen, C.P. Huang, D.L. Sparks, P.F. Sanders, and W.J.G.M. Peijnenburg. 1996. Predicting soil-water partition coefficients for cadmium. Environ. Sci. Technol. 30:3418-3424.

Levy, D. B., K. A. Barbarick, E. G. Siemer, and L. E. Sommers. 1992. Distribution and partitioning of trace metals in contaminated soils near Leadville, Colorado. J. Environ. Qual. 21:185-195.

Li, Z., and L.M. Shuman. 1996. Heavy metal movement in metal-contaminated soil profiles. Soil Science 161 (10):656-666.

Liu, C. L., M. K. Wang, T. W. Chang, and C. H. Huang. 2006. Transport of cadmium, nickel and zinc in Taoyuan red soil using one-dimensional convection-dispersion model. Geoderma. 131: 181-189.

Lyman, W. J. 1995. Transport and transformation processes, *In*: G. M. Rand (Ed.) Fundamentals of Aquatic Toxicology, Taylor & Francis, Washington DC.

Lyon, S.B. 2009. Corrosion of tin and its alloys. *In*: Richardson, T., B. Cottis, R Lindsay, S. Lyan, D. Scantlebury, H Stott, and M. Graham. (Eds), Shreir's Corrosion: Corrosion and Degradation of Engineering Materials. Elsevier, Amsterdam.Oxford. Volume 3: 2068-2077.

Maftoun, M., N. Karimian, and F. Moshiri. 2002. Sorption characteristics of copper(II) in selected calcareous soils of Iran in relation to soil properties., Commun. Soil Sci. Plant Anal. 33:13-14, 2279-2289.

Maiz, I., I. Arambarri, R. Garcia, and E. Millan. 2000. Evaluation of heavy metal availability in polluted soils by two sequential extraction procedures using factor analysis. Environ Pollut.110:3-9.

Marin, B., M. Valladon, M. Polve, and A. Monaco. 1997. Reproducibility testing of a sequential extraction scheme for the determination of trace metal speciation in a marine reference sediment by inductively coupled plasma-mass spectrometry. Anal. Chim. Acta 342:91-112.

Markiewicz-Patkowska, J., A. Hursthouse, and H. Przybyla-Kij. 2005. The interaction of heavy metals with urban soils: sorption behaviour of Cd, Cu, Cr, Pb and Zn with a typical mixed brownfield deposit. Environ. Int.31:513- 521.

Mathur, S. P., R.B. Sanderson, A. Belanger, M. Valk, E.N. Knibbe, and C.M. Preston. 1984. The effect of copper applications on the movement of copper and other elements in organic soils. Water Air Soil Pollut. 22:277-288.

McBride, M.B. 1981. Forms and distribution of copper in solid and solution phases of soil. p. 25-45. *In*: J.F. Loneragan et al. (ed.) Copper in Soils and Plants. Academic Press, Sydney, Australia.

McBride, M.B. 1994. Environmental Chemistry of Soils. Oxford University Press, Oxford.

McBride, M.B., and D.R. Bouldin. 1984. Long-term reactions of copper (II) in a contaminated calcareous soil. Soil Sci. Soc. Am. J. 48:56-59.

Melamed, R., C. Xinde, M. Chen, and Q.M. Lena. 2003. Field assessment of lead immobilization in a contaminated soil after phosphate application. The Science of the Total Environment 305:117-127.

Mermut, A.R., J.C. Jain, S. Li, R. Kerrich, L. Kozak, and S. Jana. 1996. Trace element concentrations of selected soils and fertilizers in Saskatchewan, Canada. J. Environ. Qual. 25:845-853.

Moore, H.W. 1991. Inorganic Contaminants of Surface Water. Research and Monitoring priorities. Springer-Verlag, New York, 334 pp.

Moral, R., R. J. Gilkes, and M. M. Jordán. 2005. Distribution of heavy metals in calcareous and non-calcareous soils in Spain. Water, Air, Soil Pollut. 162:127-142.

Naidu, R., R.S. Kookana, M.E. Sumner, R.D. Harter, and K.G. Tiller. 1997. Cadmium sorption and transport in variable charge soils: A review. J. Environ. Qual. 26:602-617.

Nakamaru, Y., and S. Uchida. 2008. Distribution coefficients of tin in Japanese agricultural soils and the factors affecting tin sorption behavior. J Environ Radioact 99:1003-1010.

O'Connor, G.A., H.A. Elliott, and R.K. Bastian. 2008. Degraded water reuse: An overview. J. Environ. Qual. 37:S-157–S-168.

Olivie-Lauquet, G., G. Gruau, A. Dia, C. Riou, A. Jaffrezic, and O. Henin. 2001. Release of trace elements in wetlands: role of seasonal variability. Water Res. 35:943-952.

Oorts, K. 2013. Copper. p. 367-394. *In*: Alloway B. Heavy Metals in Soils-Trace Metals and Metalloids in Soils and their Bioavailability. Springer Dordrecht Heidelberg New York London.

Ostrakhovitch, E.A., and M.G. Cherian. 2007. Tin. In: Nordberg, G.F., B.A. Fowler, M. Nordberg, L.T. Friberg. (Eds.), Handbook on the Toxicology of Metals. Third edition. Academic Press, pp. 839-859.

Pang, L., and M. E. Close. 1999. Non-equilibrium transport of Cd in alluvial gravels. J. Contam. Hydrol. 36:185– 206.

Pietrzak, U. and D.C. McPhail. 2004. Copper accumulation, distribution and fractionation in vineyard soils of Victoria, Australia, Geoderma. 122:151-166.

Press, W.H., S.A. Teukolsky, W.T. Vetterling, and B.P. Flannery. 1992. Numerical recipes in FORTRAN (2^{nd} ed.). Cambridge Univ. Press, New York.

Pueyo, M., J. Sastre, E. Hernandez, M. Vidal, J.F. Lopez-Sanchez, and G. Rauret. 2003. Prediction of trace element mobility in contaminated soils by sequential extraction. J. Environ. Qual. 32:2054-2066.

Ramírez-Pérez, A.M. , M. Paradelo, J.C. Nóvoa-Muñoz, M. Arias-Estévez, M.J. Fernández-Sanjurjo, E. Álvarez-Rodríguez, A. Núñez-Delgado.2013. Heavy metal retention in copper mine soil treated with mussel shells: Batch and column experiments. J. Hazard. Mater. 248- 249:122- 130

Ramos, L., L.M. Hernandez, and M.J. Gonzalez. 1994. Sequential fractionation of copper, lead, cadmium and zinc in soils from or near Donãna National Park. J. Environ. Qual. 23:50-57.

Rao, C. R. M., A. Sahuquillo, and J. F. Lopez-Sanchez. 2008. A review of different methods applied in environmental geochemistry for single and sequential extraction of trace elements in soils and related materials. Water, Air, and Soil Pollution. 189: 291-333.

Raven, K. P. and R. H. Loeppert. 1996. Trace element composition of fertilizers and soil amendments. Journal of Environmental Quality 26.

Rodriguez-Rubio, P., E. Morillo, L. Madrid, T. Undabeytia, and C. Maqueda, C. 2003. Retention of copper by a calcareous soil and its textural fractions: influence of amendment with two agroindustrial residues. Eur. J. Soil Sci. 54: 401-409.

Ross, S. M., ed. 1994. Toxic metals in soil-plant systems. New York: John Wiley & Sons.

Rouff, A.A., R. J. Reeder, and N.S. Fisher. 2002. Pb (II) sorption with calcite: a radiotracer study. Aquatic Geochemistry 8: 203-228.

Sauve´, S., W. Hendershot, and H.E. Allen. 2000. Solid–solution partitioning of metals in contaminated soils: Dependence of pH, total metal burden, and organic matter. Crit. Rev. Environ. Sci. Technol. 34:1125-1131.

Sayyad, G., M. Afyuni, S.F. Mousavi, K.C. Abbaspour, B.K. Richards, and R. Schulin. 2010. Transport of Cd, Cu, Pb and Zn in a calcareous soil under wheat and safflower cultivatio: A column study. Geoderma 154:311-320.

Schaecke, W., H. Tanneberg, and G. Schilling. 2002. Behavior of heavy metals from sewage sludge in a Chernozem of the dry belt in Saxony-Anhalt/Germany. J. Plant Nutr. Soil Sci. 165:609-617.

Schafer, S. G, and U. Fermfert. 1984. Tin – a toxic heavy metal? A review of the literature. Regul Toxicol Pharmacol 4:57-69.

Scott, J. S., and P. G. Smith. 1981. Dictionary of Waste and Water Treatment, Butterworths, London.

Selim, H. M. 2012. Competitive Sorption and Transport of Trace Elements in Soils and Geological Media.CRC/Taylor and Francis, Boca Raton, FL (425 p).

Selim, H. M. and D. L. Sparks. 2001. Heavy Metals Release in Soils. CRC Press, Boca Raton, FL (310 p).

Selim, H. M. and M. C. Amacher. 1988. A second order kinetic approach for modeling solute retention transport in soils. Water Resources Research 24: 2061-2075.

Selim, H.M., and L. Ma. 2001. Modeling nonlinear kinetic behavior of copper adsorption-desorption in soil. p. 189–212. *In* H.M. Selim and D.L. Sparks (ed.) Physical and chemical processes of water and solute transport/retention in soil. SSSA Spec. Publ. 56. SSSA, Madison, WI.

Selim, H.M., and L. Ma. 2001. Modeling nonlinear kinetic behavior of copper adsorption–desorption in soil. In: H.M. Selim and D.L. Sparks, editors, Physical and chemical processes of water and solute transport/retention in soil. SSSA Spec. Publ. 56. SSSA, Madison, WI. p. 189-212.

Selim, H.M., and M.C. Amacher. 1997. Reactivity and transport of heavy metals in soils. CRC Press, Boca Raton, FL.

Selim, H.M., B. Buchter, C. Hinz, and L.W. Ma. 1992. Modeling the transport and retention of cadmium in soils: Multireaction and multicomponent approaches. Soil Sci. Soc. Am. J. 56:1004-1015.

Selim, H.M.1992. Modeling the Transport and Retention of Inorganics in Soils, In: D. L. Sparks, Editor(s), Advances in Agronomy, Academic Press, 1992, Volume 47: 331-384.

Shaheen, S M., C. D. Tsadilas, T. Mitsibonas, and M. Tzouvalekas. 2009. Distribution coefficient of copper in different soils from Egypt and Greece. Commun. Soil Sci. Plant Anal. 40: 214-226.

Shaheen, S.M. 2009. Sorption and lability of cadmium and lead in different soils from Egypt and Greece. Geoderma, Volume 153(Issue 1-2): 61-68.

Sherameti, A. and A. Varma. 2010. Soil Heavy Metals. Springer-Verlag Berlin Heidelberg (492 p).

Sidle, R.C., and L.T. Kardos. 1977. Transport of heavy metals in a sludge-treated forested area. J. Environ. Qual. 6:431-437.

Sparks, D.L. 2003. Environmental soil chemistry. 2nd ed. Academic Press, San Diego, CA.

Sparks, D.L. 2011. Kinetics and Mechanisms of Soil Chemical Reactions, p.13-1 - 13-30. *In* Handbook of Soil Sciences: Properties and Processes, Second Edition. P.M. Huang, Y. Li, M. E. Sumner, eds. CRC Press, Boca Raton, FL.

Steinnes, E. 2013. Lead. P. 395-409. *In*: Alloway B. Heavy Metals in Soils: Trace Metals and Metalloids in Soils and their Bioavailability.3rd. Springer Dordrecht Heidelberg New York London.

Sterckeman, T., F. Douay, N. Proix, and H. Fourrier. 2000. Vertical distribution of Cd, Pb and Zn in soils near smelters in the North of France. Environ Pollut.107:377-389.

Sterckeman, T., F.Douay, D. Baize, H. Fourrier, N. Proix, C. Schvartz. 2004. Factors affecting trace element concentrations in soils developed in recent marine deposits from Northern France. Appl. Geochem. 19: 89-103.

Strawn, D.G., and D.L. Sparks. 1999. Sorption kinetics of trace elements in soils and soil materials.p.1-28. *In*: Selim, H.M., and K.I. Iskandar (ed.) Fate and Transport of Heavy Metals in the Vadose Zone. Lewis Publishers, Boca Raton, FL, USA.

Sukkariyah, B. F., G. Evanylo, L. Zelazny, and R. L. Chaney. 2005. Recovery and distribution of biosolids-derived trace metals in a clay loam soil. J. Environ. Qual. 34: 1843–1850.

Tack, F.M. and M.G. Verloo. 1995. Chemical speciation and fractionation in soil and sediment heavy metal analysis: a review. Intern. J. Environ. Anal. Chem. 59: 225-238.

Takeno, N. 2005. Atlas of Eh–pH diagrams. Intercomparison of thermodynamic databases. Geological Survey of Japan Open File Report No. 419.

Tessier, A., P.G.C. Campbell, and M. Bisson. 1979. Sequential extraction procedure for the speciation of particulate trace metals. Anal. Chem. 51:844-851.

Thornton, I. 1995. Metals in the Global Environment—Facts and Misconceptions, ICME, Ottawa.

Toride, N., F.J. Leij, and M. Th. van Genuchten. 1999.The CXTFIT code for estimating transport parameters from laboratory or field tracer experiments, version 2.1. Research Report No. 137, U.S. Salinity Laboratory, USDA, ARS, Riverside, CA.

Tsang, D.C.W., and I.M.C. Lo. 2006. Competitive Cu and Cd sorption and transport in soils: A combined batch kinetics, column and sequential extraction study. Environ. Sci. Technol. 40:6655–6661.

United States Environmental Protection Agency (USEPA). 1997. Ecological Risk Assessment Guidance for Superfund: Process for Designing and Conducting Ecological Risk Assessments. Interim Final. U.S. Environmental Protection Agency, Environmental Response Team (Edison, NJ). June 5, 1997.

United States Environmental Protection Agency (USEPA). 2005. Ecological Soil Screening Levels for Lead, Interim Final. Office of Solid Waste and Emergency Response. OWSER Directive 9285.7-70. 1200 Pennsylvania Ave. N.W. Washington, D.C. 20460.

Upadhyay, S.K. 2006. Chemical Kinetics and Reaction Dynamics. Springer, New York, USA. (256 p).

Ure, A. M.1991. Trace element speciation in soils, soil extracts and solutions. Microchimica Acta, 2:49-57.

van Genuchten, M.Th ., and P.J. Wierenga. 1976. Mass transfer studies in sorbing porous media: I. Analytical solutions. Soil Sci. Soc. Am. J. 40:473-481.

Venugopal, B. and T. D. Luckey. 1975. Toxicology of nonradio-active heavy metals and their salts. *In*: Luckey, T. D., B. Venugopal, and D. Hutcheson (Eds.), Heavy Metal Toxicity, Safety and Hormology, George Thieme, Stuttgart.

Vile, M.A., R.K. Wieder, and M. Novák. 1999. Mobility of Pb in Sphagnum-derived peat. Biogeochemistry 45: 35-52.

Vogeler, I. 2001. Copper and calcium transport through an unsaturated soil column. J. Environ. Qual. 30:927–933.

Wang, Y.J., Y.X. Cui, D.M. Zhou, S.Q. Wang, A.U. Xiao, R.H. Wang, and H. Zhang. 2009. Adsorption on kinetics of glyphosate and copper (II) alone and together on two types of soils. Soil Sci. Soc. Am. J. 73:1995-2001.

Wei, X.R., M.D. Hao, and M.G. Shao. 2007. Copper fertilizer effects on copper distribution and vertical transport in soils. Geoderma. 138: 213-220.

Weng, L., E.J.M. Temminghoff, S. Lofts, E. Tipping, and W.H. Van Riemsdijk. 2002. Complexation with dissolved organic matter and solubility control of heavy metals in a sandy soil. Environ. Sci. Technol. 36:4804-4810.

Yin, Y.J., H.E. Allen, C.P. Huang, D.L. Sparks, and P.F. Sanders. 1997. Kinetics of mercury(II) adsorption and desorption on soil. Environ Sci. Technol. 31:496-503.

Zemberyova, M., A.H. Zwaik, I. Farkasovska, J. Radioanal. 1998. Sequential extraction for the speciation of some heavy metals in soils. Nucl. Chem. 229: 67-71.

Zhang, H. and H.M. Selim. 2005. Kinetics of arsenate adsorption-desorption in soils. Environ. Sci. Techn. 39:6101-6108

Zhao, K. and H. M. Selim. 2010. Adsorption-Desorption Kinetics of Zn in soils: Influence of phosphate. Soil Sci. 175: 145-153

Zhu, B., and A.K. Alva. 1993. Trace metal and cation transport in a sandy soil with various amendments. Soil Sci. Soc. Am. J. 57:723-727.

CHAPTER 2. CADMIUM TRANSPORT IN ALKALINE AND ACIDIC SOILS: MISCIBLE DISPLACEMENT EXPERIMENTS[1]

2.1 Introduction

Cadmium is of potential concern as an environmental contaminant. It exhibits adverse effects on biological processes in humans, animals, and plants (Kabata-Pendias and Mukherjee, 2007). Cadmium enters the ecosystem through human activities and anthropogenic processes. Mining, phosphate fertilization, application of lime, and the utilization of biosolids amendments increase Cd levels in the soil (Alloway, 1995). It may occur in the soil as cationic and as anionic species (Kabata-Pendias and Sadurski, 2004). In the soil solution, Cd may also occur in complexes with various organic acids (Krishnamurti et al., 1997).

Cadmium behavior in soils is governed by several physical and chemical processes. It may be retained in soils through precipitation and adsorption reactions. Precipitation appears to be the predominant process in the presence of anions such as S^{2-}, CO_3^{2-}, OH^- and PO_4^{3-}, and sorption of Cd at soil mineral surfaces may occur by both specifi c and nonspecifi c processes (Naidu et al., 1997). Adsorption increases with pH and Cd may become irreversibly sorbed. Th us, the potential mobility of Cd is greatest in acidic soils (Dijkstra et al., 2004). Moreover, in oxidizing environments and alkaline soils, Cd is likely to precipitate as minerals such as octavite ($CdCO_3$) as well as CdO and $Cd(OH)_2$ (McBride, 1994; Holm et al., 1996).

During the last three decades, several models of the equilibrium and kinetic types have been proposed to describe the fate of Cd in soils. Evidence of time-dependent sorption in soils has been observed in numerous investigations (e.g., Aringhieri et al., 1985; Selim et al., 1992; Strawn and Sparks, 1999). Sidle and Kardos (1977) were among the earliest researchers to utilize

[1] This reprint originally appeared as, Elbana, T. A. and H. M. Selim. 2010. Cadmium transport in alkaline and acidic aoils: miscible displacement experiments. Soil Sci. Soc. Am. J. 74: 1956–1966. "Reprinted by Permission, ASA, CSSA, SSSA."

the convection-dispersion equation (CDE) for the description of Cu, Zn, and Cd movement in a sludge-treated forest soil. The retention mechanism was considered reversible and of the nonlinear equilibrium (Freundlich) type. In fact, nonlinearity of Cd sorption has been demonstrated by several investigators. Buchter et al. (1989) reported strong nonlinearity of a Cd sorption isotherm for a calcareous soil. Krishnamurti and Naidu (2003) reported nonlinear sorption for Palexeralf and Xerochrept soils having pH values ranging from 8.0 to 8.4. In field experiments on an alkaline soil (>40% $CaCO_3$), Moradi et al. (2005) applied the CDE to predict the mobility of Cd in soil that received repeated sludge applications; Cd concentrations were underestimated when sorption was assumed to be linear and of the equilibrium type. Improvements in predictions were realized when the mobile-immobile (or two-region) approach of van Genuchten and Wierenga (1976) was utilized. Gerritse (1996) found that BTCs of Cd from an acidic sandy soil were simulated successfully using linear sorption isotherms based on batch experiments. Chen et al. (2006) developed a simplified sequential procedure to illustrate the validity of a two-site model. Based on batch Cd adsorption experiments for two soils, they showed that combining a linear equilibrium with a first-order kinetic reaction improved the description of Cd sorption results.

A literature search revealed that Cd transport is commonly described and predicted based on linear retention where equilibrium adsorption is the dominant mechanism. In the present study, Cd mobility in soil columns and retention characteristics (adsorption-desorption) in several soils was examined. To achieve this goal, two approaches were used to describe Cd mobility in soils. One approach used the CXTFIT program, which is based on linear adsorption. The second used the MRTM, which is based on nonlinear equilibrium and kinetic adsorption–desorption for reactive chemicals in soils. The specific objectives of this study were (i) to measure the transport and retention of Cd in columns of acidic and alkaline soils, (ii) to quantify

time-dependent sorption and release and to predict the kinetics of Cd hysteresis in soils, and (iii) to predict the extent of Cd mobility and the distribution of Cd retained with depth in the soil columns.

2.2 Modeling

2.2.1 Nonlinear Model

The MRTM is schematically illustrated in Fig. 2.1. The MRTM accounts for several interactions of heavy metals with soil matrix surfaces (Selim, 1992). Based on soil heterogeneity and observed kinetics of sorption–desorption, the MRTM was proposed to describe the reactivities of heavy metals in the soil environment. Basic to the multisite approach are the concepts that the soil is made up of different constituents (soil minerals, organic matter, Fe and Al oxides) and that a solute species is likely to react with various constituents (sites) by different mechanisms. The uniqueness of this model is that its aim is to describe the reactivity of solutes with natural systems with time during transport in the soil profile. On the other hand, other commonly used models including linear, Freundlich, Langmuir, and Elovich often assume equilibrium sorption (see Selim and Amacher, 1997). Moreover, the use of such models yields a set of parameters that is only applicable for a specific reaction time. The MRTM provides a comprehensive accounting of solute sorption–desorption processes, where a single set of parameters is sought that is applicable for an entire data set and for a wide range of initial (or input) concentrations. In the model shown in Fig. 2.1, S_e represents the amount retained on equilibrium sites (mg kg^{-1}), S_1 and S_2 represent the amount retained on reversible kinetic sites (mg kg^{-1}), and S_{irr} and S_s represent the amounts irreversibly retained (mg kg^{-1}). The retention reactions associated with the MRTM are

$$S_e = K_e \left(\frac{\theta}{\rho}\right) C^N \qquad [2.1]$$

$$\frac{\partial S_1}{\partial t} = k_1 \left(\frac{\theta}{\rho}\right) C^n - k_2 S_1 \qquad [2.2]$$

$$\frac{\partial S_2}{\partial t} = \left[k_3 \left(\frac{\theta}{\rho}\right) C^n - k_4 S_2\right] - k_5 S_2 \qquad [2.3]$$

$$\frac{\partial S_s}{\partial t} = k_5 S_2 \qquad [2.4]$$

$$\frac{\partial S_{irr}}{\partial t} = k_{irr} \left(\frac{\theta}{\rho}\right) C \qquad [2.5]$$

where C is concentration in solution (mg L^{-1}), ρ is the soil bulk density (g cm^{-3}), θ is the water content (m^3 m^{-3}), N and n are dimensionless reaction orders, and t is the reaction time (h). The parameter K_e is a dimensionless equilibrium constant, and $k1$, k_2, k_3, k_4, k_5, and k_{irr} (h^{-1}) are the associated rates of reactions.

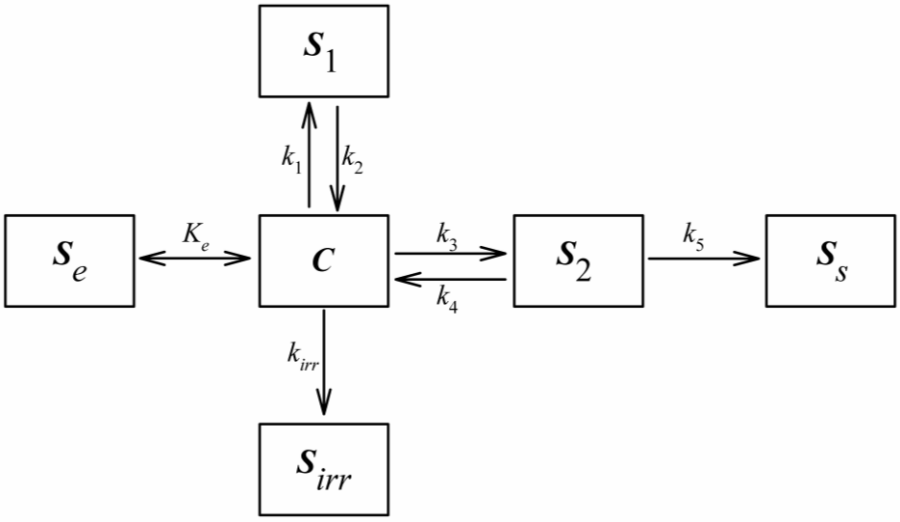

Fig. 2.1. A schematic diagram of the multireaction and transport model, where C is concentration in solution, S_e represents the amount retained on equilibrium sites, S_1 and S_2 represent the amount retained on reversible kinetic sites, S_{irr} and S_s represent the amounts irreversibly retained, and K_e, k_1, k_2, k_3, k_4, k_5, and k_{irr} are the respective reaction rates.

Incorporation of the one-dimensional solute transport CDE with the reactions given in Eq. [2.1]- [2.5] yields

$$\rho \frac{\partial S}{\partial t} + \theta \frac{\partial C}{\partial t} = \theta D \frac{\partial^2 C}{\partial z^2} - q \frac{\partial C}{\partial z} \qquad [2.6]$$

where S is the total amount sorbed,

$$S = S_e + S_1 + S_2 + S_s + S_{irr} \qquad [2.7]$$

and D is the hydrodynamic dispersion coefficient ($cm^2\ h^{-1}$), q is Darcy's water flux density ($cm\ h^{-1}$), and z is distance (cm).

The MRTM was used to describe Cd transport results from miscible displacement column experiment based on the CDE (Eq. [2.6]). To obtain model simulations of Cd transport in the soil columns, the MRTM was used along with a nonlinear least squares optimization scheme, which provided the best fit of the model to the experimental BTCs. The criteria used for estimating the goodness-of-fit of the model to the data were the coefficient of determination (r^2) and the root mean square error (RMSE).

The MRTM was also used in an independent manner to simulate adsorption and desorption data vs. time and different input (initial) concentrations. The data were obtained from the kinetic batch experiments described below. In this mode, the CDE (Eq. [2.6]) was not incorporated into the model, and the multireaction model accounted for the retention mechanisms in Eq. [2.1] – [2.5].

2.2.2 Linear Model

The program CXTFIT (Version 2.1, Toride et al., 1999) is widely used to describe the behavior of reactive chemicals in soils (e.g., Pang and Close, 1999; Tsang and Lo, 2006). This analytical model was used to solve the inverse problem based on the CDE where linear equilibrium sorption was assumed. To account for irreversible reactions of Cd in soils, the CXTFIT version selected included a sink term, which was referred to as first-order degradation or decay in CXTFIT. The CDE used by CXTFIT incorporates a first-order decay coefficient (μ) as follows:

$$R\frac{\partial C}{\partial t} = D\frac{\partial^2 C}{\partial z^2} - v\frac{\partial C}{\partial z} - \mu C \qquad [2.8]$$

where v (= q/θ) is the average pore water velocity (cm h^{-1}), R is a dimensionless retardation factor ($R = 1 + \rho K_d/\theta$), and K_d is a partitioning coefficient (L kg^{-1}). In Eq. [2.8], the term R accounts for linear equilibrium sorption. The term associated with μ is a sink term that captures irreversible retention (or removal) of a chemical directly from the soil solution based on first-order decay. Because heavy metals such as Cd do not undergo decay or degradation, we considered this term to denote irreversible retention in a similar manner or equivalent to that associated with k_{irr} (Eq. [2.5]) of the MRTM (see also Fig. 2.1). To obtain model simulations of Cd transport in soil columns, CXTFIT was used to obtain parameter estimates (R and μ) that provided the best fi t of the model to the experimental BTCs (see Toride et al., 1999).

2.3 Materials and Methods

Surface (0–40-cm) and subsurface (40–75-cm) alkaline soil samples were collected from the Bustan-3 area in the northwestern desert of Egypt. This sandy soil is classified as a Typic Torripsamment (Bakr et al., 2009). Two soil layers were sampled to quantify the impact of the presence of $CaCO_3$ on Cd mobility in this soil. The second soil was a Windsor loamy sand (a Typic Udipsamment) collected near Hanover, NH. The soil samples were analyzed for pH and organic matter using the acid dichromate oxidation method (Pansu and Gautheyrou, 2006).The total carbonate equivalent in the Bustan soil samples was determined using Collin's calcimeter (Loeppert and Suarez, 1996). Soil properties such as the pH and cation exchange capacity are given in Table 2.1.

Table 2.1. Selected physical and chemical properties of the studied soils.

	Bustan-surface	Bustan-subsurface	Windsor
pH	9.22	9.44	6.05
OM (g kg^{-1})	0.66	0.13	16.6
CEC (cmol kg^{-1})	5.60	4.84	3.28
$CaCO_3$ (%)	2.76	1.18	Nd†

† Not detected

2.3.1 Adsorption-desorption

Batch equilibration technique was used to investigate Cd adsorption using seven initial Cd concentrations (C_o) (0.004, 0.009, 0.044, 0.089, 0.178, 0.445, 0.890 mmol L^{-1}). All solutions were prepared in 0.005 mol L^{-1} KNO_3 background solution. For adsorption, 30 mL of the various $Cd(NO_3)_2$ concentrations was added to 3 g of soil in 40- mL Teflon centrifuge tubes in triplicate. The tubes were sealed and the mixtures were continuously shaken for 24 h and then centrifuged for 10 min. A 5-mL aliquot was sampled and the Cd concentration in the supernatant solution was analyzed using inductively coupled plasma-atomic emission spectrometry (Spectro Ciros charge-coupled device [CCD], Spectro Analytical Instruments, Kleve, Germany). The amounts of Cd sorbed by the soil matrix were determined by the difference between the concentrations of the supernatant and that of the initial solutions.

Immediately following 24-h adsorption, desorption commenced for the highest initial concentrations (0.178, 0.445, and 0.890 mmol L^{-1}) using successive dilutions for 12 consecutive steps (1, 2, 3, 4, 5, 6, 7, 8, 9, 10, 17, and 27 d of reaction time). In the first 10 steps, aliquots of 5 mL of the supernatant were withdrawn for Cd analysis and the remaining mixture was replaced with the 0.005 mol L^{-1} KNO_3 background solution. At the last two reaction times, 5-mL aliquots were collected and no replacement of the solution was performed. The redox potential and pH were monitored in the decanted solution at the end of each reaction time.

Following the last desorption step, four extraction steps were quantified, referred to here as exchangeable, oxidizable, carbonates and oxides, and strongly bound. The extraction method used was a modification of that of Emmerich et al. (1982). For the exchangeable phase, 37.5 mL of 0.5 mol L^{-1} KNO_3 was added to the soil and shaken for 16 h. For the oxidizable phase, 37.5 mL of 0.5 mol L^{-1} NaOH was added and shaken for 16 h. For the fraction associated with carbonates and oxides, 37.5 mL of 0.05 mol L^{-1} Na_2EDTA as a nonspecific reagent was used

(Gismera et al., 2004). Strongly bound Cd was based on extraction with 4 mol L^{-1} HNO_3 for 16 h at 70 to 80°C.

2.3.2 Miscible Displacement Experiments

The transport of Cd was investigated using the miscible displacement method described by Zhang and Selim (2006). Acrylic columns (5-cm length and 6.4-cm i.d.) were uniformly packed with air-dry soil and slowly saturated with 0.005 mol L^{-1} KNO_3 by upward flow. Input solutions were applied using a variable-speed piston pump. A pulse of approximately 10 pore volumes having a concentration of 0.890 mmol L^{-1} $Cd(NO_3)_2$ solution in 0.005 mol L^{-1} KNO_3 background solution was applied to each soil column (Table 2.2). Cadmium pulse inputs were subsequently eluted by at least 20 pore volumes of 0.005 mol L^{-1} KNO_3 solution. During leaching, the flow into the column was stopped for 2 d to evaluate the influence of flow interruption on Cd retention and transport. Physical parameters such as the moisture content (θ) and bulk density (ρ) for each column are given in Table 2.2. An additional transport column experiment was performed to quantify Cd transport using acid-washed sand material (14808-60-7, Fisher Scientific, Fairlawn, NJ). This reference sand with no clay or organic matter present (pH = 6.27, 81% sand, 19% silt) was previously used as a reference matrix for characterizing Hg retention and transport in soils (Liao et al., 2009).

To obtain independent estimates for the dispersion coefficient (*D*) in Eq. [2.6] and [2.8], separate pulses of a tracer solution were applied to each soil column aft er Cd pulse applications. The tracer used was tritium (^3H_2O) and the collected samples were analyzed using a Tri- Carb liquid scintillation β counter (Packard 2100TR, PerkinElmer, Waltham, MA). The tracer pulse was applied to assess flow characteristics by obtaining independent values for the hydrodynamic dispersion coefficient (*D*) of the classical CDE (Eq. [2.8] without the decay term). Estimates for *D* values were obtained using CXTFIT (Toride et al., 1999) and are given in Table 2.2.

Upon completion of the miscible displacement experiments, each soil column was sectioned into 1-cm increments and Cd retained by the soil was determined using the sequential extractions previously used in the batch experiments described above. Thus, the amount of Cd retained or sorbed due to pulse application vs. soil depth was quantified for all soils and the reference sand columns.

Table 2.2. Soil physical and experimental conditions of the miscible displacement columns experiments.

Matrix	Bulk density (ρ, Mg m^{-3})	Moisture content (θ, %)	Pore water velocity (cm h^{-1})	Pulse volume (P.V.)		Dispersion coefficient† (D, cm^2 h^{-1})
				^3H_2O	Cd	
Reference sand	1.622	38.8	0.940	1.48	9.23	0.515
Bustan-surface	1.839	30.6	1.321	1.32	10.12	0.881
Bustan-subsurface	1.771	33.2	1.010	1.31	10.46	2.441
Windsor soil	1.454	45.1	0.794	1.37	7.86	1.541

† Estimated by CXTFIT 2.0

2.4 Results and Discussion

2.4.1 Retention and Release

Adsorption isotherms describing the distribution of Cd sorbed and in aqueous solution are shown in Fig. 2.2. These results reflect the differences in Cd affinity among the different soils after 24 h of sorption. The Freundlich equation was used to describe such adsorption isotherms:

$$S = K_F C^b \qquad [2.9]$$

where S represents the amount sorbed (mg kg−1), KF is the Freundlich distribution coefficient (L kg^{-1}), and b is a dimensionless reaction order. The nonlinear least square optimization of SAS PROC NLIN (SAS Institute, 2000) was used to obtain best-fit parameters for the adsorption data. These isotherms show Cd sorption by all the soils to be highly nonlinear. Sorption nonlinearity also implies that the mobility of Cd in the soil tends to increase as the concentration increases. This nonlinearity is also illustrated by the small values (<1) of the Freundlich b (see Table 2.3).

The Bustan surface soil exhibited the highest affinity for Cd among the three soils. This is mainly due to its high $CaCO_3$ content. Fixation of Cd^{2+} into calcite is presumably facilitated by the similarity between the ionic radius of Ca^{2+} and Cd^{2+}. Consistent with this assumption is research by Reeder (1996) based on extended x-ray absorption fine structure that showed that Cd was bound within calcite octahedral sites. The retention of Cd on the acidic Windsor soil was dominated by clay and organic matter reactions, as documented by Lee et al. (1996) and Holm et al. (2003).

The Cd adsorption-desorption results for the three soils, shown in Fig. 2.2, indicate considerable hysteresis. This hysteretic behavior, resulting from discrepancies between the adsorption and desorption isotherms, was not surprising in view of the kinetic retention behavior of Cd in these soils and is indicative of nonequilibrium behavior of the retention mechanisms (Zhang and Selim, 2005). The family of desorption curves shown indicates a high affinity for Cd by the soil matrix. The average amounts of Cd released, as percentages of that sorbed, were 3.4, 30.7, and 35.5% for the Bustan surface, Bustan subsurface, and Windsor soils, respectively. The dashed and solid curves in Fig. 2.2 are MRTM simulations based on the kinetic fits listed in Table 2.4.

Table 2.3. Estimated Freundlich distribution coefficient (K_F) and reaction order (b) for Cd retention by the different soils (standard errors in parentheses) and coefficients of determination (r^2).

Soil	K_f (L Kg^{-1})	b	r^2
Bustan-surface	203.11 (16.854)	0.276 (0.025)	0.985
Bustan-subsurface	116.70 (9.807)	0.346 (0.024)	0.992
Windsor	99.05 (11.949)	0.459 (0.036)	0.988

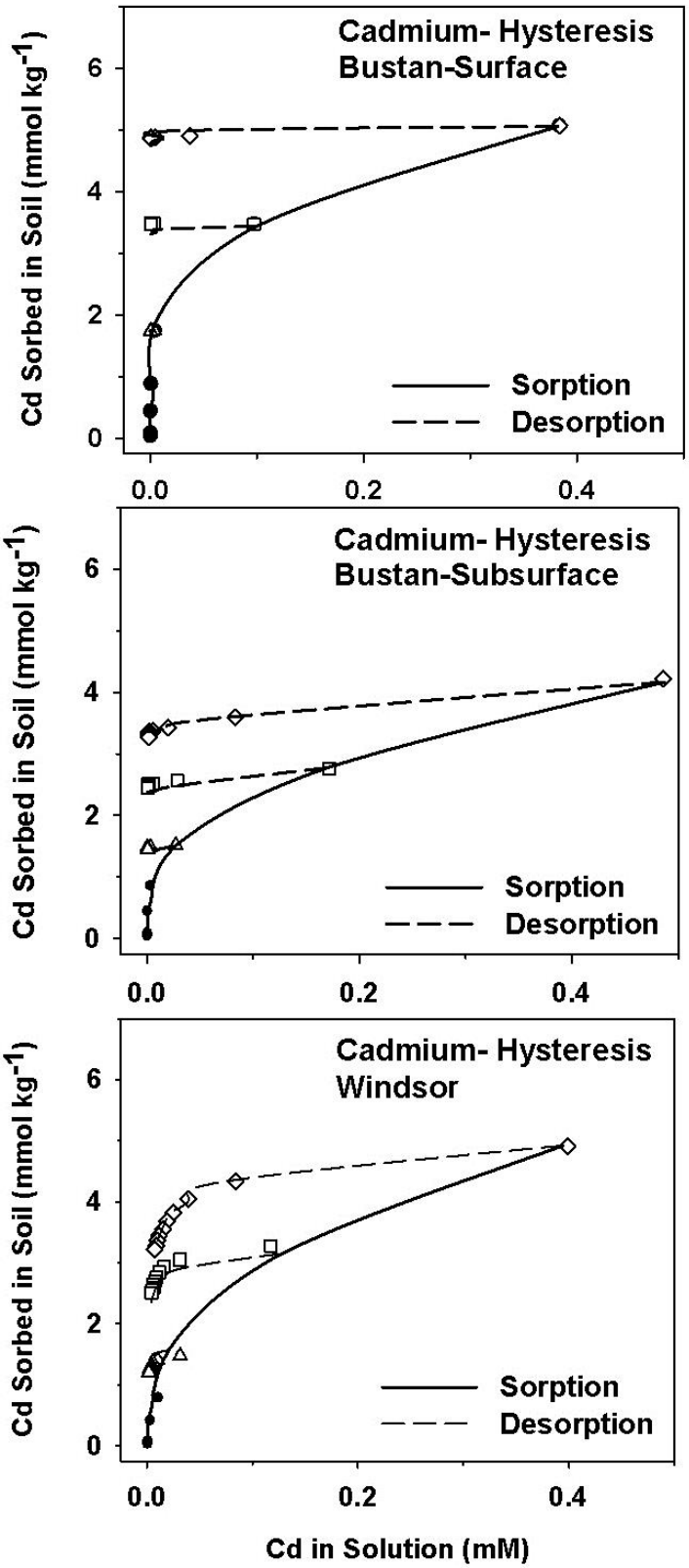

Fig. 2.2. Adsorption and desorption of Cd for the Bustan surface and subsurface and Windsor soils. The solid and dashed curves are the multireaction and transport model simulations for sorption and desorption, respectively.

Table 2.4. Goodness of several model versions for Cd retention by the Bustan surface and subsurface and the Windsor soils. Estimates of reaction rates for (standard errors in parentheses), root mean square error (RMSE), and coefficient of determination (r^2) values.

Model version†	RMSE	r^2	k_1	k_2	k_3	k_4	k_5	k_{irr}
			---------- (h^{-1}) ----------					
					Bustan soil, surface			
M1	0.7060	0.9925	0.6881 (0.0277)	0.0149 (0.0011)	---	---	---	0.0077 (0.0012)
M2	0.5904	0.9949	---	---	0.9934 (0.0076)	0.0285 (0.0004)	0.0060 (0.0001)	---
M3	0.3682	0.9981	---	---	0.8506 (0.0081)	0.0339 (0.0005)	0.0075 (0.0001)	0.0075 (0.0001)
M4	0.8906	0.9886	0.0115 (0.0008)	0.1017 (0.0079)	0.4563 (0.0156)	0.0003 (0.000023)	---	0.0137 (0.0008)
M5	0.8106	0.9916	1.0579 (0.0203)	0.0525 (0.0018)	0.1498 (0.0032)	0.0003 (0.000016)	0.0002 (0.000047)	---
					Bustan soil, subsurface			
M1	1.2235	0.9913	0.4285(0.0317)	0.0517 (0.0067)	---	---	---	0.0122 (0.0012)
M2	0.6374	0.9963	---	---	0.9945 (0.0232)	0.0951 (0.0029)	0.0145 (0.0004)	---
M3	0.6044	0.9967	---	---	1.0979 (0.0227)	0.1224 (0.0030)	0.0148 (0.0003)	0.0026 (0.0001)
M4	0.5994	0.9968	0.1509 (0.0015)	0.0028 (0.0001)	1.9582 (0.5813)	0.2843 (0.0813)	---	0.0014 (0.0005)
M5	0.6189	0.9966	0.0495 (0.0024)	0.0210 (0.0008)	1.5888 (0.0271)	0.1957 (0.0026)	0.0164 (0.0004)	---
					Windsor soil			
M1	0.8940	0.9913	0.3382 (0.0133)	0.0316 (0.0022)	---	---	---	0.0115 (0.0012)
M2	0.5413	0.9960	---	---	0.4946 (0.0091)	0.0343 (0.0016)	0.0056 (0.0005)	---
M5	0.4257	0.9975	0.1661 (0.0221)	0.0130 (0.0035)	0.4949 (0.0679)	0.0914 (0.0242)	0.0077 (0.0028)	---

† Different model version account for different Cd sorbed phases: M1 = amount retained on reversible kinetic, S_1, and irreversible, S_{irr} sites; M2 = amounts retained on reversible kinetic, S_2, and S_s; M3 = S_2, S_s, and S_{irr}; M4 = S_1, S_2 and S_{irr}; and M5 = S_1, S_2 and S_s.

2.4.2 Retention Kinetics and Sequential Extractions

In Fig. 2.3, concentration of Cd sorbed versus time is presented to illustrate Cd desorption or release with time. The Bustan-surface soil exhibited very little time-dependent Cd release. In contrast, for The Windsor and Bustan-subsurface soils, Cd desorption exhibited time-dependent behavior as shown by the continued decrease of the sorbed Cd with time. Overall, Cd release from the soil matrix was rapid during the initial stages of desorption followed by slow release (see Fig. 2.3). The MRTM model accounts for several possible interactions of Cd within the soil system. As a result, different versions of the model shown in Fig. 2.1 represent different reactions from which Cd retention mechanisms can be deduced. Several versions were examined including a three parameters model with k_1, k_2, and k_{irr} (M1), another three parameters model with k_3, k_4 and k_5 (M2), a four parameters model with k_3, k_4, k_5 and k_{irr} (M3), a five parameters model with k_1, k_2, k_3, k_4, and k_{irr} (M4), and another five parameters model with k_1, k_2, k_3, k_4, and k_5 (M5). These versions assume the presence of at least a fraction of retention sites that interacts reversibly (kinetic) and others that were kinetic but irreversible or slowly reversible. The Criteria used for estimating the goodness-of-fit of the model to the data were the r^2 and *RMSE*.

For the two Bustan soils, the surface soil layer exhibited limited Cd release with time. A four parameter model variation (k_3, k_4, k_5 and k_{irr}) consisting of one reversible and two irreversible mechanisms provided best description of the kinetic data shown in Fig. 2.3. Specifically, based on RMSE and r^2 values shown in Table 2.4, version M3 provided significantly improved simulation over M1 or M2. Five parameter model versions did not improve model predictions, which suggest over-fitting of the model (Ma and Selim, 1997). Based on the four parameters model (M3), k_3 was an order of magnitude larger than k_4 (see Table 2.4).

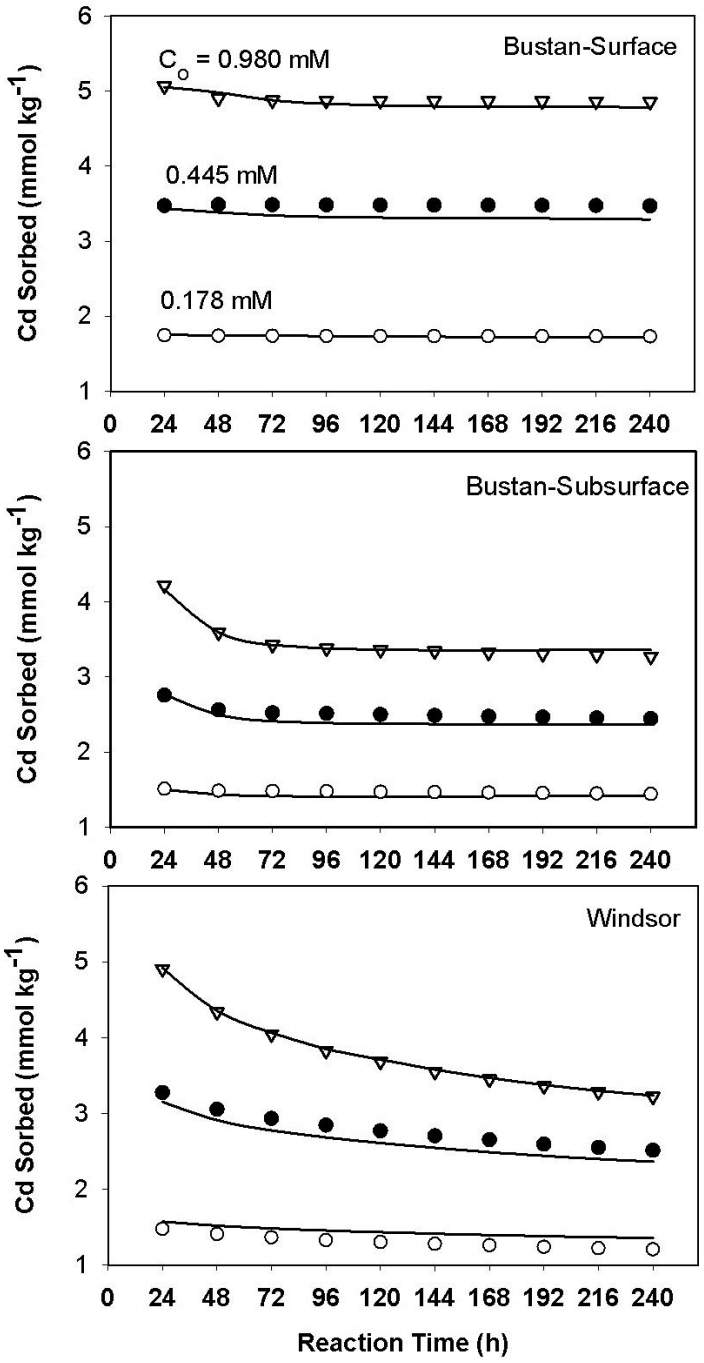

Fig. 2.3. Cadmium sorbed vs. time during release for the Bustan surface and subsurface and Windsor soils. Symbols are for different initial concentrations (C_o); solid curves are multireaction and transport model simulations.

The irreversible rates of reaction for the Bustan surface soil were higher than those for the Bustan subsurface soil. The model suggests the presence of slow reversible and irreversible mechanisms as possible Cd reactions for the two Bustan soils. This is consistent with the

exchange of Cd^{2+} for Ca^{2+} on surface sites with slow diffusion of metal ions into hydrated CaCO3, followed by superficial $(Cd,Ca)CO_3$ coprecipitation. Based on kinetic batch experiments, Pang and Close (1999) suggested that Cd precipitation was much slower than Cd sorption.

For the acidic Windsor soil, at least one reversible phase (S_1) coupled with an irreversible phase (S_s) provided a good description of the Cd kinetics (Table 2.4). Incorporation of the irreversible reaction S_{irr} did not improve the model predictions. Based on the RMSE and r^2, the five-parameter model (M5) consisting of two reversible sites (S_1 and S_2) and one irreversible phase (S_s) provided the best description of the Cd kinetics in this acidic soil.

The sequential extraction results in Table 2.5 showed that exchangeable Cd constituted 15 to 19% of the total Cd sorbed for the Windsor soil while no exchangeable forms were detected for the Bustan soils. This is a direct result of the presence of organic matter and clays in the Windsor soil. The oxidizable fraction was extremely small in all soils (<0.2%). In contrast, Cd associated with the carbonate and oxides fraction was the highest for the Bustan surface (51–69%) and Bustan subsurface (30–60%) soils. This is indicative of the high affinity of Cd for carbonates. For the Windsor soil, 19 to 31% of the Cd was associated with the oxides fraction. One assumes that the contribution of carbonates in Cd adsorption is negligible because we can presume that carbonates are absent in this acidic soil. Based on the results in Table 2.5, the fraction that represents the amount of Cd released from successive desorption steps was dependent on input Cd concentrations. In other words, the Cd fraction that was most susceptible to transport in the soil increased as the input concentration increased (from 0.178 to 0.890 mmol L^{-1}). This concentration-dependent release was consistent with the strong nonlinearity of Cd retention and it implies that the mobility of Cd tends to increase as the input Cd concentration increases.

Table 2.5. Total extracted Cd and fractions from soil batch kinetic experiments for different initial Cd concentrations.

Initial Cd	Total sorbed after 24h	Total desorbed after 28 days		Exchangeable fraction		Oxidizable fraction		Associated with carbonates/oxides		Strongly bound fraction	
Mmol L^{-1}	------ mmol kg^{-1} ------		%	mmol kg^{-1}	%	mmol kg^{-1}	%	mmol kg^{-1}	%	mmol kg^{-1}	%
					Bustan soil, surface						
0.178	1.746	0.013	0.74	ND†	ND	0.0014	0.08	1.2119	69.41	0.0488	2.80
0.445	3.472	0.033	0.96	ND	ND	0.0033	0.10	1.8512	53.31	0.0322	0.93
0.890	5.065	0.171	3.37	ND	ND	0.0066	0.13	2.5992	51.31	0.0784	1.55
					Bustan soil, subsurface						
0.178	1.513	0.0692	4.58	ND	ND	0.0002	0.01	0.9102	60.16	0.0605	4.00
0.445	2.757	0.2866	10.40	ND	ND	0.0034	0.12	1.1461	41.58	0.0368	1.34
0.890	4.220	1.2944	30.67	ND	ND	0.0064	0.15	1.2458	29.52	0.0516	1.22
					Windsor soil						
0.178	1.476	0.2912	19.73	0.282	19.11	0.0004	0.03	0.457	30.97	0.0953	6.46
0.445	3.275	0.8326	25.42	0.5591	17.07	0.0000	0.00	0.7435	22.70	0.1283	3.92
0.890	4.907	1.7437	35.54	0.7773	15.84	0.0000	0.00	0.9541	19.44	0.1300	2.65

†ND: not detected.

2.4.3 Transport

The BTCs of the applied tritium pulses in the soil columns are shown in Fig. 2.4, where the tritium concentration in the effluent is plotted against column pore volume (V/Vo), where V_o is the volume of the pore space in each soil column (cm^3). The tritium BTCs appear symmetric and were well described by the CDE. For the Bustan subsurface and Windsor soil columns, some degree of tailing was observed. Such tailing is evidence of limited physical nonequilibrium, which was probably due to intraparticle diffusion and the presence of immobile water regions (Brusseau et al., 1992). The estimated D values for the Bustan subsurface and Windsor soils were significantly larger than the D values for the Bustan surface soil and reference sand (see Table 2.2). The values of D were subsequently used in the MRTM to predict Cd transport in the different soil columns.

Cadmium mobility is illustrated by the BTCs shown in Fig. 2.5 to 2.8 and indicates significant retardation relative to tritium. For example, Cd was detected after eight effluent pore volumes for the Bustan surface soil. The maximum Cd concentration in the effluent was less than $C/C_o = 0.005$ (Co represents the Cd pulse concentration; $C_o = 890$ μmol L^{-1}). After some 50 pore volumes, the total amount of Cd in the effluent was <1% of that applied in the pulse and may thus be considered nearly immobile in the Bustan surface soil. In an effort to describe such highly immobile Cd behavior, several attempts were made to achieve convergence using the MRTM and CXTFIT. The simulation shown in Fig. 2.5 using the MRTM was obtained with $K_e = 8.056 \pm 0.166$ and $k_{irr} = 2.075 \pm 0.0185$ h^{-1} ($r^2 = 0.9329$; RMSE = 0.0006) when the MRTM was applied. On the other hand, based on CXTFIT, the best simulated BTC was obtained when $R = 20.9 \pm 0.880$ and $\mu = 2.61 \pm 0.0338$ h^{-1} were used ($r^2 = 0.6694$; RMSE = 0.0095). Simulations based on both models may be considered adequate in predicting the peak Cd concentration of the effluent solution. The Ca concentration in the effluent is also shown in Fig. 2.5 because Ca is the

dominant cation in this calcareous soil. The Ca concentration exhibited a sharp increase following the Cd pulse application. Moreover, the Cd pulse application probably resulted in nucleation of $CdCO_3$ on $CaCO_3$ as the solutions approached saturation (McBride, 1980).

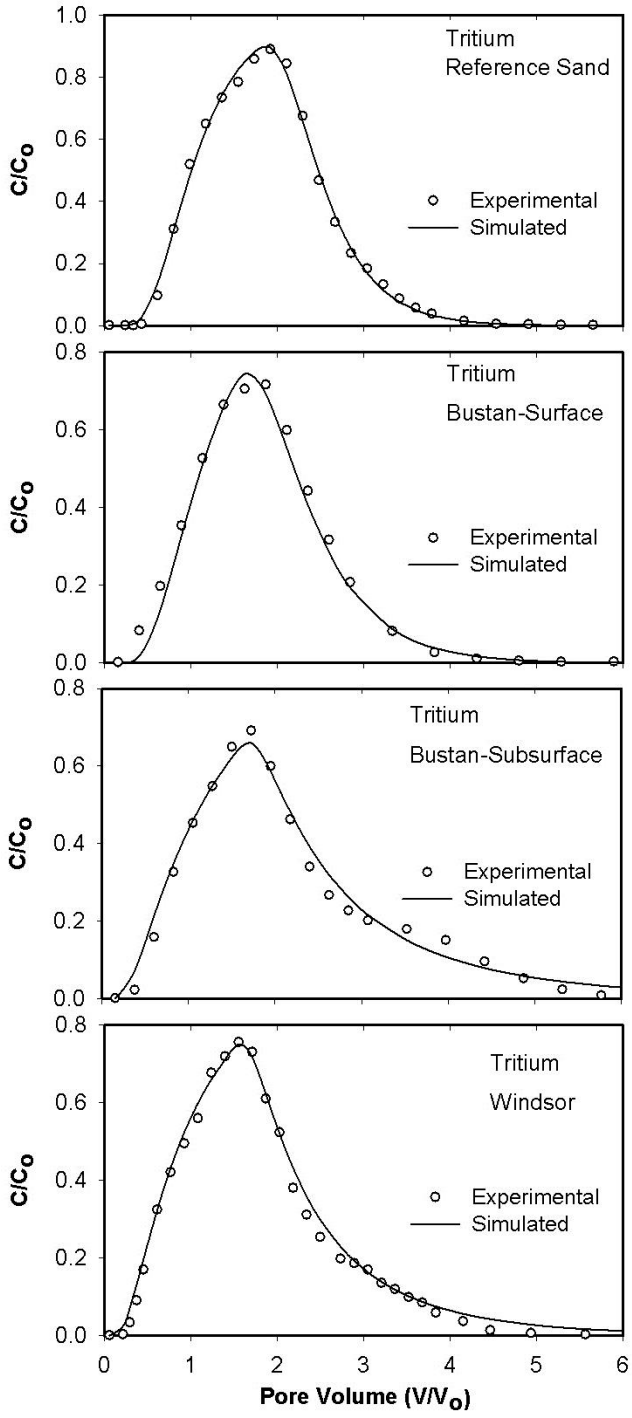

Fig. 2.4. Tritium breakthrough curves from the reference sand, Bustan surface and subsurface soil, and Windsor soil columns. Solid curves are simulations using the CXTFIT model.

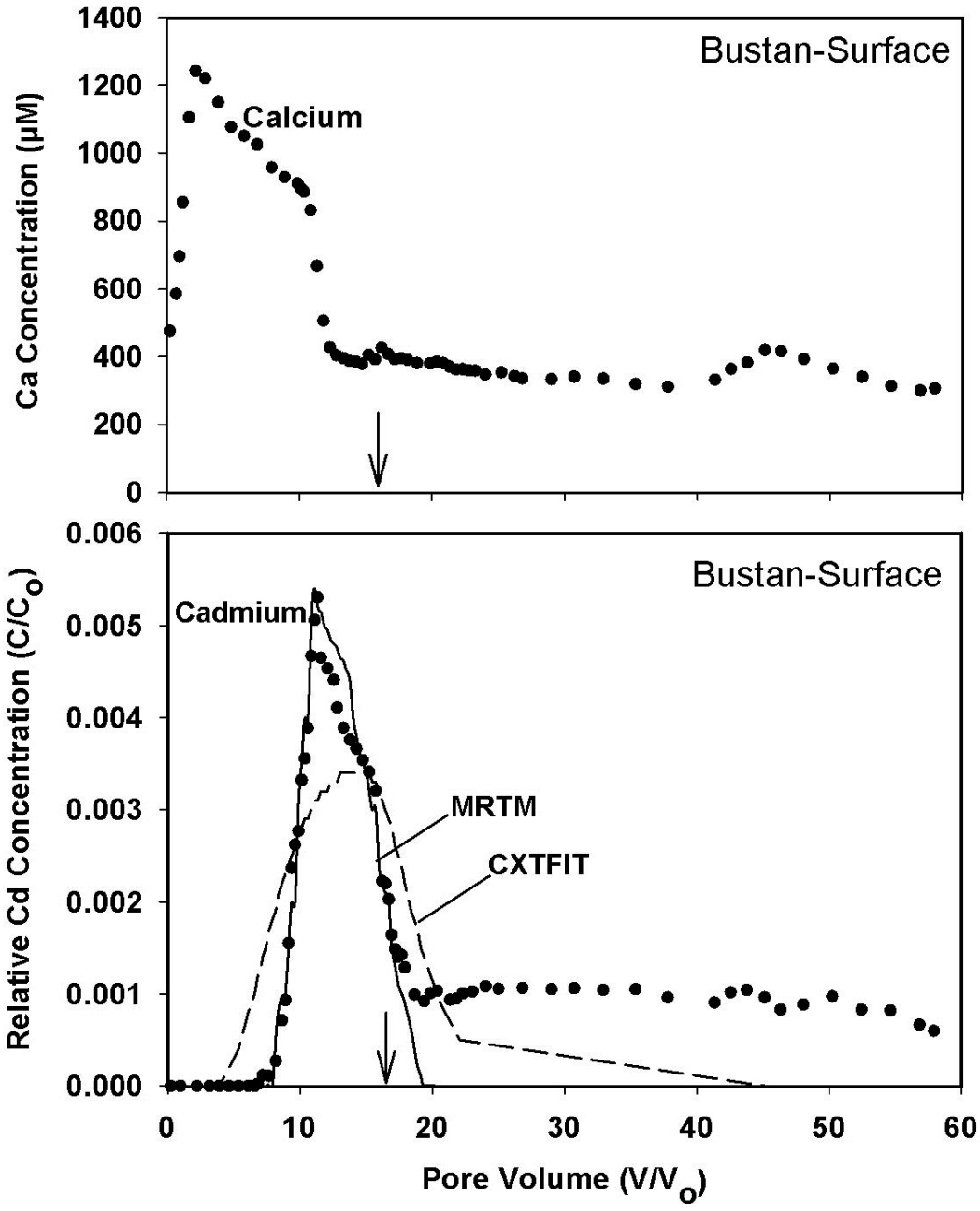

Fig. 2.5. Breakthrough results of Ca and Cd from the Bustan surface soil column. The multireaction and transport model (MRTM) and CXTFIT model simulations are denoted by the solid and dashed curves, respectively; arrows indicate when flow interruption occurred.

The Cd BTC from the Bustan subsurface soil column is shown in Fig. 2.6 and illustrates the early arrival of Cd in the effluent (three pore volumes) and a concentration maximum of C/C_o = 0.3. Moreover, based on the area under the curve, the total mass of Cd in the effluent was 30.7% of that applied. A decrease in Cd concentration in response to flow interruption was

observed. This is indicative of continued Cd sorption due to physical or chemical nonequilibrium in this soil. Several attempts were made to describe the observed BTC using different versions of the MRTM (Table 2.6). A fully kinetic MRTM version (M1) with only two phases (S_1 and S_{irr}) best described the observed BTC. Specifically, a model version that accounted for slow kinetics and irreversible reactions provided a good description of the effluent side as well as Cd concentrations during leaching in this alkaline soil (Fig. 2.6). When the linear CXTFIT was used, good overall predictions were also obtained, including the magnitude of time of peak arrival. The concentrations during leaching were underestimated, however. Parameter values that provided the best predictions using CTXFIT were $R = 14.54 \pm 0.385$ and $\mu = 0.405 \pm 0.011$ h^{-1} (r^2 = 0.9284; RMSE = 0.0239). Figure 2.6 also shows the associated BTC for Ca, which indicates a sharp rise during the Cd pulse followed by a gradual decrease during leaching.

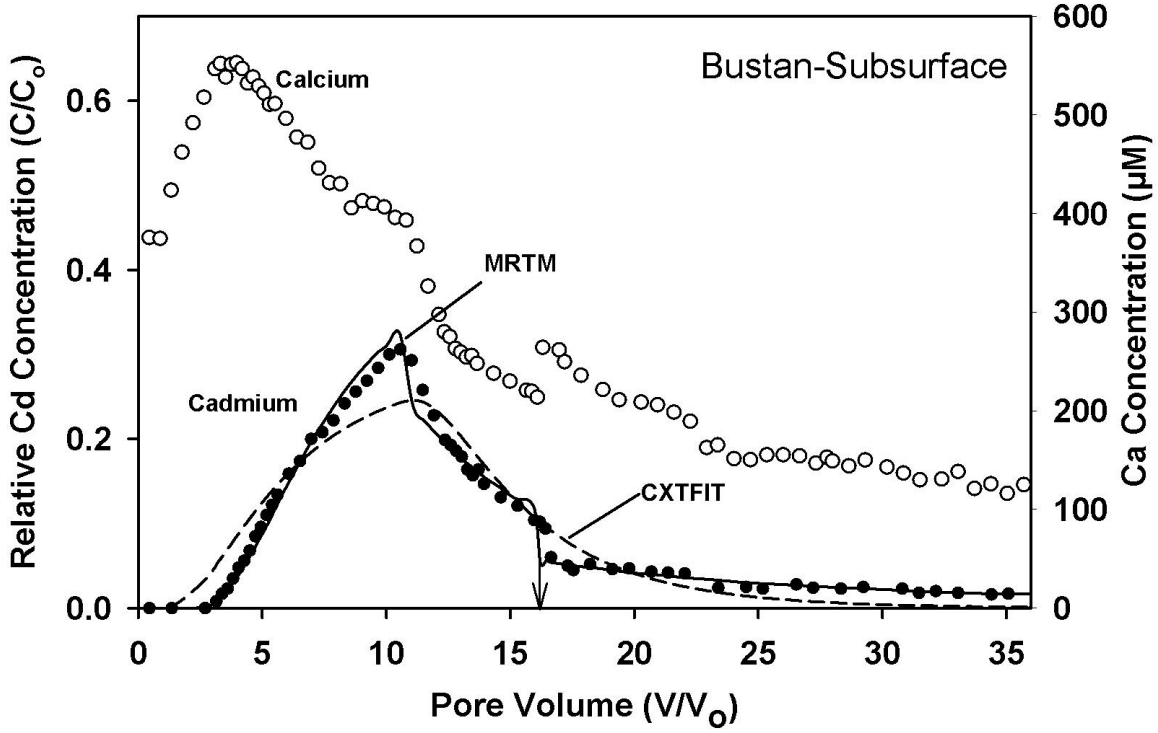

Fig. 2.6. Breakthrough results of Ca and Cd from the Bustan subsurface soil column. The multireaction and transport model (MRTM) and CXTFIT model simulations are denoted by the solid and dashed curves, respectively; the arrow indicates when flow interruption occurred.

Table 2.6. Multireaction transport model parameter estimates for Cd transport in different soil columns: model parameters estimates (standard error in parentheses), root mean square error (RMSE), and coefficient of determination (r^2) values.

Model Version†	RMSE	r^2	k_1	k_2	k_3	k_4	k_5	k_{irr}
			----------h^{-1}----------					
			Bustan-subsurface					
M1	0.0118	0.9839	20.1083 (1.0547)	0.1346 (0.0095)	----	----	----	0.2617 (0.0090)
M2	0.0195	0.9579	----	----	15.4690 (0.1892)	0.0635 (0.0010)	0.0051 (0.0003)	----
M4	0.0140	0.9807	0.1238 (0.0008)	0.0218 (0.0001)	27.5003 (0.1728)	0.2061 (0.0011)	----	0.2954 (0.0021)
M5	0.0204	0.9603	0.0403 (0.0012)	0.0065 (0.0001)	16.7148 (0.1328)	0.0721 (0.0005)	0.0059 (0.0001)	----
			Windsor Soil					
M1	0.0231	0.9195	8.1247 (0.1721)	0.1673 (0.0039)	----	----	----	0.3118 (0.0042)
M2	0.0182	0.9495	----	----	5.5504 (0.0938)	0.0402 (0.0009)	0.0111 (0.0003)	----
M5	0.0146	0.9688	2.1654 (0.2635)	0.0058 (0.0019)	7.0818 (0.1060)	0.1842 (0.0149)	0.0062 (0.0081)	----

† Different model version account for different Cd sorbed phases: M1 = amount retained on reversible kinetic, S_1, and irreversible, S_{irr} sites; M2 = amounts retained on reversible kinetic, S_2, and S_s; M3 = S_2, S_s, and S_{irr}; M4 = S_1, S_2 and S_{irr}; and M5 = S_1, S_2 and S_s.

The mobility of Cd in the Windsor soil is shown in Fig. 2.7, where a gradual increase of the adsorption (left) side of the BTC can be observed, with a peak concentration of C/C_o = 0.25. This was followed by slow Cd release during leaching. The amount of Cd recovered in the effluent solution after 30 pore volumes was 21% of that applied. In this acidic Windsor soil, Ca concentrations in the effluent give the appearance of competitive sorption between Ca and Cd. The applied Cd increased the Ca concentration in the effluent, with the highest Ca concentration (470 μmol L−1) at three pore volumes. Decreased Ca and Cd concentrations due to flow interruption were observed, followed by extensive tailing of the BTC depicting slow release during leaching. Modeling efforts for the Windsor soil are shown by the curves in Fig. 2.7 and clearly illustrate the capability of the MRTM to provide good predictions of Cd BTCs. For this soil, the best MRTM prediction was realized using Version M5, which accounts for two kinetic ($S_1$and S_2) and an irreversible reaction (S_s). The estimated model parameters are given in Table 2.6. Simulation of the Cd BTC using CXTFIT is also shown in Fig. 2.7. The simulation predicted an earlier arrival of Cd than that measured, with somewhat lower peak concentrations. Nevertheless, the CXTFIT simulations well predicted the peak arrival time. The estimated parameters associated with CXTFIT were R = 6.788 ± 0.304 and μ = 0.418 ± 0.011 h^{-1} (r^2 = 0.7973; RMSE = 0.0364).

For the reference sand, the BTC indicates that Cd exhibited early arrival, along with concentration maxima nearly equal to that of the applied Cd in the pulse (Fig. 2.8). The Cd BTC resembled that for tritium as a tracer solute. This is an indication that equilibrium was dominant for Cd transport in this sand column. In fact, complete recovery of the applied Cd was obtained (97.6%), which indicates that little if any Cd was retained by the reference sand. Good prediction of the measured BTC was obtained using CXTFIT with R = 1.952 ± 0.035 and RMSE = 0.0634. Equally good predictions were realized when the MRTM was used where nonlinear reversible

kinetics with the S_1 phase was assumed. Best-fit parameters obtained were n = 0.905, k_1 = 0.437 h^{-1}, and k_2 = 0.3420 h^{-1} along with a lower value for the RMSE of 0.0443 compared with CXTFIT. The magnitude of these rate coefficients suggests the presence of a rapid reversible mechanism for Cd retention that is consistent with the observed BTC for this reference sand.

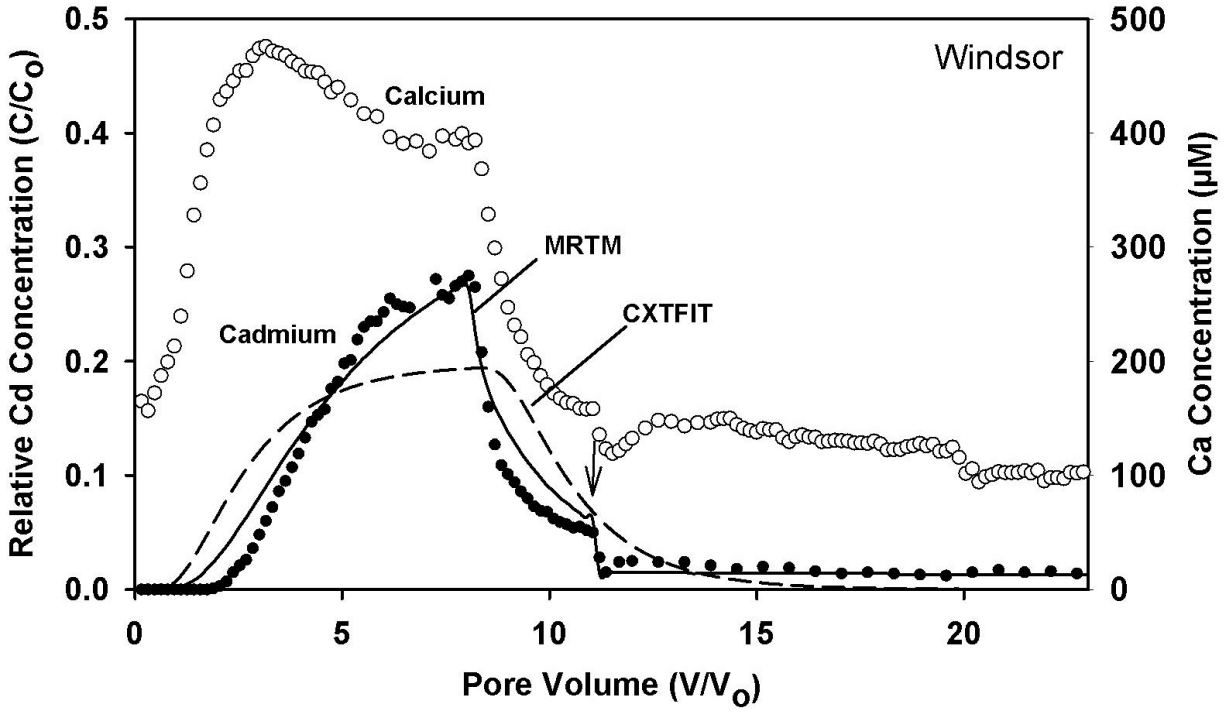

Fig. 2.7. Breakthrough results of Ca and Cd from the Windsor soil column. The multireaction and transport model (MRTM) and CXTFIT model simulations are denoted by the solid and dashed curves, respectively; the arrow indicates when flow interruption occurred.

The distributions of sorbed Cd vs. depth in the three soil columns are given in Table 2.7. Consistent with the batch results, sorbed Cd for the Bustan soils was associated with the carbonates and oxides fraction. For the Windsor soil and the reference sand, sorbed Cd was primarily in the exchangeable and carbonates and oxides fractions. Sorbed Cd vs. depth is shown in Fig. 2.9 along with the MRTM and CXTFIT simulations. The MRTM and CXTFIT were used to simulate Cd sorbed vs. depth where no inverse modeling was performed. Rather, the model parameters used were those utilized for the BTC simulations. The simulated results showed

adequate overall predictions of the measured results. Poor predictions were realized for the first section of the Bustan surface soil column (Fig. 9), however. This may be a result of the limited Cd mobility in that soil. We recognize that measured Cd based on sequential extractions oft en yields less than total recovery. Several studies reported that the sum of Cd fraction measurements represent 78 to 90% of the total sorbed (Emmerich et al., 1982; Dowdy et al., 1991; Han and Banin, 1999). Therefore, based on these simulations, the use of the MRTM and CXTFIT are recommended for providing overall estimates of the levels of Cd retained by the soil with depth.

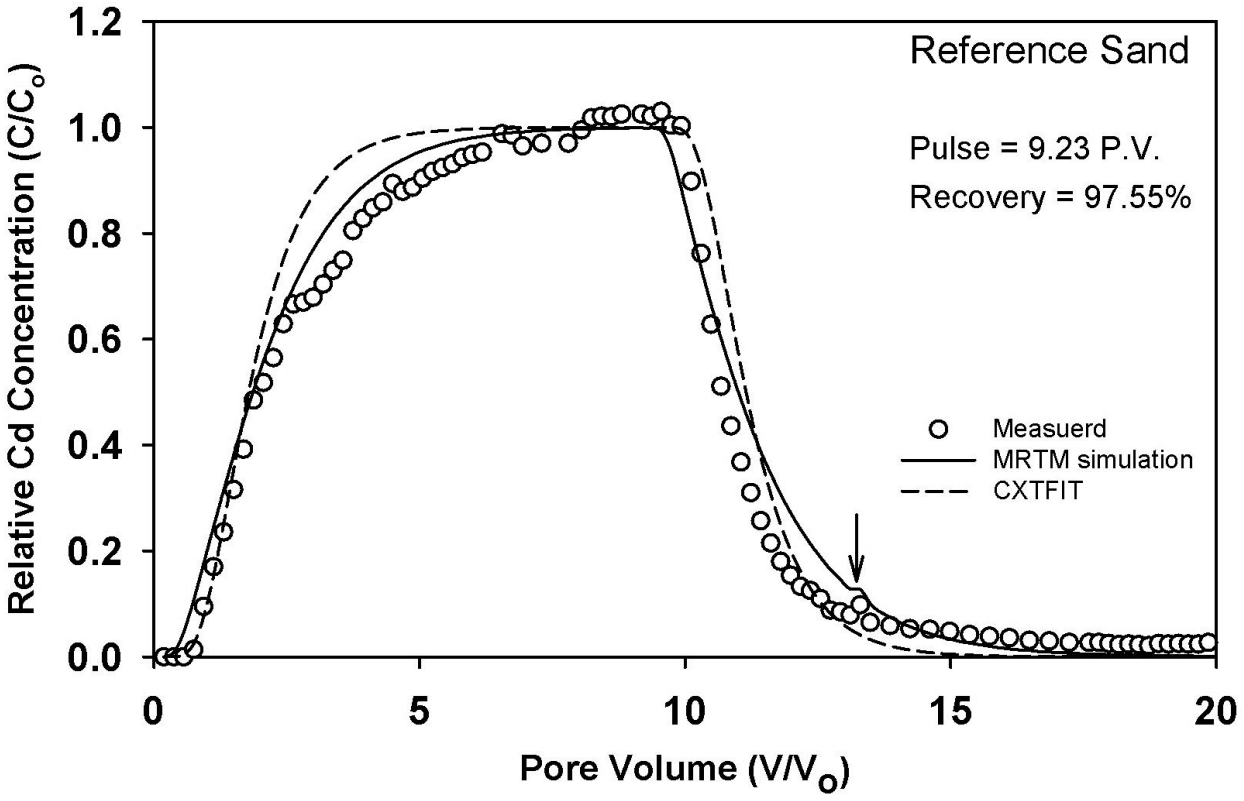

Fig. 2.8. Cadmium breakthrough results from the reference sand column. The multireaction and transport model (MRTM) and CXTFIT model simulations are denoted by the solid and dashed curves, respectively; the arrow indicates when flow interruption occurred.

Table 2.7. Total extracted (or sorbed) Cd and the different fractions from sectioned soil columns.

Depth	Total Cd sorbed	Exchangeable fraction		Oxidizable fraction		Associated with carbonates/oxides		Strongly bound	
cm	----- µmol kg^{-1} -----		%	µmol kg^{-1}	%	µmol kg^{-1}	%	µmol kg^{-1}	%
				Reference sand					
0-1	80.4	25.29	31.45	ND†	0.00	50.05	62.24	5.07	6.30
1-2	89.7	35.39	39.45	ND	0.00	46.13	51.42	8.19	9.13
2-3	127.0	42.47	33.45	ND	0.00	73.34	57.77	11.14	8.78
3-4	123.0	48.62	39.54	ND	0.00	63.86	51.93	10.49	8.53
4-5	128.5	50.21	39.09	ND	0.00	67.69	52.70	10.54	8.21
				Bustan soil, surface					
0-1	1824.9	ND	0.00	22.55	1.24	1772.29	97.12	30.03	1.65
1-2	1635.4	ND	0.00	9.33	0.57	1606.72	98.25	19.35	1.18
2-3	1224.3	ND	0.00	5.88	0.48	1201.41	98.13	17.01	1.39
3-4	377.6	ND	0.00	0.00	0.00	372.11	98.54	5.52	1.46
4-5	267.4	ND	0.00	0.00	0.00	236.23	88.35	31.14	11.65
				Bustan soil, subsurface					
0-1	624.8	2.40	0.38	14.31	2.29	599.10	95.88	9.03	1.45
1-2	1282.2	92.53	7.22	13.22	1.03	1157.97	90.31	18.47	1.44
2-3	1401.2	60.77	4.34	12.16	0.87	1306.78	93.26	21.51	1.54
3-4	608.5	ND	0.00	5.76	0.95	591.49	97.21	11.21	1.84
4-5	480.3	ND	0.00	4.52	0.94	465.82	96.99	9.92	2.07
				Windsor Soil					
0-1	1804.7	937.24	51.93	ND	0.00	813.85	45.10	53.64	2.97
1-2	1070.3	492.87	46.05	ND	0.00	527.36	49.27	50.04	4.68
2-3	1032.1	420.97	40.79	ND	0.00	569.63	55.19	41.53	4.02
3-4	614.5	199.18	32.41	1.03	0.17	382.05	62.17	32.27	5.25
4-5	591.5	200.94	33.97	0.65	0.11	354.13	59.87	35.76	6.05

† Not detected.

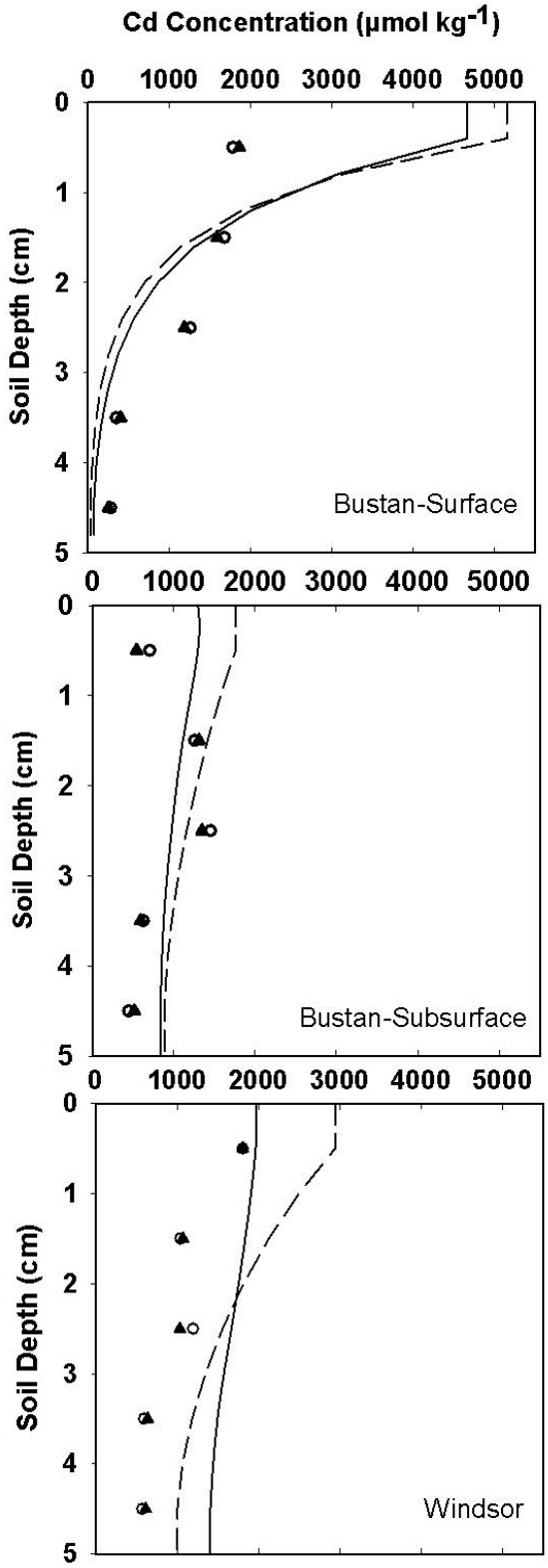

Fig. 2.9. Cadmium sorbed vs. column depth based on soil extractions. Solid and dashed curves represent the multireaction and transport model (MRTM) and CXTFIT model predictions, respectively; closed and open symbols are experimental measurements and represent different replications.

2.5 Conclusions

Cadmium retention exhibited strong nonlinear and kinetic behavior for all three soils. Such strong sorption was accompanied by slow release with time. Moreover, Cd was nearly immobile in the calcareous Bustan surface soil, whereas 30 and 20% of the applied Cd was mobile in the Bustan subsurface and Windsor soil columns. The use of a multireaction model that accounts for nonlinear equilibrium and kinetic reactions was capable of describing the kinetic behavior of Cd sorption and release for all the soils. The MRTM was also capable of describing Cd BTCs for all the soil columns. The CXTFIT model adequately predicted the peak location of all BTCs but underestimated Cd arrival and effluent concentrations during leaching. The results of sorbed Cd vs. soil depth showed that Cd was associated with the carbonate fraction for the alkaline Bustan soils and with exchangeable and oxides fractions for the acidic Windsor soil.

2.6 References

Alloway, B.J. 1995. The origins of heavy metals in soils. p. 38–57.*In*: Alloway, B.J. (ed.), Heavy metals in soils. Blackie Academic and Professional, London, UK.

Aringhieri, R., P. Carrai, and G. Petruzzelli. 1985. Kinetics of Cu^{2+} and Cd^{2+} adsorption by an Italian soil. Soil Sci. 139:197–204.

Bakr, N., M.H. Bahnassy, M.M. El-Badawi, G.W. Ageeb, and D.C. Weindorf. 2009. Land capability evaluation in newly reclaimed areas: a case study in Bustan 3 area, Egypt. Soil Surv. Horiz. 51:90-95.

Brusseau, M.L., R.E. Jessup, and P.S.C. Rao. 1992. Modeling solute transport influenced by multiprocess nonequilibrium and transformation reactions. Water Resour. Res. 28:175–182.

Buchter, B., B. Davidoff, M.C. Amacher, C. Hinz, I.K. Iskander and H.M. Selim . 1989. Correlation of Freundlich Kd and n retention parameters with soils and elements. Soil Sci. 148: 370–379.

Chen, W., A.C. Chang, L. Wu, and A.L. Page. 2006. Modeling dynamic sorption of cadmium in cropland soils. Vadose Zone J. 5:1216–1221.

Dijkstra, J.J., J.C.L. Meeussen, and R.N.J. Comans. 2004. Leaching of heavy metals from contaminated soils: an experimental and modeling study. Environ. Sci. Technol. 38: 4390–4395.

Dowdy, R.H., J.J. Latterll, T.D. Henesly, R.B. Grossman, and D.L. Sullivan. 1991. Trace metal movement in an Aeric Ochraqualf following 14 years of annual sludge applications. J. Environ. Qual. 20:119–123.

Emmerich W.E., L. J. Lund, A.L. Page and A.C. Chang. 1982. Solid phase forms of heavy metal in sewage sludge-treated soils. J. Environ. Qual. 11:178-181.

Gerritse, R.G. 1996. Dispersion of cadmium in columns of saturated sandy soils. J. Environ. Qual. 25:1344-1349.

Gismera, M. J., J. Lacal, , P. da Silva, , R. Garcia, , M. T. Sevilla, , and J. R. Procopio. 2004. Study of metal fractionation in river sediments. A comparison between kinetic and sequential extraction procedures. Environ. Pollut. 127:175–182.

Han, F.X., and A. Banin. 1999. Long-term transformations and redistribution of potentially toxic heavy metals in arid-zone soils. II.Under field capacity regime.Water Air Soil Pollut. 114:221–250.

Holm, P.E., B.B.H. Andersen, and T.H. Christensen. 1996. Cadmium solubility in aerobic soils. Soil. Sci. Soc. Am. J. 60, 775–780.

Holm, P.E., H. Rootzen, O.K. Borgaard, J.P. Moberg, , and T.H. Christensen. 2003. Correlation of cadmium distribution coefficient to soil characteristics. J. Environ. Qual. 32: 138–145.

Kabata-Pendias A, and A.B. Mukherjee. 2007. Trace elements from soil to human. Springer. 556 pp.

Kabata-Pendias A, and W. Sadurski. 2004. Trace elements and compounds in soil p 79–99. *In*: E. Merian et al. (ed) Elements and their compounds in the environment, Wiley-VCH, Weinheim.

Krishnamurti G.S.R., P.M. Huang and K.C.J. van Rees. 1997. Kinetics of cadmium release from soils as influenced by organic acids: implication in cadmium availability, J. Environ. Qual. 26:271–277.

Krishnamurti, G.S.R., and R. Naidu. 2003. Solid-solution equilibria of cadmium in soils. *Geoderma* 113**:** 17–30.

Lee, S.Z., H.E. Allen, C.P. Huang, D.L. Sparks, P.F. Sanders, and W.J.G.M. Peijnenburg. 1996. Predicting soil-water partition coefficients for cadmium. Environ. Sci. Technol. 30: 3418–3424.

Liao, L., H.M. Selim, and R.D. DeLaune. 2009. Mercury adsorption-desorption and transport in soils. J. Environ. Qual. 38: 1608–1616.

Loeppert, R.H., and D.L. Suarez. 1996. Carbonate and gypsum. p. 437–474. *In* D.L. Sparks et al. (ed.) Methods of soil analysis. Part 3. 3rd ed. SSSA Book Ser. 5. SSSA, Madison, WI.

Ma, L., and H.M. Selim. 1997. Evaluation of nonequilibrium models for predicting atrazine transport in soils. Soil Sci. Soc. Am. J. 61: 1299–1307.

McBride, M. B. 1980. Chemisorption of Cd^{2+} on calcite surfaces. Soil Sci. Soc. Am. J. 44:26–28.

McBride, M.B. 1994. Environmental Chemistry of Soils. Oxford University Press, Oxford.

Moradia, A., K.C., Abbaspourb, and M. Afyuni. 2005. Modelling field-scale cadmium transport below the root zone of a sewage sludge amended soil in an arid region in central Iran. J. Contam. Hydrol. 79:187– 206.

Naidu, R., R.S. Kookana, M.E. Sumner, R.D. Harter, and K.G. Tiller. 1997. Cadmium sorption and transport in variable charge soils: A review. J. Environ. Qual. 26:602–617.

Pang, L., and M. E. Close. 1999. Non-equilibrium transport of Cd in alluvial gravels. J. Contam. Hydrol. 36:185– 206.

Pansu M**.,** and J. Gautheyrou. 2006, *Handbook of Soil Analysis - Mineralogical, Organic and Inorganic Methods.* Springer, Berlin.

Reeder, R.J. 1996. Interaction of divalent cobalt, zinc, cadmium, and barium with the calcite surface during layer growth. Geochim. Cosmochim. Acta. 60:1543–1552.

SAS Institute. 2000. SAS/STAT user's guide, version 8; SAS Institute, Cary, North Carolina.

Selim, H. M. 1992. Modeling the Transport and Retention of Inorganics in Soils. Adv. Agron. 47: 331-384.

Selim, H. M. and M. C. Amacher. 1997. Reactivity and Transport of Heavy Metals in Soils. CRC, Boca Raton.

Selim, H.M., B. Buchter, C. Hinz, and L.W. Ma. 1992. Modeling the transport and retention of cadmium in soils: Multireaction and multicomponent approaches. Soil Sci. Soc. Am. J. 56:1004–1015.

Sidle, R.C., and L.T. Kardos. 1977. Transport of heavy metals in a sludge-treated forested area. J. Environ. Qual. 6:431–437.

Strawn, D.G., and D.L. Sparks. 1999. Sorption kinetics of trace elements in soils and soil materials. In: Selim, H.M., and K.I. Iskandar (ed.) Fate and Transport of Heavy Metals in the Vadose Zone. Lewis Publishers, Boca Raton, FL, USA, p.1–28.

Toride, N., F.J. Leij, and M. Th. van Genuchten. 1999.The CXTFIT code for estimating transport parameters from laboratory or field tracer experiments, version 2.1. Research Report No. 137, U.S. Salinity Laboratory, USDA, ARS, Riverside, CA.

Tsang, D.C.W., and I.M.C. Lo. 2006. Competitive Cu and Cd sorption and transport in soils: A combined batch kinetics, column and sequential extraction study. Environ. Sci. Technol. 40:6655–6661.

van Genuchten, M.Th ., and P.J. Wierenga. 1976. Mass transfer studies in sorbing porous media: I. Analytical solutions. Soil Sci. Soc. Am. J. 40:473–481.

Zhang, H., and H. M. Selim. 2005. Kinetics of arsenate adsorption-desorption in soils. Environ. Sci. Technol. 39:6101–6108.

Zhang, H., and H. M. Selim. 2006. Modeling the transport and retention of arsenic (V) in soils. Soil Sci. Soc. Am. J. 70: 1677–1687.

CHAPTER 3. COPPER MOBILITY IN ACIDIC AND ALKALINE SOILS: MISCIBLE DISPLACEMENT EXPERIMENTS[2]

3.1 Introduction

Modeling copper (Cu) mobility in soil is necessary for pollution control as well as plant nutrition management. Copper is an essential micronutrient required in the growth of both plants and animals (Kabata-Pendias and Pendias, 2001). However, at elevated levels Cu harmfully affects the environment (Alloway 1995). In agroecosystems, Cu is extensively used in the form of fertilizers (Holmgren et al., 1993; Mermut et al., 1996), and bactericides and fungicides (Epstein and Bassein, 2001). Copper is susceptible to accumulation in surface soil layers due to strong bindings to organic matter (OM), clay minerals, and oxides of Fe, Al, and Mn (Kabata-Pendias and Sadurski 2004, Ma et al., 2006). Moreover, Cu reactivities and transport in soils is often observed for extended periods of time (Pietrzak and McPhail, 2004).

Extensive mobility of Cu in soils has been observed. In fact, appreciable leaching of Cu in soil profiles has been shown in humus-poor acidic soils (Mathur et al., 1984), and in soils which received repeated application of Cu fertilizer in alkaline soils (Wei et al., 2007). Sparks (2003) stated that mobility and fate of heavy metals such as Cu in soils are affected by soil properties and is reflected by the partitioning between the soil and solution. Copper retention in soils was found to be significantly correlated with soil pH, OM, cation exchange capacity (CEC), amorphous Fe, Al, Si, and Mn oxides, and clay content (Chen et al., 1999; Adriano, 2001; Shahen et al., 2009). Moreover, soil-solution parameters such as ionic strength, competing and counter ions have been shown to influence the adsorption of metals in soils (Harter and Naidu, 2001).

[2] This reprint originally appeared as, Elbana, T. A. and H M. Selim. 2011. Copper mobility in acidic and alkaline soils: miscible displacement experiments. Soil Sci. Soc. Am. J. 75:2101–2110. “Reprinted by Permission, ASA, CSSA, SSSA."

Copper retained in the soil is commonly associated with various soil components including OM, clays, carbonate, and Fe and Mn oxides (Tessier et al., 1979; Emmerich et al., 1982; Baker and Senft 1995). These components exhibit varying potential for retention as well as release Cu in soils. He et al. (2006) suggested that based on column leaching, short-term Cu pulse was primarily due to the exchangeable Cu fraction. They also found that, based on batch extractions, carbonate-bound and exchangeable fractions contribute to long-term Cu release from sandy soils.

Recent Cu kinetic behavior studies in soils have been investigated by several scientists including Florido et al. (2010), Wang et al. (2009), and Lopez-Periago et al. (2008) among others. Lopez-Periago et al. (2008) studied Cu retention and release kinetics by several acidic soils using the stir-flow batch method. Their results indicated that Cu retention was 10 times faster than that for Cu release where hysteretic behavior was dominant for all soils. Kinetic of Cu retention during adsorption was investigated by Wang et al. (2009) based on batch techniques. Their results illustrated that Cu adsorption varied extensively among the different soils. The Elovick and power function models were successful in describing the kinetics of adsorption for all soils. Studies on Cu mobility in soils include Chang et al. (2001) who performed Cu and Cd miscible displacement column experiments on a lateritic silty-clay soil. They found that theoretical Cu and Cd BTCs simulated based on Freundlich nonlinear retardation factors provided better predictions than when linear adsorption was assumed. Vogeler (2001) described movement of Cu in soil column leaching experiments performed under unsaturated flow conditions where a Cu solution was continuously applied. Attempts were made to describe Cu concentration in the effluent based on the convection–dispersion solute transport equation (CDE) where ion exchange for a Cu–Ca binary system was assumed as the governing retention mechanism. Measured Cu results were significantly retarded when compared to CDE simulation,

however. As a result, the authors suggested that nonexchange processes are also involved in Cu transport in soils. The study of Florido et al. (2010) is one of the few papers where kinetic adsorption was incorporated in modeling of Cu transport in fixed beds. Copper BTCs were generated from fixed beds of grapevine OM that received continuous pulse of Cu solutions. Adequate description of BTCs effluent Cu concentrations were achieved when the CDE accounted for linear equilibrium and first-order kinetic adsorption.

A literature search revealed that few studies attempted to describe Cu transport where retention was not restricted to linear adsorption where local equilibrium was assumed. In this study, the focus was to describe Cu transport based on multiple component or multisite approaches where adsorption was accounted for based on several nonlinear reactions of the kinetic as well as equilibrium types. To achieve this goal, Cu transport experiments on different soils were performed using miscible displacement column that received Cu pulses then leached with Cu-free solution. The specific objectives of this study were:

1. To quantify the sorption of Cu on acidic and alkaline soils;
2. To quantify the kinetics of Cu retention during transport in soil columns using miscible displacement, and
3. To test the predictive capability of kinetic multireaction modeling approaches to describe Cu transport and reactivity of Cu in soils.

3.2 Multireaction Model

The MRTM is schematically illustrated in Fig.3.1. MRTM accounts for several interactions of heavy metals with soil matrix surfaces soils (Selim, 1992). Based on soil heterogeneity and observed kinetics of sorption–desorption, MRTM was proposed to describe the reactivities of heavy metals in the soil environment. Basic to the multi-site approach is that the soil is made up of different constituents (soil minerals, OM, Fe and aluminum oxides), and that a

solute species is likely to react with various constituents (sites) by different mechanisms. The retention reactions associated with MRTM are,

$$S_e = K_e \left(\frac{\theta}{\rho}\right) C^N \qquad [3.1]$$

$$\frac{\partial S_1}{\partial t} = k_1 \left(\frac{\theta}{\rho}\right) C^n - k_2 S_1 \qquad [3.2]$$

$$\frac{\partial S_2}{\partial t} = \left[k_3 \left(\frac{\theta}{\rho}\right) C^n - k_4 S_2\right] - k_5 S_2 \qquad [3.3]$$

$$\frac{\partial S_s}{\partial t} = k_5 S_2 \qquad [3.4]$$

$$\frac{S_{irr}}{\partial t} = k_{irr} \left(\frac{\theta}{\rho}\right) C \qquad [3.5]$$

where C is concentration in solution (mg L^{-1}), ρ is the soil bulk density (g cm^{-3}), θ is the soil moisture content (cm^3 cm^{-3}), and t is the reaction time (h). In the model, S_e represents the amount retained on equilibrium sites (mg kg^{-1}); S_1 and S_2 represent the amount retained on reversible kinetic sites (mg kg^{-1}); S_{irr} and S_s represent the amounts irreversibly retained (mg kg^{-1}). Parameter K_e is a dimensionless equilibrium constant, and k_1, k_2, k_3, k_4, k_5, and k_{irr} (h^{-1}) are the associated rates of reactions, and n is dimensionless reaction order commonly < 1.

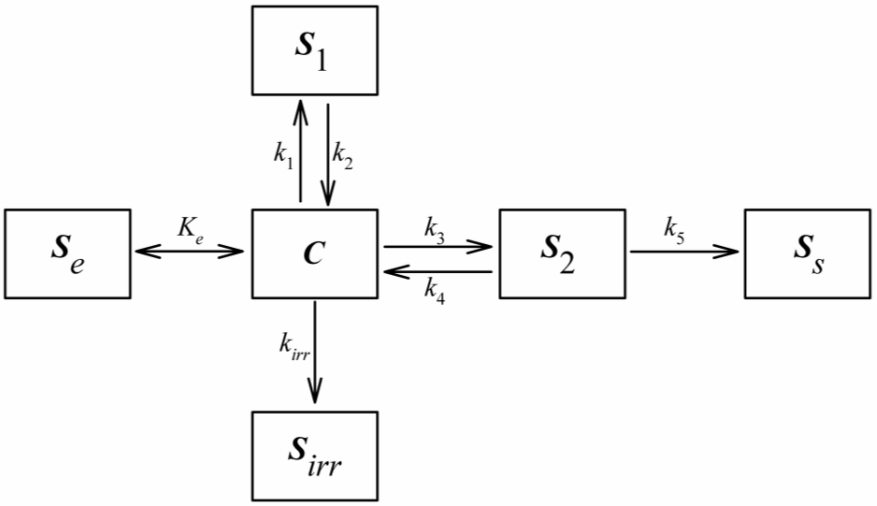

Fig. 3.1. Schematic of the multireaction and transport model (MRTM).

Incorporation of the one-dimensional CDE with the reactions given in eqs. [3.1]-[3.5], yields

$$\rho \frac{\partial S}{\partial t} + \theta \frac{\partial C}{\partial t} = \theta D \frac{\partial^2 C}{\partial z^2} - q \frac{\partial C}{\partial z} \qquad [3.6]$$

where S is the total amount sorbed,

$$S = S_e + S_1 + S_2 + S_s + S_{irr} \qquad [3.7]$$

and D is the hydrodynamic dispersion coefficient ($cm^2\ h^{-1}$), q is Darcy's water flux density ($cm\ h^{-1}$), and z is distance (cm).

The MRTM model was used to describe Cu transport BTCs from our column experiments based on the CDE of eq. [3.6]. To obtain model simulations of Cu transport in the soil columns, MRTM was used along with a nonlinear least-squares optimization scheme, which provided best-fit of the model to the experimental BTCs. Criteria used for estimating the goodness-of-fit of the model to the data were the coefficient of determination (r^2) and the root mean square error (*RMSE*) statistics.

3.3 Materials and Methods

Surface (0-40 cm) and subsurface (40-75 cm) soils were collected from an area near Bustan-3 in the Northwestern desert of Egypt. This sandy calcareous soil is classified as Typic Torripsamments, (Bakr et al., 2009) and the top two soil layers were sampled to quantify the impact of $CaCO_3$ on Cu mobility in this soil. The second soil is a Windsor loamy sand collected near Hanover, NH. Selected soil physical and chemical properties were determined in our laboratory and are given in Table 3.1. NaOAc at pH 8.2 and NH_4OAc at pH 7 methods were used for determining CEC in alkaline and acidic soils, respectively (Pansu and Gautheyrou, 2006). Moreover, column transport experiments were performed to quantify Cu transport in acid washed sand material (Fisher Scientific: 14808-60-7). This sand material with no clay and organic matter (pH=6.27; sand=81%, silt=19%) was previously used as a reference matrix in recent Hg transport experiments (Liao et al., 2009).

3.3.1 Adsorption Isotherms

To assess the retention capability of the soils used to retain Cu, adsorption isotherms were measured. The batch equilibration technique was used where a wide range of initial Cu concentrations (C_o) were used (0.05, 0.10, 0.20, 0.53, 1.02, 2.10, and 4.4 mmol L^{-1}). Due to the anticipated high affinity of Cu retention by our calcareous soils, initial Cu concentrations of 6.3, 9.4, and 12.6 mmol L^{-1} were also used for Bustan soils. All solutions were prepared in 0.005 mol L^{-1} KNO_3 as a background solution. Adsorption was performed in triplicate where 3-g sample of each soil were placed in Teflon centrifuge tubes and mixed with 30 mL solution of known Cu concentrations described above. The tubes were sealed and the mixtures were continuously shaken for 24 h and then centrifuged for 10 min. A 5-mL aliquot was sampled and Cu concentration in the supernatant solution was analyzed using inductively coupled plasma-atomic emission spectrometry (ICP-AES) (Spectro Citros CCD, Spectro Analytical Instruments, Kleve, Germany). The amount of Cu sorbed by the soil matrix was determined by the difference between the concentrations of the supernatant and that of the initial solutions.

Table 3.1. Selected physiochemical properties of the studied soil and its soil classification.

	Bustan-surface	Bustan-subsurface	Windsor
Soil taxonomy	---- Typic Torripsamments ----		Typic Udipsamments
pH (1 :2.5)	9.22	9.44	6.05
OM (g kg^{-1}) †	0.66	0.13	16.6
CEC (cmol kg^{-1})	5.60	4.84	3.28
$CaCO_3$ (%)	2.76	1.18	ND¶
Citrate-bicarbonate-dithionite (CBD)			
Fe g kg^{-1}	4.175	1.261	3.885
Al g kg^{-1}	0.986	0.353	1.322
Mn g kg^{-1}	0.200	0.042	0.129

† OM, organic matter, CEC, cation exchange capacity.¶ ND, not detected

3.3.2 Miscible Displacement

To quantify the mobility of Cu in the above soils, a series of miscible displacement column experiments as described by Zhang and Selim (2006) were performed. Acrylic columns

(5-cm in length and of 6.4-cm i.d.) were uniformly packed with air-dry soil and were slowly water-saturated with a background solution of 0.005 mol L^{-1} KNO_3. To ensure water-saturation, upward flow in the soil columns was maintained. Constant flux was controlled by a piston pump (FMI lab pump, Model QG 6, Fluid Metering Inc, Oyster Bay, NY) where some 20 pore volumes of the background solution were applied at the desired flow rate. Following saturation a pulse of 3.15 mmol L^{-1} Cu (in the form of $(NO_3)_2$) in 0.005 mol L^{-1} KNO_3 was introduced into each column which was followed by several pore volumes of 0.005 mol L^{-1} KNO_3 copper-free solution. The volume of the applied Cu pulse ranged from 8 to 10 pore volumes (see table 3.2). Effluent samples collected from each miscible displacement column experiments were analyzed by ICP–AES (Spectro Citros CCD, model CCD; Spectro Analytical Instruments, Kleve, Germany).

Table 3.2. Soil physical and experimental conditions of the miscible displacement columns experiments.

Column	Matrix	Bulk density, ρ (Mg m^{-3})	Moisture content, θ (m^3 m^{-3})	Pore water velocity (cm h^{-1})	Pulse input (pore volumes)		Dispersion coefficient, D (cm^2 h^{-1})
					^3H_2O	Cu	
101	Bustan-surface	1.77	0.334	1.053	1.32	10.08	0.881
102	Bustan-surface	1.70	0.356	4.610	1.87	59.01	0.863
201	Bustan-subsurface	1.74	0.343	1.084	1.31	10.62	2.441
202	Bustan-subsurface	1.74	0.342	4.982	1.95	49.83	1.207
301	Windsor soil	1.46	0.449	0.787	1.37	8.61	1.541
302	Windsor soil	1.45	0.454	3.748	1.88	49.63	1.650
401	Reference sand	1.63	0.386	1.048	1.47	11.97	0.515

Low Cu recovery in the effluent solution from our miscible displacement column experiments was observed. For the calcareous soils, the low recoveries were associated with effluent concentrations not exceeding 1% of that applied. Moreover, more than 95% of applied Cu was retained by the soil. To achieve recovery of Cu in the effluent solution, additional column experiments were performed where a large pulse of the Cu solution (some 50 pore

volumes) was applied to each soil column. Physical parameters for each column such as bulk density, soil moisture content, are given in Table 3.2.

To describe the flow characteristic in each soil column, a pulse of tracer solution (tritium, ^3H_2O) was applied to each column subsequent to Cu pulse application. The collected tritium samples were analyzed using a Tri-Carb liquid scintillation β counter (Packard-2100 TR). The tracer pulse was applied to obtain independent estimates for the hydrodynamic dispersion coefficient (D) of the CDE equation. Estimates for D values were obtained using CXTFIT (Toride et al., 1999) and are given in Table 3.2.

3.4 Results and Discussion

3.4.1 Sorption Isotherms

Copper adsorption isotherms for the different soils are shown in Fig. 3.2. The amount of Cu retained from the soil solution reflects the extent of Cu affinity among the different soils after 24 h equilibration time. The Freundlich equation was used to describe the adsorption isotherms,

$$S = K_F C^b \qquad [3.8]$$

where S represents the amount of Cu sorbed (mg kg^{-1}), K_F is the Freundlich distribution coefficient where units depends on the units of C and S used in measuring, and b is a dimensionless reaction order. Bustan surface soil exhibited highest Cu affinity as depicted by increased Cu sorbed as the concentration of Cu in solution increased. Bustan surface soil had the highest estimated K_F followed by Bustan subsurface and Windsor soil (see Table 3.3). Moreover, for Bustan surface soil, the Freundlich parameter b was > 1 which suggests greater affinity for sorption. Freundlich b value of 1.14 for Cu adsorption on a New Mexico calcareous soil (with $CaCO_3$ of 7.39%) was reported by Buchter et al. (1989). Based on these results, it is likely that a fraction of Cu was specifically or irreversibly sorbed on the $CaCO_3$ fraction. Consistent with these results is recent work of Shaheen et al. (2009) indicating highest b values

(b = 0.93) for adsorption of Cu on a calcareous soil whereas lowest values (b =0.19) associated with a sandy soil with low carbonates.

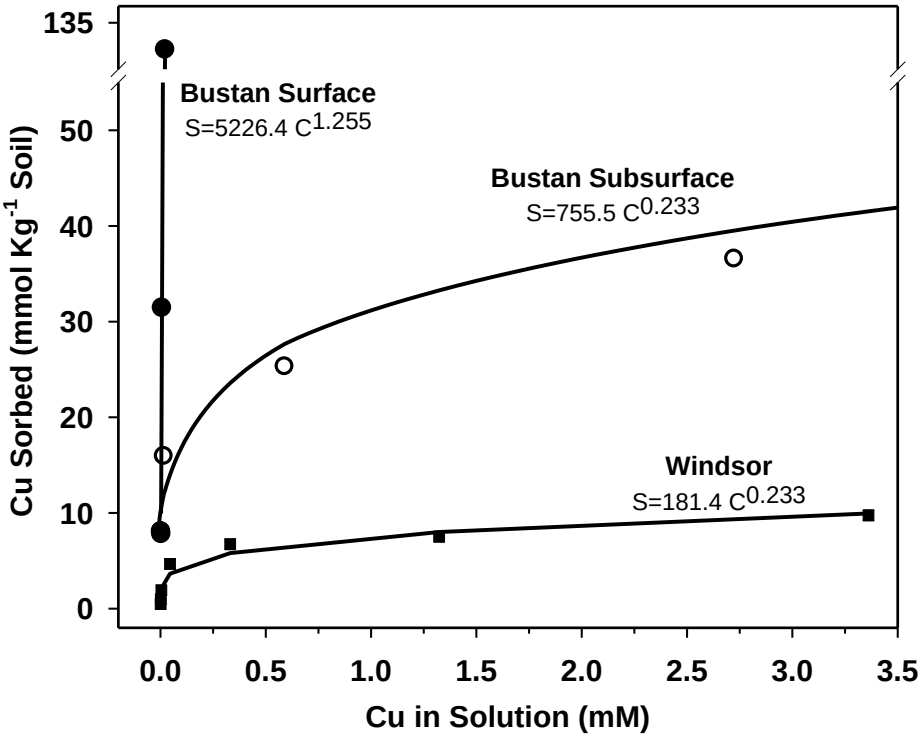

Fig. 3.2. Cu adsorption isotherms for Windsor, Bustan-surface, and Bustan-subsurface soils. Solid curves are Freundlich model calculations.

Based on Chen et al. (1999) and Adriano (2001) among others, with decreasing soil pH a marked decrease in the number of sites available for Cu sorption was observed. The acidic Windsor soil exhibited relatively low affinity for Cu adsorption when compared with the alkaline Bustan soils. The estimated Freundlich K_F was more than an order of magnitude less than that associated with Bustan surface soil (Table 3.3). Copper sorption by acidic soils such as Windsor was primarily due to oxides and hydroxides of Fe, Al, and Mn as well as OM (Adriano, 2001).

Table 3.3. Estimated Freundlich parameters and their standard errors (SE) for Cu retention by the different soils.

Soil	K_F	b	r^2
Bustan-surface	5226.4±(165.7)	1.255±(0.090)	0.992
Bustan-subsurface	755.5±(124.7)	0.233±(0.030)	0.972
Windsor	181.36±(27.6)	0.233±(0.034)	0.950

3.4.2 Tracer Transport

Breakthrough of the applied tritium pulses in the different soil columns are shown in Fig. 3.3. Here relative tritium concentration in the effluent (C/C_o) as a function of effluent pore volumes eluted (V/V_o) are presented. Here V_o represents the volume of soil-pore space within each soil column (cm^3). The tritium BTC from the reference sand column appear symmetric and exhibited no tailing as illustrated in Fig. 3.3. Such observations are consistent with the assumption that the reference sand is a nonreactive porous medium. On the other hand, tritium BTC from the Bustan and Windsor soil columns exhibited varying degrees of asymmetry. Tritium transport in Windsor soil was characterized by asymmetric BTC with rapid increase in concentration of the effluent (left hand) side of the BTC (Fig. 3.3). This was followed by extended tailing during leaching which confirms the extent of physical non-equilibrium for Windsor soil. Tritium transport in Bustan surface and subsurface soils did not exhibit extensive asymmetry when compared to the BTC for the Windsor soil. Nevertheless, some BTC tailing was observed which is evidence of limited physical nonequilibrium likely due to intraparticle diffusion and the presence of immobile water regions (Brusseau et al., 1992).

The solid curves shown in Fig. 3.3 are simulations of tritium BTCs based on the advection-dispersion equation for solute transport in soils. All tritium BTCs for Bustan and Windsor soils as well as for the reference sand were successfully simulated with $r^2 > 0.98$**.** The estimated D values for Windsor soil ranged from 1.54-1.65 $cm^2\ h^{-1}$ and were significantly larger than D values for the reference sand of 0.515 $cm^2\ h^{-1}$ (see Table 3.2). In contrast, for Bustan subsurface soil the estimated D values ranged from 1.204-2.441 $cm^2\ h^{-1}$. For Bustan subsurface soil the estimated D values were much higher than those for Bustan surface soil (0.863 to 0.881 $cm^2\ h^{-1}$) which indicates higher degree of flow variation and physical heterogeneity for the Bustan subsurface soil layer.

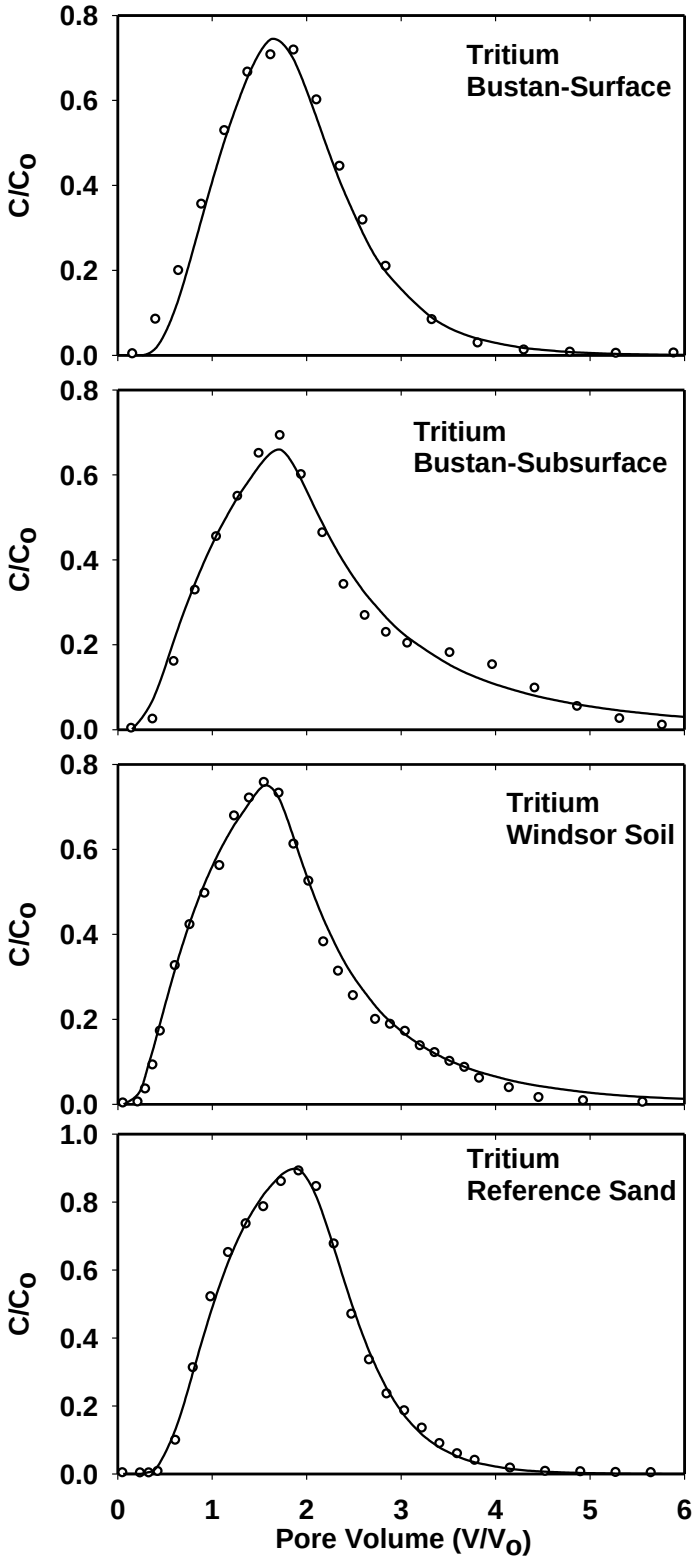

Fig. 3.3. Tritium breakthrough curves (BTCs) from the reference sand, Bustan-surface, Bustan-subsurface, and Windsor soil columns. Circle symbols for measured data. Solid curves are simulations using the CXTFIT model.

3.4.3 Copper Transport

Copper BTC from the reference sand column is shown in Fig. 3.4. Here a Cu pulse of 12 pore volumes was applied to the column then leached with a Cu-free solution. The BTC indicates that Cu exhibited early arrival along with concentration maxima equals that of the applied Cu pulse. In fact, the BTC showed resemblance that for tritium as tracer solute shown in earlier (see Fig. 3.3). Based on effluent Cu concentrations, complete recovery of applied Cu was obtained (99.3%). This indicates that little if any Cu was retained by the reference sand matrix. Good prediction of measured BTC was realized when MRTM was used where a reversible kinetic S_1 phase was assumed. Best-fit parameters obtained were n= 0.704, k_1= 0.369±0.027 h^{-1}, and k_2= 0.333±0.028 h^{-1} along with a low value for RMSE of 0.0152. The magnitude of these rate coefficients suggests low affinity of the reference sand material to retain Cu which is consistent with the observed BTC.

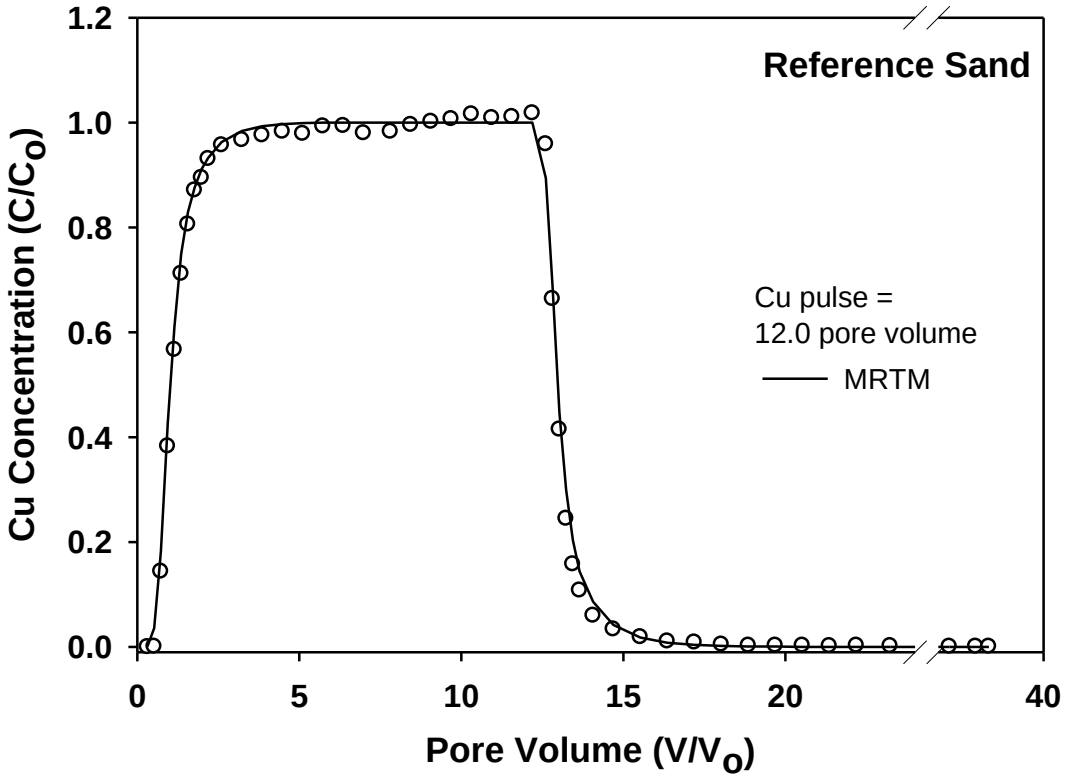

Fig. 3.4. Copper breakthrough curve (BTC) for the reference sand. Solid curve is multireaction and transport model (MRTM) simulation.

Copper mobility in the soil columns is illustrated by the BTCs shown in Figs. 3.5 to 3.10. These BTCs indicate significant Cu retardation or delayed movement in comparison to those of the reference sand. Such Cu retardation was as much as 10 pore volumes before Cu was observed in the effluent solution. For Bustan soil, the BTCs associated with Cu pulses of short duration (about 10 pore volumes) are shown in Fig. 3.5 and clearly illustrate the strong affinity for Cu by the surface and the subsurface Bustan soils. These BTCs are characterized by low peak concentrations as well as extremely low recovery. In fact, the total amounts of Cu recovered in the effluent solution were 0.4% and 0.6% of that applied in the pulse for Bustan surface and subsurface soil columns, respectively. Moreover, peak Cu concentration in the effluent was less than C/C_o=0.01 (C_o represents the Cu pulse concentration; C_o = 3.15 mmol L^{-1}). Such strong affinity and low Cu mobility in Bustan soils is a direct consequence of the presence of $CaCO_3$ and to a lesser extent to the presence of Fe, Al, and Mn oxides (see Table 3.1). Based on extended X-ray absorption fine-structure (EXAFS) spectroscopy, Elzinga and Reeder (2002) showed that Cu occupy Ca sites in the calcite structure forming inner-sphere Cu sorption complexes. One may consider such strongly bound Cu as irreversibly sorbed.

In an effort to describe the behavior of Cu as depicted by the BTCs in Fig. 3.5, several attempts were made to achieve convergence using MRTM. Best MRTM simulations are based on the dominance of irreversible sorption (S_{irr}) and to a lesser extent equilibrium sorption. For Bustan surface, best simulation was obtained using k_{irr} of 2.270 ± 0.0268 h^{-1} and K_e of 1.572 ± 0.084 (r^2 = 0.6349; RMSE = 0.0008) whereas for the Bustan subsurface, best-fit parameters were k_{irr} = 3.254 ± 0.0409 h^{-1} and K_e = 19.096 ± 0.513 (r^2 = 0.9153; RMSE = 0.0007). In Fig. 3.5 we also show Ca concentration in the effluent since it represents the dominant cation in this calcareous soil. Calcium concentration exhibited a sharp increase of concentration following Cu pulse application. Ponizovsky et al. (2007) reported equivalence of Cu sorbed amounts and Ca,

Mg, Na, and H cations released in soil solution, and the regressions between the sorbed amount of Cu and these cations expressed in mole kg^{-1} was close to linear with slopes of 0.8 to 1.1.

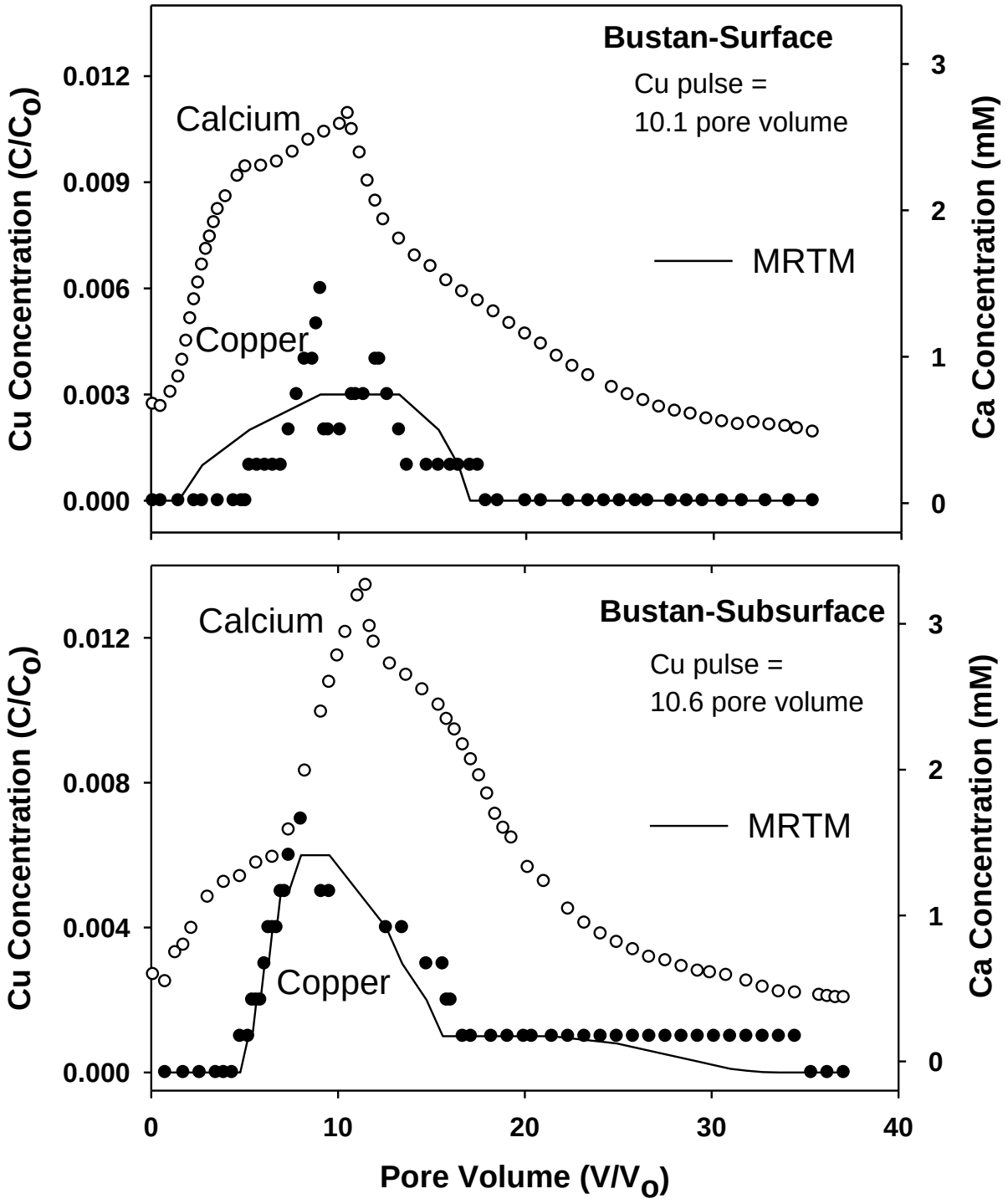

Fig. 3.5. Breakthrough results of Ca and Cu from the Bustan surface (top) and Bustan subsurface (bottom) soil columns. Solid curve is multireaction and transport model (MRTM) simulation.

The BTC from the Bustan surface column that received a Cu pulse for a long duration (59 pore volumes) is shown in Fig. 3.6. The BTC exhibited late arrival of Cu in the effluent solution (of 10 pore volumes) with a concentration maxima of C/C_o of 0.4. Based on the area under the curve, the total amount of Cu in the effluent was 27% of that applied, which further supports the strong affinity of this calcareous soil for Cu. The results in Fig. 3.6 also show Ca concentration in the effluent solution, which exhibited a sharp increase in concentration in response to the Cu pulse application. A slow and continued decrease in Ca concentration was observed following the Cu pulse application (> 60 pore volumes). The overall shape of both Cu and Ca BTCs give rise to the possibility of competitive sorption or ion exchange of Ca and Cu in this soil.

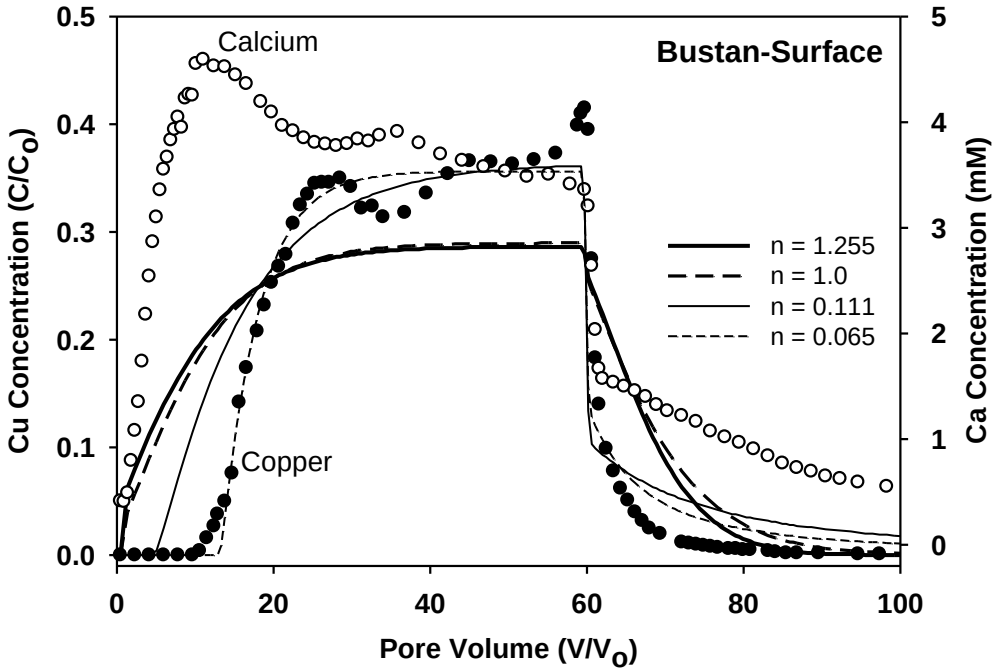

Fig. 3.6. Breakthrough results of Ca and Cu from the Bustan surface soil column with a Cu pulse of 59.0 pore volumes. Solid and dashed curves represent multireaction and transport model (MRTM) simulation using different *n* values.

The solid curve shown in Fig. 3.6 represents MRTM simulation (version M1) where only the reversible phase (S_1) and irreversible phase (S_{irr}) were considered. Other versions of the model were also considered and provided poor predictions of the measured BTC (see Table 3.4). The inadequate predictions shown in Fig. 3.6 are likely due to the use of a nonlinear reaction

order n > 1 in MRTM model calculations. Actual n value used in the model was 1.255 and was based on the isotherm results for the calcareous Bustan surface soil given in Fig. 3.2 (also see Table 3. 3). In fact, when n = 1 was used, improved simulations were not achieved (see dashed curve in Fig. 3.6). The use of n > 1 in eq. [3.1]-[3.3] is unusual since n less than unity is measured for most trace elements (see Buchter et al., 1989 and Selim and Amacher, 1997). In fact, we are unaware of models where nonlinear isotherms with n > 1 were implemented to describe BTC of reactive solutes in soils. The work of Selim et al. (2004) is one of the few where n > 1 was successfully used to describe BTCs for SO_4 continuous pulse input into columns from a forest Swedish subsurface soil layers. The solid curve shown in Fig. 3.6 represents MRTM simulation when irreversible adsorption was accounted for based on nonlinear rather than a linear reaction mechanism. Specifically the irreversible form used with n of 1.255 was,

$$S_{irr} = k_{irr}\left(\frac{\theta}{\rho}\right) C^{1.255} \qquad [3.9]$$

Such predictions were superior than all other predictions. We recognize that n>1 implies convex isotherms which were also obtained for a calcareous soil by Buchter et al. (1989). Convex isotherms imply strong binding or irreversible sorption which is illustrated by the low recovery of applied Cu in Bustan surface soil column.

Vogeler et al. (2001) described the movement of Cu in soil column leaching experiments based on CDE where ion exchange for a Cu-Ca binary system was assumed as the governing retention mechanism. Since ion exchange is fully reversible, it is not surprising that Vogeler et al. (2001) obtained less than adequate predictions from their Cu transport experiments. The dashed curve shown in Fig. 3.7 represents predictions based on ion exchange modeling which accounted for reversible as well as irreversible sorption.

Table 3.4. Multireaction transport model parameter estimates for Cu transport in Bustan surface soil (long pulse): model parameter estimated standard error (SE), root mean square error (RMSE), and coefficient of determination (r^2) values.

Model version†	RMSE	r^2	n	k_1	SE	k_2	SE	k_3	SE	k_4	SE	k_5	SE	k_{irr}	SE
				---------- h^{-1} ----------											
M1	0.0842	0.7559	1.255††	0.668	0.229	0.264	0.096	----	----	----	----	----	----	1.191	0.036
M1 (with n=1)	0.0821	0.7858	1.000†††	2.302	0.753	0.250	0.088	----	----	----	----	----	----	1.180	0.036
M1 (n fitted)	0.0547	0.9033	0.111±0.015	99.252	19.722	0.0958	0.0269	----	----	----	----	----	----	0.9573	0.023
M1 (n fitted)	0.0309	0.9636	0.065±0.003	311.214	12.64	0.219	0.008	----	----	----	----	----	----	0.977	0.012
M2	0.0904	0.7077	1.255	----	----	----	----	1.096	0.263	0.201	0.095	0.108	0.018	----	----

† M1 = S_1 and S_{irr} (k_1,k_2, and K_{irr}); M2 = S_2 and S_s (k_3,k_4, and k_5)
†† n is based on adsorption isotherm.
††† *n=1 assumed value*.

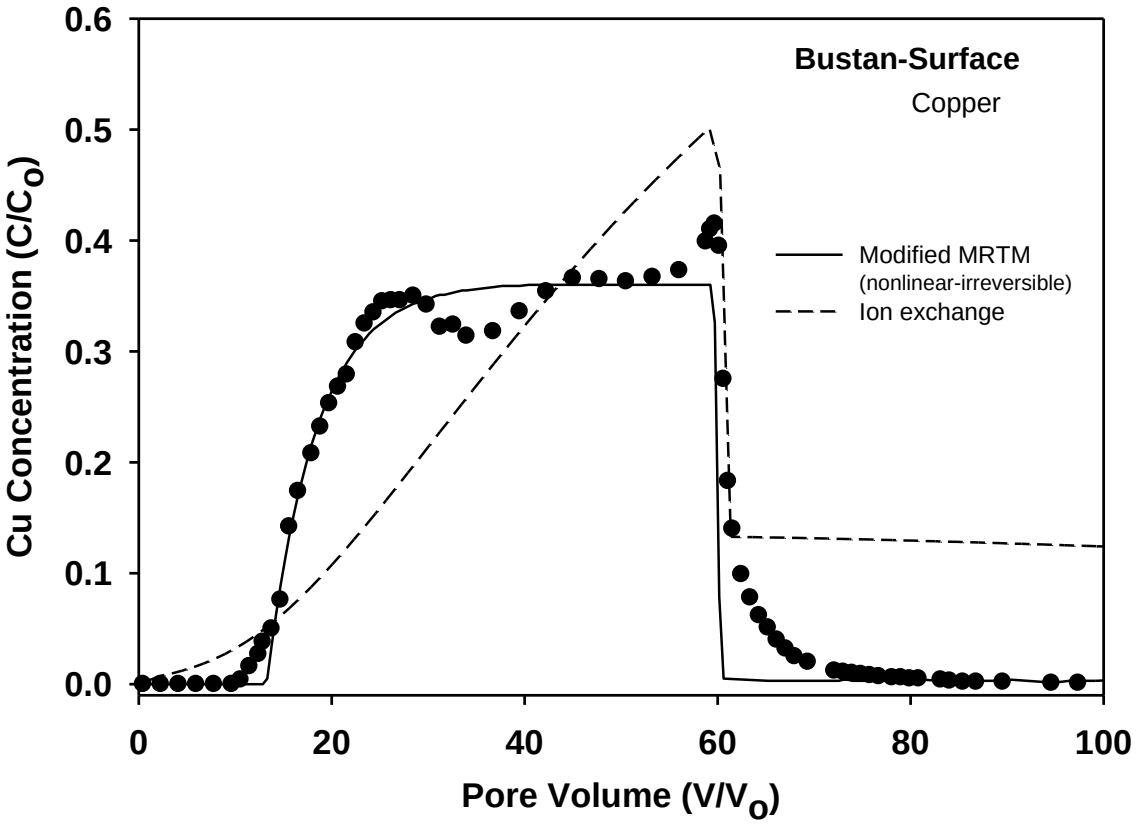

Fig.3.7. Breakthrough results of Cu from the Bustan surface soil column with a Cu pulse of 59.0 pore volumes.

To depict BTC behavior, the equilibrium assumption was relaxed and the kinetic ion exchange formulation of Selim et al. (1992) was invoked,

$$\frac{dX}{dt} = \alpha(X^* - X) \qquad [3.10]$$

$$X = \frac{KY}{1+(K-1)Y} \qquad [3.11]$$

Where X is the equivalent fraction (Cu in our case) on the exchanger phase $(X=S/\Omega)$ where Ω is the cation-exchange (or sorption) capacity of the soil ($mmol_c\ kg^{-1}$), and Y is equivalent ionic fraction in the solution phase (C/C_T) where C_T is the total concentration ($mmol_c\ L^{-1}$) and is the sum of ion (cationic) species in solution. The term κ is the selectivity coefficient or a separation factor for the affinity of ions on exchange sites (dimensionless). In eq. [3.10] X^* represent the equilibrium sorbed amount (at time t), and α is an apparent rate coefficient (h^{-1}). Additional

details of ion exchange modeling are discussed in Zhou and Selim (2001) and Vogeler (2001). Irreversible sorption was also incorporated into the ion-exchange formulation in a similar manner to that of eq. [3.5]. The resulting predictions based on ion exchange modeling shown in Fig. 3.7 captures the overall trend of the BTC for Cu.

We recognize that a drawback of the models used above is that they do not account for the release or dissolution/precipitation of carbonates which dominate trace element reactvities in calcareous soils. Several efforts to quantify Ca dissolution from carbonates are reported in the literature. Such efforts are based on principals of chemical models. The chemical model of Plummer et al. (1978) for pure systems is used as the basis for of transport and requires comprehensive set of parameters such as surface area of calcite among others. Modifications to chemical models have been proposed to improve Ca dissolution/precipitation modeling in soil systems (see Suarez and Simenek, 1997). Recently Kaufmanna and Dreybrodt (2007) presented a solution to the problem of dissolution of limestone covered by a water film open to a CO_2-containing atmosphere. Their system of equations is based in part on Ca concentration at the boundary surface and diffusional-mass transport of the dissolved species from and towards the water–limestone interface. Their approach is restricted to a flat surface and is yet to be extended to calcareous soils under saturated or unsaturated flow conditions.

Copper transport in Bustan subsurface soil is shown in Fig. 3.8. Here some 60 pore volumes of Cu pulse were introduced to the column which resulted in increased Cu mobility when compared to earlier BTC associated with a short Cu pulse of only 10 pore volumes (see Fig. 3.5 and 3.8). This increased mobility is manifested by the large recovery in the effluent of some 60% of the applied pulse as well as high BTC peak concentration of C/C_o of 0.86. Gradual increase of the adsorption (left) side of the BTC was observed which was followed by extended or slow Cu release during leaching. The associated BTC for Ca exhibited a gradual decrease in

concentration after reaching maxima during the early stage of Cu pulse application. The gradual decrease in Ca concentration was associated with a corresponding increase of Cu concentration. The MRTM version (M2) with a reversible phase (S_2) and irreversible phase (S_s) provided the best description of the measured BTC (Fig. 3.8). Other model versions provided less than adequate predictions with lower r^2 and higher RMSE (see Table 3.5).

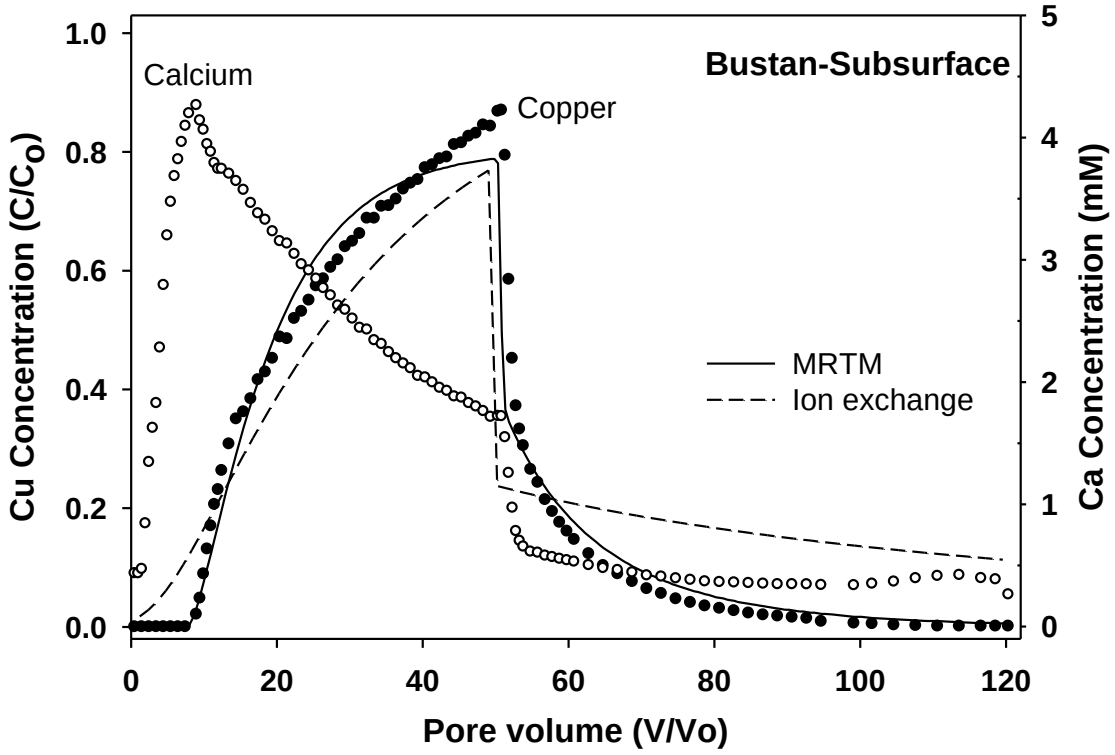

Fig. 3.8. Breakthrough results of Ca and Cu from the Bustan subsurface soil column with a Cu pulse of 59.0 pore volumes. Solid and dashed curves represent multireaction and transport model (MRTM) and ion exchange model simulations, respectively.

As such one may regard S_2 as outer sphere complexation or ion exchange whereas S_s may be considered as a representation of strongly bound Cu via inner sphere complexation. Unlike the simulations for Bustan surface soil, no adjustments of the value of parameter n were required. In all simulations the n value (n = 0.23) used was that from the isotherm shown of Fig. 3.2. Moreover, such BTC prediction is considered adequate and confirms in part earlier work of He et

al. (2006). These authors argued that short-term Cu leaching was likely due to exchange reactions whereas carbonate-bound contribute to long-term Cu release.

The mobility of Cu in the acidic Windsor soil is illustrated by the BTCs shown in Figs. 3.9 and 3.10. The BTC shown in Fig 3.9 which is associated with the short Cu pulse (8.6 pore volumes) appeared narrow with a peak concentration C/C_o of only 0.25. This was followed by gradual decrease in concentration or slow release of retained Cu in the soil during leaching. Moreover, the total amount of Cu recovered in the effluent solution was only 11.4% of that applied. In contrast, for the long Cu pulse application (49.6 pore volumes) resulted in a wide BTC which appeared somewhat symmetrical with a high concentration maxima (C/C_o of 0.9) (see Fig. 3.10). In addition, some 85.8% of the applied Cu in the pulse was recovered in the effluent solution. The high recovery for the BTC shown in Fig. 3.10 was due in part to the fivefold increase in flow velocity when compared to that associated with the short pulse.

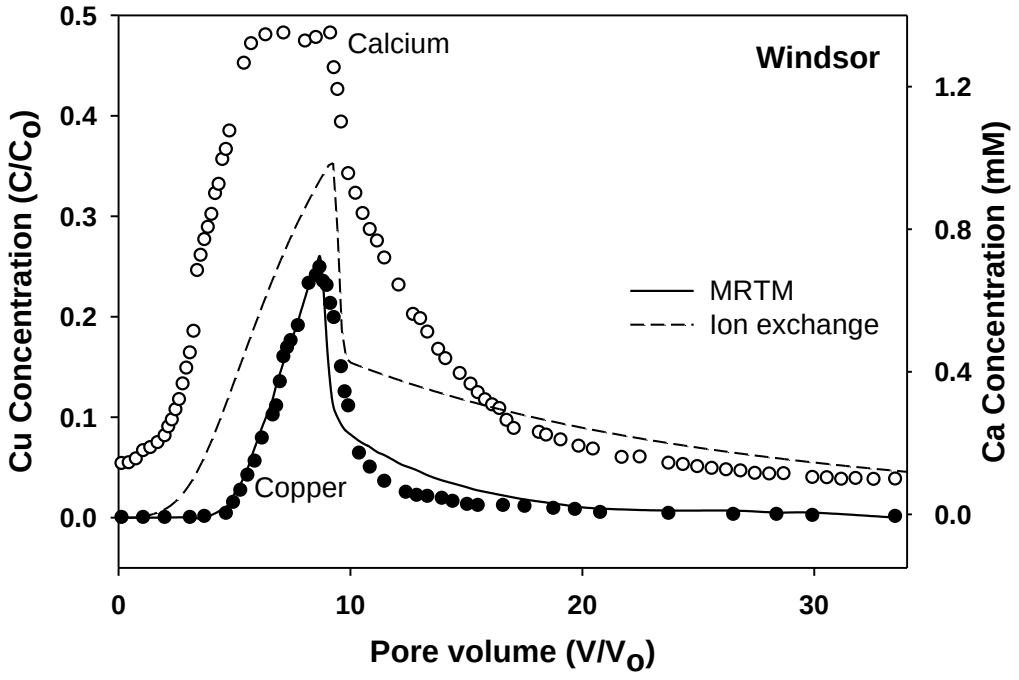

Fig.3.9. Breakthrough results of Ca and Cu from the Windsor soil column with a Cu pulse of 8.6 pore volumes. The multireaction transport model (MRTM) and ion exchange model simulations denoted by solid and dashed curves, respectively.

Table 3.5. Multireaction transport model parameter estimates for Cu transport in Bustan-subsurface and Windsor soils columns: model parameter estimated standard error (SE), root mean square error (RMSE), and coefficient of determination (r^2) values.

Model version†	RMSE	r^2	k_1	SE	k_2	SE	k_3	SE	k_4	SE	k_5	SE	k_{irr}	SE
			----------h^{-1}----------											
Bustan-subsurface (Long pulse)														
M1	0.0647	0.9647	137.818	8.279	0.162	0.013	----	----	----	----	----	----	0.295	0.015
M2	0.0530	0.9702	----	----	----	----	129.109	5.452	0.115	0.007	0.011	0.001	----	----
Windsor Soil (Short pulse)														
M1	0.0382	0.8418	32.903	0.596	0.104	0.001	----	----	----	----	----	----	0.300	0.012
M2	0.0246	0.9110	----	----	----	----	30.7427	0.1506	0.0554	0.0002	0.0077	0.0001	----	----
Windsor Soil (Long pulse)														
M1	0.0412	0.9913	125.190	3.517	0.426	0.013	----	----	----	----	----	----	0.079	0.004
M2	0.0363	0.9922	----	----	----	----	124.236	4.608	0.395	0.018	0.014	0.001	----	----

†:M1 = S_1 and S_{irr} (k_1,k_2, and K_{irr}); M2 = S_2 and S_s (k_3,k_4, and k_5)

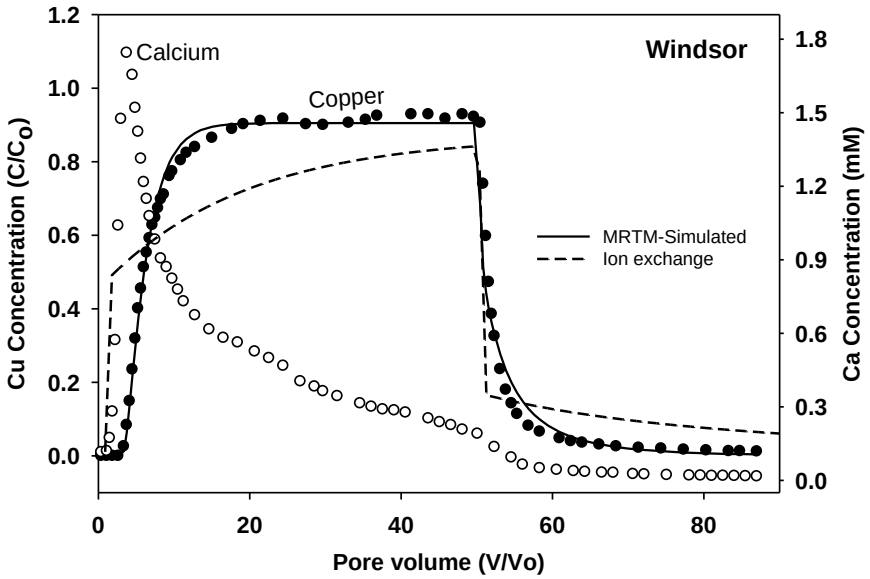

Fig.3.10. Breakthrough results of Ca and Cu from the Windsor soil column with a Cu pulse of 49.6 pore volumes. The multireaction transport model (MRTM) and ion exchange model simulations denoted by solid and dashed curves, respectively.

Numerous studies suggested that for acidic soils such as Windsor soil, Cu retention with Fe and Al oxides are the dominant sorption mechanisms (Chen et al., 1999; Adriano, 2001; Shaheen et al. (2009), among others). The data shown in Fig. 3.9 and 3.10 also indicate that the applied Cu resulted in an increased Ca concentration in the effluent solution followed by extensive tailing or slow release during leaching. Maximum Ca concentrations were observed during Cu pulse application which is likely due to Ca-Cu ion exchange as a primary retention mechanism for acidic soils (Vogeler, 2001).

Simulations using MRTM describing Cu BTCs for Windsor soil columns are illustrated by the curves shown in Figs. 3.9 and 3.10. These model simulations are indications that MRTM provides good predictions of Cu transport regardless of the size of applied input Cu pulse or the flow velocity in the soil columns. Best simulations of the Cu BTCs shown were obtained using version M2 which accounts for a fully reversible kinetic phase (S_2) and irreversible phase (S_s). The estimated model parameters and RMSE and r^2 values are given in Table 3.5. Earlier work of Selim and Ma (2001) suggested that irreversible phase (S_s) was needed in to account for surface

precipitation reactions of Cu on soils with high content of Fe and Al oxides such as our Windsor soil. In contrast, S_{irr} irreversible sites are conceptually representation of direct precipitation from solution. Based on batch kinetic studies, Selim and Ma (2001) concluded that the use of S_s over S_{irr} provided significant improvements in simulation of the kinetic Cu adsorption and release from soils. In this study, there was a significant improvement between goodness-of-fit of MRTM formulations with two different types of irreversible sites (see M1 and M2 in Table 3.5 and Figs. 3.9 and 3.10). Efforts to describe these Cu results based on ion exchange modeling are also shown in Figs. 3.9 and 3.10. These simulations of Cu behavior in Windsor soil are best regarded as an overall approximation. These simulations suggest that improvements in predictions based on ion exchange processes are needed.

In summary, sorption batch and miscible displacement column techniques were used to assess Cu sorption and mobility in an acidic and alkaline soils. Breakthrough results indicate that Cu mobility may be regarded as immobile in the alkaline soil columns when short Cu pulse was applied. A large Cu pulse inputs ($\geq$ 50 pore volumes) resulted in higher Cu mobility in the alkaline soils, with recoveries of 27% and 60% from the surface and subsurface soil columns, respectively. The respective recoveries from the acidic Windsor soil were 11.4% and 85.8% associated with a short and long pulse applications. MRTM was successful in describing the BTCs for all soil columns except those from the surface alkaline soil with high $CaCO_3$ content. Improved predictions were obtained when nonlinear kinetic irreversible reaction was incorporated into the MRTM model.

3.5 References

Adriano, D.C. 2001. Trace elements in terrestrial environments: biogeochemistry, bioavailability and risk of metals. 2nd ed. Springer, New York.

Alloway, B.J. 1995. The origins of heavy metals in soils. p. 38–57.*In*: Alloway, B.J. (ed.), Heavy metals in soils. Blackie Academic and Professional, London, UK.

Baker, D.E., and J.P. Senft. 1995. Copper. p. 179–205. *In* Alloway, B.J. (ed.) Heavy metals in soils. Blackie Academic & Professional, London, UK.

Bakr, N., M.H. Bahnassy, M.M. El-Badawi, G.W. Ageeb, and D.C. Weindorf. 2009. Land capability evaluation in newly reclaimed areas: A case study in Bustan 3 area, Egypt. Soil Surv. Horiz. 50:90–95.

Brusseau, M.L., R.E. Jessup, and P.S.C. Rao. 1992. Modeling solute transport influenced by multiprocess nonequilibrium and transformation reactions. Water Resour. Res. 28:175–182.

Buchter, B., B. Davidoff , M.C. Amacher, C. Hinz, I.K. Iskander, and H.M. Selim. 1989. Correlation of Freundlich K_d and *n* retention parameters with soils and elements. Soil Sci. 148:370–379.

Chang, C. M., M. K. Wang, T. W. Chang, and C. Lin. 2001. Transport modeling of copper and cadmium with linear and nonlinear retardation factors. Chemosphere 43:1133–1139.

Chen, M., L.Q. Ma, and W.G. Harris. 1999. Baseline concentrations of 15 trace elements in Florida surface soils. J. Environ. Qual. 28: 1173–1181.

Elzinga, E.J. and R.J., Reeder. 2002. X-ray absorption spectroscopy study of Cu^{2+} and Zn^{2+} adsorption complexes at the calcite surface: implications for site specific metal incorporation preferences during calcite crystal growth. Geochimica et Cosmochimica Acta. 66: 3943-3954.

Emmerich, W.E., L.J. Lund, A.L. Page, and A.C. Chang. 1982. Solid phase forms of heavy metal in sewage sludge-treated soils. J. Environ. Qual. 11:178–181.

Epstein, L. and S. Bassein. 2001. Pesticide applications of copper on perennial crops in California, 1993 to 1998. J. Environ. Qual. 30:1844–1847.

Florido, A., C. Valderrama, J. A. Arevalo, I. Casas, M. Martinez, and N. Miralles. 2010. Application of two sites non-equilibrium sorption model for the removal of Cu(II) onto grape stalk wastes in a fixed-bed column. Chem. Eng. J., 156: 298–304.

Harter, R.D., and R. Naidu. 2001. An assessment of environmental and solution parameter impact on trace-metal sorption by soils. Soil Sci. Soc. Am. J. 65:597–612.

He, Z.L., M. Zhang, X.E. Yang, and P.J. Stoffella. 2006. Release behavior of copper and zinc from sandy soils. Soil Sci. Soc. Am. J. 70:1699–1707.

Holmgren, G.G.S., M.W. Meyer, R.L. Chaney, and R.B. Daniels. 1993. Cadmium, zinc, copper and nickel in agricultural soils in the United States of America. J. Environ. Qual. 22:335–348.

Kabata-Pendias, A., and H. Pendias. 2001. Trace elements in soils and plants. 3rd ed. CRC Press, Boca Raton, FL.

Kabata-Pendias, A., and W. Sadurski. 2004. Trace elements and compounds in soil. p. 79–99. *In* E. Merian et al. (ed.) Elements and their compounds in the environment. Wiley-VCH, Weinheim, Germany.

Kaufmann, G., and W. Dreybrodt. 2007. Calcite dissolution kinetics in the system $CaCO_3$–H_2O–CO_2 at high undersaturation. Geochim. Cosmochim. Ac. 71:1398-1410.

Liao, L., H.M. Selim, and R.D. DeLaune. 2009. Mercury adsorption–desorption and transport in soils. J. Environ. Qual. 38:1608–1616.

Ma, Y., E. Lombi, A.L. Nolan, and M.J. McLaughlin. 2006. Short-term natural attenuation of copper in soils: effect of time, temperature, and soil characteristics. Environ Toxic Chem. 25:652–658.

Mathur, S. P., R.B. Sanderson, A. Belanger, M. Valk, E.N. Knibbe, and C.M. Preston. 1984. The effect of copper applications on the movement of copper and other elements in organic soils. Water Air Soil Pollut. 22:277-288.

Mermut, A.R., J.C. Jain, S. Li, R. Kerrich, L. Kozak, and S. Jana. 1996. Trace element concentrations of selected soils and fertilizers in Saskatchewan, Canada. J. Environ. Qual. 25:845–853.

Pansu, M., and J. Gautheyrou. 2006. Handbook of soil analysis: Mineralogical, organic and inorganic methods. Springer-Verlag, Berlin.

Pietrzak U. and D.C. McPhail. 2004. Copper accumulation, distribution and fractionation in vineyard soils of Victoria, Australia, Geoderma. 122:151–166.

Plummer, L.N., T.M. Wigley, and D.L. Parkhurst. 1978. The kinetics of calcite dissolution in CO_2 systems at 5° to 50°C and 0.0 to 1.0 atm CO_2. Am. J. Sci. 278:179-216.

Ponizovsky, A. A., H. E. Allen, and A. J. Ackerman. 2007. Copper activity in soil solutions of calcareous soils. Environ. Pollut. 145:1–6.

Selim, H.M. 1992. Modeling the transport and retention of inorganics in soils. Adv. Agron. 47:331–384.

Selim, H. M., and M. C. Amacher. 1997. Reactivity and Transport of Heavy Metals in Soils. CRC,Boca Raton, FL (240 p).

Selim, H.M., B. Buchter, C. Hinz, and L.W. Ma. 1992. Modeling the transport and retention of cadmium in soils: Multireaction and multicomponent approaches. Soil Sci. Soc. Am. J. 56:1004–1015.

Selim, H.M., G.R. Gobran, X. Guan, and N. Clarke. 2004. Mobility of sulfate in forest soils: Kinetic modeling. J. Environ. Qual. 33: 488-495.

Selim, H.M., and L. Ma. 2001. Modeling nonlinear kinetic behavior of copper adsorption-desorption in soil. p. 189–212. *In* H.M. Selim and D.L. Sparks (ed.) Physical and

chemical processes of water and solute transport/retention in soil. SSSA Special publication no. 56. SSSA, Madison, WI.

Shaheen, S. M., C. D. Tsadilas, T. Mitsibonas, and M. Tzouvalekas. 2009. Distribution coefficient of copper in different soils from Egypt and Greece. Commun. Soil Sci. Plant Anal. 40: 214–226.

Sparks, D.L. 2003. Environmental soil chemistry. 2nd ed. Academic Press, San Diego, CA.

Suarez, D L, and J Simunek. 1997. Unsatchem: unsaturated water and solute transport model with equilibrium and kinetic chemistry. Soil Sci. Soc. Am. J. 61:1633–1646.

Tessier, A., P.G.C. Campbell, and M. Bisson. 1979. Sequential extraction procedure for the speciation of particulate trace metals. Anal. Chem. 51:844–851.

Toride, N., F.J. Leij, and M.Th . van Genuchten. 1999. The CXTFIT code for estimating transport parameters from laboratory or field tracer experiments, version 2.1. Res. Rep. 137. U.S. Salinity Lab., Riverside, CA.

Vogeler, I. 2001. Copper and calcium transport through an unsaturated soil column. J. Environ. Qual. 30:927–933.

Wang, Y., Y. Cuia, D. Zhou, S. Wang, A. Xiao, R. Wang, and H. Zhang. 2009. Adsorption kinetics of glyphosate and copper (II) alone and together on two types of soils. Soil Sci. Soc. Am. J.

Xiaorong, W., H. Mingde, and S. Mingan. 2007. Copper fertilizer effects on copper distribution and vertical transport in soils. Geoderma. 138: 213–220.

Zhang, H., and H.M. Selim. 2006. Modeling the transport and retention of arsenic(V) in soils. Soil Sci. Soc. Am. J. 70:1677–1687.

Zhou, L., and H.M. Selim. 2001. Solute transport in layered soils: nonlinear and Kinetic Reactivity. Soil Sci. Soc. Am. J. 65:1056–1064.

CHAPTER 4. COPPER TRANSPORT IN CALCAREOUS SOILS: SECOND-ORDER MODELING[3]

4.1 Introduction

The reactivities of heavy metals and their transport in the soil profile play a significant role in their bioavailability and leaching losses beyond the root zone. Soil contamination by heavy metals from mining, industrial, agricultural, and geological sources poses a serious risk because of their high toxicity to human health as well as negative environmental impact on the ecosystem. Transport of toxic metals in the vadose zone and aquifers may lead to further contamination of surface and groundwater (National Research Council, 2003).

Copper exhibits a strong affinity to various soil constituents such as organic matter, clay minerals, and metal hydroxides with varying strengths (Adriano, 2001; Kabata-Pendias and Sadurski, 2004; Han, 2007). Copper in a calcareous soil is found primarily in nonexchangeable form and possibly adsorbed on surfaces as hydroxy or hydroxycarbonate species (McBride and Bouldin, 1984). Rodriguez-Rubio et al. (2003) suggested that Cu was preferentially retained in calcareous soils through precipitation of CuO, $Cu_2(OH)_2CO_3$, or $Cu(OH)_2$ and by adsorption on soil carbonates. Elzinga and Reeder (2002) used extended x-ray absorption fine-structure (EXAFS) spectroscopy to characterize Cu adsorption complexes at the calcite surface. They observed that Cu occupied Ca sites in the calcite structure and formed inner sphere Cu adsorption complexes at calcite surfaces. The EXAFS results revealed that the precipitation of malachite [$Cu_2(OH)_2CO_3$] did not take place in Cu–calcite suspensions at Cu concentration of 5.0 and 10.0 μmol L^{-1}.

Heavy metal retention is commonly associated with the release of divalent cations such as Ca and Mg (Madrid and Diaz-Barrientos, 1992; Wang et al., 2009). In calcareous soils,

[3] This reprint originally appeared as, Elbana, T.A. and H. M. Selim. 2012. Copper transport in calcareous soils: miscible displacement experiments and second-order modeling. Vadose Zone J. 11(2). "Reprinted by Permission, ASA, CSSA, SSSA."

Ponizovsky et al. (2007) found that Cu retention is accompanied by the release of Ca, Mg, Na, and H cations in the soil solution and that the total amount of cations released was equal to the amount of Cu sorbed. Moreover, they observed that carbonates exhibited stronger binding for Cu than soil organic matter. Describing the release of cations such as Ca in the presence of carbonates has not been successful. Goldberg et al. (2007) concluded that surface complexation modeling approaches were not successful for the prediction of Se(IV) adsorption when the soil contained >1.6% inorganic C. Elzahabi and Yong (2001) concluded that at high pH and carbonate contents, heavy metals retained in the soil were mainly as carbonate salts. When the pH of the soil decreases, carbonate dissolution increases and ionic exchange becomes the principal retention mechanism of heavy metals.

Several studies have attempted to model Cu reactivities and transport in soils. For example, He et al. (2006) found that the release of Cu at short times was probably due to the exchangeable fraction. In contrast, long-term leaching experiments showed that the exchangeable and carbonate-bound fractions were the primary contributors to Cu release. Selim and Ma (2001) investigated the adsorption of Cu with time for a wide range of input Cu concentrations. They also quantified the desorption and the hysteretic effect of Cu release in soils. They found that the use of multiple reaction approaches such as SOTS and the multireaction model were capable of describing the observed nonlinear kinetic behavior of Cu in soils during adsorption as well as during desorption. Tsang and Lo (2006) showed that a first-order, two-site nonequilibrium model, with one site representing instantaneous sorption and the other rate-limited sorption, provided better simulation of Cu BTCs than an equilibrium transport model.

Lafuente et al. (2008) quantified the competitive mobility of six metals—Cr, Cu, Pb, Ni, Zn, and Cd—in columns having $CaCO_3$ contents ranging between 5.9 and 12.0%. They found that >90% of all applied heavy metals were retained by the soil. They also found that Cu was less

mobile than Ni and Cd. In a recent study, Sayyad et al. (2010) used undisturbed 50-cm columns to quantify the mobility of Cu, Cd, Pb, and Zn in soils having $CaCO_3$ contents ranging from 35.6 to 37.6%. Their BTCs results indicated that Cu was more mobile than Zn and Pb.

A literature search revealed that several studies have been conducted to investigate Cu mobility and release in acidic as well as alkaline soils (Sidle et al., 1977; Zhu and Alva, 1993; Chang et al., 2001; Bang and Hesterberg, 2004; Wang et al., 2009; Sayyad et al., 2010). Only a few studies, however, aimed at modeling Cu transport in soils, especially alkaline calcareous soils, have been done. In this study, we focused on quantifying the mobility and retention of Cu in calcareous soils based on miscible displacement column experiments.

Specifically, our objectives were:

i. to quantify the transport and retention of Cu in calcareous soils,

ii. to assess how carbonates removal from soil enhances mobility of Cu,

iii. to assess the capability of two modeling approaches (SOTS and CXTFIT) in describing the mobility of Cu, and

iv. to simulate the distribution of Cu with soil depth with and without the presence of $CaCO_3$.

4.2 Second-Order Two-Site Model

Basic to the second-order formulation is the assumption that a limited number of sites are available for solute adsorption in soils. As a result, the reaction rate is a function of the solute concentration in the soil solution and the availability of adsorption sites on soil matrix surfaces. Specifically, retention mechanisms are assumed to depend on the number of sites (ϕ) that are available for solute adsorption in soils (Selim and Amacher 1997; Zhang and Selim, 2011). The model also assumes that a fraction of the total sorption sites is rate limited, while the remaining fractions interact rapidly or instantaneously with the solute in the soil solution. The sorbed

phases S_e, S_k, and S_{irr} are in direct contact with the solute in the solution phase (C) and are governed by concurrent reactions (see Fig. 4.1). Specifically, C is assumed to react rapidly and reversibly with the equilibrium phase S_e. The relations between C and S_k and S_{irr} are governed by reversible nonlinear and irreversible linear kinetic reactions, respectively. A second irreversible reaction was assumed as a consecutive reaction of the S_k phase into a less accessible or strongly retained phase S_s. Therefore, the model formulation can be expressed as

$$S_e = K_e \theta\ C\ \varphi \qquad [4.1]$$

$$\frac{\partial S_k}{\partial t} = k_1 \theta\ C\ \varphi - (k_2 + k_3) S_k \qquad [4.2]$$

$$\frac{\partial S_s}{\partial t} = k_3 S_k \qquad [4.3]$$

$$\rho \frac{\partial S_{irr}}{\partial t} = k_{irr}\ \theta\ C \qquad [4.4]$$

Here ϕ is related to the sorption capacity (S_{max}) by:

$$S_{max} = \varphi + S_e + S_k + S_s + S_{irr} \qquad [4.5]$$

where ϕ and S_{max} (μg solute g^{-1} soil) are the unoccupied (or vacant) and total sorption sites on soil surfaces, respectively. The total sorption sites S_{max} was considered as an intrinsic soil property and is time invariant. In addition, S_e is the amount retained on equilibrium-type sites (μg g^{-1}), S_k is the amount retained on kinetic-type sites (μg g^{-1}), S_s is the amount retained irreversibly by consecutive reaction (μg g^{-1}), and S_{irr} is the amount retained irreversibly by a concurrent type of reaction (μg g^{-1}). The reaction rate coefficients are K_e (mL μg^{-1}), k_1 (mL μg^{-1} h^{-1}), k_2 (h^{-1}), k_3 (h^{-1}), and k_{irr} (h^{-1}), while C is the solute concentration (μg mL^{-1}), θ is the volumetric water content (mL mL^{-1}), and t is the reaction time (h).

At any time t, the total amount of solute sorbed by the soil matrix, S, can be expressed as

$$S = S_e + S_1 + S_2 + S_s + S_{irr} \qquad [4.6]$$

The above reactions were incorporated into the advection–dispersion equation (ADE) as

$$\theta \frac{\partial C}{\partial t} + \rho \frac{\partial S}{\partial t} = \frac{\partial}{\partial x}\left(D\theta \frac{\partial C}{\partial x}\right) - q \frac{\partial C}{\partial x} \qquad [4.7]$$

where x is distance (cm), D is the hydrodynamic dispersion (cm^2 h^{-1}), ρ is the bulk density of the soil (g mL^{-1}), and q is steady Darcy's water flux density (cm h^{-1}). For the reactive transport of Cu in soils, the second term in Eq. [4.7], $\partial S/\partial t$, was accounted for using the second-order approach described above in Eq. [4.1–4.5].

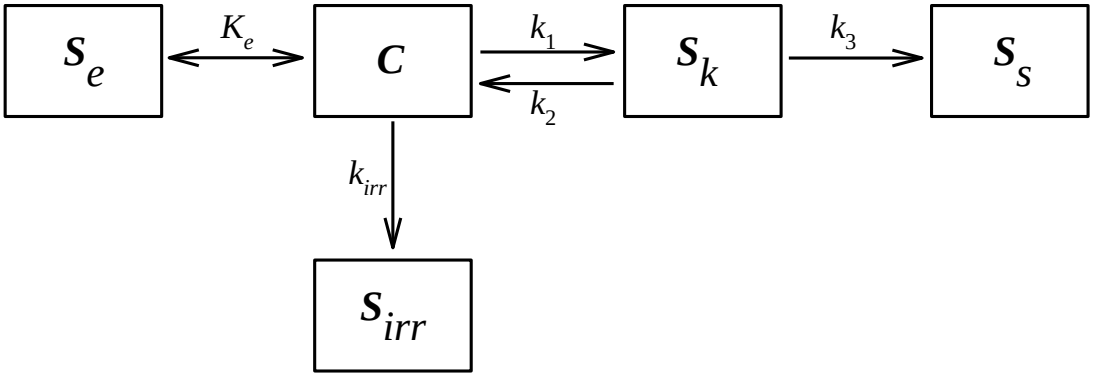

Fig. 4.1. A schematic of the second-order, two-site (SOTS) model for retention of reactive chemicals in soils, where C is the solute in the solution phase, S_e is the amount retained on equilibrium-type sites, S_k is the amount retained on kinetic-type sites, S_s is the amount retained irreversibly by consecutive reaction, S_{irr} is the amount retained irreversibly by concurrent type of reaction, and K_e, k_1, k_2, k_3, and k_{irr} are reaction rates.

A finite difference (Crank–Nicholson forward–backward) method was used to provide numerical solutions of the transport equation subject to a solute-free initial condition:

$$C(x, t = 0) = 0 \qquad [4.8]$$

and upper and lower boundary conditions:

$$vC - D\frac{\partial C}{\partial x}|_{(x=0,t)} = \begin{cases} vC_o & 0<t\leq t_o \\ 0 & t>t_o \end{cases} \qquad [4.9]$$

$$\frac{\partial C}{\partial x}(x = L, t) = 0 \qquad [4.10]$$

where C_o is the input Cu concentration (μg mL^{-1}), t_o is the duration of the Cu input pulse (h), L is the length of the soil column (cm), and v (cm h^{-1}) is the pore water velocity (q/θ). The kinetic retention processes of the SOTS model (Eq. [4.1–4.5]) were solved using the fourth-order

Runge–Kutta method. The BTC data from column experiments were fitted to the models described above using the Levenberg–Marquardt nonlinear least square optimization method (Press et al., 1992). Statistical criteria used for estimating the goodness-of-fit of the models to the data were the coefficients of determination, r^2, and the root mean square error (RMSE):

$$RMSE = \sqrt{\frac{\sum(C_{ops}-C)^2}{n_o-n_p}} \qquad [4.11]$$

where C_{ops} is the observed Cu concentration at time t, C is the simulated Cu concentration at time t, n_o is the number of measurements, and n_p is the number of fitted parameters.

We also utilized a linear model to describe Cu transport from the miscible displacement column experiments. Specifically, we used CXTFIT as described by Toride et al. (1999). This analytical model was utilized to solve the inverse problem based on the ADE where linear equilibrium sorption was assumed. To account for irreversible reactions of Cu in soils, the CXTFIT version selected included a sink term, which was referred to as first-order degradation or decay in CXTFIT. The ADE used after the incorporation of a first-order decay (sink) term is

$$R\frac{\partial C}{\partial t} = D\frac{\partial^2 C}{\partial z^2} - v\frac{\partial C}{\partial z} - \mu C \qquad [4.12]$$

where R is a dimensionless retardation factor ($R = 1 + \rho K_d/\theta$) and K_d is a partitioning coefficient (mL g^{-1}). In Eq. [4.12], the term R accounts for linear equilibrium sorption. The rate coefficient μ (h^{-1}) associated with the sink term (μC) captures irreversible retention (or removal) of a chemical directly from the soil solution based on first-order decay. Because heavy metals such as Cu do not undergo decay or degradation, we consider this term to be for irreversible retention in a similar manner or equivalent to that associated with k_{irr} (Eq. [4]) of the SOTS model (see also Fig. 4.1). To obtain model simulations of Cu transport in soil columns, CTXFIT was utilized to obtain parameter estimates (R and μ) that provided the best fit of the model to the experimental BTCs.

4.3 Materials and Methods

The soil selected for this study was Bustan soil (a Typic Torripsamment) located in the northwestern desert of Egypt. Soil samples from this alkaline soil were collected from surface (0–40 cm) and subsurface (40–75 cm) layers. Selected chemical properties including pH, organic matter, cation exchange capacity, and total carbonate equivalent for these soil layers are given in Table 4.1. In addition, sodium citrate–dithionite was used to extract oxides and hydroxides of Fe, Al, and Mn (Loeppert and Inskeep, 1996).

Table 4.1. Selected physiochemical properties of the soils used in this study.

	Bustan-surface soil	Bustan-subsurface soil
pH (1 :2.5)	9.22	9.44
Organic matter (g Kg^{-1})	0.66	0.13
Cation exchange capacity (cmol kg^{-1})	5.60	4.84
$CaCO_3$ (%)	2.76	1.18
Citrate-bicarbonate-dithionite (CBD)		
Fe g kg^{-1}	4.175	1.261
Al g kg^{-1}	0.986	0.353
Mn g kg^{-1}	0.200	0.042

4.3.1 Sorption

Adsorption of Cu was studied using the batch method described by Selim and Amacher (1997). Triplicate 3-g samples of each soil were placed in 40-mL polypropylene tubes and mixed with 30-mL solutions of known Cu concentrations. Ten initial Cu concentrations (C_o) (0.05, 0.10, 0.20, 0.53, 1.02, 2.10, 4.4, 6.3, 9.4, and 12.6 mmol L^{-1}) were used. Reagent-grade $Cu(NO_3)_2$ was prepared in 0.005 mol L^{-1} KNO_3 background solution. The samples were shaken at 150 rpm on a reciprocal shaker for 24 h and subsequently centrifuged for 10 min at 1300 xg. A 5-mL aliquot was sampled from the supernatant and the collected samples were analyzed for total Cu concentration using inductively coupled plasma–atomic emission spectrometry (ICP–AES; Spectro Citros CCD). The fraction of Cu adsorbed by the soil was calculated based on the change in concentration in the solution (before and after each adsorption). We also conducted a

similar batch study with surface soil after removal of the carbonates present in the soil. Carbonate removal was performed using NaOAc at pH 5 as described by Kunze and Dixon (1986).

4.3.2 Miscible Displacement Experiments

To quantify the mobility of Cu in the Bustan soil, column experiments were also performed using the miscible displacement technique as described by Selim and Amacher (1997). Acrylic columns (5 cm in length and 2.62-cm i.d.) were uniformly packed with air-dry soil and were slowly water saturated with a background solution of 0.005 mol L^{-1} KNO_3 where upward flow was maintained. Constant flux was controlled by a piston pump (Fluid Metering Inc. lab pump, Model QG6), with some 20 pore volumes of the background solution applied at a constant flow rate. Following saturation, a pulse having a concentration of 3.15 mmol L^{-1} Cu $(NO_3)_2$ in 0.005 mol L^{-1} KNO_3 background solution was applied to each soil column. The volume of the applied Cu pulse and the physical parameters for each soil column (e.g., moisture content, θ, and bulk density, ρ) are given in Table 4.2. The Cu pulse input was subsequently eluted by at least 20 pore volumes of 0.005 mol L^{-1} KNO_3 solution. Effluent samples were collected using an ISCO fraction collector. Concentrations of Cu and Ca in the collected effluent samples from each miscible displacement column experiment were analyzed by ICP–AES (Spectro Citros CCD). These miscible displacement experiments were performed on both soil layers as well as on the surface layer after carbonate removal.

Table 4.2. Soil physical and experimental conditions of the miscible displacement columns experiments.

Matrix	Bulk density (ρ, g mL^{-1})	Moisture content (θ, mL mL^{-1})	Pore water velocity (cm h^{-1})	Pulse input (Pore volumes)		Dispersion coefficient (D, cm^2 h^{-1})
				^3H_2O	Cu	
Surface	1.70	0.36	4.610	1.87	59.01	0.863±0.049
Subsurface	1.74	0.34	4.982	1.95	49.83	1.207±0.095
Surface (carbonates removed)	1.78	0.33	5.061	2.43	54.66	2.344±0.109

To obtain independent estimates of the dispersion coefficient (*D*), separate pulses of a tracer solution were applied to each soil column subsequent to the Cu pulse applications. The tracer used was tritium (^3H_2O) and the collected samples were analyzed using a Tri-Carb liquid scintillation β counter (Packard-2100 TR). Estimates for *D* values were obtained using CXTFIT (Toride et al., 1999) and are given in Table 4.2. Values of *D* were subsequently used in the SOTS model to predict Cu transport in the different soil columns. Following the leaching of the applied Cu pulse, the soil column was sectioned into 1-cm increments and Cu retained by the soil was determined using four chemical sequential extractions: exchangeable, oxidizable, carbonate and oxide associated, and strongly bound (Emmerich et al., 1982). For the exchangeable phase, 25 mL of 0.5 mol L^{-1} KNO_3 was added to the soil and shaken for 16 h. For the oxidizable phase, 25 mL of 0.5 mol L^{-1} NaOH was added and shaken for 16 h. Similarly, 25 mL of 0.05 mol L^{-1} Na_2EDTA as a nonspecific reagent was used for the fraction associated with carbonates and oxides (Gismera et al., 2004). The strongly bound Cu fraction was determined from extraction with 23 mL of 4 mol L^{-1} HNO_3 for 16 h at 70 to 80°C.

4.4 Results and Discussion

4.4.1 Sorption Isotherms

The results of the batch equilibration experiments are shown in Fig. 4.2 and reflect the differences in Cu affinities between the surface and subsurface Bustan soil. These isotherms, which show the concentration in soil solution *C* vs. the amount sorbed by the soil matrix *S*, are highly nonlinear and illustrate strong Cu sorption. The Freundlich equation was utilized to describe the adsorption isotherms:

$$S = K_f C^b \qquad [4.13]$$

where *S* is the amount sorbed (μg g^{-1}), K_f is the Freundlich distribution coefficient (mL g^{-1}), and *b* is a dimensionless reaction order. The surface soil exhibited the highest affinity for Cu, with a

K_f value of 5226 mL g^{-1} and b = 1.255 (see Table 4.3). For the subsurface soil, Cu retention was much lower than for the surface soil, with a K_f of 755.5 mL g^{-1} and b = 0.233. When the carbonates were removed from the surface soil, Cu sorption decreased significantly (K_f of 83.7 mL g^{-1} and b = 0.418), which illustrates the dominant contribution of the carbonate fraction to Cu sorption. These results are consistent with the recent work of Shaheen et al. (2009) on Egyptian soils, which showed a b value of 0.93 for Cu adsorption in a calcareous soil and a b of 0.19 for a sandy soil with low carbonate content.

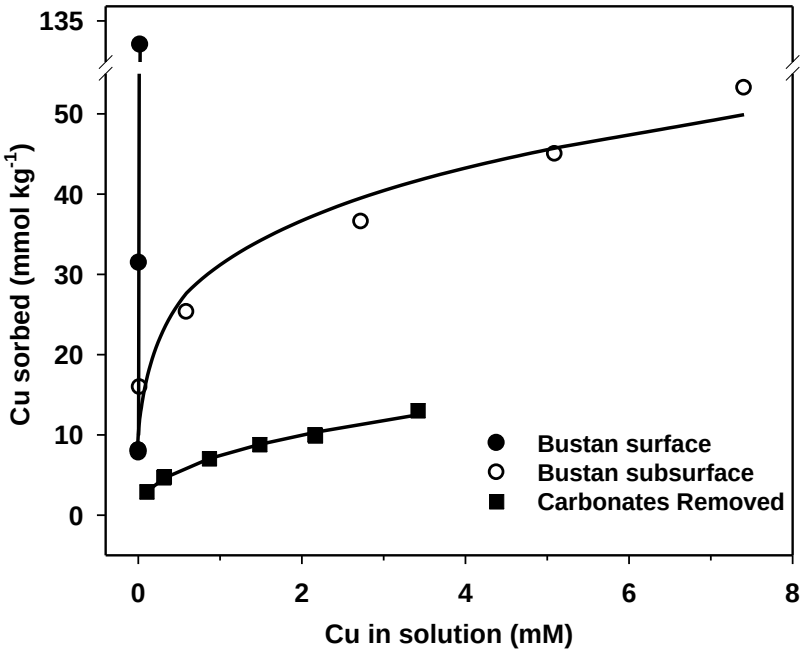

Fig. 4.2. Copper adsorption isotherms for Bustan surface soil, subsurface soil, and surface soil after removal of carbonate. The solid curves are Freundlich model calculations.

Table 4.3. Estimated Freundlich and Langmuir parameters and their standard errors (SE) for Cu retention by the different soils.

Soil	----------Freundlich model†----------			---------Langmuir Model‡---------		
	K_f (mL g^{-1})	b	r^2	S_{max} (μg g^{-1})	K_L (mL μg^{-1})	r^2
Surface	5226.4±165.7	1.255±0.090	0.992	NA§	NA	NA
Subsurface	755.5±124.7	0.233±0.030	0.972	3436±460	0.019±0.011	0.906
Surface (carbonates removed)	83.7±8.4	0.418±0.021	0.975	902.3±63.8	0.021±0.005	0.912

† K_f Freundlich adsorption coefficient; b, reaction order. ‡ S_{max}, adsorption maximum; K_L, Langmuir coefficient related to binding strength. § NA, estimation Langmuir parameter was not applicable for the surface soil

The adsorption isotherms of Fig. 4.2 were also described using the Langmuir equation:

$$S = \frac{S_{max} K_L C}{1 + K_L C} \qquad [4.14]$$

where S_{max} is the sorption capacity (μg g^{-1}) and K_L (mL μg^{-1}) is a Langmuir coefficient related to the binding strength. The use of the Langmuir isotherm for the surface soil was not successful. For the subsurface soil and for the surface soil when carbonates were removed, however, the use of the Langmuir model was successful (see Table 4.3). The Langmuir isotherm is derived by assuming a finite number of uniform adsorption sites and the absence of lateral interaction between adsorbed species; both assumptions are violated in soils particularly at high solution metal concentrations (Goldberg and Criscenti, 2008). The sorption capacity for the subsurface soil was about four times higher (S_{max} = 3436 ± 460 μg g^{-1}) than the surface soil with carbonates removed (S_{max} = 902 ± 63 μg g^{-1}). These results indicate that the fraction of Cu is probably sorbed specifically onto the $CaCO_3$ constituent.

4.4.2 Copper Transport

Copper BTCs, shown in Fig. 4.3 and 4.4, exhibited a gradual decrease in concentration during leaching or desorption (right side of the BTCs) as well as asymmetry of the BTCs from the calcareous soil layers. The slow release during leaching and the lack of a sharp front of the sorption side of the BTCs are features indicative of kinetic reactivities of Cu in these soils, where reversible and irreversible sorption may be dominant. In addition, incomplete Cu breakthrough was obtained from the two columns, i.e., <100% recovery of the Cu applied.

For the Bustan surface soil, after leaching with some 40 pore volumes, the Cu recovery in the effluent was only 27% of that applied. Such low Cu recovery in the effluent was not surprising for this calcareous surface soil, as evidenced by the strong Cu retention exhibited by adsorption from the batch experiments. Other features of strong Cu retention by the surface layer

include extensive retardation, as depicted by the delayed arrival of Cu in the effluent solution (14 pore volumes), and a peak concentration C/C_o of only 0.415. The Cu BTC for the Bustan subsurface soil layer indicated less retardation than that observed for the surface layer. Specifically, Cu arrival in the effluent was detected after eight pore volumes, with a peak concentration (C/C_o) of 0.87.

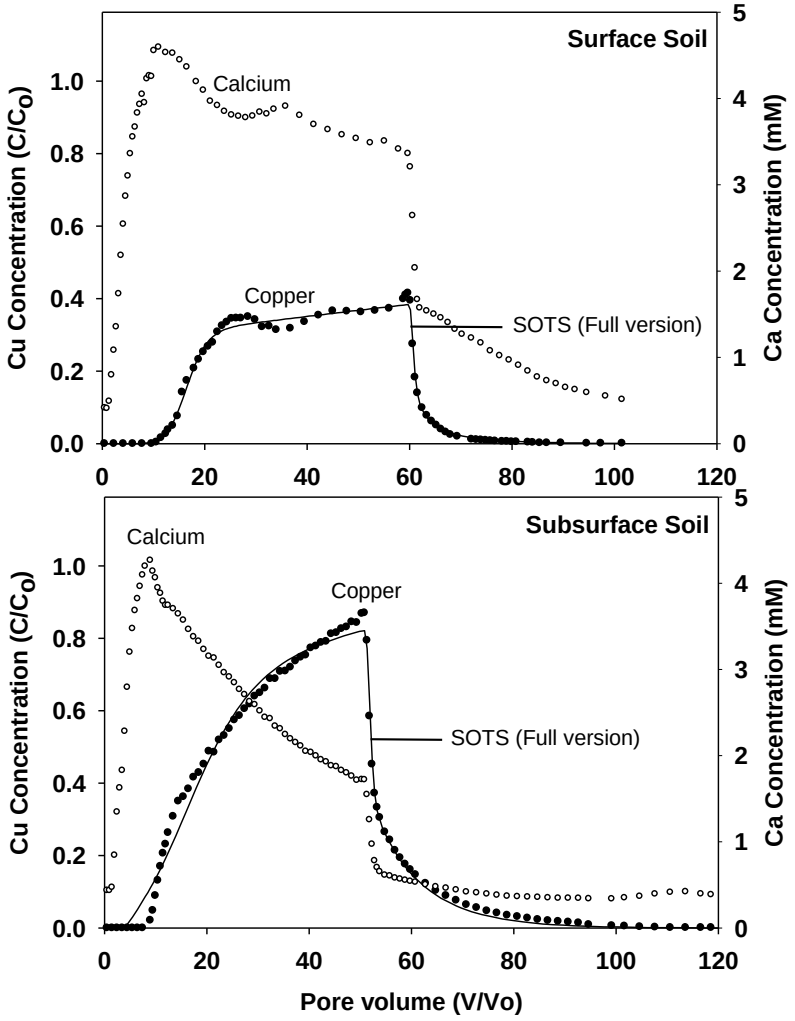

Fig. 4.3. Breakthrough results of Cu and Ca from surface soil (top) and subsurface soil (bottom). Solid curves are simulations using the second-order, two-site (SOTS) model version V1 (full model).

Based on the area under the curve, the amount of Cu recovery in the effluent for the subsoil was 60% of that applied, compared with only 27% for the surface layer. These BTC results are consistent with earlier retention findings illustrated by the isotherms of Fig. 4.2.

Because the experiment results in Fig. 4.3 show strong retardation of Cu breakthrough in the effluent accompanied by slow release during leaching, the use of models that account for reversible and irreversible processes is justified. The solid curves in Fig. 4.3 are simulations using the SOTS model.

The SOTS model accounts for equilibrium and kinetic reversible mechanisms as well irreversible reactions of reactive solutes in soils. Comparison of calculated BTCs and measured Cu effluent concentrations illustrates the capability of the SOTS model in predicting Cu mobility in the surface and subsurface columns (Fig. 4.4). Model calculations well described the adsorption (left) side as well as the leaching or desorption sides of Cu transport for both soils. The goodness of model simulations given by r^2 and the total sum of RMSEs is supportive of the SOTS model in describing the measured Cu results (see Table 4.4). In fact, high r^2 values (>0.99) and low RMSE values were realized for both soils. The associated model parameters (K_e, k_1, k_2, k_3, k_{irr}, and S_{max}) along with their standard errors of estimates are also presented in Table 4.4.

Because Cu recoveries in the effluent from the calcareous surface and subsurface Bustan soil columns were limited to 27 and 60% of the amount applied, a significant amount of Cu was strongly sorbed. Irreversible or slowly reversible reactions are the likely mechanisms for strongly sorbed Cu in these soils. As shown in Fig. 4.1, the SOTS model accounts for irreversible retention in two ways. One is a concurrent irreversible reaction (S_{irr}) and the second is a consecutive irreversible reaction (S_s). In the simulations shown in Fig. 4.3, we utilized the full model (Version 1, V1) which accounts for both irreversible mechanisms. In Fig. 4.4, the simulations shown were obtained with only the consecutive irreversible phase accounted for (i.e., $k_{irr} = 0$). This model version (V2) produced equally good results when compared with simulations based on the full version (V1) shown in Fig. 4.3. Other model versions were

calculated including the concurrent model (V3) (BTCs not shown). Based on the overall descriptions of the BTCs as well as r^2 and RMSE values, none of these versions produced equally good description of Cu BTCs as those of V1 and V2. The associated model parameters for all model versions examined (K_e, k_1, k_2, k_3, k_{irr}, and S_{max}) along with their standard errors of estimates are given in Table 4.4.

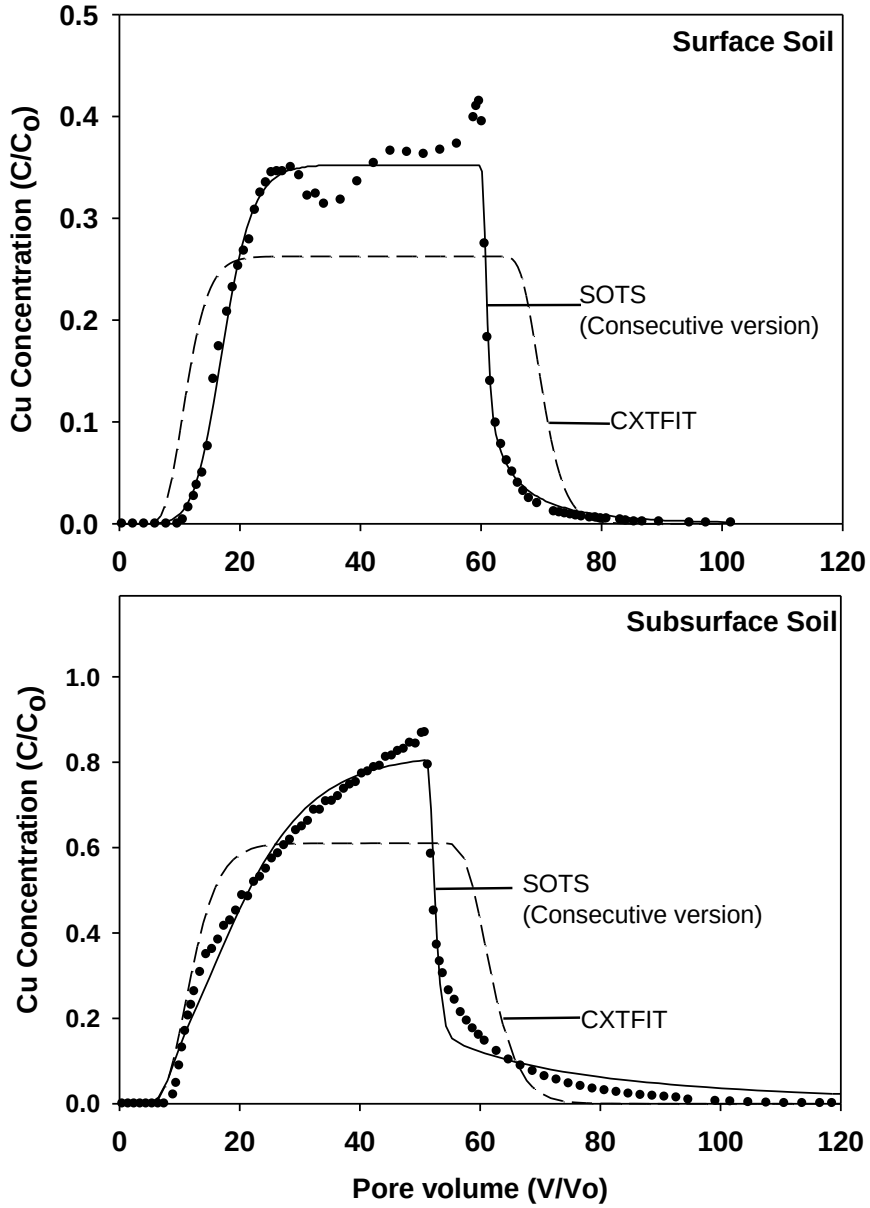

Fig. 4.4. Breakthrough results of Cu from surface soil (top) and subsurface soil (bottom). Solid curves are simulations using the consecutive version (V2 using the amount retained on equilibrium-type sites, *Se*, the amount retained on kinetic-type sites, S_k, and the amount retained irreversibly by consecutive reaction, S_s) of the second-order, two-site (SOTS) model. Dashed curves represent CXTFIT simulations.

We should emphasize that for surface and subsurface soil columns, model versions V1 and V2 provided a good description of the Cu BTCs shown in Fig. 4.3 and 4.4 and that of the amount irreversibly sorbed. Based on model simulations, 96 and 99% of the amount sorbed was accounted for in the consecutive phase (S_s) using V1 and V2, respectively. Such a finding is consistent with that of Selim and Ma (2001), who successfully used the SOTS model to describe Cu sorption–desorption from batch experiments on a McLaren soil. They concluded that the use of a consecutive reaction provided improved description of sorption kinetics and hysteresis of Cu when compared with the concurrent irreversible reaction.

The Ca concentration in the effluent from the surface and subsurface soils are shown in Fig. 4.3. For the surface soil column, the Ca BTC exhibited a sharp increase following the Cu pulse application, with a maximum concentration of 4.59 mmol L^{-1}. For the subsurface soil column, the maximum concentration was 4.26 mmol L^{-1} with a gradual Ca decrease following the Cu pulse application. These results are consistent with recent studies by Ponizovsky et al. (2007) and Wang et al. (2009), who showed that Cu retention was accompanied by the release of cations in the soil solution.

Simulations using CXTFIT are shown in Fig. 4.4. For both the surface and subsurface soil columns, the CXTFIT simulations show early arrival of the Cu BTCs and failure to describe the tailing of the leaching right side of the BTCs. In addition, the concentration peak maxima of the BTCs were underestimated. The model parameters that provided the best prediction using CXTFIT were $R = 12.69 \pm 0.63$ and $\mu = 1.295 \pm 0.038$ h^{-1} ($r^2 = 0.647$, RMSE = 0.094) for the surface soil column. The respective values for the subsurface soil column were $R = 13.13 \pm 0.65$ and $\mu = 0.504 \pm 0.035$ h^{-1} ($r^2 = 0.811$, RMSE = 0.1377).

Table 4.4. Second-order two-site (SOTS) model parameter estimates for Cu transport in surface soil, subsurface soil, and surface soil after carbonate removal: estimates of adsorption maximum (S_{max}) and reaction rates (K_e, k_1, k_2, k_3, and k_{irr}) ± their standard errors, with root mean square error (RMSE), and coefficient of determination (r^2).

Model version†	RMSE	r^2	S_{max}	K_e	k_1	k_2	k_3	k_{irr}
			μg g^{-1}	mL μg^{-1}	mL μg^{-1} h^{-1}	----------	h^{-1}	----------
Surface Soil								
V1	0.0105	0.9957	379.21±6.95	0.01194±0.0008	0.02066±0.00133	0.0609±0.0050	0.0889±0.0021	0.00047±0.00004
V2	0.0149	0.9914	429.21±8.35	0.01010±0.0008	0.01430±0.00090	0.0351±0.0032	0.0709±0.0015	------
V3	0.0562	0.8814	2911.13±138.64	0.00034±0.0001	0.00031±0.00011	0.2314±0.0772	------	0.00038±0.00003
V4	0.0696	0.8089	2685.92±135.99	0.00032 ±0.0001	0.00046±0.00004	0.00096±0.0004	------	------
V5	0.0570	0.8757	2908.81±135.53	------	0.00055±0.00012	0.3426±0.0817	------	0.00039±0.00003
Surface Soil (Carbonates Removed)								
V1	0.0564	0.9923	342.22±6.02	0.0170±0.0001	0.0020±0.0002	0.0138±0.0017	0.0486±0.0042	0.000011± 0.000001
V2	0.0591	0.9917	350.91±7.30	0.0171±0.0001	0.0017±0.0001	0.0096±0.0007	0.0410±0.0031	------
V3	0.0148	0.9986	468.57±6.83	0.0073±0.0003	0.0022+0.0001	0.1244±0.0044	------	0.00031±0.00001
V4	0.0350	0.9939	353.05±7.99	0.0130±0.0007	0.0026±0.0001	0.0466±0.0023	------	------
V5	0.0341	0.9926	619.33±14.49	------	0.0045±0.0002	0.2614±0.0163	------	0.00036±0.00002
Subsurface Soil								
V1	0.0316	0.9905	1020.08±95.13	0.0034±0.0005	0.0015±0.0002	0.1310±0.0243	0.0086±0.0069	0.0006±0.00003
V2	0.0398	0.9852	686.99±24.38	0.0084±0.0006	0.0024±0.0002	0.0175±0.0025	0.0137±0.0016	------
V3	0.0316	0.9904	1127.24±25.06	0.0030±0.0003	0.0013±0.0001	0.1540±0.0176	------	0.0006±0.00003
V4	0.0477	0.9783	842.32±22.56	0.0087±0.0006	0.0013±0.0001	0.0058±0.0007	------	------
V5	0.0485	0.9784	1264.78±30.72	------	0.0044±0.0007	0.4872±0.0732	------	0.0007±0.00004

† V1 = amount on equilibrium-type sites (S_e), amount retained on kinetic-type sites (S_k), amount retained irreversibly by consecutive reaction (S_s), amount retained irreversibly by concurrent reaction (S_{irr}) and reaction rates (K_e, k_1,k_2, k_3 and k_{irr}); V2 = S_e, S_k, and S_s with (K_e, k_1,k_2, and k_3); V3 = S_e, S_k and S_{irr} with (K_e, k_1,k_2, and k_{irr}); V4 = S_e and S_k (K_e, k_1, and k_2); V5 = S_k and S_{irr} with (k_1,k_2, and k_{irr}).

The influence of the removal of carbonates from the surface soil on Cu mobility and reactivity is illustrated by the BTC shown in Fig. 4.5. The BTC is characterized by early arrival of Cu in the effluent (three pore volumes) and a peak concentration C/C_o of 1.0. Moreover, 87% of the applied Cu was recovered in the effluent solution. In contrast, only 27% was recovered when the carbonates were not removed. The associated Ca BTC exhibited slow release during leaching, with a maximum concentration of only 0.71 mmol L^{-1} compared with 4.59 mmol L^{-1} from the surface soil when the carbonates were removed.

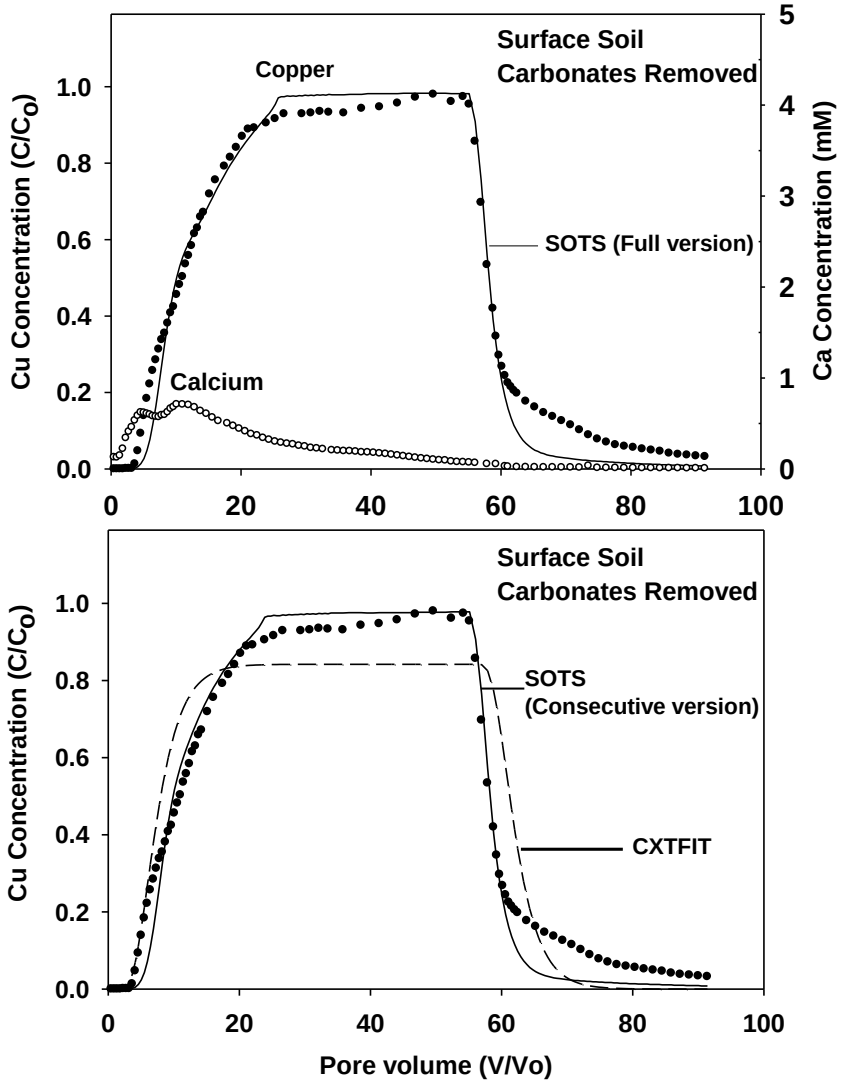

Fig. 4.5. Breakthrough results of Cu and Ca from the surface soil after removal of carbonate. Solid curves are simulations using the full version (V1) and consecutive version (V2, disregarding the amount retained irreversibly by concurrent type of reaction) of the second order, two-site (SOTS) model. The dashed curve represents CXTFIT simulations.

Good description of the BTC was obtained using the SOTS model versions V1 and V2, as shown in Fig. 4.5. Other model versions also produced equally good descriptions of the BTC. The associated model parameters for all model versions along with their standard errors of estimates are given in Table 4.4. The use of CXTFIT provided a good overall description of the BTC; however, CXTFIT failed to describe the slow release of Cu during leaching. The CXTFIT parameter values that provided the best predictions were $R = 8.16 \pm 0.23$ and $\mu = 0.177 \pm 0.016$ h^{-1} ($r^2 = 0.910$, RMSE = 0.116).

4.4.3 Copper Distribution with Depth

The results of the distribution of Cu retained vs. soil depth following the termination of the miscible displacement experiments are given in Table 4.5. For the surface soil, the amount of Cu retained ranged from 13.60 to 24.65 mmol kg^{-1}, whereas for the subsurface soil it ranged from 2.43 to 16.98 mmol kg^{-1}. As expected, when the carbonates were removed, a low amount of Cu was retained in the soil (<3.5 mmol kg^{-1}). In general, the amount of Cu retained by each soil is reflected by the amount leached or recovery in the effluent solution. The lowest amount of Cu retained was for the soil column when the carbonates were removed. The results presented in Table 4.5 also indicate that a major portion of the retained Cu was associated with the carbonate and oxide fraction (53.9–69.2%). This amount decreased sharply when the carbonates were removed, where the carbonate and oxide fraction ranged from 9.6 to 20.6% and that associated with the exchangeable fraction ranged from 58.3 to 78.8%.

Sorbed Cu vs. depth is shown in Fig. 4.6 along with SOTS and CXTFIT model simulations. The two models were used to predict the amount of Cu sorbed vs. depth where no inverse modeling was performed. Rather, the model parameters used were those utilized for the BTC simulations. Simulated results showed good predictions of the Cu distribution for the surface soil when the carbonates were removed. In contrast, poor predictions were realized for

both surface and subsurface soil columns. Based on the sum of all fractions, Cu recoveries were 74.6 and 83.0% of the total sorbed from the surface and subsurface soil columns, respectively. For the soil when carbonates were removed, only 64.6% was recovered, which may be due to the small amount of Cu recovered from the entire column (7.5 mg). For the surface and subsurface soil columns, the respective mass recoveries for Cu were 58.8 and 29.2 mg, respectively. Such incomplete recoveries of retained Cu are consistent with the earlier work of Emmerich et al. (1982) and Han and Banin (1999), among others, who reported that the sum of heavy metal fraction measurements represented 78 to 90% of the total amount sorbed.

Table 4.5. Total extracted Cu and the different fractions from sectioned soil column.

Depth	Total Cu sorbed	Exchangeable fraction		Oxidizable fraction		Associated with carbonates/oxides		Strongly bound	
cm	mmol kg^{-1}	mmol kg^{-1}	%	mmol kg^{-1}	%	mmol kg^{-1}	%	mmol kg^{-1}	%
Surface Soil									
0-1	19.30	0.02	0.09	5.42	28.08	13.36	69.22	0.50	2.61
1-2	21.87	0.02	0.10	7.51	34.33	14.02	64.09	0.32	1.48
2-3	21.15	0.01	0.06	7.18	33.95	13.61	64.33	0.35	1.66
3-4	24.65	0.01	0.04	8.27	33.56	15.68	63.61	0.69	2.79
4-5	13.60	0.01	0.05	4.88	35.85	8.06	59.30	0.65	4.80
Removed Carbonate Soil									
0-1	1.33	0.78	58.26	0.10	7.42	0.27	20.63	0.18	13.69
1-2	2.24	1.54	69.01	0.07	3.19	0.35	15.62	0.27	12.17
2-3	2.57	1.94	75.25	0.04	1.48	0.31	12.21	0.28	11.06
3-4	3.28	2.58	78.81	0.06	1.97	0.31	9.55	0.32	9.66
4-5	3.42	2.58	75.56	0.10	2.86	0.37	10.84	0.37	10.74
Subsurface Soil									
0-1	2.43	0.002	0.07	0.72	29.48	1.49	61.31	0.22	9.14
1-2	9.56	0.006	0.06	4.06	42.48	5.28	55.26	0.21	2.20
2-3	16.98	0.009	0.05	6.63	39.04	9.96	58.66	0.38	2.24
3-4	10.45	0.005	0.05	4.40	42.13	5.63	53.90	0.41	3.92
4-5	10.53	0.008	0.07	4.49	42.65	5.70	54.13	0.33	3.15

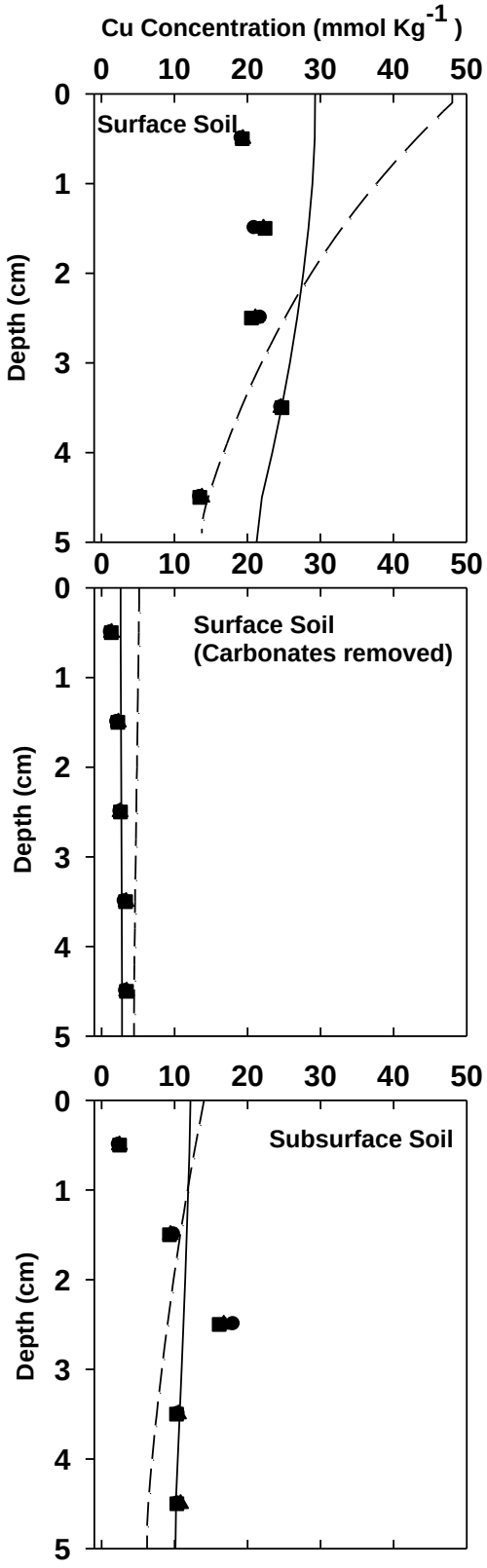

Fig. 4.6. Copper sorbed vs. column depth based on soil extractions. Solid and dashed curves represent the second-order, two-site (SOTS) model and CXTFIT predictions, respectively. Symbols are experimental measurements and represent different replications.

4.5 Conclusions

Surface and subsurface samples were used to investigate Cu reactivity and mobility in calcareous soils. Sorption isotherms were nonlinear and exhibited strong Cu sorption for all soils. The results of Cu sorption on soil when the carbonates were removed indicated that a major fraction of Cu was specifically sorbed onto $CaCO_3$ constituents. Breakthrough results indicated that Cu recovery in the effluent was 27, 60, and 87% for the surface, subsurface, and surface soil when carbonates were removed, respectively. Simulations using the linear model, for both the surface and subsurface soil columns, failed to predict early arrival of the Cu BTCs and the tailing during leaching. The use of a SOTS model provided good prediction of Cu arrival in the effluent, concentration maxima, and the slow release during leaching. We thus recommend that the SOTS model, which accounts for kinetic reversible and irreversible retention mechanisms, is used for predicting Cu transport in calcareous soils.

4.6 References

Adriano, D.C. 2001. Trace elements in terrestrial environments: biogeochemistry, bioavailability and risk of metals. Second edition. Springer, New York.

Bang, J., and D. Hesterberg. 2004. Dissolution of trace element contaminants from two coastal plain soils as affected by pH. J. Environ. Qual. 33:891–901.

Chang, C. M., M. K. Wang, T. W. Chang, and C. Lin. 2001. Transport modeling of copper and cadmium with linear and nonlinear retardation factors. Chemosphere 43:1133–1139.

Elzahabi, M., and R.N. Yong. 2001. pH influence on sorption characteristics of heavy metal in the vadose zone. Eng. Geol. 60:61–68.

Elzinga, E.J. and R.J., Reeder. 2002. X-ray absorption spectroscopy study of Cu^{2+} and Zn^{2+} adsorption complexes at the calcite surface: implications for site specific metal incorporation preferences during calcite crystal growth. Geochim. Cosmochim. Acta. 66: 3943-3954.

Emmerich W.E., L. J. Lund, A.L. Page and A.C. Chang. 1982. Solid phase forms of heavy metal in sewage sludge-treated soils. J. Environ. Qual. 11:178-181.

Gismera, M. J., J. Lacal, , P. da Silva, , R. Garcia, , M. T. Sevilla, , and J. R. Procopio. 2004. Study of metal fractionation in river sediments. A comparison between kinetic and sequential extraction procedures. Environ. Pollut. 127:175–182.

Goldberg, S. and L.J. Criscenti. 2008. Modeling adsorption of metals and metalloids by soil components. p. 215-264. *In* A. Violante, P.M. Huang, and G.M. Gadd (ed). Biophysico-chemical processes of heavy metals and metalloids in soil environments. John Wiley&Sons, Inc.

Goldberg, S., S.M. Lesch, and D.L. Suarez. 2007. Predicting selenite adsorption by soils using soil chemical parameters in the constant capacitance model. Geochim. Cosmochim. Acta 71:5750-5762.

Han F.X. 2007. Binding and distribution of trace elements among solid-phase components in arid zone soils. pp. 131-167. *In* B. J. Alloway, and J. K. Trevors (ed.) Biogeochemistry of trace elements in arid environments, Springer Netherlands.

Han, F.X., and A. Banin. 1999. Long-term transformations and redistribution of potentially toxic heavy metals in arid-zone soils. II.Under field capacity regime.Water Air Soil Pollut. 114:221–250.

He, Z.L., M. Zhang, X.E. Yang, and P.J. Stoffella. 2006. Release behavior of copper and zinc from sandy soils. Soil Sci. Soc. Am. J. 70:1699–1707.

Kabata-Pendias, A., and W. Sadurski. 2004. Trace elements and compounds in soil. p. 79–99. *In* E. Merian et al. (ed.) Elements and their compounds in the environment. Wiley-VCH, Weinheim, Germany.

Kunze, G.W., and J.B. Dixon. 1986. Pretreatment for mineralogical analysis. p. 92–95. *In* A Klute (ed.) Methods of soil analysis. Part 1. 2nd. ed. Agron. Monogr. 9. ASA and SSSA, Madison, WI.

Lafuente, A.L., C. Gonzalez, J.R. Quintana, A. Vazquez, A. Romero. 2008. Mobility of heavy metals in poorly developed carbonate soils in the Mediterranean region. Geoderma 145:238–244.

Loeppert, R.H., and W.P. Inskeep. 1996. Iron. p. 639–664. In D.L. Sparks (ed.) Methods of soil analysis. Part 3. SSSA Book Ser. no. 5. SSSA, Madison, WI.

Madrid, L. and E. Diaz-Barrientos. 1992. Influence of carbonate on the reaction of heavy metals in soils. J. Soil Sci. 43:709–721.

McBride, M.B., and D.R. Bouldin. 1984. Long-term reactions of copper (II) in a contaminated calcareous soil. Soil Sci. Soc. Am. J. 48:56–59.

National Research Council. 2003. Bioavailability of Contaminants in Soils and sediments: Processes, Tools and Applications. National Academies Press, Washington, D.C.: p.240.

Ponizovsky, A. A., H. E. Allen, and A. J. Ackerman. 2007. Copper activity in soil solutions of calcareous soils. Environ. Pollut. 145:1–6.

Press, W.H., S.A. Teukolsky, W.T. Vetterling, and B.P. Flannery. 1992. Numerical recipes in FORTRAN (2nd ed.). Cambridge Univ. Press, New York.

Rodriguez-Rubio, P., E. Morillo, L. Madrid, T. Undabeytia, and C. Maqueda, C. 2003. Retention of copper by a calcareous soil and its textural fractions: influence of amendment with two agroindustrial residues. Eur. J. Soil Sci. 54: 401–409.

Sayyad, G., M. Afyuni, S.F. Mousavi, K.C. Abbaspour, B.K. Richards, and R. Schulin. 2010. Transport of Cd, Cu, Pb, and Zn in a calcareous soil under wheat and safflower cultivation – a column study. Geoderma. 154:311–320.

Selim, H.M., and L. Ma. 2001. Modeling nonlinear kinetic behavior of copper adsorption-desorption in soil. p. 189–212. *In* H.M. Selim and D.L. Sparks (ed.) Physical and chemical processes of water and solute transport/retention in soil. SSSA Special publication no. 56. SSSA, Madison, WI.

Selim, H.M., and M.C. Amacher. 1997. Reactivity and transport of heavy metals in soils. CRC Press, Boca Raton, FL.

Shaheen, S. M., C. D. Tsadilas, T. Mitsibonas, and M. Tzouvalekas. 2009. Distribution coefficient of copper in different soils from Egypt and Greece. Commun. Soil Sci. Plant Anal. 40: 214–226.

Sidle, R.C., L.T. Kardos, and M.Th. van Genuchten. 1977. Heavy metals transport model in a sludge-treated soil. J. Environ. Qual. 6:438–445.

Toride, N., F.J. Leij, and M. Th. van Genuchten. 1999. The CXTFIT code for estimating transport parameters from laboratory or field tracer experiments, version 2.1. Research Report No. 137, U.S. Salinity Laboratory, USDA, ARS, Riverside, CA.

Tsang, D.C.W., and I.M.C. Lo. 2006. Competitive Cu and Cd sorption and transport in soils: a combined batch kinetics, column and sequential extraction study. Environ. Sci. Technol. 40:6655–6661.

Wang, Y.J, Y.X., Cui, D.M., Zhou, S.Q., Wang, A.U., Xiao, R.H. Wang, and H. Zhang. 2009. Adsorption kinetics of glyphosate and copper(ii) alone and together on two types of soils. Soil Sci. Soc. Am. J. 73:1995–2001.

Zhang, H. and H M. Selim. 2011. Second-order modeling of arsenite transport in soils. Journal of Contaminant Hydrology 126:121–129.

Zhu, B., and A.K. Alva. 1993. Trace metal and cation transport in a sandy soil with various amendments. Soil Sci. Soc. Am. J. 57:723–727.

CHAPTER 5. LEAD MOBILITY IN ALKALINE SOILS: INFLUENCE OF CADMIUM AND COPPER

5.1 Introduction

Understanding mobility of heavy metal in soils and factors that govern their retention is essential for quantifying their potential contamination. Lead (Pb) is an inorganic pollutant which is conservative pollutant and poses risks to soils and water resources. Lead is strongly bound to humic matter in organic-rich soils and to iron oxides in mineral soils, and is rather immobile in soils except at extremely high concentrations (Steinnes, 2013). Hooda and Alloway (1998) reported that soil pH, cation exchange capacity (CEC), clay content, $CaCO_3$, organic matter (OM), were positively correlated with Pb sorption in soil.

Cadmium is another heavy metal that is toxic at very low exposure levels. Kabata-Pendias and Mukherjee (2007) reported that soil Cd concentration is estimated to range between 0.06 and 1.1 mg kg^{-1} with an average 0.5 mg kg^{-1}. Cadmium is known to be relatively mobile compared to Pb in most soils (Schmitt and Sticher, 1986; Kabata-Pendias and Sadurski 2004; Campbell et al., 2006; Dong et al., 2009). In aerobic soils, precipitation is unlikely to control Cd solubility unless at excessive Cd contamination and at pH values >7.0 (Smolders and Mertens, 2013). In contrast to Pb and Cd, Copper (Cu) is an essential micronutrient required in the growth of both plants and animals (Kabata-Pendias and Pendias, 2001). However, elevated soil Cu concentrations cause toxic effects in all terrestrial organisms (Alloway, 1995; Oorts, 2013). Appreciable leaching of Cu in soil profiles has been shown in humus-poor acidic soils (Mathur et al., 1984), and in soils which received repeated application of Cu fertilizer in alkaline soils (Wei et al., 2007).

Quantifying the proportions of metals bound to different soil constituents is important to the understanding of heavy metal behavior and fate in soils. The mobility and bioavailability of

metals in soil depend on the strength of the bond between the heavy metal and soil surface as well as the properties of the soil solution (Filgueiras et al., 2002). Pb speciation research shows that Pb fractionation depends on soil properties and total amount of pollution loading. Marin et al. (1997) applied a sequential extraction scheme and found that Pb was essentially extracted from the Fe-Mn oxides fraction with 32% of the total (11.01 mg kg^{-1}) whereas the 5.5% and 4.5% were associated with the exchangeable and OM fractions, respectively. Whereas, less than 0.1% of Pb was associated with Fe-Mn oxides in the 60-85 cm layer which contained around 6 g kg^{-1} total Pb, and more than 45% associated with the OM/sulfides fraction. In order to evaluate Pb mobility in soil, Maiz et al. (2000) used two different sequential extraction procedures to evaluate Pb availability from contaminated soils. They found that 15% of the total Pb was bound with the exchangeable and carbonate fractions whereas 17% and 4% were associated with Fe-Mn oxides and the organic matter/sulphide fractions, respectively. Alhough chemical speciation is time consuming and expensive (Tack and Verloo, 1995), these methods provide imperative knowledge about element mobility and availability in soils (Filgueiras et al., 2002).

Numerous studies were carried out to quantify the competitive effect of several heavy metals on Pb retention and mobility in soils. In batch experiments, Schmitt and Sticher (1986) reported a higher availability of Cd, Cu, and Pb when applied concurrently due to competition for available sorption sites. Their results from sorption batch experiments indicated that the Pb-saturation level decreased from 6.33 mg g^{-1} for a single Pb solution to 1.72 mg g^{-1} when a mixed solution of Pb, Cu, and Cd was applied. Lu and Xu (2009) evaluated the competitive adsorption of four heavy metals Cd, Cu, Zn and Pb and found that Pb was the most strongly sorbed metal by the studied soils. They reported weaker competition at low initial concentrations on the adsorption complex.

Chotpantarat et al. (2012) showed that the maximum sorption capacity of Pb in a single system was higher than those in binary and multi-metal systems of Ni, Mn, and Zn through lateritic soil columns. Fonseca et al. (2011) studied sorption and transport of Cr, Cd, Cu, Zn and Pb to evaluate the co-contamination of a loamy sand soil by single and multiple heavy metals. Their results for Pb showed that the soil exhibited higher sorption capacity for noncompetitive compared with Pb competitive sorption. Nevertheless, Pb exhibited a slightly higher retardation in the competitive scenario under flow condition.

A literature search revealed that numerous studies were carried out to quantify competitive sorption in soils. However, only a few studies focused on competitive transport in a system of multiple heavy metals including Pb. In this study, miscible displacement column experiments and sequential extraction were used to assess Pb mobility and reactivity in alkaline soils. The specific objectives were (1) to quantify the mobility and fractionation of Pb in alkaline soils, and (2) to assess the competitive effect of Cd and Cu on Pb transport in alkaline soils.

5.2 Materials and Methods

Surface (0-40 cm) and subsurface (40-75 cm) soils were collected from an area near Bustan-3 in the Northwestern desert of Egypt. This sandy calcareous soil is classified as Typic Torripsamments, (Bakr et al., 2009) and the top two soil layers were sampled to quantify the impact of $CaCO_3$ on Pb mobility in this soil. Selected soil physical and chemical properties were determined in our laboratory and are given in Table 5.1. The NaOAc at pH 8.2 method was used for determining CEC in this alkaline soil (Pansu and Gautheyrou, 2006). In addition, washed sea sand (Fisher Scientific: 14808-60-7) was used as a reference material where no clay and organic matter were present. Liao et al. (2009) used this sand material previously as a reference matrix to study the mobility of Hg in this reference material.

Table 5.1. Selected physiochemical properties of the studied soils and reference sand material.

Soil	Bustan-surface	Bustan-subsurface	Reference Sand
Soil taxonomy	Typic Torripsamments		
pH (1 :2.5)	9.22	9.44	6.7
Organic matter (g kg^{-1})	0.66	0.13	n.d†
Cation exchange capacity (cmol kg^{-1})	5.60	4.84	n.d
$CaCO_3$ (%)	2.76	1.18	n.d
Citrate-bicarbonate-dithionite (CBD)			
Fe g kg^{-1}	4.175	1.261	0.023
Al g kg^{-1}	0.986	0.353	0.043
Mn g kg^{-1}	0.200	0.042	n.d

† Not detected

Two miscible displacement column experiments as described by Zhang and Selim (2006) were carried out to study the mobility of Pb, Cd, and Cu. Acrylic columns (5-cm in length and of 6.4-cm i.d.) were uniformly packed with air-dry soil and were slowly water-saturated with a background solution of 5 mmol L^{-1} KNO_3. To insure water-saturation, upward flow in the soil columns was maintained. Constant flux was controlled by a piston pump (FMI lab pump, Model QG 6, Fluid Metering Inc, Oyster Bay, NY) where some 20 pore volumes of the background solution were applied at the desired flow rate. Following saturation two pulses of 0.497 mmol L^{-1} Pb (in the form of $(NO_3)_2$) in 5 mmol L^{-1} KNO_3 were introduced into Bustan surface and Bustan subsurface soil columns. Each pulse was eluted by several pore volumes of 5 mmol L^{-1} KNO_3 lead-free solution for leaching. Subsequently, pulses of 0.925 mmol L^{-1} Cd followed by pulses of 1.176 mmol L^{-1} Cu were introduced into Bustan surface and Bustan subsurface soil columns, respectively (see Table 5.2). Each pulse was eluted by several pore volumes of the background solution (5 mmol L^{-1} KNO_3). The flow into the columns was stopped for 2d to evaluate the influence of flow interruption on Pb, Cd, and Cu retention and transport.

Table 5.2. Soil physical and experimental conditions of the miscible displacement columns experiments.

Matrix	Bulk density, ρ (Mg m^{-3})	Moisture content, θ (m^3 m^{-3})	Pore water velocity (cm h^{-1})	Pulse (pore volumes)		
				Pb	Cd	Cu
Bustan-surface	1.839	0.306	1.258	20.12	11.28	12.13
Bustan-subsurface	1.771	0.332	1.061	20.08	9.97	10.23
Reference Sand-I	1.634	0.383	0.892	11.33	---	---
Reference Sand-II	1.672	0.369	0.938	11.99	---	---

Upon completion of the miscible displacement experiments, each soil column was sectioned into 1-cm increments and Pb, Cd, and Cu retained by the soil were determined using sequential extractions. Four extraction steps were quantified, referred to here as exchangeable, oxidizable, carbonates and oxides, and strongly bound. The extraction method used was a modification of that of Emmerich et al. (1982). For the exchangeable phase, 37.5 mL of 0.5 mol L^{-1} KNO_3 was added to the soil and shaken for 16 h. For the oxidizable phase, 37.5 mL of 0.5 mol L^{-1} NaOH was added and shaken for 16 h. For the fraction associated with carbonates and oxides, 37.5 mL of 0.05 mol L^{-1} Na_2EDTA as a nonspecific reagent was used (Gismera et al., 2004). Strongly bound element was based on extraction with 4 mol L^{-1} HNO_3 for 16- h at 70 to 80°C. Thus, the amounts of Pb, Cd, and Cu retained or sorbed due to pulse application versus soil depth were quantified for the Bustan soil columns.

Since extremely low Pb recovery in the effluent solution from the miscible displacement experiments was observed for Bustan surface and subsurface soils, two column experiments were performed using acid-washed sand material (Fisher Scientific: 14808-60-7). The properties of reference material with no clay and organic matter and sand=81% and silt=19% are given in Table 5.1. In column I, a Pb pulse having a concentration of 0.483 mmol L^{-1} Pb was introduced whereas for column II, Pb concentration in the pulse was 5 times higher (2.413 mmol L^{-1} Pb). In

both columns, a stop-flow of 2 d during Pb application was performed in order to evaluate the influence of flow interruption on Pb retention and transport. Upon completion of the miscible displacement experiments, each reference sand column was sectioned into 1-cm increments and Pb retained by the soil was determined using an Innov-X Delta Premium PXRF as a screening method (USEPA, 2007). Thus, the amount of Pb retained or sorbed versus soil depth due to pulse application was quantified for the reference sand columns.

5.3 Results and Discussion

5.3.1 Transport in Surface Soil

Results for Pb, Cd, and Cu concentrations in the effluent solution from the Bustan surface soil is given in Fig 5.1. The results are presented as relative concentrations (C/C_o) versus effluent pore volumes eluted (V/V_o). Here C is the concentration in the effluent and C_o is that of the input pulse solution, V is the total volume of effluent (cm^3) at any time t, and V_o represents the volume of soil-pore space within the soil column (cm^3). The results indicate extremely low Pb concentrations in the effluent throughout the experiment. In contrast, Fig. 5.1 indicates distinct breakthrough curves (BTCs) for Cd and Cu. This soil column received a pulse of Pb which was followed by a Cd pulse and a Cu pulse in a consecutive manner as described previously. The two vertical lines (dashed) in Fig. 5.1 delineate when the Cd pulse and the Cu pulse were applied, respectively.

Results for Pb are further presented in Fig. 5.2 on an expanded scale and show that Pb was not detected during pulse application and leaching. In fact Pb was detected only after some 50 pore volumes as a result of Cd and Cu pulse applications. Specifically, the highest Pb concentrations of C/C_o of 0.018 - 0.02 were detected during Cu pulse application. After 100 pore volumes, the total amount of Pb recovered in the effluent solution was <0.5% of that applied. Such extremely low mobility and thus high affinity of Pb is likely due to the presence of $CaCO_3$

in this alkaline soil (see Table 5.1). Hooda and Alloway (1998) indicated that soil pH and $CaCO_3$ content were positively correlated with Pb sorption in soils. Rouff et al. (2005) found that, based on X-ray absorption near-edge structure (XANES) studies, Pb adsorption is dominate at pH of 8.2.

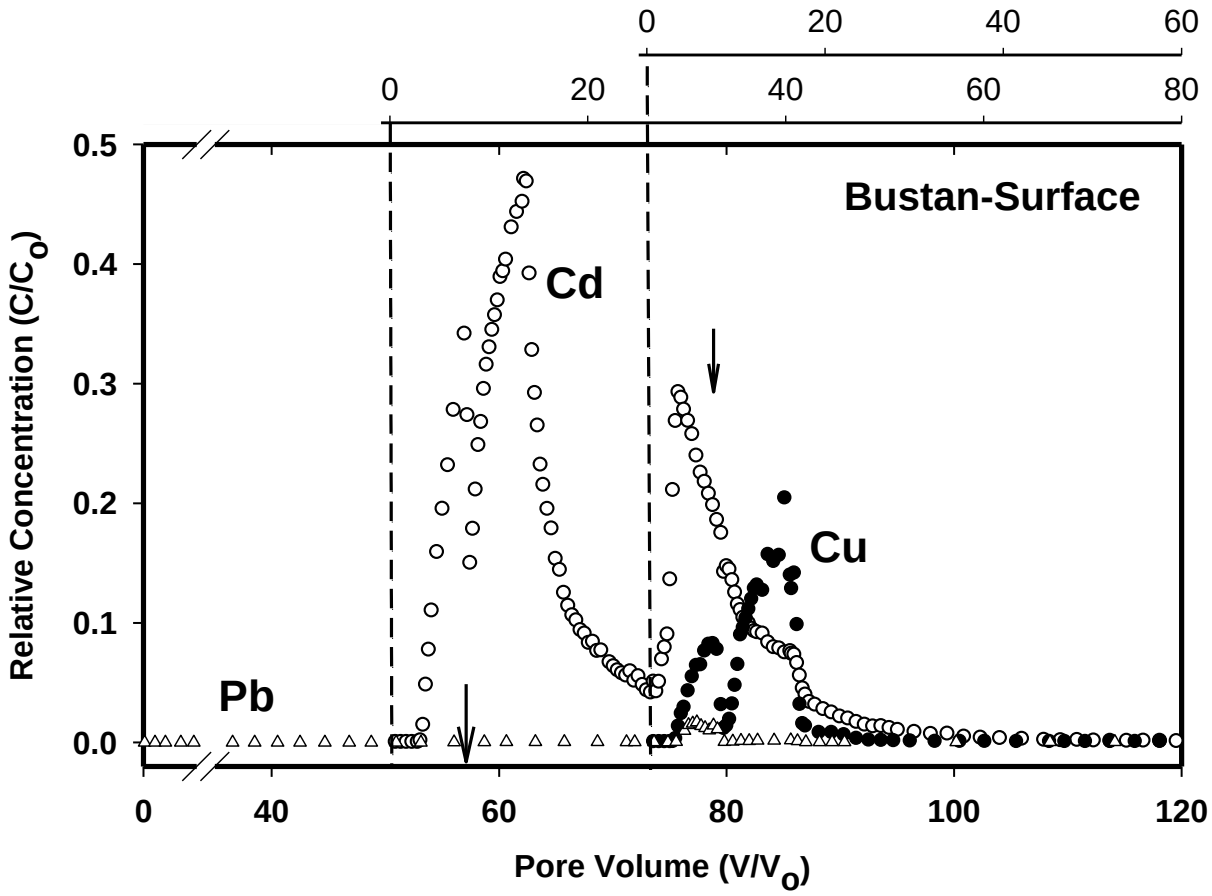

Fig.5.1. Breakthrough results of Pb, Cd, and Cu from the Bustan surface soil column; vertical dashed lines indicate the starting of Cd and Cu pulses; vertical solid arrows indicate when the flow interruption occurred.

Cadmium BTC shown in Fig. 5.1 exhibited higher mobility compared to Pb in this surface soil. High Cd mobility is illustrated by the early Cd detection in the effluent solution (two pore volumes) and a high peak concentration (C/C_o = 0.47) was observed by the end of the Cd pulse. A subsequent Cd BTC was also observed as a consequence of the Cu pulse application. This subsequent BTC with peak concentration of C/C_o = 0.293 is a clear indication of competitive behavior of the incoming Cu that resulted in the release of retained Cd in this soil.

We should emphasize here that total recovery of Cd was not attained. In fact 47% of applied Cd was retained which illustrates the affinity of Cd in this alkaline soil. Moreover, the BTCs for Cd indicated extended tailing which is indicative of slow Cd release from this soil. During the column experiment, two stop-flow or flow interruptions occurred. A decrease in Cd concentration in the effluent solution in response to the stop-flow events was observed (see arrows in Fig. 5.1). Such concentration decrease is indicative of continued Cd sorption from the soil (Reedy et al 1996; Brusseau et al., 1997).

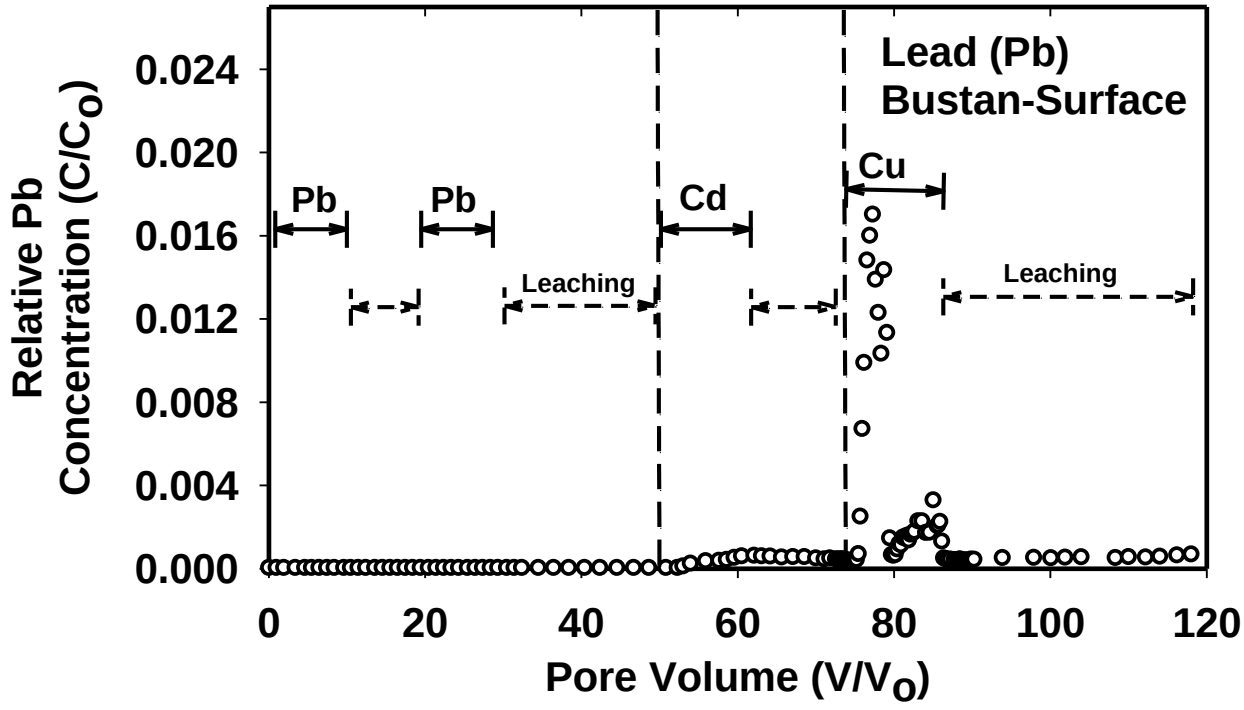

Fig. 5.2. Breakthrough results of Pb from the Bustan surface soil column; solid and dashed horizontal arrows indicate pore volumes of different elements or leaching solutions.

Based on the results shown in Fig. 5.1 it is obvious that much stronger Pb retention occurred when compared to Cd under flow conditions. In an alkaline soil (Entisol), Shaheen (2009) showed that stronger Pb sorption than Cd where the distribution coefficients for Pb and Cd were 4833.7 L Kg^{-1} and 78.8 L Kg^{-1}, respectively. These findings are in agreement with the

results presented here. Elbana and Selim (2010) studied the retention and mobility of Cd in the soil used here where no Pb or Cu were applied. Their results indicated that Cd was nearly immobile where 99% of applied Cd was retained by the soil with maximum Cd concentration less than C/C_o = 0.005. Their results are contrary to our finding of high mobility of Cd as shown in Fig. 5.1. Therefore, results from the current study revealed that Pb strongly competed with Cd for available sorption sites. This resulted in reduced affinity and greater mobility for Cd in this soil.

For Cu, BTC results indicated lower effluent concentrations when compared with Cd in where peak concentration reached C/C_o of 0.204 (see Fig.5.1). Based on the BTC results, the total amount of Cu retained by the soil column was >91% of that applied. Also a sharp decrease of Cu concentration in effluent in response to the flow interruption was observed. Such a behavior is likely due to chemical and to a lesser extent physical or nonequilibrium processes under water-flow conditions (Reedy et al 1996; Brusseau et al., 1997). In a previous Cu transport study on this soil where no Pb or Cd pulses were applied, Elbana and Selim (2011) found that Cu exhibited limited mobility with total Cu recovery in the effluent solution of only 0.4%. They also observed that peak Cu concentration did not exceed C/C_o of 0.01. As a result a 9% increase in the amount of effluent solution based on the BTC results of Fig. 5.1 is due mainly to the strong retention of Pb and Cd on the available sorption sites of the soil matrix. Therefore we conclude that Pb and Cd resulted in enhanced mobility of Cu due to their competition for available sorption sites.

Results of pH and Ca concentrations in the effluent solution from the surface soil are given in Fig. 5.3. The pH ranged from 6 to 8 with an average of 6.8 during the Pb pulse with a subsequent increase during Cd and Cu pulses above pH of 7. Calcium measurements indicated an increase as a result of Pb, Cd, and Cu pulse applications. Moreover, increases in Ca

concentrations due to flow interruption were consistent throughout the flow experiment. These increases are indicative of the kinetic and competitive Pb, Cd, and Cu retention on Ca release in this alkaline soil.

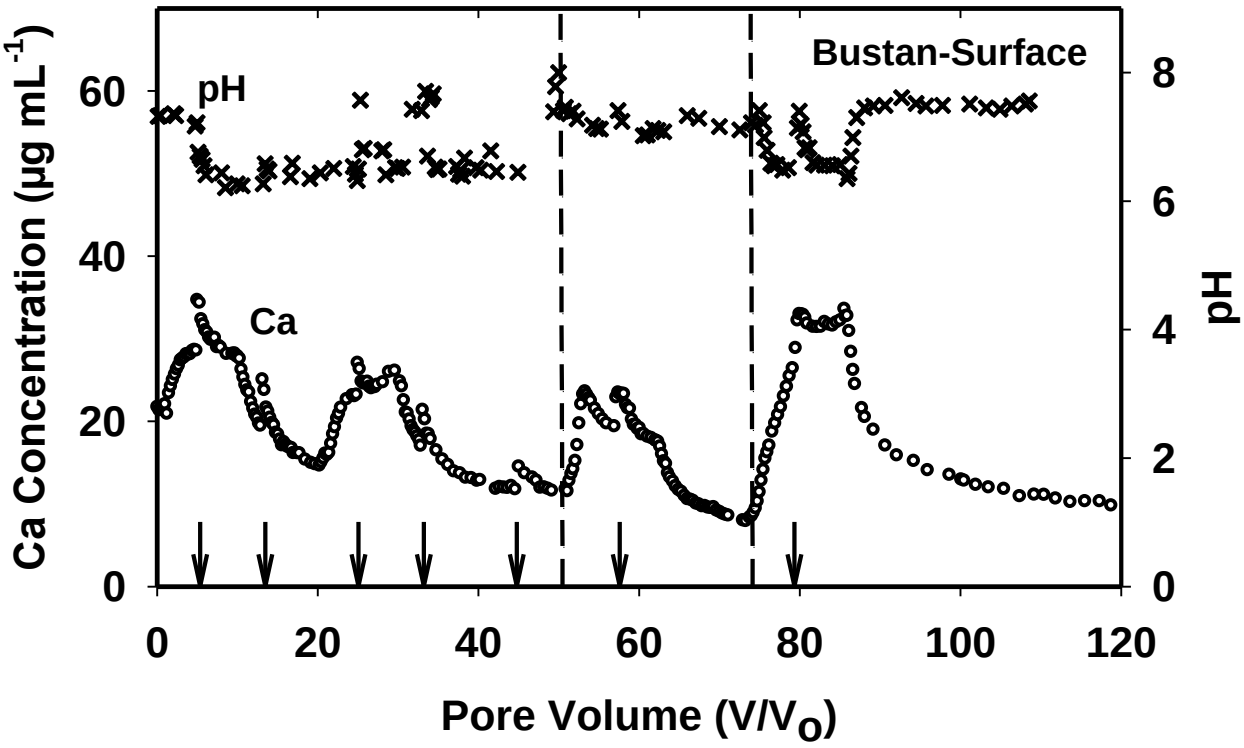

Fig. 5.3. Breakthrough results of Ca from the Bustan surface soil column; dashed horizontal lines indicate starting of Cd and Pb pulses; vertical solid arrows indicate when the flow interruption occurred. The pH measurements were represented on secondary Y axis.

The results of the distribution of Pb, Cd, and Cu retained by the soil matrix versus column depth following the termination of the experiments are shown in Fig. 5.4. These distributions illustrate distinct differences among these heavy metals. Highest amount retained was observed for Pb whereas Cd showed the lowest amount retained. In addition, a sharp decrease in concentration with depth was observed for Pb and Cu and to a lesser extent for Cd. These results provide essential information on the extent of the affinity as well as mobility of Pb, Cd, and Cu in this soil.

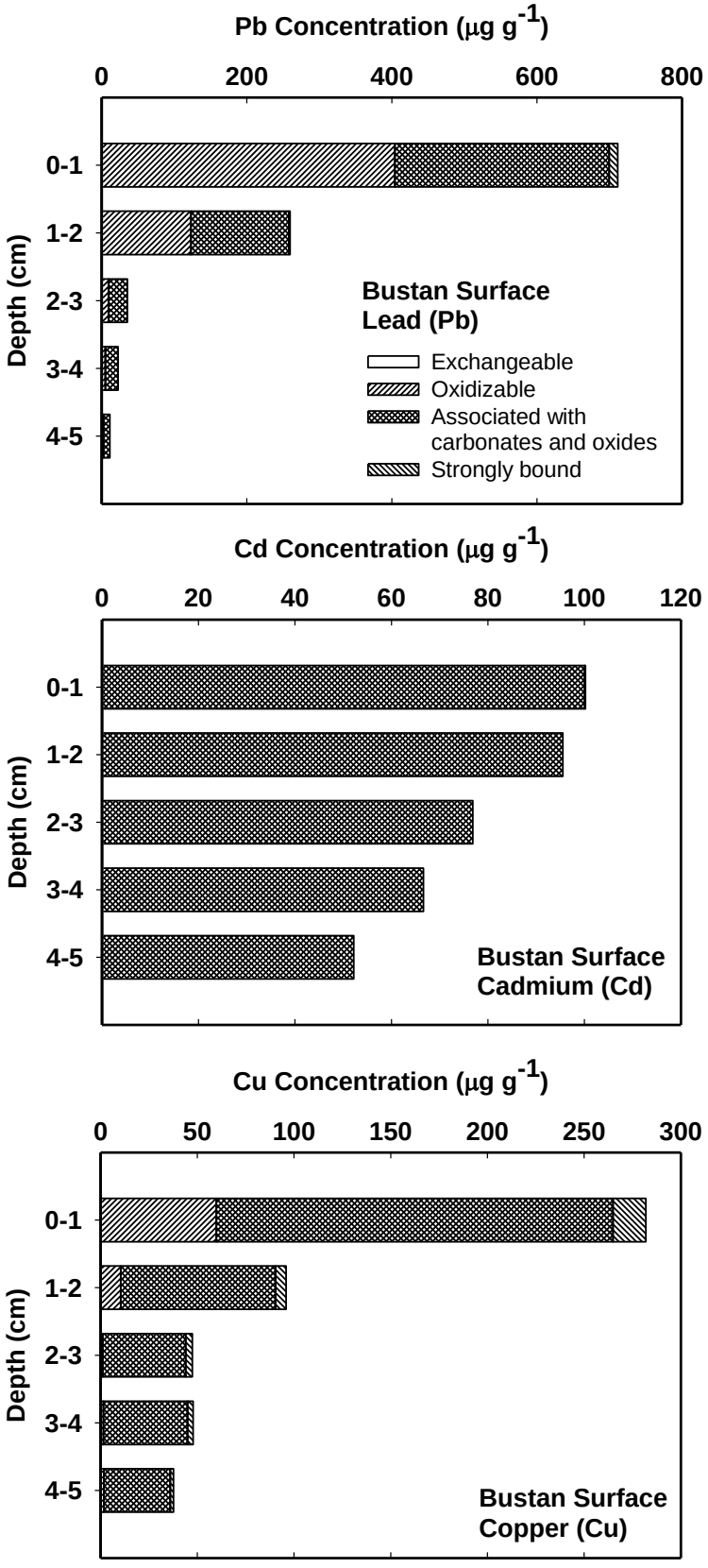

Fig. 5.4. Different Pb, Cd, and Cu fractions from sectioned soil columns for Bustan surface soil.

As depicted in Fig 5.4, strong Pb retention was observed with 93% of the total amount retained remained near the soil surface (0-2 cm). Such strong Pb retention was anticipated based on the effluent results presented earlier. Moreover, the Pb retained by the soil matrix was mainly associated with the oxidizable as well as the carbonate and oxides fractions. Davidson et al. (1998) reported that for a contaminated surface soil layer (2-13 cm) Pb was associated with the Fe-Mn oxides and OM/sulfides fractions. For Cu, the distribution indicated highest retention near the soil surface indicative of high sorption and limited mobility. Based on sequential analysis, the amount of retained Cu was in the oxidizable, carbonate and oxides, and strongly bound fractions. In other words, Cu was not present in the exchangeable fraction which is similar to that for Pb (see Fig. 5.4). Balasoiu et al. (2001) referred to strong affinity of Cu by the soil as indicative to Cu retained on organic matter by complexation rather than by ion exchange.

In contrast to the Pb and Cu distribution patterns exhibited in Fig. 5.4, Cd distribution vs depth indicated lowest amount retained with a gradual decrease with depth. These findings support the BTC results where high concentrations of Cd in the effluent solution were observed for an extended flow period (or pore volumes) (see Fig. 5.1). The Cd distribution also showed that the amount retained was mainly associated with the carbonates and oxides fraction. Moral et al. (2005) reported that for calcareous soils Cd was recovered mainly in the sorbed-carbonate and strongly bound fraction.

5.3.2 Transport in Subsurface Soil

Results for Pb, Cd, and Cu concentrations in the effluent solution from the subsurface alkaline soil are given in Fig 5.5. The results are analogous to those from the surface soil (column I) shown in Fig 5.1. Specifically, extremely low Pb concentrations in the effluent solution was obtained whereas distinct breakthrough curves (BTCs) for Cd and Cu. Results for Pb on an expanded scale showed that Pb was detected as a result of Cd and Cu pulse applications

(see Fig. 5.6). Moreover, despite the lower $CaCO_3$ content in the subsurface (see Table 1), the amount of Pb retained by each column was similar ~ 99.5% of that applied. For Cd and Cu, the recoveries in the effluent solution were 46.1% and 2.41%, respectively. For column I, the respective values were 47% and 8%. Response to flow interruption during Cd and Cu application was similar to that for column I indicative of strong kinetic sorption reactions. It is difficult to explain the lower Cd and Cu peak concentrations in column II compared to column I, however.

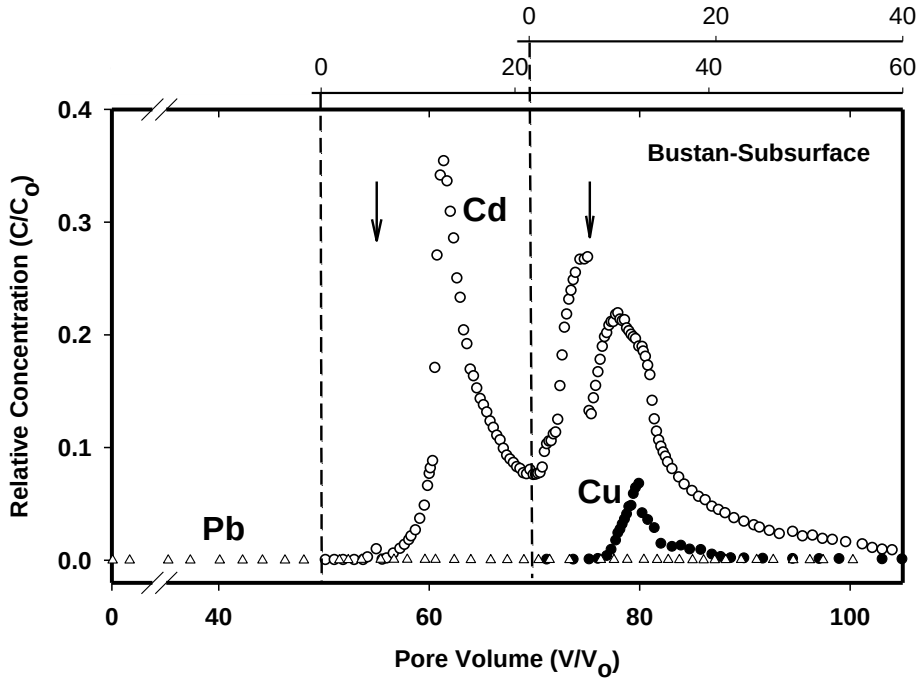

Fig. 5.5. Breakthrough results of Pb, Cd, and Cu from the Bustan subsurface soil column; vertical dashed lines indicate the starting of Cd and Cu pulses; vertical solid arrows indicate when the flow interruption occurred.

Changes in pH and the amount of Ca released from column II is shown in Fig 5.7 and indicated a clear increase in Ca release resulting from Pb, Cd and Cu applications. The pH changes during the miscible displacement experiment for column II exhibited low fluctuations due to pulse applications when compared to that for column I. The amount of heavy metals retained versus depth of the subsurface column is shown in Fig 5.8. Although similar distribution patterns were observed for the subsurface when compared to the surface layer, several distinct differences were observed. For all three heavy metals, lower amounts retained by the subsurface

soil were obtained when compared to the surface soil. Leaching to lower depth (>2cm) was observed for Cu. Moreover, unlike the surface soil, significant Cd in the exchangeable (at 0-1 cm depth) was measured in the subsurface layer.

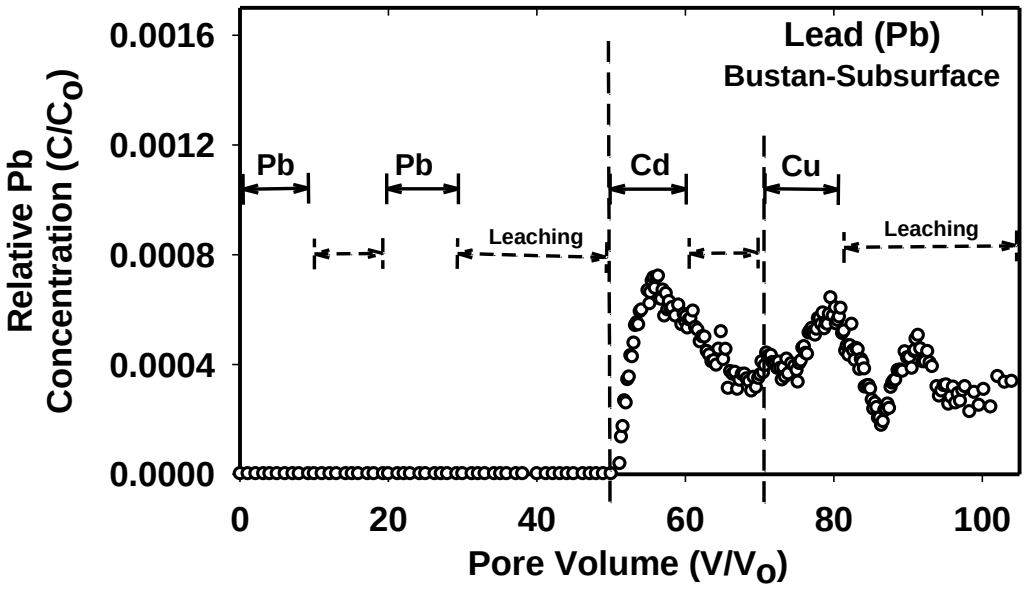

Fig. 5.6. Breakthrough results of Pb from the Bustan subsurface soil column; solid and dashed horizontal arrows indicate pore volumes of different elements or leaching solutions.

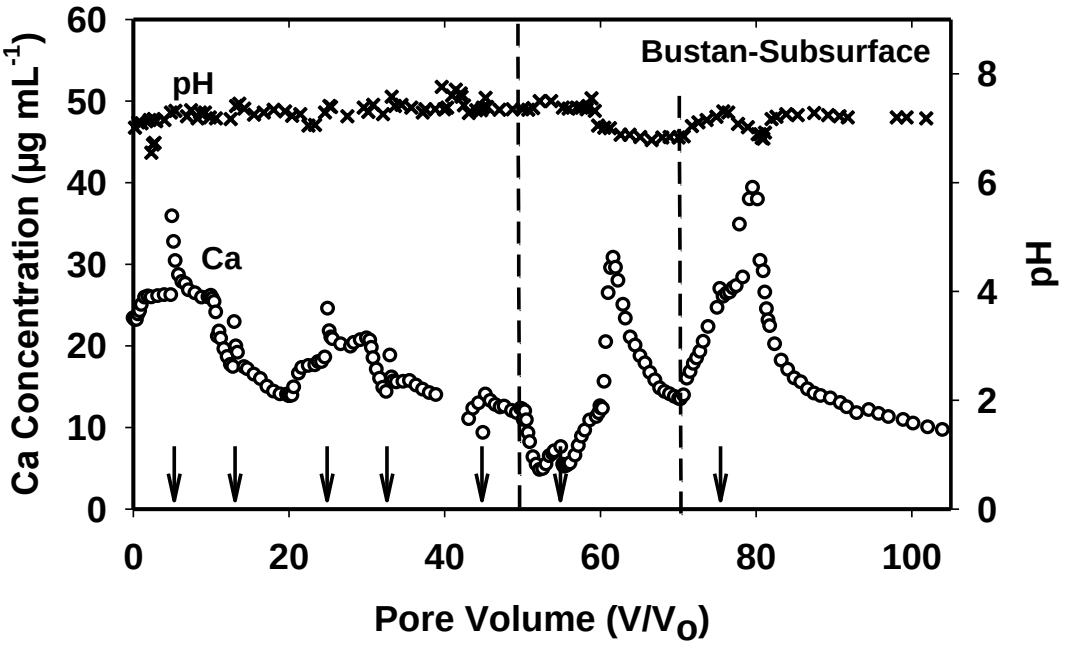

Fig. 5.7. Breakthrough results of Ca from the Bustan surface soil column; dashed horizontal lines indicate starting of Cd and Pb pulses; vertical solid arrows indicate when the flow interruption occurred. The pH measurements were represented on secondary Y axis.

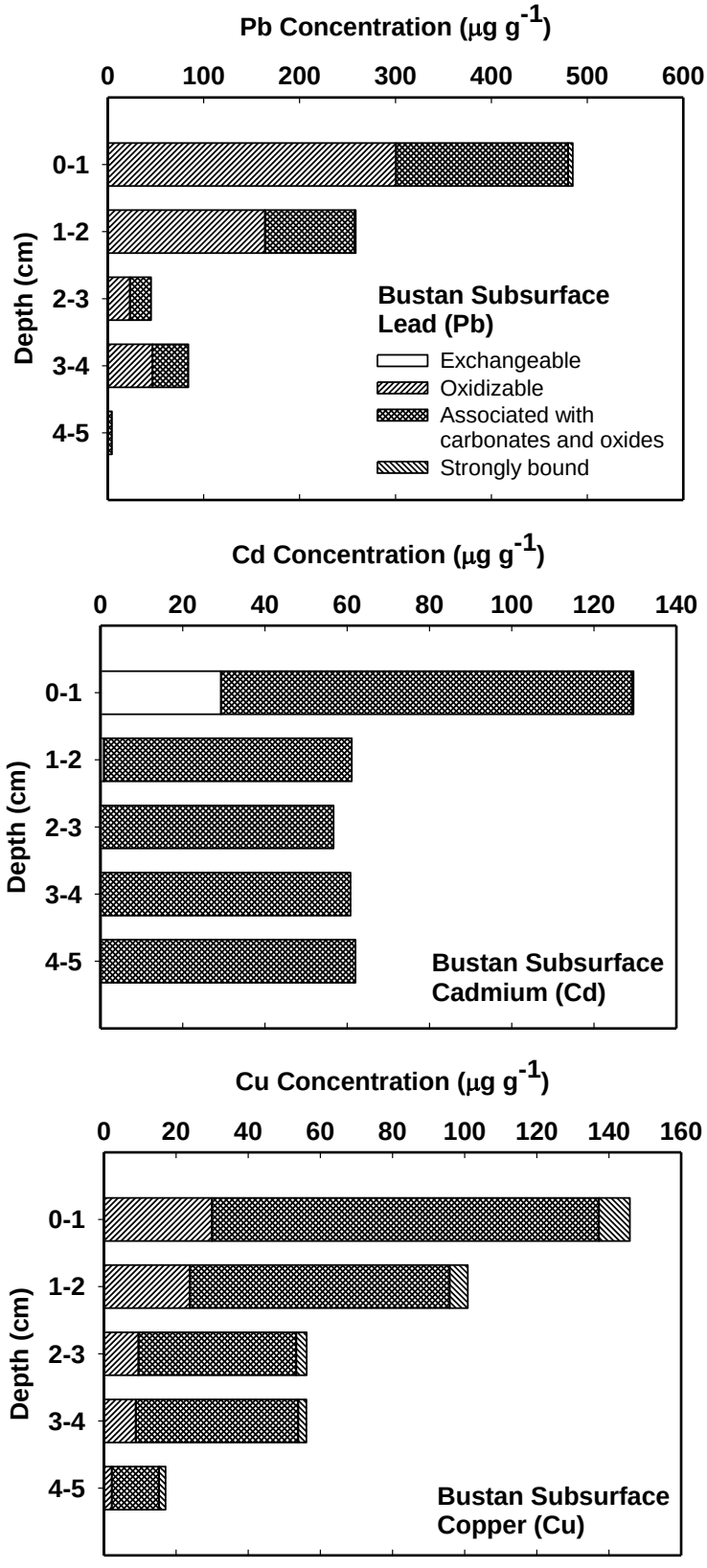

Fig. 5.8. Different Pb, Cd, and Cu fractions from sectioned soil columns for Bustan subsurface soil.

5.3.3 Transport in Reference Sand

Lead BTCs for the reference sand columns (I and II) are shown in Fig 5.9 and 5.10. The major difference between the two columns is that of the Pb concentration in the input pulse; 0.483 and 2.413 mmol L^{-1}, respectively. These figures also illustrated Ca release versus pore volume from the two columns. For column I, the BTC exhibited early arrival (only 1 pore volume) and peak concentration of C/C_o of 0.8 (see Fig. 5.9). In addition, the total amount of Pb in the effluent solution was 60% of that Pb applied. The response to flow interruption shown in Fig. 5.9 is indicative of strong retention where kinetic reactions are dominated. The lack of total recovery of Pb in this reference sand was surprising because this matrix is devoid of organic matter and clays. In fact recent published work on this reference sand indicated complete recovery for Zn, Cd, and Cu (Selim et al., 2013, Elbana and Selim 2010, 2011).On the other hand, Liao et al., (2009) found that Hg transport in this sand material was highly retarded, with only 17% recovery for that applied Hg. They suggested that Hg retention was likely due to adsorption by quartz as well as iron and aluminum oxides. Sheppard and Sheppard (1991) reported that only 33% of added Pb was leached through a sandy soil depth greater than 50 cm.

Results of Pb in the effluent from the reference sand column II is given in Fig. 10. This BTC illustrated that a five-fold increase in Pb input concentration resulted in that peak concentrations reached that of the input pulse in a relatively short time. Moreover, response to flow interruption was less obvious than for column I. The release of Ca in response to introducing Pb solution is also illustrated by the curve shown in Fig. 5.10. Based on the area under the BTC, the total amount of Pb in the effluent was 94.3% of that Pb applied. This high recovery is much higher than that from column I with only 60% recovery. Nevertheless, because of the difference in the input Pb pulse concentrations, the amount retained by each reference sand column was relatively similar. Therefore, based on these results we conclude that sorption

capacity for Pb in this reference sand material was attained. This finding is further supported by the Pb distribution of the amount retained versus depth in both soil columns. In fact, the range of amount of Pb retained was similar for both columns with somewhat lower concentration at the second depth (1-2 cm) for column II (see Fig. 5.11).

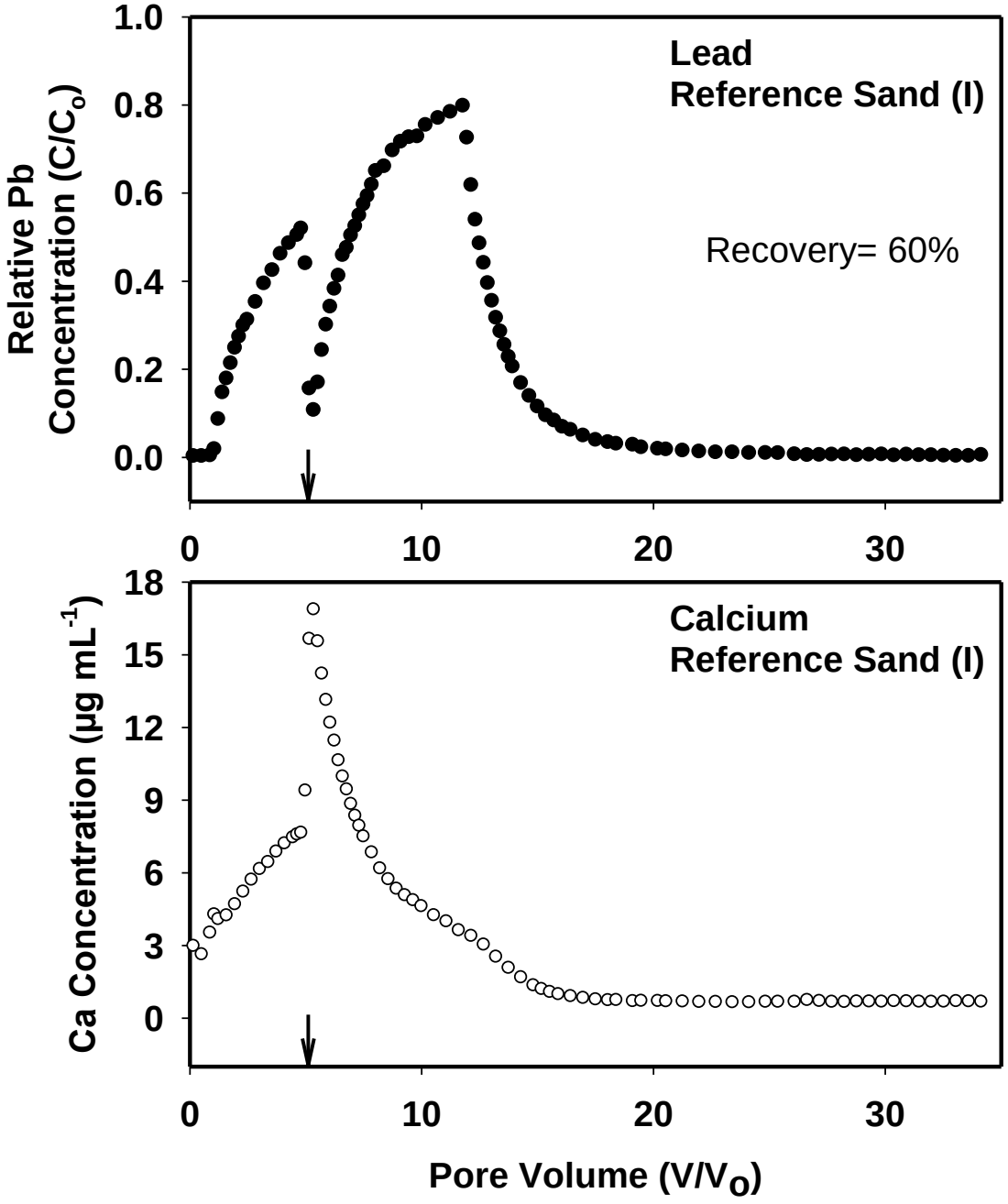

Fig. 5.9. Breakthrough results of Pb (top) and Ca (bottom) from the reference sand column when pulse of 0.483 mmol L^{-1} of Pb was introduced; the arrow indicates when flow interruption occurred.

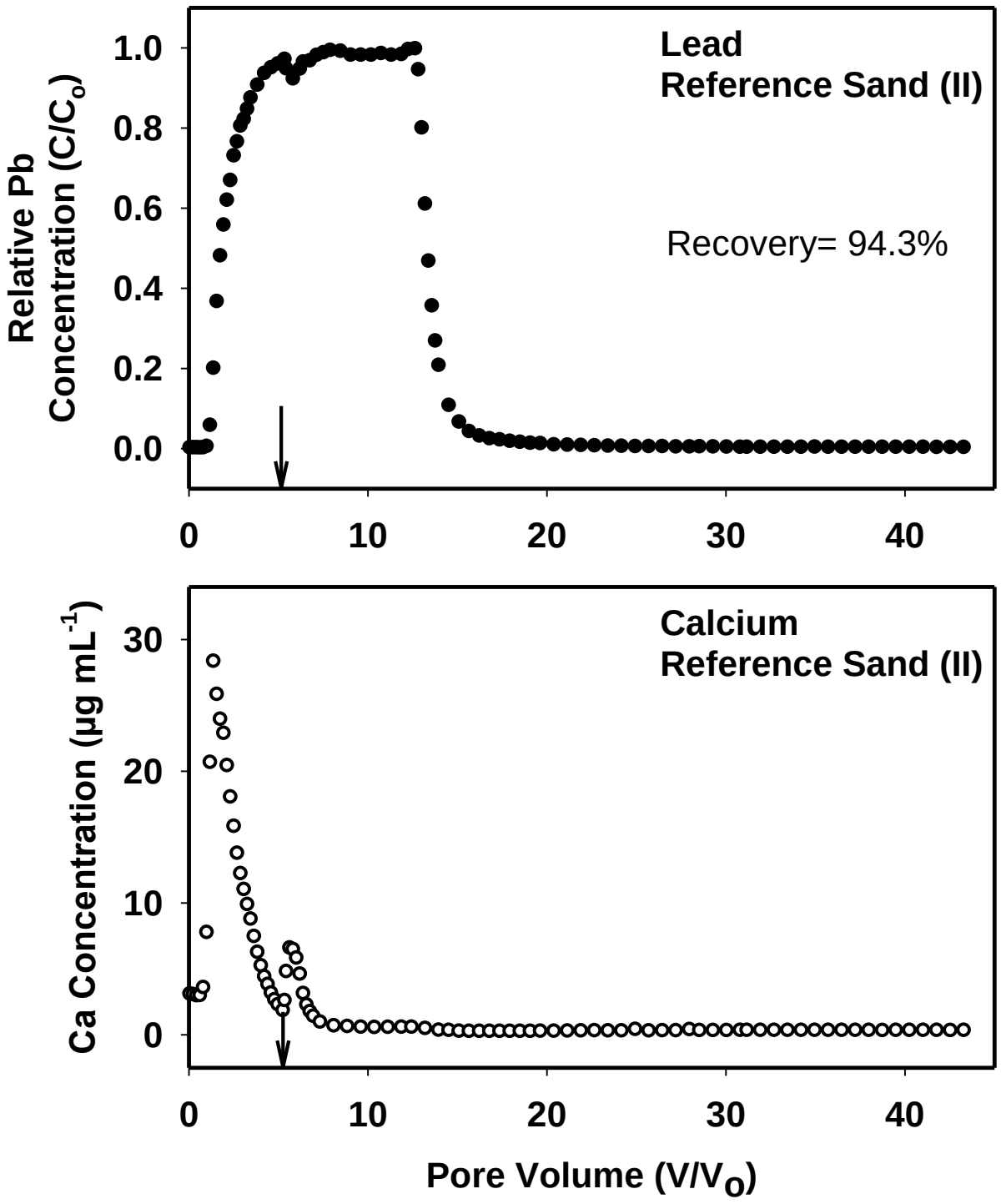

Fig. 5.10. Breakthrough results of Pb from the reference sand column when pulse of 2.413 mmol L^{-1} was introduced; the arrow indicates when flow interruption occurred.

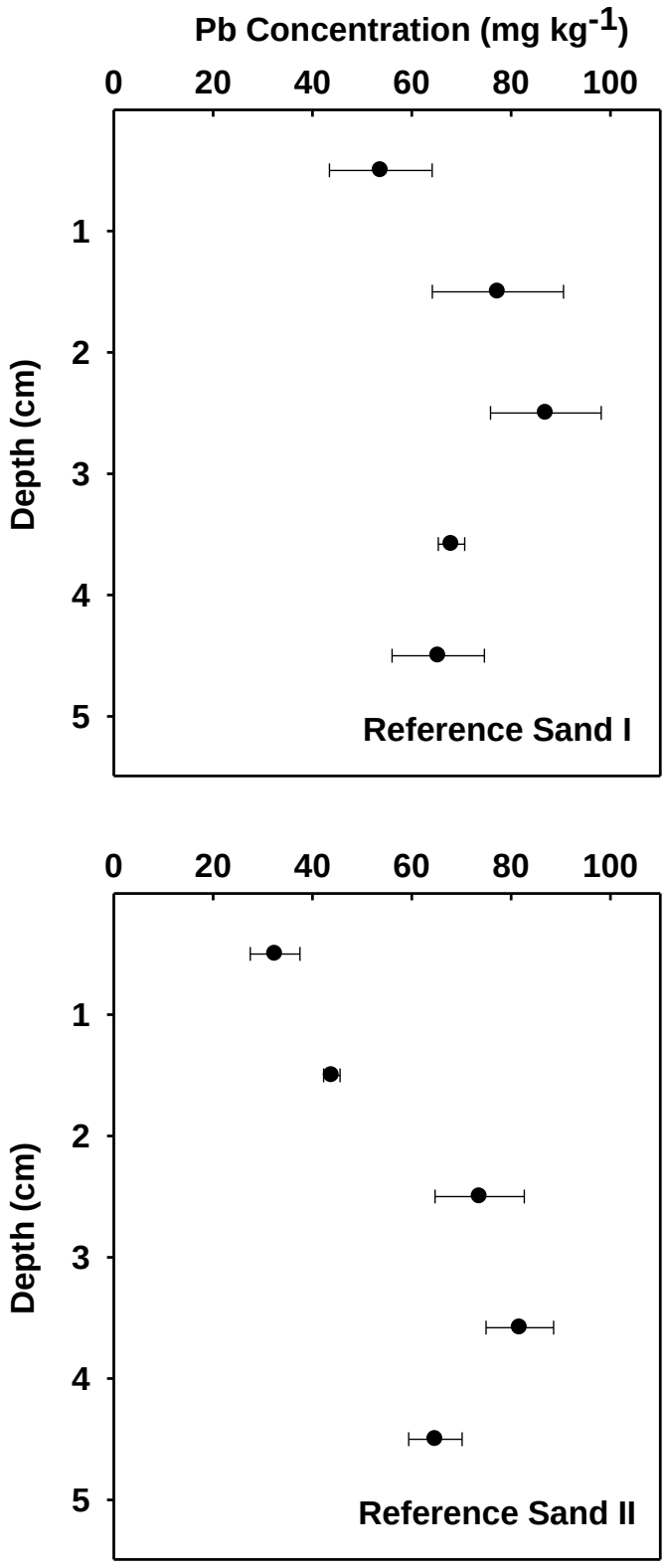

Fig 5.11. Lead sorbed vs. reference sand columns depth based on XRF scanning when a pulse of 0.483 mmol L^{-1} (top) and 2.413 mmol L^{-1} (bottom) of Pb were introduced.

5.4 Conclusions

Surface and subsurface soil materials were used to investigate Pb mobility in an alkaline soil and the subsequent influence of Cd and Cu on Pb release. Miscible displacement column experiments indicated that Pb is strongly sorbed (99.5%) with less than 0.5% recovery of Pb mobility in the effluent solution. The influence of subsequent Cd and Cu pulse applications did not result in Pb release from both surface and subsurface soils. Distribution of the amount of heavy metals retained versus depth in the soil column indicated that more than 85 to 93% of Pb applied was retained in the surface 2 cm. In addition, Pb was mainly associated with oxidizable as well as the carbonate and oxides fractions. Based on effluent results, the surface and subsurface soil exhibited affinity in the order of Pb>Cu>Cd. On the other hand, Pb exhibited high mobility when applied to the reference sand and that the amounts retained by each reference sand column were similar regardless of Pb concentration of the input pulse. Therefore, we conclude that sorption capacity for Pb in this reference sand material was attained.

5.5 References

Alloway, B.J. 1995. The origins of heavy metals in soils. p. 38–57.*In*: Alloway, B.J. (ed.), Heavy metals in soils. Blackie Academic and Professional, London, UK.

Bakr, N., M.H. Bahnassy, M.M. El-Badawi, G.W. Ageeb, and D.C. Weindorf. 2009. Land capability evaluation in newly reclaimed areas: A case study in Bustan 3 area, Egypt. Soil Surv. Horiz. 50:90–95.

Balasoiu, C.F., G.J. Zagury, L. Deschenes. 2001. Partitioning and speciation of chromium, copper, and arsenic in CCA-contaminated soils: influence of soil composition. Sci. Total Environ. 280:239–255.

Brusseau, M.L., Q.H. Hu, and R. Srivastava. 1997. Using flow interruption to identify factors causing nonideal contaminant transport. J. Contam. Hydrol. 24:205–219.

Campbell, C. G., F. Garrido, V. Illera, and M.T. García-González 2006. Transport of Cd, Cu and Pb in an acid soil amended with phosphogypsum, sugar foam and phosphoric rock. Appl. Geochem. 21:1030-1043.

Chotpantarat S., S.K. Ong, C. Sutthirat, K. Osathaphan. 2012. Competitive modeling of sorption and transport of Pb^{2+}, Ni^{2+}, Mn^{2+} and Zn^{2+} under binary and multi-metal systems in lateritic soil columns. Geoderma.189-190: 278-287.

Davidson, C.M., A.L. Duncan, D. Littlejohn, A.M. Ure, and L.M. Garden. 1998. A critical evaluation of the three-stage BCR sequential extraction procedure to assess the potential mobility and toxicity of heavy metals in industrially-contaminated land. Anal. Chim Acta. 363:45–55.

Dong, D., X. Zhao, X. Hua, J. Liu, and M. Gao. 2009. Investigation of the potential mobility of Pb, Cd and Cr(VI) from moderately contaminated farmland soil to groundwater in Northeast. China. Journal of Hazardous Materials 162:1261–1268.

Elbana, T. A. and H M. Selim. 2010. Cadmium transport in alkaline and acidic Soils: miscible displacement Experiments. Soil Sci. Soc. Am. J. 74: 1956–1966.

Elbana, T. A. and H M. Selim. 2011. Copper mobility in acidic and alkaline soils: miscible displacement experiments. Soil Sci. Soc. Am. J. 75:2101–2110.

Emmerich, W.E., L.J. Lund, A.L. Page, and A.C. Chang. 1982. Solid phase forms of heavy metal in sewage sludge-treated soils. J. Environ. Qual. 11:178–181.

Filgueiras, A.V., I. Lavilla, C. Bendicho. 2002. Chemical sequential extraction for metal portioning in environmental solid samples. J. Environ. Monit. 4: 823-857.

Fonseca, B., H. Figueiredo, J. Rodrigues, A. Queiroz, and T. Tavares. 2011. Mobility of Cr, Pb, Cd, Cu and Zn in a loamy soil: a comparative study. Geoderma 164:232–237.

Gismera, M.J., J. Lacal, P. da Silva, R. Garcia, M.T. Sevilla, and J.R. Procopio. 2004. Study of metal fractionation in river sediments: A comparison between kinetic and sequential extraction procedures. Environ. Pollut. 127:175–182.

Hooda, P.S. and B.J. Alloway. 1998. Cadmium and lead sorption behaviour of selected English and Indian soils. Geoderma. 84:121-134.

Kabata-Pendias A, A. B. Mukherjee. 2007. Trace elements from soil to human. Heidelberg, Germany: Springer Verlag; 550 pp.

Kabata-Pendias A, and W. Sadurski. 2004. Trace elements and compounds in soil p 79–99. *In*: E. Merian et al. (ed) Elements and their compounds in the environment, Wiley-VCH, Weinheim.

Kabata-Pendias, A., and H. Pendias. 2001. Trace elements in soils and plants. 3rd ed. CRC Press, Boca Raton, FL.

Liao, L., H.M. Selim, and R.D. DeLaune. 2009. Mercury adsorption–desorption and transport in soils. J. Environ. Qual. 38:1608–1616.

Lu, S.G. and Q.F Xu. 2009. Competitive adsorption of Cd, Cu, Pb and Zn by different soils of Eastern China. Environmental Geology. 57:685-693.

Maiz, I., I. Arambarri, R. Garcia, and E. Millan. 2000. Evaluation of heavy metal availability in polluted soils by two sequential extraction procedures using factor analysis. Environ Pollut.110:3-9.

Marin, B., M. Valladon, M. Polve, and A. Monaco. 1997. Reproducibility testing of a sequential extraction scheme for the determination of trace metal speciation in a marine reference sediment by inductively coupled plasma-mass spectrometry. Anal. Chim. Acta 342:91-112.

Mathur, S. P., R.B. Sanderson, A. Belanger, M. Valk, E.N. Knibbe, and C.M. Preston. 1984. The effect of copper applications on the movement of copper and other elements in organic soils. Water Air Soil Pollut. 22:277-288.

Moral, R., R. J. Gilkes, and M. M. Jordán. 2005. Distribution of heavy metals in calcareous and non-calcareous soils in Spain. Water, Air, Soil Pollut. 162:127-142.

Oorts, K. 2013. Copper. P. 367-394. *In*: Alloway B. Heavy Metals in Soils: Trace Metals and Metalloids in Soils and their Bioavailability.3rd. Springer Dordrecht Heidelberg New York London.

Pansu, M., and J. Gautheyrou. 2006. Handbook of soil analysis: Mineralogical, organic and inorganic methods. Springer-Verlag, Berlin.

Ponizovsky, A.A., H.E. Allen, and A.J. Ackerman. 2007. Copper activity in soil solutions of calcareous soils. Environ. Pollut. 145:1–6.

Reedy, O.C., P.M. Jardine, G.V. Wilson, and H.M. Selim. 1996. Quantifying the diffusive mass transfer of nonreactive solutes in columns of fractured saprolite using flow interruption. Soil Sci. Soc. Am. J. 60:1376–1384.

Rouff, A.A., E.J. Elzinga, R.J. Reeder, and N.S. Fisher. 2005. The influence of pH on the kinetics, reversibility and mechanisms of Pb(II) sorption at the calcite-water interface. Geochim. Cosmochim. Acta. 69:5173–5186.

Schmitt H, H. Sticher. 1986. Prediction of heavy metal contents and displacement in soils. Z. Pflanzenernaehr. Bodenk. 149: 157-171.

Schmitt H, H. Sticher. 1986. Prediction of heavy metal contents and displacement in soils. Z. Pflanzenernaehr. Bodenk. 149: 157-171.

Selim, H.M., T.A. Elbana, K. Zhao, J. Xu, and E.L. Fergusson. 2013. Miscible displacement of zinc in soil columns: linear and nonlinear modeling. Soil Sci. Soc. Am. J. 77.

Shaheen, S.M. 2009. Sorption and lability of cadmium and lead in different soils from Egypt and Greece, Geoderma 153 (2009) 61–68.

Sheppard, S.C., and M. I. Sheppard. 1991. Lead in boreal soils and food plants. Water Air Soil Pollut 57–58:79–91.

Smolders, E., and J. Mertens, 2013. Cadmium. P. 283-311. *In*: Alloway B. Heavy Metals in Soils: Trace Metals and Metalloids in Soils and their Bioavailability.3rd. Springer Dordrecht Heidelberg New York London.

Steinnes, E. 2013. Lead. P. 395-409. *In*: Alloway B. Heavy Metals in Soils: Trace Metals and Metalloids in Soils and their Bioavailability.3rd. Springer Dordrecht Heidelberg New York London.

Tack F.M., and M.G. Verloo. 1995. Chemical speciation and fractionation in soil and sediment heavy metal analysis: a review. Int. J. Environ. Anal. Chem. 59: 225-238.

Tsang, D.C.W., and I.M.C. Lo. 2006. Competitive Cu and Cd sorption on and transport in soils: A combined batch kinetics, column and sequential extraction study. Environ. Sci. Technol. 40:6655–6661.

USEPA (U.S. Environmental Protection Agency). 2007. Method 6200: Field Portable X-Ray Fluorescence Spectrometry for the Determination of Elemental Concentrations in Soil and Sediment. P 6200-1:6200-32 *In*: Test Methods for Evaluating Solid Waste, Physical/Chemical Methods (SW-846). http://www.epa.gov/epawaste/hazard/testmethods/sw846/online/index.htm

Wei, X.R., M.D. Hao, and M.G. Shao. 2007. Copper fertilizer effects on copper distribution and vertical transport in soils. Geoderma. 138: 213–220.

Zhang, H., and H.M. Selim. 2006. Modeling the transport and retention of arsenic (V) in soils. Soil Sci. Soc. Am. J. 70:1677–1687.

CHAPTER 6. REACTIVITY OF LEAD AND TIN IN SOILS: SORPTION-DESORPTION EXPERIMENTS

6.1 Introduction

Lead (Pb) is a naturally occurring element which can be found in all environmental media: air, soil, sediment, and water. According to the U.S. Environmental Protection Agency, the concentrations of Pb in soils that are protective of ecological receptors as known as ecological soil screening levels (Eco-SSLs) are 11, 56, and 120 ppm for birds, mammals, and plants respectively, (USEPA 2005). Plant toxicity levels of Pb in soils are not easy to evaluate, but it is generally agreed that a soil Pb concentration ranging from 100 to 500 mg kg^{-1} is considered as excessive (Kabata-Pendias and Pendias, 2001). Pb concentrations vary from one soil to another due to the variation in soil physiochemical characteristics and the occurrence of anthropogenic sources of Pb contamination. Lead is relatively highly sorbed on soils; soil pH, cation exchange capacity (CEC), clay content, $CaCO_3$, organic matter (OM), were positively correlated with Pb sorption in soils (Hooda and Alloway, 1998). Lead sorption isotherms were strongly nonlinear and the sorption capacity increased from 3.22 mg g^{-1} at pH = 2.0 to 7.59 mg g^{-1} at pH = 5.5 (Martínez-Villegas et al., 2004). Soil OM has a significant effect on Pb-sorption capacity, Strawn and Sparks (2000) found that removing of OM decreased 40% of Pb sorption comparing with untreated soil. Moreover, McKenzie (1980) found that Pb adsorption by Mn oxides was up to 40 times greater than Pb adsorption by Fe oxides and no evidence for oxidation of Pb nor the formation of specific Pb-Mn minerals was found.

Lead fractionation depends on soil properties and total amount of pollution loading. Marin et al. (1997) found that Pb was essentially extracted from the Fe-Mn oxides fraction with 32% of the total (11.01 mg kg^{-1}) whereas 5.5 and 4.5% were associated with the exchangeable and OM fractions, respectively. Also, Davidson et al. (1998) studied Pb fractionation in an

industrially contaminated site. They reported that for the surface layer (2-13 cm) contained 600 mg kg^{-1} total Pb, 32 and 25% of Pb were associated with Fe-Mn oxides and OM/sulfides fractions, respectively. Whereas less than 0.1% of Pb associated with Fe-Mn oxides in the deep layer (60-85 cm) that contained around 6000 mg kg^{-1}, and more than 45% associated with OM/sulfides fraction. In addition to soil properties, land use influences Pb fractionation in soil. Chrastný et al (2012) found that higher amount of exchangeable Pb was found in forest land compared to pasture land and the Pb was mainly associated with reducible and oxidizable fractions in contaminated organic soil horizons.

Numerous studies were carried out to explore the competitive effect of other heavy metals on Pb retention in soils. In batch experiments, Schmitt and Sticher (1986) reported a higher availability of Cd, Cu, and Pb when applied concurrently due to competition for sorption sites. Their results from sorption batch experiments indicated that Pb-saturation level decreased from 6.33 mg g^{-1} for single Pb solution to 1.72 mg g^{-1} when a mix solution of 18:59:1 as Pb: Cu: Cd was applied. Lu and Xu (2009) evaluated the competitive adsorption of four heavy metals Cd, Cu, Zn and Pb and found that Pb was the most strongly sorbed metal by the studied soils. They reported weaker competition for low initial concentrations due to the extent of available sorption sites for most cations in the adsorption complex. Fonseca et al. (2011) studied sorption and transport of Cr, Cd, Cu, Zn and Pb to evaluate the co-contamination of a loamy sand soil by single and multiple heavy metals. Their results for Pb showed that multiple heavy metals reduced Pb sorption capacity, whereas soils exhibited higher Pb retention when noncompetitive sorption of Pb was occurred. Recently, Chotpantarat et al. (2012) showed that compatitive sorption (binary and multi-metal systems) of Ni, Mn, Zn, and Pb reduced the sorption capacity of Pb on lateritic soil under flow conditions.

Tin (Sn) occurs in the Earth's crust at an average concentration above 2 mg kg^{-1} with two oxidation states, +2 and +4 stannous and stannic, respectively (Kabata-Pendias and Mukherjee, 2007). In contaminated soils and sediments, Sn concentration may be highly elevated up to 1000 mg kg^{-1} (Schafer and Fembert, 1984; Bryan and Langston, 1992). There is a relatively small dataset concerning inorganic tin in soil, and no suggestion that levels are sufficiently high to cause toxicity (Clifford et al., 2010). Various versions of Eh–pH diagrams for inorganic Sn have been constructed (Takeno, 2005) and Sn may exist in different species such as Sn^{4+}, Sn^{2+}, $Sn(OH)_2(aq)$, $Sn(OH)_2(S)$, Sn $(OH)_2^{2+}$ among others. Tin exhibits high potential to be sorbed and retained on soil. Some inorganic tin compounds dissolve in water, whereas most inorganic tin compounds bind to soils and sediments (Ostrakhovitch and Cherian, 2007). Nakamaru and Uchida (2008) studied Sn sorption behavior in Japanese soils using ^{113}Sn tracer, and reported that Sn distribution coefficient, K_d, ranged between 128 and 1590000 L kg^{-1}. Unexpectedly, the authors found that the K_d values increased with decreasing pH. Moreover, they found that the major fraction of soil-sorbed Sn was associated with OM or Al/Fe- (hydro) oxides fractions. Hou et al. (2006) showed that Sn occurred in relatively diverse fractions and the concentrations of Sn in the residues were large in clay-rich soils. They found that the average proportions of the mobilizable (exchangeable, carbonate-bound, metal-organic complex, easily reducible metal oxide-bound) fractions of Sn was 36$\pm$16%, whereas 40$\pm$13% associated with the residues.

Literature review revealed that several studies accounted for the sorption of inorganic Sn on soil whereas it appears that no studies have been carried out to explore the competitive sorption between Pb and Sn in soils. In the current research, the retention behavior of Sn and Pb in acid soils was studied and simulated. The specific objectives of this study were to (i) measure the sorption-desorption of single and binary systems of Sn and Pb in two acid soils, (ii) quantify

the fractionation of Sn and Pb in the studied soils before and after desorption experiment, and (iii) simulate the retention kinetics of Sn and Pb using second-order two-site models.

6.2 Materials and Methods

6.2.1 Sorption and Release

Two soils were selected for this study, Olivier (fine-silty, mixed, active, thermic Aquic Fraglossudalfs) and Windsor (mixed, mesic Typic Udipsamments) soils. Selected chemical properties including pH, OM, and CEC are given in Table 6.1. Additionally, sequential extraction of Fe, Al, and Mn were carried out according to Amacher (1996). For the exchangeable phase 10 ml of 0.1 *M* $Mg(NO_3)_2$ was added to the 0.5 g soil and shaken for 2 h. Subsequently, the metal oxides fraction extracted by 40 ml of oxalate solution, followed by 25 ml of pH 2, 30% H_2O_2 to extract metals associated with the OM phase.

Table 6.1. Selected physical and chemical properties of the studied soils.

	Olivier	**Windsor**
pH (1 :2.5)	5.80	6.05
Total Carbon (g kg^{-1})	21.28	11.92
CEC (cmol kg^{-1})	8.6	3.28
Sequential Extraction		
Fe (mmole kg^{-1})		
Exchangeable	0.015	0.013
Associate with oxides	146.2	174.0
Associate with OM	7.829	4.732
Al (mmole kg^{-1})		
Exchangeable	0.107	Nd†
Associate with oxides	110.6	180.3
Associate with OM	57.2	13.3
Mn (mmole kg^{-1})		
Exchangeable	0.447	0.262
Associate with oxides	13.5	4.799
Associate with OM	0.084	0.350

† Not detected

Retention of Pb and Sn was studied using the batch method described by Selim and Amacher (1997). Two sets of duplicate 3-g samples of each soil were placed in 40-mL

polypropylene tubes and mixed with 30-mL solutions of known Pb concentrations. Specifically, six initial Pb concentrations (C_o) (0.125, 0.186, 0.428, 0.932, 1.933, and 3.804 mmol L^{-1}) were used; the respective concentrations in µg mL^{-1} are 26, 38.5, 88.6, 193.2, 400, and 788.2. Reagent-grade $Pb(NO_3)_2$ was prepared in 5 mmol L^{-1} $Ca(NO_3)_2$ background solution. The samples were shaken at 150 rpm on a reciprocal shaker for 1d for one set and 7d for the another set and subsequently centrifuged for 10 min at 1300 xg. A 5-mL aliquot was sampled from the supernatant and the collected samples were analyzed for total Pb concentration using inductively coupled plasma–atomic emission spectrometry (ICP–AES; Spectro Citros CCD). The fraction of Pb sorbed by the soil was calculated based on the change in concentration in the solution (before and after each adsorption). For the 1d-set, immediately following 1d sorption, desorption commenced for the highest two initial concentrations (1.933, and 3.804 mmol L^{-1}) using successive dilutions for 10 consecutive steps (3 d of reaction time for each step).

Similarly, two sets of duplicate 3-g samples of each soil were used to study sorption-desorption of Sn by the two soils. Six initial Sn concentrations (C_o) (0.122, 0.369, 0.946, 1.844, 3.624, and 5.405 mmol L^{-1}) were used; the respective concentrations in µg mL^{-1} are 14.5, 43.8, 112.3, 218.9, 430.2, and 641.6. Reagent-grade $SnCl_2$ was prepared in 5 mmol L^{-1} $Ca(NO_3)_2$ background solution. The samples were shaken at 150 rpm on a reciprocal shaker for 24 h for one set and 7 d for the another set and subsequently centrifuged for 10 min at 1300 xg. A 5-mL aliquot was sampled from the supernatant and the collected samples were analyzed for total Sn concentration using ICP–AES. Immediately following 1d sorption, desorption commenced for the highest initial concentrations (3.624 and 5.405 mmol L^{-1}) using successive dilutions for 10 consecutive steps (3d of reaction time for each step). To study the influence of Sn and Pb on the retention and release of each other, the above mentioned Pb batch experiments were also carried out where different levels of Sn concentrations were added into the background solutions. Two

levels of Sn were used; namely 1.685and 3.370 mmol L^{-1}. The form of Sn used was $SnCl_2$ in 5 mmol L^{-1} $Ca(NO_3)_2$ as the background solution. Release of Al, Fe, and Mn into the effluent was monitored during all batch experiments as well as the change in solution pH.

In order to quantify the amount of metals associated with various phases, following the 7d sorption and the last desorption step for 1d Sorption/30d desorption-experiment, three selective extraction steps were used, referred to here as exchangeable, organic matter, and metal oxide fractions according to Amacher (1996). Based on mass balance calculations, the metal residue was determined to quantify the strongly bound fraction in each soil.

6.2.2 Sorption Isotherms and Kinetic Modeling

Sorption isotherms describe the distribution of metal concentration in aqueous phase and sorbed on the soil. The Freundlich equation was utilized to describe such adsorption isotherms,

$$S = K_F C^b \qquad [6.1]$$

where S represents the amount sorbed (µg g^{-1}), C is the concentration in solution µg mL^{-1}, b is a dimensionless reaction order and K_F is the Freundlich distribution coefficient (mL g^{-1}).

Adsorption isotherms of Pb and Sn also were described using the Langmuir equation,

$$S = \frac{S_{max} K_L C}{1 + K_L C} \qquad [6.2]$$

Where S_{max} is the sorption capacity (µg g^{-1}) and K_L (mL µg^{-1}) is a Langmuir coefficient related to the binding strength. Nonlinear least square optimization of SAS PROC NLIN (SAS Institute, 2011) was used to obtain best-fit parameters for the adsorption data using both models.

Second-Order Two-Site (SOTS) model was used in this study to simulate Sn and Pb sorption-desorption isotherms and the kinetics of Pb reactivity in soils. Basic to the second-order formulation is the assumption that a limited number of sites are available for solute adsorption in soils. Furthermore, the reaction rate is a function of the solute concentration in the soil solution

and the availability of adsorption sites on soil matrix surfaces. Specifically, retention mechanisms are assumed to depend not only on C but also the number of sites (φ) that are available for solute adsorption in soils (Selim and Amacher. 1988; Selim and Amacher, 1997). The model also assumes that a fraction of the total sorption sites is rate limited, while the remaining fractions interact rapidly or instantaneously with the solute in the soil solution. The sorbed phases S_e, S_k, and S_{irr} are in direct contact with the solute in the solution phase (C) and are governed by concurrent reactions (see Fig. 6.1). Specifically, C is assumed to react rapidly and reversibly with the equilibrium phase S_e. The relations between C and S_k and S_{irr} are governed by reversible nonlinear and irreversible linear kinetic reactions, respectively. A second irreversible reaction was assumed as a consecutive reaction of the S_k phase into a less accessible or strongly retained phase S_s. Therefore, the model formulation can be expressed as

$$S_e = K_e \theta\, C\, \varphi \qquad [6.3]$$

$$\frac{\partial S_k}{\partial t} = k_1 \theta C \varphi - (k_2 + k_3) S_k \qquad [6.4]$$

$$\frac{\partial S_s}{\partial t} = k_3 S_k \qquad [6.5]$$

$$\rho \frac{\partial S_{irr}}{\partial t} = \theta\, k_{irr} C \qquad [6.6]$$

Here φ is related to the sorption capacity (S_{max}) by:

$$S_{max} = \varphi + S_e + S_k + S_s + S_{irr} \qquad [6.7]$$

where φ and S_{max} (μg solute g^{-1} soil) are the unoccupied (or vacant) and total sorption sites on soil surfaces, respectively. The total sorption sites S_{max} was considered as an intrinsic soil property and is time invariant. In addition, S_e is the amount retained on equilibrium-type sites (μg g^{-1}), S_k is the amount retained on kinetic-type sites (μg g^{-1}), S_s is the amount retained irreversibly by consecutive reaction (μg g^{-1}), and S_{irr} is the amount retained irreversibly by a concurrent type of reaction (μg g^{-1}). The equilibrium constant is K_e (mL μg^{-1}), the reaction rate

coefficients are k_1 (mL μg^{-1} h^{-1}), k_2 (h^{-1}), k_3 (h^{-1}), and k_{irr} (h^{-1}), while C is the solute concentration (μg mL^{-1}), θ is the volumetric water content (mL mL^{-1}), and t is the reaction time (h).

At any time t, the total amount of solute sorbed by the soil matrix, S, can be expressed as

$$S = S_e + S_k + S_s + S_{irr} \qquad [6.8]$$

Statistical criteria used for estimating the goodness-of-fit of the models to the data were the coefficients of determination, r^2, and the root mean square error (RMSE):

$$RMSE = \sqrt{\frac{\sum(C_{ops}-C)^2}{n_o-n_p}} \qquad [6.9]$$

where C_{ops} is the observed metal concentration at time t, C is the simulated metal concentration at time t, n_o is the number of measurements, and n_p is the number of fitted parameters.

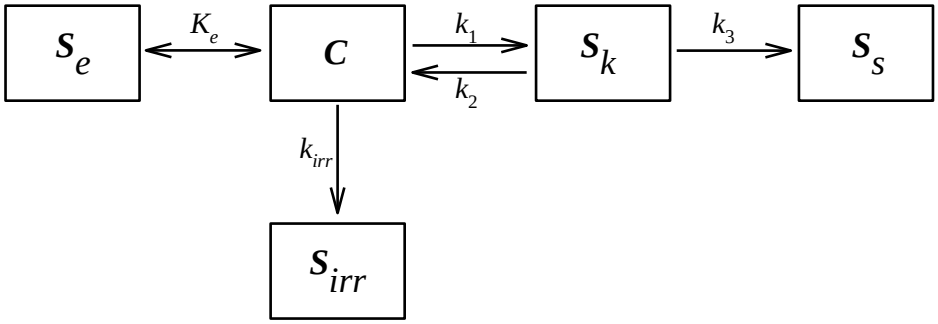

Fig. 6.1. A schematic of the second-order, two-site (SOTS) model for retention of reactive chemicals in soils, where C is the solute in the solution phase, S_e is the amount retained on equilibrium-type sites, S_k is the amount retained on kinetic-type sites, S_s is the amount retained irreversibly by consecutive reaction, S_{irr} is the amount retained irreversibly by concurrent type of reaction, and K_e, k_1, k_2, k_3, and k_{irr} are reaction rates.

6.3 Results and Discussion

6.3.1 Sorption Isotherm

Both Windsor and Olivier soils exhibited high affinity for Sn. For a single Sn system, the sorption isotherms indicated that sorption maxima did not converged within the experimental time frame where more than 99.5% of the added Sn concentrations were sorbed by both soils (Fig. 6.2). Based on coefficient of determination (r^2) and the standard error for the estimated

Freundlich and Langmuir parameters, the use of Langmuir isotherm for both soils was not successful. Freundlich equation provided poor simulations for the Sn isotherms and the reaction order values, *b*, were 2.46 and 3.72 for Olivier and Windsor soils, respectively (Table 6.2). Such high sorption and *b* values much greater than 1 imply irreversible or nonspecifically sorption (Selim et al., 2004; Elbana and Selim, 2011). The sorption isotherms for Windsor soil exhibited slope increases for large initial Sn concentrations and slope reversal was observed for the largest additions (see Fig 6.2). Uygur and Rimmer (2000) explained this change of slope as evidence of precipitation. Strong Sn sorption on Japanese agricultural soils with K_d value of 1,590,000 L kg^{-1} was reported by Nakamaru and Uchida (2008).

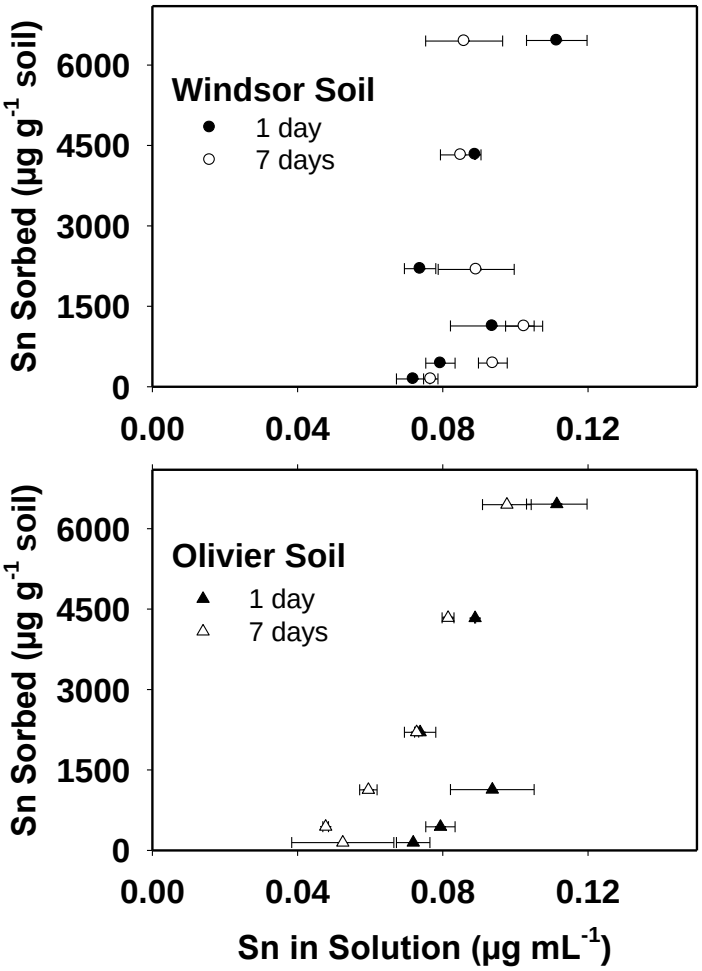

Fig. 6.2. Sn sorption isotherms for Windsor (top) and Oliver (bottom) soils for 1d and 7d sorption experiments, symbols are experimental measurements and represent different replications.

Table 6.2 Estimated Freundlich and Langmuir parameters ± their standard errors (SE) for single Pb, single Sn, and Pb retention in the presence of different Sn concentrations by Windsor and Olivier soils for one and seven days-sorption experiments.

Ion		Soil	Freundlich model			Langmuir Model		
			K_f (μg^{1-b} g^{-1} mL^b)	b	r^2	S_{max} (μg g^{-1})	K_L (mL μg^{-1})	r^2
---- Sn ----	Single	Windsor-1day	$1.94x10^7$±4.97 $x10^7$	3.72±1.13	0.5645	$2.07x10^7$±$2.08x10^{11}$	0.001±14.9	0.2460
		Windsor-7day	NA†	NA	----	NA	NA	----
		Olivier-1day	$1.52x10^6$±1.02 $x10^6$	2.46±0.29	0.9226	$3.24x10^7$±$1.62x10^{11}$	0.001±6.39	0.5891
		Olivier-7day	$1.27x10^7$±1.31 $x10^7$	3.27±0.43	0.9102	$3.24x10^7$±$2.57x10^{11}$	0.001±10.1	0.4843
---------- Pb ----------	Single	Windsor-1day	1790.1±186.4	0.205±0.021	0.9418	4617.6±250.0	3.290±0.884	0.9429
		Windsor-7day	1978.7±234.8	0.220±0.026	0.9247	5133.1±347.6	2.993±0.999	0.9173
		Olivier-1day	1068.7±96.1	0.249±0.018	0.9791	4197.9±338.9	0.106±0.045	0.8993
		Olivier-7day	1366.3±125.5	0.217±0.018	0.9686	4015.1±299.0	1.027±0.475	0.8948
	Mix with 200 µg mL^{-1} (1.685 mmol L^{-1}) Sn	Windsor-1day	709.7±55.1	0.295±0.015	0.9887	3825.9±274.3	0.058±0.018	0.9251
		Windsor-7day	779.0 ±48.8	0.292±0.012	0.9923	3975.2±283.3	0.074±0.024	0.9232
		Olivier-1day	659.4±21.9	0.290±0.006	0.9979	3632.0±277.0	0.038±0.012	0.9231
		Olivier-7day	573.7±21.3	0.313±0.007	0.9978	3593.4±274.6	0.046±0.016	0.9177
	Mix with 400 µg mL^{-1} (3.370 mmol L^{-1}) Sn	Windsor-1day	367.5±25.3	0.365±0.024	0.9789	3487.1±141.6	0.020±0.003	0.9823
		Windsor-7day	330.8 ±48.8	0.410±0.014	0.9945	4230.8±291.9	0.015±0.003	0.9661
		Olivier-1day	254.8±16.2	0.392±0.012	0.9958	3098.1±194.5	0.013±0.003	0.9646
		Olivier-7day	138.7±21.6	0.511±0.029	09856	3911.2±643.8	0.007±0.003	0.9210

† NA, estimation was not applicable; data did not converge with the model.

For the single Pb sorption, Pb sorption isotherms describing the distribution of sorbed Pb versus Pb in aqueous solution are shown in Fig. 6.3. These results reflect the differences in Pb affinity among the different soils after 1d and 7d of sorption. These isotherms showed that Pb sorption by Windsor and Olivier soils to be highly nonlinear. This nonlinearity is also illustrated by the small values (<1) of the Freundlich *b* (see Table 6.2). Specifically, the reaction order values, *b*, were 0.205 to 0.220 and 0.217 to 0.249 for Windsor and Olivier soils, respectively. Also, the parameter "*b*" is a joint measure of both the relative magnitude and diversity of energies associated with a particular sorption process (Weber et al., 1992).

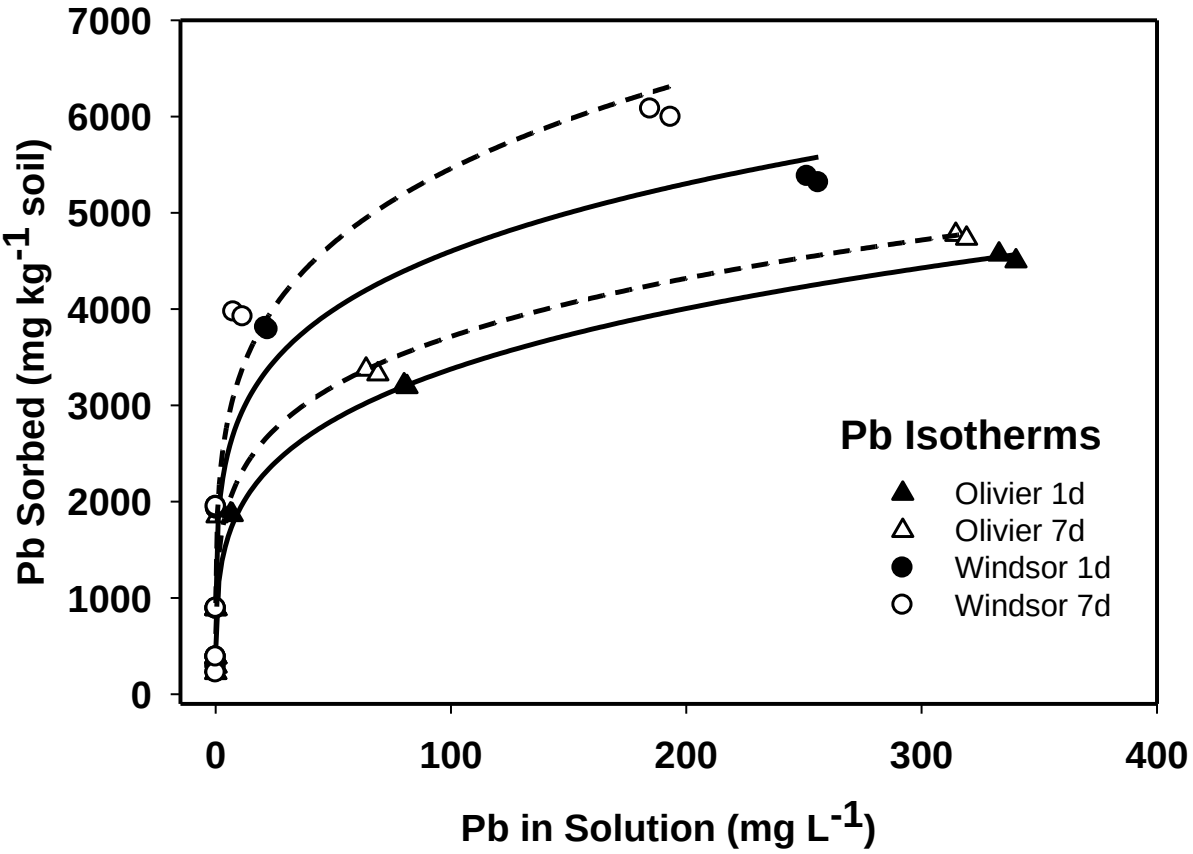

Fig. 6.3. Lead sorption isotherms for Windsor and Oliver soils for 1d and 7d sorption experiments, symbols are experimental measurements and represent different replications. Solid and dashed curves are Freundlich calculations.

Freundlich isotherms revealed that the retention characteristics of Pb were affected by increasing equilibration time from 1d to 7d. Increasing equilibration time led to increase the

value of K_F in both soils (Table 6.2). In Windsor and Olivier soils Pb exhibited lower affinity compared to Sn. Based on Langmuir fitting, Winsor soil exhibited Pb sorption capacity, S_{max}, of 4618±250 μg g^{-1} and 5133±348 μg g^{-1} for 1d and 7d, respectively. Whereas, the respective values for Olivier soil were 4198±339 μg g^{-1} and 4015±299 μg g^{-1}. Such variation in S_{max} indicated time dependent Pb sorption for Windsor soil.

The presence of Sn in the background solution reduced Windsor and Olivier soil's Pb-affinity as depicted by lowering K_F values and increasing *b* value (see Fig 6.4 and Table 6.2). For Windsor soil in a mixed system of Pb and Sn with Sn of 1.685 mmol L^{-1}, the K_F was reduced from 1790 and 1979 mL g^{-1} to 710 and 779 mL g^{-1} for 1d and 7d, respectively. Whereas the mixed system of Pb with 3.370 mmol L^{-1} Sn reduced K_F to 368 and 331 mL g^{-1} for 1d and 7d, respectively (Table 6.2). Similarly for Olivier soil, the mixed system of Pb with 1.685 mmol L^{-1} Sn reduced K_F from 1069 and 1366 mL g^{-1} to 659 and 574 mL g^{-1} for 1d and 7d, respectively. Whereas the mixed system of Pb with 3.370 mmol L^{-1} Sn reduced K_F to 255 and 139 mL g^{-1} for 1d and 7d, respectively. Moreover, the presence of Sn with Pb as a binary system reduced the values of Langmuir parameters (S_{max} and K_L). The reduction of maximum sorption capacity of Pb due to the presence of other metals such as Ni, Mn, and Zn was a result of competition for sorption sites (Chotpantarat et al., 2012).This decrease in maximum sorption and binding strength parameters were indicative of the reduction effect of Sn on Pb sorption by Windsor and Olivier soils.

The influence of the presence of different Pb concentration in the soil solution on Sn sorption is presented in Fig. 6.5. Results indicated no significant effect of Pb on Sn retention in both Windsor and Olivier soils. The presence of three different Pb concentrations (200, 400, and 800 μg mL^{-1}) mixed with two different initial Sn concentrations (200 and 400 μg mL^{-1}) revealed that the average Sn sorbed amounts on Windsor soil were 1933±7 μg kg^{-1} and 3872±6 μg kg^{-1}

when 200 µg mL^{-1} and 400 µg mL^{-1} Sn initial concentrations were applied, respectively. Whereas the respective values for Oliver soil were 1928±13 and 3864±4 µg kg^{-1}, respectively. Moreover, these results showed almost complete Sn sorption on the studied soils since more than 99.9% of the initial Sn was sorbed.

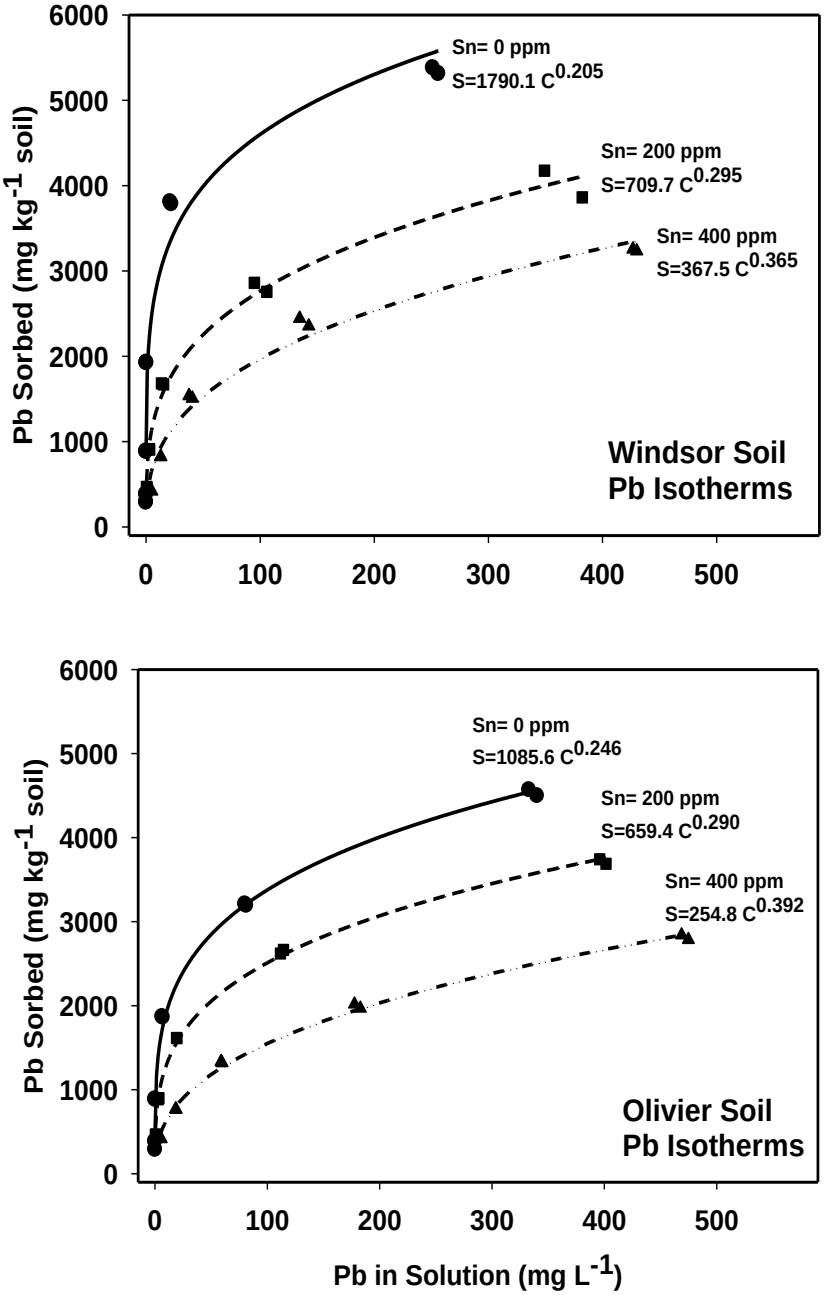

Fig. 6.4. Lead sorption isotherms for Windsor (top) and Olivier (bottom) soils. Different symbols represent the experimental results in the presence of different Sn levels added (0, 200, and 400 ppm) in the soil solution. Solid and dashed curves represent calculations using the Freundlich model equestion (6.1).

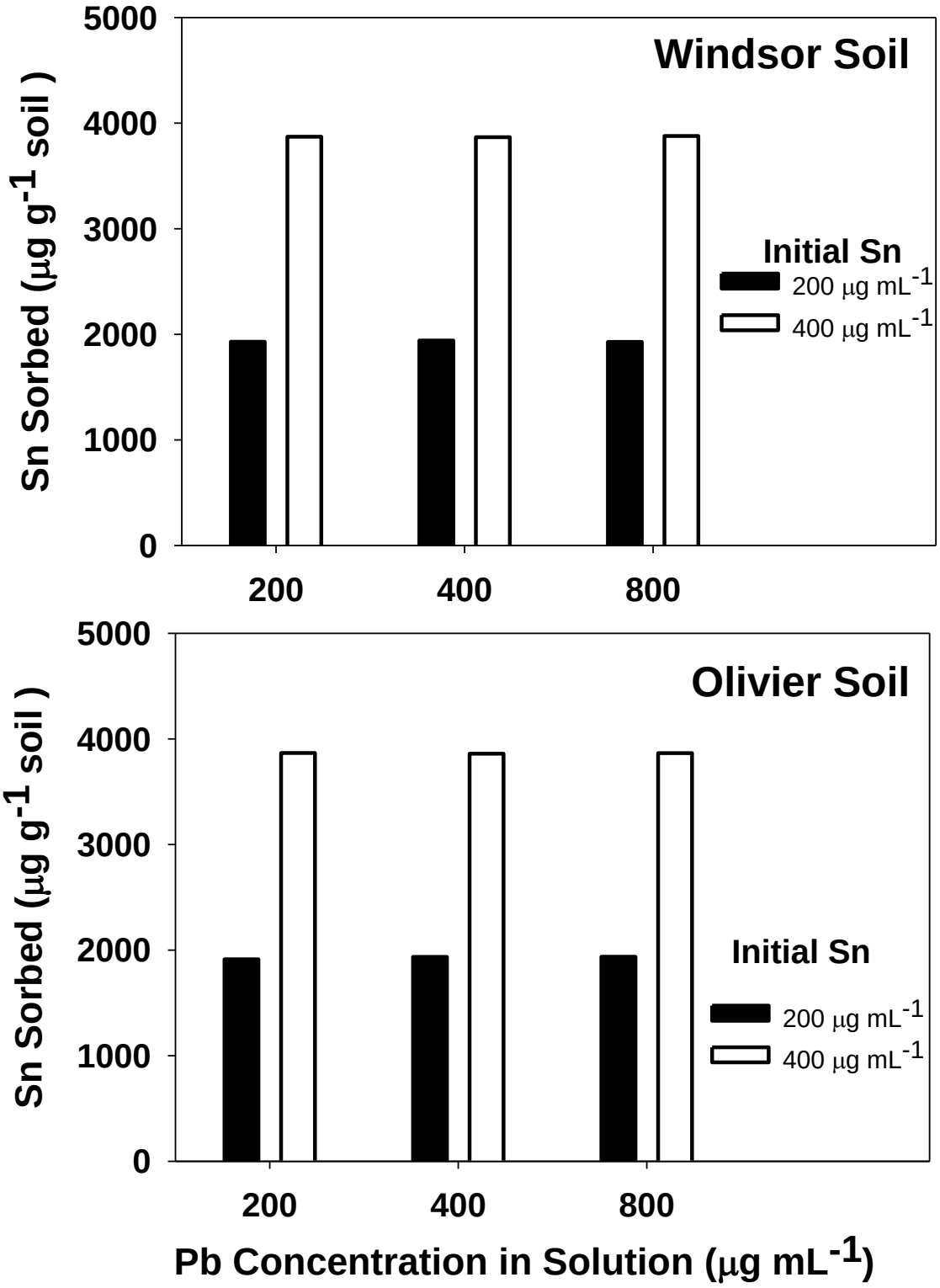

Fig. 6.5. Effect of different Pb levels added (0, 200, and 400 ppm) into the background solutions on the sorption amount of Sn after 1d sorption experiment.

6.3.2 Hysteresis and Retention Kinetics

Sorption-desorption results of Sn by Windsor and Olivier soils indicated exceptionally strong Sn retention on these soils. Specifically, less than 0.001% of sorbed Sn was released after 30d of 10 successive dilutions consecutive steps. For Windsor soil, the sorbed Sn amounts immediately following 1d sorption were 36.49±0.05 mmole kg^{-1} and 54.40±0.07 mmole kg^{-1} for the highest initial concentrations of 3.624 and 5.405 mmol L^{-1}, respectively. The respective values after 30d desorption were 36.47±0.04 mmole kg^{-1} and 54.38±0.07 mmole kg^{-1}. Similarly for Olivier soil, the sorbed Sn amounts following 1d sorption were 36.55±0.08 and 54.58±0.01 mmole kg^{-1} for the highest initial concentrations of 3.62 and 5.41 mmol L^{-1}, respectively. The respective values after 30d desorption were 36.54±0.08 and 54.56±0.01 mmole kg^{-1}. Consistent with our results, Herting et al. (2008) showed that no measurable Sn release was detected over 2 years in a field study in an urban environment (the detection limit of 0.001 µg mL^{-1}).

Sorption-desorption results of Pb by Windsor and Olivier soils shown in figures 6.6 and 6.7, respectively, exhibited considerable hysteresis. This hysteretic behavior of Pb resulting from discrepancies between sorption and desorption isotherms depended on the concentration of Sn in the system. These isotherms, which showed the concentration in soil solution (*C*) vs. the amount sorbed by the soil matrix (*S*), were highly nonlinear and illustrate strong Pb sorption. The presence of Sn reduced the sorbed Pb. Specifically, for Windsor soil, the highest sorbed amounts were 25.81, 19.40 and 15.66 mmole kg^{-1} in the presence of Sn concentration of 0, 1.685, and 3.370 mmol L^{-1}, respectively (see also Fig. 6.6). For Olivier soil, the respective amount of Pb sorbed were 21.88, 17.93 and 13.57 mmole kg^{-1}, respectively.

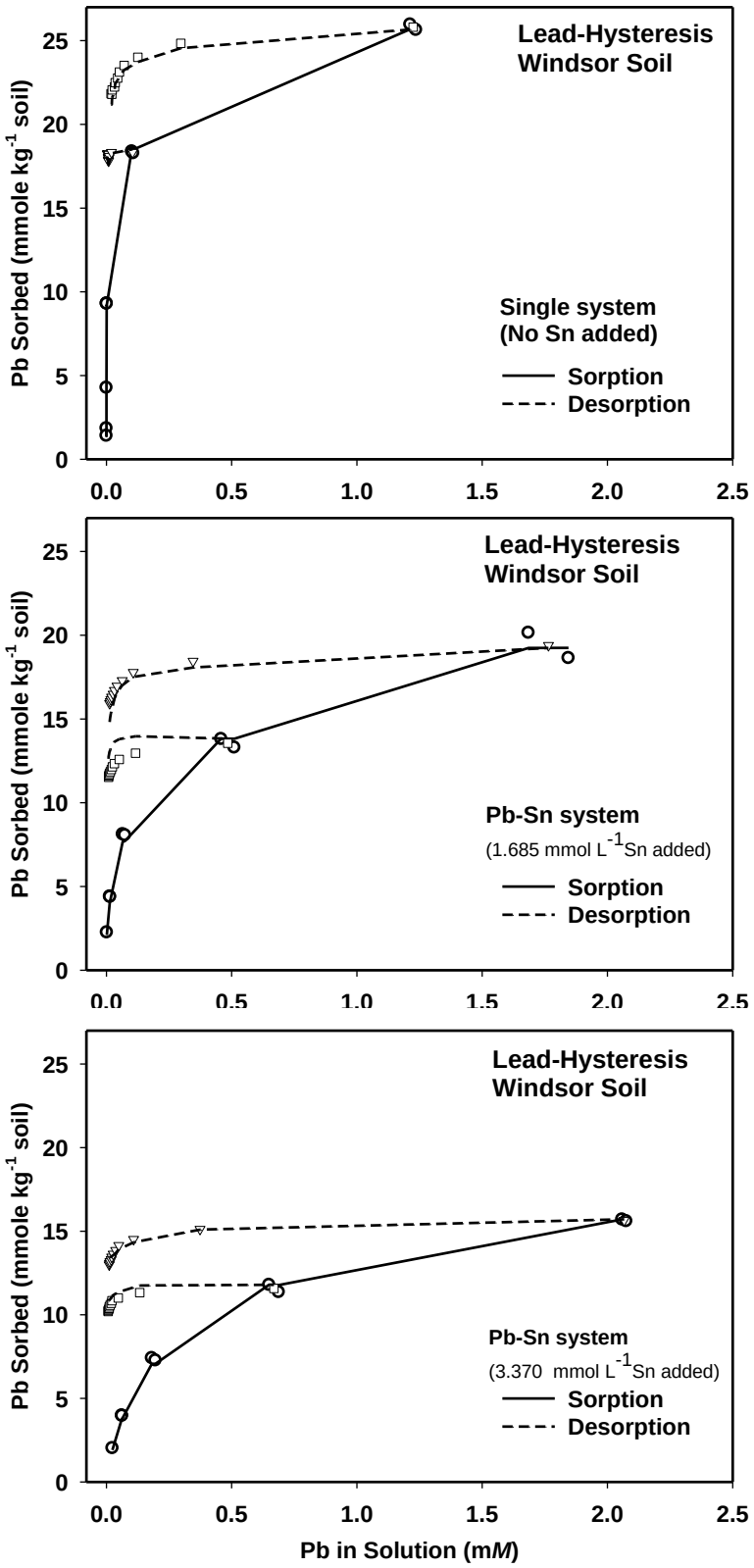

Fig 6.6. Sorption and desorption of Pb for the Windsor soil in the presence of different Sn levels (0, 1.685, and 3.370 mmol L^{-1}) in soil solutions. The solid and dashed curves are the second-order two-site model simulations for sorption and desorption, respectively.

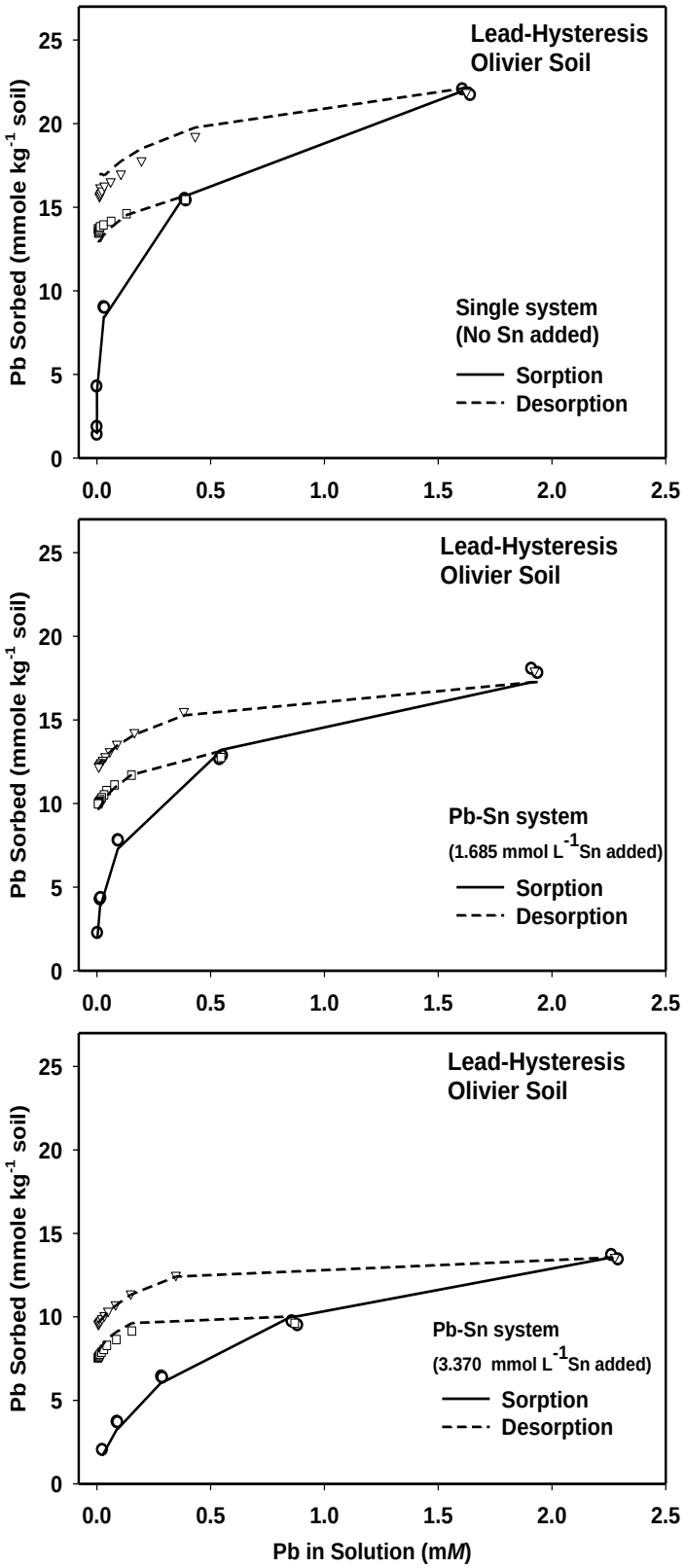

Fig. 6.7. Sorption and desorption of Pb for the Olivier soil in the presence of different Sn levels (0, 1.685, and 3.370 mmol L^{-1}) in soil solutions. The solid and dashed curves are the second-order two-site model simulations for sorption and desorption, respectively.

Concentrations of Pb sorbed versus time during Pb desorption or release are illustrated in Figures 6.8 and 6.9. In the absence of Sn, average amounts of Pb released from Windsor soil, as percentage of that sorbed, were 2.96 and 15.74% for C_o of 1.933 and 3.804 mmol L^{-1}, respectively. In the presence of 1.685 mmol L^{-1} Sn, the respective average amounts of Pb released were 15.01 and 17.91%. The respective average amounts of Pb released were 11.90 and 16.99% in the presence of 3.370 mmol L^{-1} Sn (Fig. 6.8). For low and high initial Pb concentrations, time-dependent behavior of released Pb from Windsor soil showed the continued decreasing of sorbed Pb with time in the presence of Sn. Whereas this kinetic behavior was not distinct when low initial Pb concentration (1.933 mmol L^{-1}) was applied in absence of Sn (Fig. 6.8). For Olivier soil, in the absence of Sn, 12.92 and 28.47% of Pb was released for the highest initial Pb concentrations of 1.933 and 3.804 mmol L^{-1}, respectively. In the presence of 1.685 mmol L^{-1} Sn in soil solutions, the respective average Pb released were 21.75 and 31.97%. Whereas, the respective average amounts of Pb released were 21.59 and 29.58% in the presence of 3.370 mmol L^{-1} Sn (Fig. 6.9). The results showed that Olivier soil exhibited much more time-dependent for Pb release compared to Windsor soil where 12.92 to 31.97% of Pb was released within the 30d desorption time. Also, the mixing of Pb with Sn led to release of more than 20% of sorbed Pb within desorption period. Overall, Pb released from Oliver soil was rapid during the initial stages of desorption, followed by slow release (see Fig. 6.9).

6.3.3 SOTS Modeling

Attempts to describe the Pb release results using SOTS model described earlier are illustrated by the solid curves shown in in Figures 6.8 and 6.9. The SOTS simulations based on kinetic fits listed in Table 6.3. The SOTS model accounts for several possible equilibrium and kinetic interactions of Pb in soil. As a result, different versions of the model shown in Fig. 6.1 represent different reactions from which one can deduce Pb retention mechanisms.

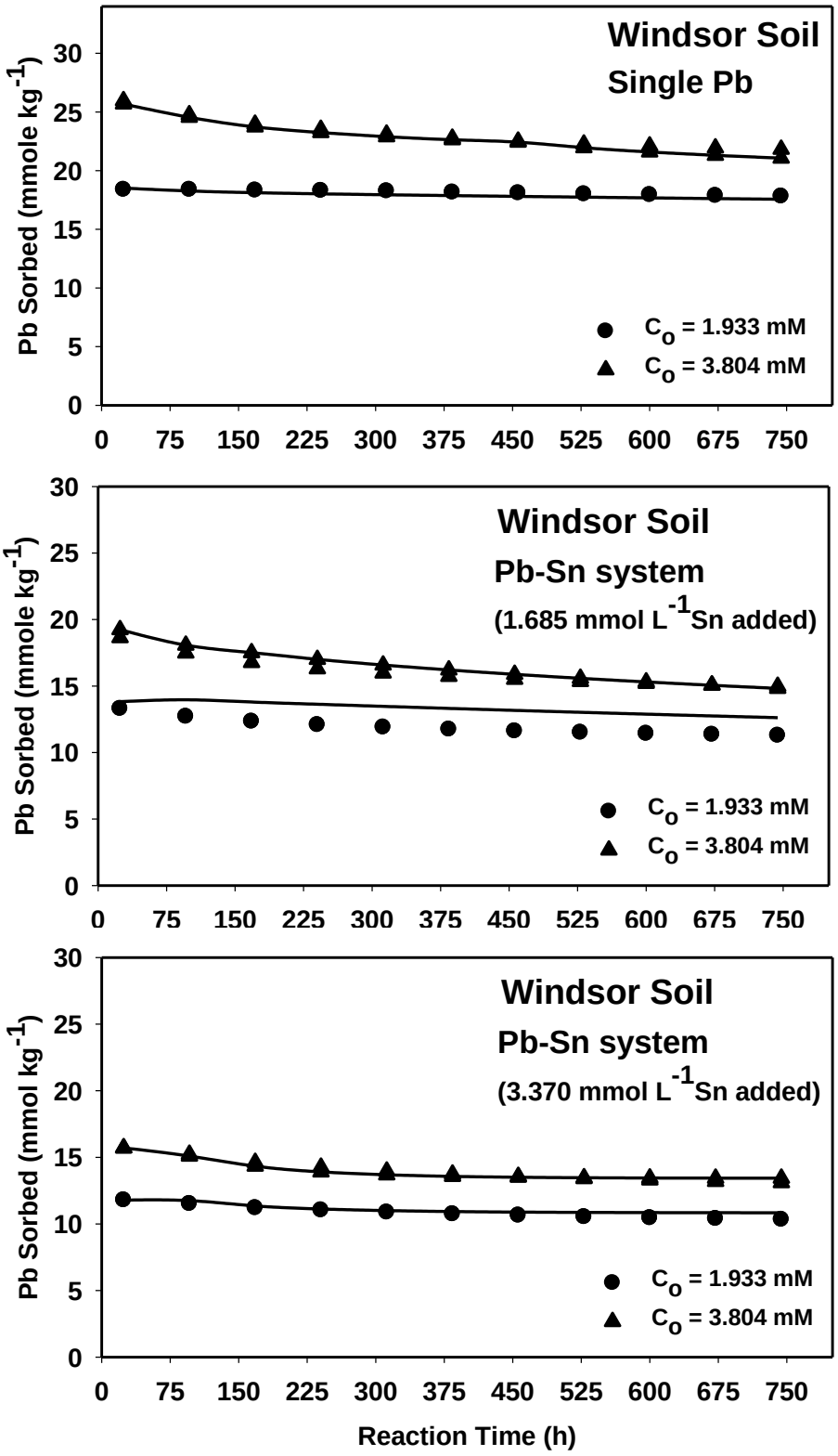

Fig. 6.8. Lead sorbed vs. time during release for Windsor soil. Symbols are for different initial concentrations (C_o); the solid curves are the second-order two-site model simulations.

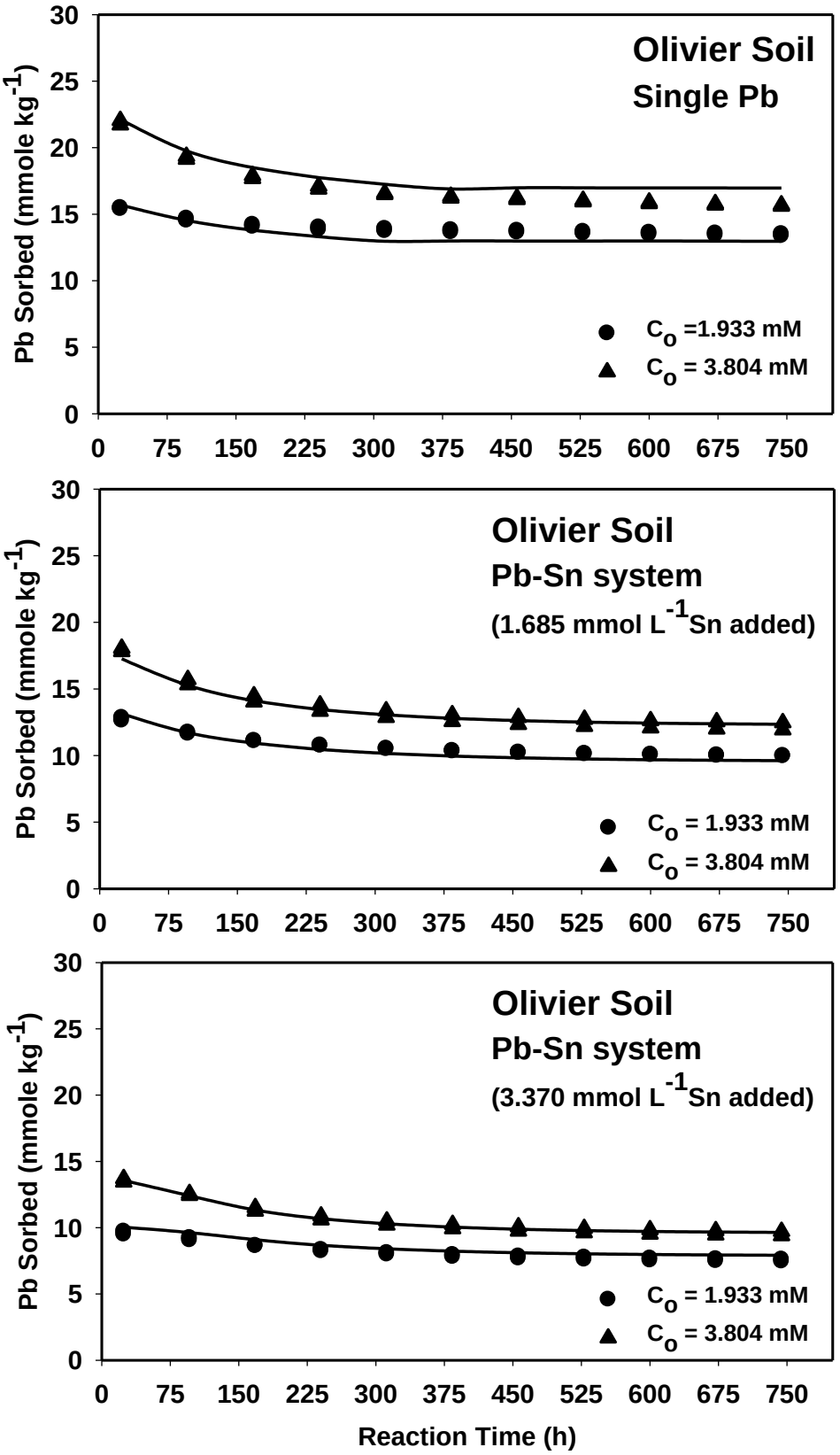

Fig. 6.9. Lead sorbed vs. time during release for Olivier soil. Symbols are for different initial concentrations (C_o); the solid curves are the second-order two-site model simulations.

Table 6.3 Second-order, two-site (SOTS) model parameter estimates for Pb retention by Windsor and Olivier soils reaction rates (K_e, k_1, k_2, k_3, and k_{irr}) ± their standard errors, with root mean square error (RMSE) and coefficient of determination (r^2).

Model Version†	*RMSE*	r^2	K_e	K_1	K_2	k_3	k_{irr}
			mL μg^{-1}	mL μg^{-1} h^{-1}	---------- h^{-1} ----------		
Windsor Soil with no Sn							
M1	2.650	0.9979	0.2225±0.0079	0.0023±0.0004	0.0010±0.0002	---	---
M2	4.066	0.9946	---	0.0152±0.0001	0.0395±0.0002	0.0013±0.00002	---
M3	4.883	0.9932	---	0.0010±0.0001	0.0039±0.0007	---	0.0052±0.0001
Windsor Soil with 200 ppm Sn							
M1	6.360	0.9931	0.0048+0.0008	0.0005+0.00004	0.0008+0.0002	---	---
M2	8.748	0.9872	---	0.0128+0.00002	0.2858+0.001	0.0064+0.0007	---
M3	8.202	0.9936	---	0.00016+0.00003	0.0054+0.0019	---	0.00023+0.00003
Windsor Soil with 400 ppm Sn							
M1	5.406	0.9968	0.0023+0.00002	0.0003+0.00001	0.0007+0.0001	---	---
M2	4.013	0.9985	---	0.0003+0.00001	0.0075+0.0016	0.0038+0.0007	---
M3	2.979	0.9989	---	0.0001+0.00001	0.0108+0.0012	---	0.00017+0.00001
Olivier Soil with no Sn							
M1	6.468	0.9931	0.0137±0.0001	0.0008±0.0001	0.0022±0.0005	---	---
M2	5.002	0.9952	---	0.0130±0.00004	0.3623±0.0035	0.0030±0.00003	---
M3	11.085	0.9886	---	0.0003±0.00004	0.0085±0.0039	---	0.0002±0.00004
Olivier Soil with 200ppm Sn							
M1	7.243	0.9948	0.0039+0.0006	0.00048+0.00004	0.0027+0.0005	---	---
M2	5.604	0.9964	---	0.0073+0.0001	0.3459+0.0285	0.0042+0.0005	---
M3	6.955	0.9957	---	0.00027+0.00003	0.0106+0.0020	---	0.00014+0.00002
Olivier Soil with 400 ppm Sn							
M1	6.420	0.9969	0.00215+0.00001	0.00022+0.00001	0.0015+0.0002	---	---
M2	3.751	0.9988	---	0.00022+0.00001	0.0075+0.0011	0.0033+0.0005	---
M3	3.413	0.9989	---	0.00012+0.00001	0.0088+0.0008	---	0.00010+0.00001

†: M1 = S_e and S_k (K_e, k_1, and k_2,); M2 = S_k, and S_s (k_1,k_2, and k_3); M3 = S_k and S_{irr} (k_1,k_2, and k_{irr}).

Several versions were examined including; (M1) a three parameters model with k_1, k_2, and k_e, (M2) another three parameters model with k_1, k_2 and k_3, and (M3) a three parameters model with k_1, k_2, and k_{irr}. To arrive at the simulation shown, the SOTS model was used in an inverse mode with nonlinear least square approximation. As a result, a set of best estimates criteria used for estimating the goodness-of-fit of the model to the data were r^2 and *RMSE*. For Windsor soil, considering reversible kinetic site, S_k, and instantaneous equilibrium type site, S_e in version M1 provided the best simulation for Pb reactivity for single Pb or Pb-Sn binary system were 1.685 mmol L^{-1}Sn mixed with the background solutions. Whereas, reversible kinetic site, S_k, and linear kinetic reaction, S_{irr} in version M3 provided the best simulation for Pb reactivity when Pb-Sn binary system with 3.37 mmol L^{-1}Sn mixed with the background solutions (Table 6.3). Based on these kinetic simulations, the SOTS model successfully simulated sorption-desorption isotherms for Windsor soil as illustrated by solid and dashed curves in Fig. 6.7. For Olivier soil, despite single or binary system, version M2, that accounted for the reversible kinetic site, S_k and the consecutive reaction on S_s sites, provided the best simulation for Pb reactivity based on r^2 and *RMSE* statistics (see Fig. 6.1 and Table 6.3). In fact, versions M2 and M3 that accounted for kinetic and irreversible reactions equally provided good simulation for the kinetic behavior in the presence of different levels of Sn (see Table 6.3).

6.3.4 Lead and Tin Influence on Release of Al, Fe, and Mn

The induced releases of Al, Fe, and Mn from Windsor and Olivier soils versus the sorbed Pb or Sn are presented in Figures 6.10 and 6.11. Sorption of Pb increased the release of Al, Fe, and Mn from both soils. Specifically, a positive correlation was observed between Mn released from Windsor soil where 0.18 and 0.43 mmole kg^{-1} associated with the lowest and the highest sorbed Pb, respectively (Fig. 6.10). This released Mn was higher than that one found in the exchangeable form (Table 6.1). Windsor soil exhibited low Fe released with average of 0.008

mmole kg^{-1} which was less than the extractable exchangeable Fe, 0.013 mmole kg^{-1} (see Table 6.1). The maximum released Al (0.246 mmole kg^{-1}) found to be associated with the highest sorption of Pb (25.81 mmole kg^{-1}). For Olivier soil, limited Fe released (average of 0.001 mmole kg^{-1}) associated with Pb sorption whereas the maximum Al released was 0.237 mmole kg^{-1}. Again, positive correlation was observed between released Mn and sorbed Pb where 1.37 and 2.58 mmole kg^{-1} associated with the lowest and the highest sorbed Pb, respectively (Fig. 6.10). The amount of released Mn from Olivier soil was 5 times or higher than that amount was released from Windsor soil. Moreover, Fig. 6.10 shows the relation between the solution pH and the sorbed Pb after 1d. For Windsor soil the pH decreased from 5.95 to 4.47 with average of 5.44 whereas the respective pH values for Olivier soil were 5.87 to 4.48 with average of 5.33.

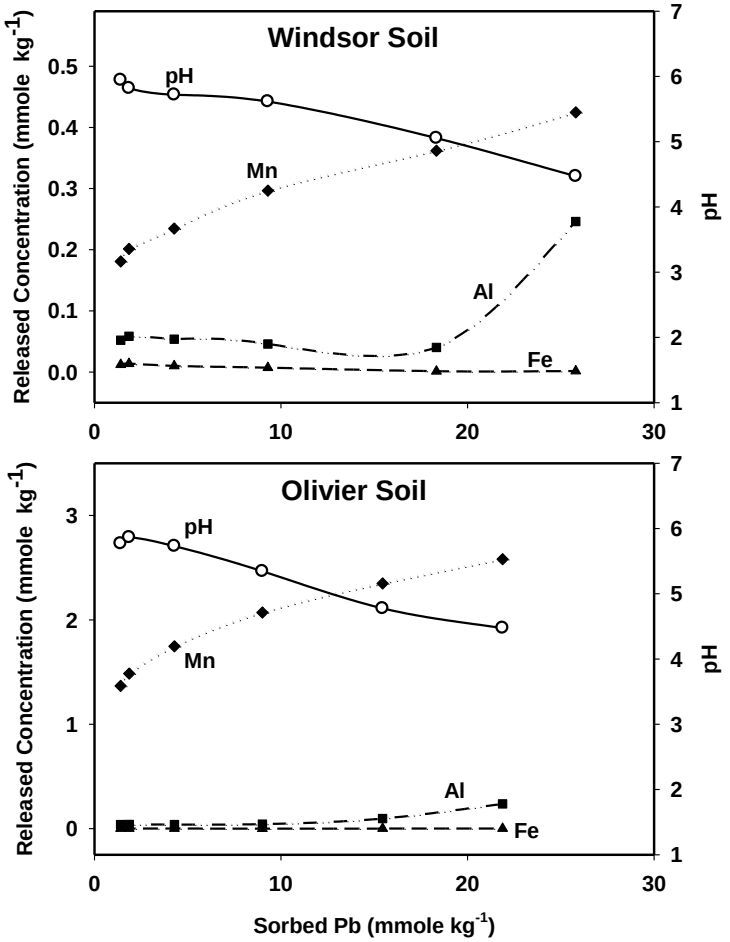

Fig. 6.10. Induced releases of Al, Fe, and Mn versus the sorbed amount of Pb after 1d sorption for Windsor and Olivier soils. The measured pH in the solution is shown in secondary Y axis.

Sorption of Sn increased the induced releases of Al, Fe, and Mn from both soils. For Windsor soil, positive correlation was observed between Mn released and the sorbed Sn where 0.38 and 2.43 mmole kg^{-1} of the released Mn was associated with the lowest (1.2 mmole kg^{-1}) and the highest (54.4 mmole kg^{-1}) Sn sorption, respectively. The respective Al amount released ranged between 0.05 and 8.82 mmole kg^{-1} whereas, the respective Fe released values ranged between 0.02 and 7.7 mmole kg^{-1} (Fig. 6.11). The maximum released of Mn from Windsor soil due to Sn sorption found to be 5 times higher than that Mn released due to Pb sorption. Moreover, the released Al and Fe from Olivier soil significantly increased by 1 and 3 orders of magnitude, respectively, compared to releases associated with Pb sorption. For Olivier soil, 2.3 and 11.7 mmole kg^{-1} of released Mn was associated with the lowest (1.2 mmole kg^{-1}) and the highest (54.4 mmole kg^{-1}) Sn sorption. The respective values of released Fe were 0.0 and 11.2 mmole kg^{-1} whereas, the respective released Al values were 0.01 and 2.6 mmole kg^{-1}.

Figure 6.11 shows the relation between the solution pH and the sorbed Sn after 1d. The higher sorbed Sn associated with the lower pH. For Windsor soil, the pH decreased from 5.89 to 3.03 with average of 4.68 whereas the respective values for Olivier soil were 5.09 to 2.63 with average of 4.37. Results of induced element released from soil due to Sn sorption revealed that Al and Fe were affected with pH decrease significantly whereas Mn did not exhibit this behavior. Generally, this significant decrease in solution pH associated with Sn sorption could partially explain the increase releases of Mn, Al, and Fe. Despite the fact that until now there is no suggestion about Sn toxicity levels (Clifford et al., 2010), the current research indicated that contamination with Sn led to release of substantial amount of Al, Fe, and Mn that could be leached from soil or cause toxicity for plants due to excessive available level.

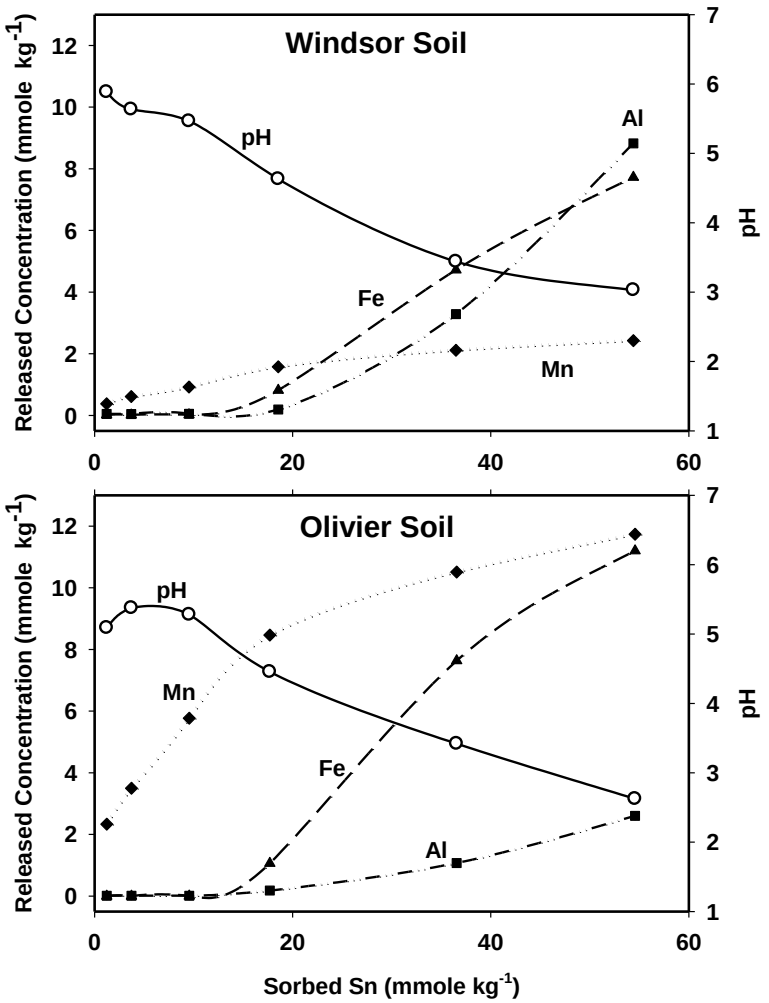

Fig. 6.11. Induced releases of Al, Fe, and Mn versus the sorbed amount of Sn after 1d sorption for Windsor and Olivier soils. The measured pH in the solution is shown in secondary Y axis.

6.3.5 Lead and Tin Sequential Extractions

Tin and Pb sequential extraction results for Windsor and Olivier soils are shown in Tables 6.4 and 6.5, respectively. Results revealed that Sn was mainly associated with the oxides fraction while no exchangeable Sn was detected for both soils. Specifically, for Windsor soil, after 7d of sorption, 88.2 to 96.3% of Sn was associated with the oxides fraction, whereas the respective values after 30d desorption were 71.5 to 88.7% (Table 6.4). The Sn fraction associated with the OM after 7d sorption ranged from 3.0 to 6.5% which was reduced to 0.02% after 30d desorption. For Olivier soil, 3.5 to 6.3% of Sn was associated with the OM fraction after 7d sorption and was decreased to 0.8% after 30d desorption.

Table 6.4 Total extracted and fractions of Sn and Pb from Windsor soil batch kinetic experiments for different initial concentrations.

		Description	Initial Pb or Sn	Total sorbed after 7d	Total sorbed after 1d	Total desorbed after 30 d	Exchangeable fraction	Associated with oxides	Associated with OM	Strongly bound fraction
			mmol L^{-1}	--mmole kg^{-1}--		---------- mmole kg^{-1} (%) ----------				
---- Sn ----	Single	Sorption (7d)	3.624	36.424	---	---	0.0 (0.0)	32.120 (88.2)	1.079 (2.96)	3.224 (8.9)
			5.405	54.326	---	---	0.0 (0.0)	52.293 (96.3)	3.549 (6.53)	---
		1d sorption-30d desorption	3.624	---	36.488	0.019 (0.05)	0.0 (0.0)	26.09 (71.5)	0.007 (0.02)	10.372 (28.4)
			5.405	---	54.399	0.020 (0.04)	0.0 (0.0)	48.243 (88.7)	0.010 (0.02)	6.126 (11.3)
---------- Pb ----------	Single	Sorption (7d)	1.933	19.045	---	---	1.039 (5.46)	12.045 (63.24)	0.135 (0.71)	5.826 (30.59)
			3.804	29.134	---	---	3.521 (12.09)	14.312 (49.12)	1.519 (5.21)	9.782 (33.58)
		1d sorption-30d desorption	1.933	---	18.334	0.542 (2.96)	0.337 (1.84)	10.126 (55.23)	0.008 (0.04)	7.320 (39.93)
			3.804	---	25.805	4.063 (15.75)	0.665 (2.58)	12.960 (50.22)	0.248 (0.96)	7.868 (30.49)
	Mix with 1.685 mmol L^{-1} Sn	Sorption (7d)	1.933	14.128	---	---	1.625 (11.50)	12.360 (87.49)	0.231 (1.64)	---
			3.804	20.526	---	---	3.346 (16.30)	17.168 (83.64)	0.497 (2.42)	---
		1d sorption-30d desorption	1.933	---	13.554	2.034 (15.01)	0.172 (1.27)	8.158 (60.19)	0.017 (0.13)	3.174 (23.42)
			3.804	---	19.395	3.461 (17.84)	0.394 (2.03)	12.646 (65.20)	0.010 (0.05)	2.884 (14.87)
	Mix with 3.370 mmol L^{-1} Sn	Sorption (7d)	1.933	12.043	---	---	1.354 (11.24)	10.603 (88.04)	0.150 (1.25)	---
			3.804	18.016	---	---	2.494 (13.84)	13.755 (76.35)	0.225 (1.25)	1.542 (8.56)
		1d sorption-30d desorption	1.933	---	11.576	1.378 (11.90)	0.113 (0.98)	5.588 (48.27)	0.0 (0.0)	4.496 (38.84)
			3.804	---	15.654	2.659 (16.99)	0.266 (1.70)	7.743 (49.46)	0.0 (0.0)	4.987 (31.86)

Table 6.5 Total extracted and fractions of Sn and Pb from Olivier soil batch kinetic experiments for different initial concentrations.

		Description	Initial Pb or Sn	Total sorbed after 7d	Total sorbed after 1d	Total desorbed after 30 d	Exchangeable fraction	Associated with oxides	Associated with OM	Strongly bound fraction
			mmol L^{-1}	--mmole kg^{-1}--		---------- mmole kg^{-1} (%) ----------				
---- Sn ----	Single	Sorption (7d)	3.624	36.533	---	---	0.0 (0.0)	37.875 (103.7)	1.276 (3.5)	---
			5.405	54.328	---	---	0.0 (0.0)	52.351 (96.4)	3.419 (6.3)	---
		1d sorption-30d desorption	3.624	---	36.553	0.013 (0.04)	0.0 (0.0)	36.239 (99.2)	0.280 (0.8)	0.02 (0.05)
			5.405	---	54.575	0.013 (0.02)	0.0 (0.0)	57.342 (105.1)	0.436 (0.8)	---
---------- Pb ----------	Single	Sorption (7d)	1.933	16.163	---	---	2.837 (17.55)	10.813 (66.90)	0.144 (0.89)	2.368 (14.65)
			3.804	22.940	---	---	6.567 (28.63)	11.745 (51.20)	0.111 (0.48)	4.518 (19.69)
		1d sorption-30d desorption	1.933	---	15.450	1.996 (12.92)	0.641 (4.15)	9.389 (60.77)	0.084 (0.54)	3.339 (21.61)
			3.804	---	21.881	6.231 (28.48)	0.789 (3.61)	11.185 (51.12)	0.063 (0.29)	3.613 (16.51)
	Mix with 1.685 mmol L^{-1} Sn	Sorption (7d)	1.933	12.468	---	---	2.899 (23.25)	8.252 (60.19)	0.033 (0.26)	1.284 (10.30)
			3.804	17.991	---	---	5.923 (32.92)	10.613 (58.99)	0.289 (1.61)	1.166 (6.48)
		1d sorption-30d desorption	1.933	---	12.753	2.773 (21.74)	0.290 (2.27)	9.478 (74.32)	0.014 (0.11)	0.198 (1.55)
			3.804	---	17.932	5.732 (31.97)	0.427 (2.38)	12.278 (68.47)	0.413 (2.30)	---
	Mix with 3.370 mmol L^{-1} Sn	Sorption (7d)	1.933	9.042	---	---	2.451 (27.11)	5.693 (62.96)	0.109 (1.21)	0.789 (8.73)
			3.804	16.167	---	---	5.294 (32.75)	9.100 (56.29)	0.085 (0.53)	1.688 (10.44)
		1d sorption-30d desorption	1.933	---	9.617	2.076 (21.59)	0.222 (2.31)	5.842 (60.75)	0.028 (0.29)	1.449 (15.07)
			3.804	---	13.574	4.015 (29.58)	0.325 (2.39)	8.047 (59.28)	0.021 (0.15)	1.167 (8.60)

For Windsor soil, the sequential extraction results of single Pb after 7d sorption indicated that 5.5-12.1%, 49.1-63.2%, 0.71-5.21% and 30.6-33.6% were associated with the exchangeable, oxides, OM, and strongly bound fractions, respectively. The respective values after the 30d desorption decreased to 1.84-2.58%, 50.22-55.23%, 0.04-0.96%, and 30.5-39.9% (see Table 6.4). In agreement with these results, Marin et al. (1997) showed that Pb was essentially extracted from the Fe-Mn oxides fraction with 32% whereas the 5.5 and 4.5% were associated with the exchangeable and OM fractions, respectively. When Pb was mixed with 1.685 mmol L^{-1} Sn, 60.2 to 87.5% and 0.0 to 23.4% of Pb were associated with the oxides and the strongly bound fractions, respectively. Moreover, the exchangeable fraction ranged from 11.5 to 16.3% and 1.3 to 2.0% after 7d sorption and 30d desorption, respectively (Table 6.4). However, when Pb was mixed with 3.370 mmol L^{-1} Sn, 48.3 to 88.0% and 8.6 to 38.8% of Pb were associated with the oxides and the strongly bound fractions, respectively. The exchangeable fraction ranged from 11.2 to 13.8% and 1.0 to 1.7% after 7d sorption and 30d desorption, respectively (Table 6.4). Generally, based on the sorbed amount of Pb after 7d sorption, mixing the Pb with Sn affected Pb fractionation in Winsor soil by increasing the portion associated with exchangeable and oxides fractions whereas existence of Sn in the system reduced the strongly bound fraction.

On the other hand, for Olivier soil, the sequential extraction results of single Pb after 7d sorption indicated that 17.55-28.63%, 51.20-66.90%, 0.48-0.89% and 14.65-19.69% were associated with exchangeable, oxides, OM, and strongly bounded, respectively. The respective values after 30d desorption were 3.61-4.15%, 51.12-60.77%, 0.29-0.54%, and 16.51-21.61% (See Table 6.5). When Pb was mixed with 1.685 mmol L^{-1} Sn, 59.0 to 74.3% and 1.6 to 10.3% of Pb were associated with oxides and the strongly bound fractions, respectively. Moreover, 23.3 to 32.9% and 2.3 to 2.4% of Pb were associated with the exchangeable fraction after 7d sorption and 30 d desorption, respectively (Table 6.5). When Pb was mixed with 3.370 mmol L^{-1} Sn, 56.3

to 63.0% and 8.7 to 15.1% of Pb were associated with the oxides and the strongly bound fractions, respectively. Whereas, the exchangeable fractions were 27.1 to 32.8% and 2.3 to 2.4% after 7d sorption and 30d desorption, respectively (Table 6.5). On the whole, based on the sorbed amount of Pb after 7d sorption, presence of Sn affected Pb fractionation in Olivier soil by slightly increasing the exchangeable fraction and decreasing the strongly bound fraction.

6.4 Conclusions

Sorption batch and sequential extraction experiments were carried out to assess the retention and reactivity of Sn and Pb in soils. Isotherm results exhibited highly nonlinear sorption for both heavy metals. Lead isotherms indicated a Freundlich exponent parameter *b* of 0.204 and 0.249 for Windsor and Olivier soils, respectively. The respective values for Sn were greater than 1 (2.46 and 3.72) which implies irreversible sorption. Since that Sn was almost completely sorbed, the contamination with Sn resulted in reducing sorption of Pb by both soils as evidenced by lowering the maximum sorption capacity. Also, Sn contamination led to release of substantial amount of Al, Fe, and Mn that could cause toxicity for plants due to excessive available level of these elements. Moreover, Sn was nearly irreversible in the studied soils where more than 99% of the added Sn was retained by soil and did not desorbed during experimental time. Whereas, Pb exhibited kinetic behavior where 3-15% and 13-28% of Pb were released for Windsor and Olivier soils, respectively during desorption. The use of a SOTS model that accounts for nonlinear equilibrium and kinetic reactions was capable of describing the kinetic behavior of Pb sorption and release in Windsor and Olivier soils. The sequential extraction experiments' results revealed that the most susceptible Pb fraction to release from the studied soil was raised by increasing the input concentration of single Pb or by mixing it with Sn. This concentration-dependent release is consistent with the strong nonlinearity of Pb retention and implies that mobility of Pb tends to increase as the inputs of Pb concentration elevate.

6.5 References

Amacher, M.C. 1996. Nickel, Cadmium, and lead. P. 739-768. In: Sparks (ed.) Methods of soil analysis: chemical methods. Part 3. SSSA No.5. ASA-CSSA-SSSA, Madison, WI.

Bryan, G. W, and W.J. Langston. 1992. Bioavailability, accumulation and effects of heavy metals in sediments with special reference to United Kingdom estuaries: a review. Environ. Pollut. 76, 89-131.

Chotpantarat S., S.K. Ong, C. Sutthirat, K. Osathaphan. 2012. Competitive modeling of sorption and transport of Pb^{2+}, Ni^{2+}, Mn^{2+} and Zn^{2+} under binary and multi-metal systems in lateritic soil columns. Geoderma.189-190: 278-287.

Chrastný V., M. Komárek, J. Procházka, L. Pechar, A. Vaněk, V. Penížek, and J. Farkaš. 2012. 50 years of different landscape management influencing retention of metals in soils. J Geochem Explor. 115:59-68.

Clifford, M.J, G.M. Hilson, and M.E Hodson. 2010. Tin and mercury. *In* P Hooda (Ed.) Trace Elements in Soils. Wiley/ Blackwell. P:497 – 513.

Davidson, C.M., A.L. Duncan, D. Littlejohn, A.M. Ure, A.M., and L.M. Garden. 1998. A critical evaluation of the three-stage BCR sequential extraction procedure to assess the potential mobility and toxicity of heavy metals in industrially-contaminated land. Anal. Chim. Acta. 363: 45–55.

Elbana, T. A. and H M. Selim. 2011. Copper mobility in acidic and alkaline soils: miscible displacement experiments. Soil Sci. Soc. Am. J. 75:2101–2110.

Fonseca, B., H. Figueiredo, J. Rodrigues, A. Queiroz, and T. Tavares. 2011. Mobility of Cr, Pb, Cd, Cu and Zn in a loamy soil: a comparative study. Geoderma 164:232–237.

Herting, G., S. Goidanich, I.O. Wallinder, and C. Leygraf. 2008. Corrosion-induced release of Cu and Zn into rainwater from brass, bronze and their pure metals. A 2-year field study; Environ. Monit. Assess. 144:455–461.

Hooda, P.S. and B.J. Alloway. 1998. Cadmium and lead sorption behaviour of selected English and Indian soils. Geoderma, 84:121-134.

Hou, H., T. Takamatsu, M.K. Koshikawa, M. Hosomi. 2006. Concentrations of Ag, In, Sn, Sb and Bi, and their chemical fractionation in typical soils in Japan. European Journal of Soil Science 57: 214–227.

Kabata-Pendias A, and A.B. Mukherjee. 2007. Trace elements from soil to human. Springer. 556 pp.

Kabata-Pendias, A., and H. Pendias. 2001. Trace elements in soils and plants. 3rd ed. CRC Press, Boca Raton, FL.

Lu, S.G. and Q.F Xu. 2009. Competitive adsorption of Cd, Cu, Pb and Zn by different soils of Eastern China. Environmental Geology. 57:685-693.

Marin, B., M. Valladon, M. Polve, and A. Monaco. 1997. Reproducibility testing of a sequential extraction scheme for the determination of trace metal speciation in a marine reference sediment by inductively coupled plasma-mass spectrometry. Anal. Chim. Acta. 342:91–112.

McKenzie R.M. 1980.The adsorption of lead and other heavy metals on oxides of manganese and iron, Aust. J. Soil Res. 18:61-73.

Nakamaru Y and S. Uchida. 2008. Distribution coefficients of tin in Japanese agricultural soils and the factors affecting tin sorption behavior. J Environ Radioact 99:1003–1010.

Ostrakhovitch, E.A., and M.G. Cherian. 2007. Tin. In: Nordberg, G.F., B.A. Fowler, M. Nordberg, L.T. Friberg. (Eds.), Handbook on the Toxicology of Metals. Third edition. Academic Press, pp. 839–859.

SAS 9.3. 2011. Foundation for Microsoft® Windows® SAS Institute Inc., Cary, NC, USA.

Schafer S. G, and U. Fermfert. 1984. Tin – a toxic heavy metal? A review of the literature. Regul Toxicol Pharmacol 4:57–69.

Schmitt H, H. Sticher. 1986. Prediction of heavy metal contents and displacement in soils. Z. Pflanzenernaehr. Bodenk. 149: 157-171.

Selim, H. M. and M. C. Amacher. 1988. A second order kinetic approach for modeling solute retention transport in soils. Water Resources Research 24: 2061-2075.

Selim, H.M., and M.C. Amacher. 1997. Reactivity and transport of heavy metals in soils. CRC Press, Boca Raton, FL.

Selim, H.M., G.R. Gobran, X. Guan, and N. Clarke. 2004. Mobility of sulfate in forest soils: Kinetic modeling. J. Environ. Qual. 33: 488-495.

Takeno N .2005. Atlas of Eh–pH diagrams. Intercomparison of thermodynamic databases. Geological Survey of Japan Open File Report No. 419.

USEPA. 2005. Ecological Soil Screening Levels for Lead, Interim Final. Office of Solid Waste and Emergency Response. OWSER Directive 9285.7-70. 1200 Pennsylvania Ave. N.W. Washington, D.C. 20460.

Uygur, V., and D. L. Rimmer. 2000. Reactions of zinc with iron-oxide coated calcite surface at alkaline pH. Eur. J. Soil. Sci.51:511-516.

Weber Jr. W.J, P.M. McGinley, and L.E. Katz. 1992. A distributed reactivity model for sorption by soils and sediments. 1. conceptual basis and equilibrium assessments. Environ Sci Technol. 26:1955–1962.

CHAPTER 7. INFLUENCE OF TIN ON LEAD MOBILITY IN SOILS

7.1 Introduction

Lead (Pb) is a persistent pollutant that adversely affects environmental resources and human health. According to the U.S. Environmental Protection Agency (USEPA), the concentrations of Pb in soils that are protective of ecological receptors the ecological soil screening levels (Eco-SSLs) are 11, 56, and 120 ppm for birds, mammals, and plants respectively, (USEPA 2005). Lead enters the soil through natural processes such as weathering of the parent material and/or anthropogenic sources. Many anthropogenic sources for Pb contamination have been reported. Steinnes (2013) listed automobile exhausts, mining and smelting, sewage sludge, shooting ranges, and urban soils as sources for Pb pollution. The estimated average Pb for different soils is 25 mg kg^{-1}, whereas soil Pb concentration ranging from 100 to 500 mg kg^{-1} is considered as excessive (Kabata-Pendias and Pendias 2001). High level of Pb with values of 0.3-1.6% and 1.2-3.1% for surface (0-10cm) and subsurface (10-20cm) soils, respectively were reported for areas in the vicinity of industrial plants. Examples include Pb contamination due to battery recycling and salvage yards with discharge of waste oil (Melamed et al. 2003).

Tin (Sn) occurs in the earth's crust at an average concentration above 2 mg kg^{-1} and with possible oxidation states, +2 (stannous) and +4 (stannic) (Kabata-Pendias and Mukherjee, 2007). In contaminated soils and sediments, Sn concentration may be highly elevated to over 1000 mg kg^{-1} (Schafer and Fembert 1984; Bryan and Langston, 1992). Tin exhibits a high potential to be sorbed and retained by soils. Some of inorganic tin compounds dissolve in water, whereas most inorganic Sn compounds strongly bind to soils and sediments (Ostrakhovitch and Cherian, 2007).

Lead mobility in soils is controlled by soil characteristics and environmental conditions. Soil pH, cation exchange capacity (CEC), clay content, $CaCO_3$, and organic matter (OM), were

positively correlated with Pb sorption in soil (Hooda and Alloway, 1998). This is supported with various studies, e.g., Martínez-Villegas et al. (2004) that showed that Pb sorption isotherms were strongly nonlinear and the sorption capacity increased with increasing pH. Strawn and Sparks (2000) found that removing OM decreased Pb sorption by 40% compared to untreated soil. Moreover, McKenzie (1980) found that Pb sorption by Mn oxides was up to 40 times greater than that by Fe oxides and no evidence for oxidation of Pb or the formation of specific Pb-Mn minerals was found.

Physical and chemical soil properties govern Pb mobility. Barkouch et al. (2007) studied Pb transport in laboratory soil columns; their results showed that increasing bed height, water–soil surface contact, and particulate bed tortuosity led to higher contact time, thus higher Pb retention by soils. Whereas Pb retention was decreased as a result of increasing flow rate and pulse volume. On the other hand, the occurrence of certain chemicals affects retention and mobility of Pb in soil. Garrido et al. (2006) showed the potential of industrial by-products such as phosphogypsum, sugar foam, and phosphoric rock in influencing the Pb mobility in acid soils. Karathanasis et al. (2005) showed the potential of colloids derived from biosolid wastes to co-transport Pb in subsurface soil environments. They explained that the colloid and metal mobility were enhanced by decreasing solution pH and colloid size, and increasing OM. This resulted in higher elution of sorbed and soluble metal loads through metal–organic complex formation. At a Pb-contaminated site Melamed et al. (2003) found that a mixture of H_3PO_4 and $Ca(H_2PO_4)_2$ or phosphate rock was effective in immobilizing Pb with minimum adverse impacts associated with pH reduction. Vile et al. (1999) found that soluble Pb^{2+} was retained in the peat through physiochemical binding to organic matter, and as such Pb^{2+} was largely immobile in peat even under conditions of a fluctuating water table.

Numerous studies were carried out to study the competitive effect of other heavy metals on Pb retention and mobility in soils. In batch experiments, Schmitt and Sticher (1986) reported a higher availability of Cd, Cu, and Pb when applied concurrently due to competition for available sorption sites. Their results from sorption batch experiments indicated that Pb-saturation level decreased from 6.33 mg/g for single Pb solution to 1.72 mg/g when a mixed solution of Pb, Cu, and Cd was applied. Lu and Xu (2009) evaluated the competitive adsorption of Cd, Cu, Zn and Pb and found that Pb was the most strongly sorbed metal by the soils studied. They reported weaker competition at low initial concentrations due to the extent of available sorption sites for most cations in the adsorption complex. Chotpantarat et al. (2012) showed that the maximum sorption capacity of Pb in a single system was higher than in binary and multi-metal systems of Ni, Mn, and Zn through lateritic soil columns. Fonseca et al. (2011) studied sorption and transport of Cr, Cd, Cu, Zn and Pb and found that Pb exhibited higher sorption capacity for noncompetitive compared with Pb competitive sorption; Pb exhibited a slightly higher retardation in the competitive scenario under flow conditions, however.

Simulation of Pb transport in soils is a prerequisite for predicting the risk of heavy metal mobility in contaminated sites. A literature review revealed that only a few studies provided simulation for Pb transport, although, several studies were carried out to study Pb behavior in soils. Hanna et al. (2009) successfully simulated Pb elution from contaminated roadside soils. They used surface complexation modeling by assuming a single type of binding sites for all oxides. Based on soil column leaching experiments, Dong et al. (2009) quantified the maximum amount of element that can be loaded and the mass of the adsorbent. They provided acceptable simulation for Pb leaching based on non-linear regression of the breakthrough data using a Thomas algorithm. Recently, modeling studies based on two-site nonequilibrium models have been implemented for strongly sorbed elements (Fonseca et al., 2011; Chotpantarat et al., 2012).

Moreover, there are numerous studies on heavy metal competition based on batch experiments, whereas only a few considered competitive sorption under flow conditions. In this study, the influence of Sn on Pb mobility was investigated. A miscible displacement technique was used to quantify the competitive Sn-Pb interaction. Moreover, simulation by second-order two-site transport models were implemented (Selim and Amacher 1997). Specifically, the objectives of this work were to: 1) quantify Pb sorption in two soils in a single system and in a binary Sn-Pb one, 2) quantify Sn and Pb transport in the two soils, and 3) simulate heavy metal mobility in soil based on nonlinear equilibrium-kinetic models.

7.2 Materials and Methods

Two soils were selected for this study, Olivier (fine-silty, mixed, active, thermic Aquic Fraglossudalfs) and Windsor (mixed, mesic Typic Udipsamments) soils. Selected chemical properties including pH, OM, and CEC are given in Table 7.1. In addition, sequential extraction of Fe, Al, and Mn were carried out according to Amacher (1996). For the exchangeable phase 10 ml of 0.1 *M* $Mg(NO_3)_2$ was added to 0.5 g soil and shaken for 2 h. Subsequently, the metal oxides fraction was extracted with 40 ml of oxalate solution, followed by 25 ml of pH 2, 30% H_2O_2 to extract metals associated with the OM phase.

7.2.1 Sorption

Sorption of Pb and Sn was studied using the batch method described by Selim and Amacher (1997). Duplicate 3-g samples of Windsor and Olivier soils were placed in 40-mL polypropylene tubes and mixed with 30-mL solutions of known Pb concentrations. Specifically, six initial Pb concentrations (C_o) (0.125, 0.186, 0.428, 0.932, 1.933, and 3.804 mmol L^{-1}) were used; the respective concentrations in µg mL^{-1} are 26, 38.5, 88.6, 193.2, 400, and 788.2. Reagent-grade $Pb(NO_3)_2$ was prepared in 5 mmol L^{-1} $Ca(NO_3)_2$ background solution. The samples were shaken at 150 rpm on a reciprocal shaker for 24h and subsequently centrifuged for

10 min at 1300 xg. A 5-mL aliquot was sampled from the supernatant and the collected samples were analyzed for total Pb concentration using inductively coupled plasma–atomic emission spectrometry (ICP–AES; Spectro Citros CCD). The fraction of Pb sorbed by the soil was calculated based on the change in concentration in the solution (before and after each adsorption). To study the influence of Sn on Pb retention, the above mentioned Pb batch experiments were also carried out in the presence of different levels of Sn concentrations in solution. Two levels of Sn were used; 1.685 and 3.370 mmol L^{-1} (200 and 400 µg mL). The form of Sn used was $SnCl_2$ prepared in 5 mmol L^{-1} $Ca(NO_3)_2$ as the background solution.

Table 7.1. Selected physical and chemical properties of the studied soils.

	Olivier	Windsor
pH (1 :2.5)	5.80	6.05
Total Carbon (g Kg^{-1})	21.28	11.92
CEC (cmol kg^{-1})	8.6	3.28
Sequential Extraction		
Fe (mmole kg^{-1})		
Exchangeable	0.015	0.013
Associate with oxides	146.2	174.0
Associate with OM	7.829	4.732
Al (mmole kg^{-1})		
Exchangeable	0.107	Nd†
Associate with oxides	110.6	180.3
Associate with OM	57.2	13.3
Mn (mmole kg^{-1})		
Exchangeable	0.447	0.262
Associate with oxides	13.5	4.799
Associate with OM	0.084	0.350

† Not detected

7.2.2 Miscible Displacement Experiments

To quantify the mobility of Pb and Sn in Windsor and Olivier soils, column experiments were carried out using the miscible displacement technique as described by Selim and Amacher (1997). Acrylic columns (5 cm in length and 6.4-cm i.d.) were uniformly packed with air-dry soil and slowly saturated with a background solution of 5 mmol L^{-1} $Ca(NO_3)_2$ where upward flow was maintained. Constant flux was controlled by a piston pump (Fluid Metering Inc. lab pump,

Model QG6), with some 20 pore volumes of the background solution applied at a constant flow rate. Following saturation, input solutions of Sn and Pb were introduced in consecutive pulses into each column as well as mixed pulse was applied for each soil (see Table 7.2). Pulses were prepared in 5 mmol L^{-1} $Ca(NO_3)_2$ background solution. The volume of the applied Sn or Pb pulses and the physical parameters for each soil column (e.g., moisture content,θ, and bulk density, ρ) are given in Table 7.2. The metal pulse input was subsequently eluted by 5 mmol L^{-1} $Ca(NO_3)_2$ solution for leaching. Effluent samples were collected using an ISCO fraction collector. Concentrations of Pb, and Sn in the effluent solution were analyzed by ICP–AES (Spectro Citros CCD). Changes in pH in the effluent were also monitored. Additionally, K, Mg, Al, Fe, and Mn analysis were carried out in the effluent solution.

Table 7.2. Soil physical and experimental conditions of the miscible displacement columns experiments.

Matrix	Pb/Sn sequence	Bulk density (ρ, g mL^{-1})	Moisture content (θ, mL mL^{-1})	Pore water velocity (cm h^{-1})	Pulse input			
					Pore volumes		Concentration (mmol L^{-1})	
					Pb	Sn	Pb	Sn
Windsor	Pb→Sn	1.185	0.553	0.593	37.9	38.9	0.917	1.356
	Sn→Pb	1.188	0.552	0.632	42.3	41.6	0.920	1.287
	Pb&Sn	1.188	0.552	0.585	---- 41.8 ----		0.954	1.307
	Sn only	1.190	0.551	0.620	---	169.9	---	1.387
Olivier	Pb→Sn	1.245	0.530	0.663	44.1	44.4	0.921	1.303
	Sn→Pb	1.240	0.532	0.670	41.9	41.8	0.897	1.452
	Pb&Sn	1.234	0.534	0.651	--- 41.9 ---		0.945	1.613
	Sn only	1.252	0.528	0.599	---	176.2	---	1.382
Reference Sand	Pb only	1.634	0.383	0.876	11.4	---	0.929	---
	Sn only	1.653	0.376	0.808	---	18.9	---	1.570

Column transport experiments were carried out to quantify Pb and Sn transport in a nonreactive medium using acid washed sand material (Fisher Scientific: 14808-60-7). In this

reference sand no clay and organic matter were present (pH = 6.27; sand = 81%; silt = 19). It was previously used as a reference matrix for characterizing Hg, Cd, and Cu mobility in soils (Liao et al., 2009; Elbana and Selim 2010, 2011).

Upon completion of the miscible displacement experiments, each soil column was sectioned into 0.5 or 1-cm increments and Sn and Pb retained by the soil were determined using an Innov-X Delta Premium PXRF as a screening method (USEPA, 2007). Thus, the amounts of Sn and Pb retained or sorbed versus soil depth due to pulse application were quantified for all soils and the reference sand columns.

To obtain independent estimates of the dispersion coefficient (*D*), separate pulses of a tracer solution were applied to each soil column subsequent to the heavy metal pulse applications. Tritium (^3H_2O) was used as a tracer and the collected samples were analyzed using a Tri-Carb liquid scintillation β counter (Packard-2100 TR). Estimates for *D* values were obtained using CXTFIT (Toride et al., 1999). Values of *D* were subsequently used in the SOTS model to predict Pb and Sn transport in the different soil columns.

7.2.3 Modeling with Second-Order Two-Site Model

Basic to the second-order formulation is the assumption that a limited number of sites are available for solute adsorption in soils. As a result, the reaction rate is a function of the solute concentration in the soil solution and the availability of adsorption sites on soil matrix surfaces. Specifically, retention mechanisms are assumed to depend not only on concentration in solution, *C*, but also the number of sites (φ) that are available for solute adsorption in soils (Selim and Amacher. 1988; Selim and Amacher 1997). The model also assumes that a fraction of the total sorption sites is rate limited, while the remaining fractions interact rapidly or instantaneously with the solute in the soil solution. The sorbed phases S_e, S_k, and S_{irr} are in direct contact with the solute in the solution phase (*C*) and are governed by concurrent reactions (see Fig. 7.1).

Specifically, C is assumed to react rapidly and reversibly with the equilibrium phase S_e. The relations between C and S_k and S_{irr} are governed by reversible nonlinear and irreversible linear kinetic reactions, respectively. A second irreversible reaction was assumed as a consecutive reaction of the S_k phase into a less accessible or strongly retained phase S_s. Therefore, the model formulation can be expressed as

$$S_e = K_e \theta\ C\ \varphi \qquad [7.1]$$

$$\frac{\partial S_k}{\partial t} = k_1 \theta\ C\ \varphi - (k_2 + k_3) S_k \qquad [7.2]$$

$$\frac{\partial S_s}{\partial t} = k_3 S_k \qquad [7.3]$$

$$\rho \frac{\partial S_{irr}}{\partial t} = \theta\ k_{irr} C \qquad [7.4]$$

Here φ is related to the sorption capacity (S_{max}) by:

$$S_{max} = \varphi + S_e + S_k + S_s + S_{irr} \qquad [7.5]$$

where φ and S_{max} (μg solute g^{-1} soil) are the unoccupied (or vacant) and total sorption sites on soil surfaces, respectively. The total sorption sites S_{max} was considered as an intrinsic soil property and is time invariant. In addition, S_e is the amount retained on equilibrium-type sites (μg g^{-1}), S_k is the amount retained on kinetic-type sites (μg g^{-1}), S_s is the amount retained irreversibly by consecutive reaction (μg g^{-1}), and S_{irr} is the amount retained irreversibly by a concurrent type of reaction (μg g^{-1}). The equilibrium constant is K_e (mL μg^{-1}). The reaction rate coefficients are, k_1 (mL μg^{-1} h^{-1}), k_2 (h^{-1}), k_3 (h^{-1}), and k_{irr} (h^{-1}), while C is the solute concentration (μg mL^{-1}), θ is the volumetric water content (mL mL^{-1}), and t is the reaction time (h).

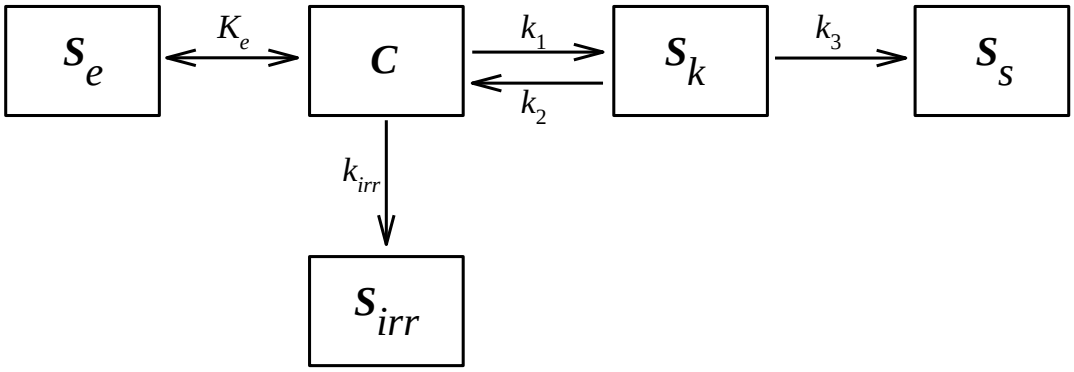

Fig. 7.1. A schematic of the second-order, two-site (SOTS) model for retention of reactive chemicals in soils, where *C* is the solute in the solution phase, *S*e is the amount retained on equilibrium-type sites, S_k is the amount retained on kinetic-type sites, S_s is the amount retained irreversibly by consecutive reaction, S_{irr} is the amount retained irreversibly by concurrent type of reaction, and K_e, k_1, k_2, k_3, and k_{irr} are reaction rates.

At any time *t*, the total amount of solute sorbed by the soil matrix, *S*, can be expressed as

$$S = S_e + S_k + S_s + S_{irr} \qquad [7.6]$$

The above reactions were incorporated into the advection–dispersion equation (ADE) as

$$\theta \frac{\partial C}{\partial t} + \rho \frac{\partial S}{\partial t} = \frac{\partial}{\partial t}\left(D\theta \frac{\partial C}{\partial x}\right) - q \frac{\partial C}{\partial x} \qquad [7.7]$$

where *x* is distance (cm), *D* is the hydrodynamic dispersion (cm^2 h^{-1}), ρ is the bulk density of the soil (g mL^{-1}), and *q* is steady Darcy's water flux density (cm h^{-1}). For the reactive transport of Pb in soils, the second term in Eq. [7.7], $\partial S/\partial t$, was accounted for using the second-order approach described above in Eq. [7.1–7.5]. A finite difference (Crank–Nicholson forward–backward) method was used to provide numerical solutions of the transport equation subject to a solute-free initial condition:

$$C(x, t = 0) = 0 \qquad [7.8]$$

and the boundary conditions:

$$vC - D\frac{\partial C}{\partial x}|_{(x=0,t)} = \begin{cases} vC_o & 0<t\leq t_o \\ 0 & t>t_o \end{cases} \qquad [7.9]$$

$$\frac{\partial C}{\partial x}(x = L, t) = 0 \qquad [7.10]$$

where C_o is the input Pb concentration (μg mL^{-1}), t_o is the duration of the Pb input pulse (h), L is the length of the soil column (cm), and v (cm h^{-1}) is the pore water velocity (q/θ). The kinetic retention processes of the SOTS model (Eq. [7.1–7.5]) were solved using the fourth-order Runge–Kutta method. The BTC data from column experiments were fitted to the models described above using the Levenberg–Marquardt nonlinear least square optimization method (Press et al., 1992). Statistical criteria used for estimating the goodness-of-fit of the models to the data were the coefficients of determination, r^2, and the root mean square error (RMSE):

$$RMSE = \sqrt{\frac{\sum(C_{ops}-C)^2}{n_o-n_p}} \qquad [7.11]$$

where C_{ops} is the observed Pb concentration at time t, C is the simulated Pb concentration at time t, n_o is the number of measurements, and n_p is the number of fitted parameters.

7.3 Results and Discussion

7.3.1 Sorption Isotherms

Lead sorption isotherms that depict the distribution between aqueous and sorbed phases for Pb in the presence of different levels of Sn (0, 200, and 400 ppm) are shown in Fig. 7.2. These sorption isotherms exhibited nonlinear Pb sorption behavior and the effect of Sn is clearly depicted indicating a decreased Pb sorption with increasing Sn concentration. Adsorption isotherms of Pb were described using the Langmuir equation,

$$S = \frac{S_{\max} K_L C}{1+K_L C} \qquad [7.12]$$

where S represents the amount sorbed (μg kg^{-1}), S_{max} is the sorption capacity (μg g^{-1}), C is the concentration in solution μg mL^{-1}, and K_L (mL μg^{-1}) is a Langmuir coefficient related to binding strength. The nonlinear least square optimization of SAS PROC NLIN (SAS Institute, 2011) was used to obtain best-fit parameters for the sorption data. Both Windsor and Olivier soils exhibited

high sorption affinity for Pb when no Sn was added to the soil solutions. The maximum sorption capacities were 4617.6 μg g^{-1} and 4197.9 μg g^{-1} for Windsor and Olivier soils, respectively (Table 7.3). A range of 5813 to 12902 μg g^{-1} was reported for S_{max} in moderately neutral contaminated soils (Dong et al., 2009); whereas a S_{max} of 2000 to 12000 μg g^{-1} was reported for acid urban soils (Li, 2006). As shown in Fig. 7.2, the mixing of 200 μg mL^{-1} and 400 μg mL^{-1} of Sn in the soil solutions decreased Pb maximum sorption capacity, S_{max}, by 17.1% and 24.5%, respectively for the Windsor soil, whereas, the respective values for the Oliver soil were 12.2% and 23.8%. Fig. 7.2 showed that the nonlinearity of Pb-sorption in both soils implies that the mobility of Pb in the soil tends to increase as the concentration of Pb or Sn increases in the input solution. Our results indicated that Sn is capable of competing with Pb on sorption sites and reduce Pb sorption capacities and binding strengths on the Windsor and Oliver soils (Table7.3). Reduction of Pb sorption due to competition was reported by many authors. Schmitt and Sticher (1986) showed that mixing Pb with Cd (1:1) reduced the S_{max} from 6330 μg g^{-1} (noncompetitive) to 4680 μg g^{-1} (competitive). Recently, Chotpantarat et al. (2012) showed the decrease in Pb sorption on soils when Pb was mixed in binary systems with Mn, Ni, or Zn.

Table 7.3 Estimated Langmuir parameters and their standard errors (SE) for Pb retention in the presence of different Sn concentrations by Windsor and Olivier soils after 1day-sorption experiments.

Soil	Sn (μg g^{-1})	S_{max} (μg g^{-1})	K_L (mL μg^{-1})	r^2
Windsor	0	4617.6±250.0	3.290±0.884	0.943
	200	3825.9±274.3	0.058±0.018	0.925
	400	3487.1±141.6	0.020±0.003	0.982
Olivier	0	4197.9±338.9	0.106±0.045	0.899
	200	3632.0±277.0	0.038±0.012	0.923
	400	3098.1±194.5	0.013±0.003	0.965

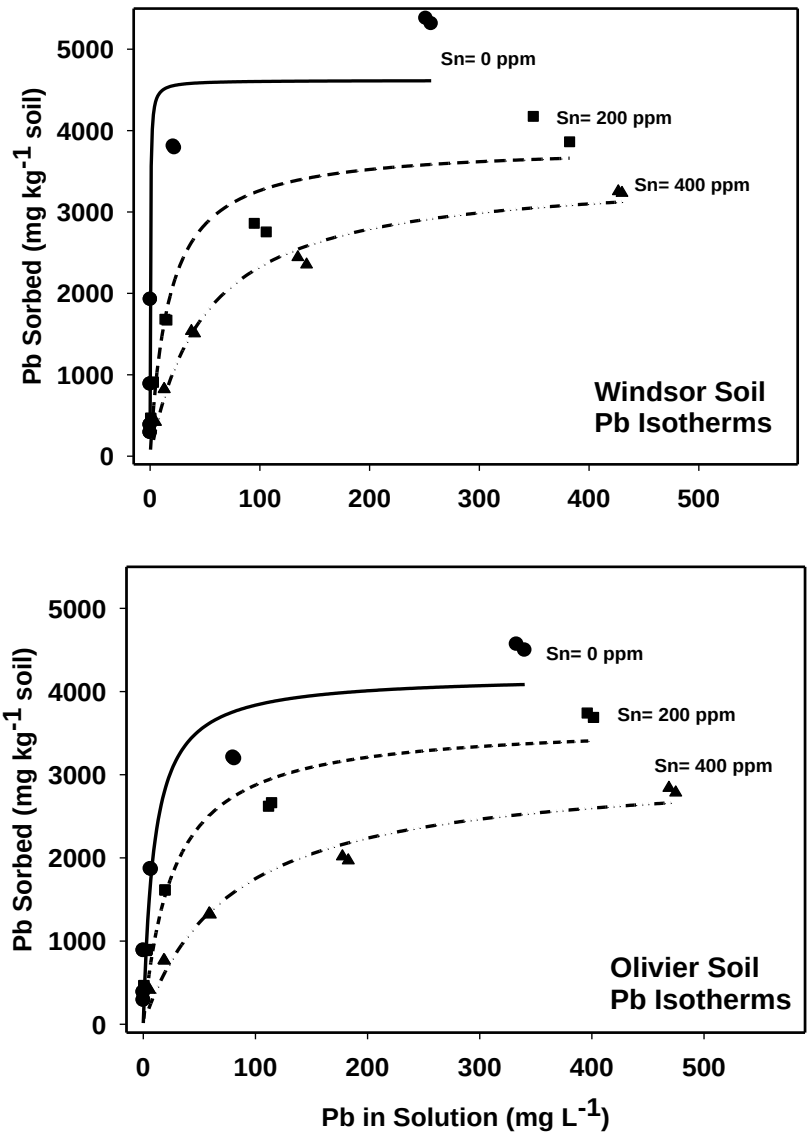

Fig. 7.2. Langmuir sorption isotherm for Pb retention in the presence of different Sn concentrations by Windsor and Olivier soils after 1 day-sorption experiments.

7.3.2 Tracer Transport

Breakthrough of the applied tritium pulses in the different soil columns is shown in Fig.7. 3. Here relative tritium concentration in the effluent (C/C_o) as a function of effluent pore volumes eluted (V/V_o) are presented. Here V_o represents the volume of soil-pore space within each soil column (cm^3). The tritium BTC from the reference sand column appears symmetric and exhibited no tailing as illustrated in Fig. 7.3. Such observations are consistent with the assumption that the reference sand is a nonreactive porous medium.

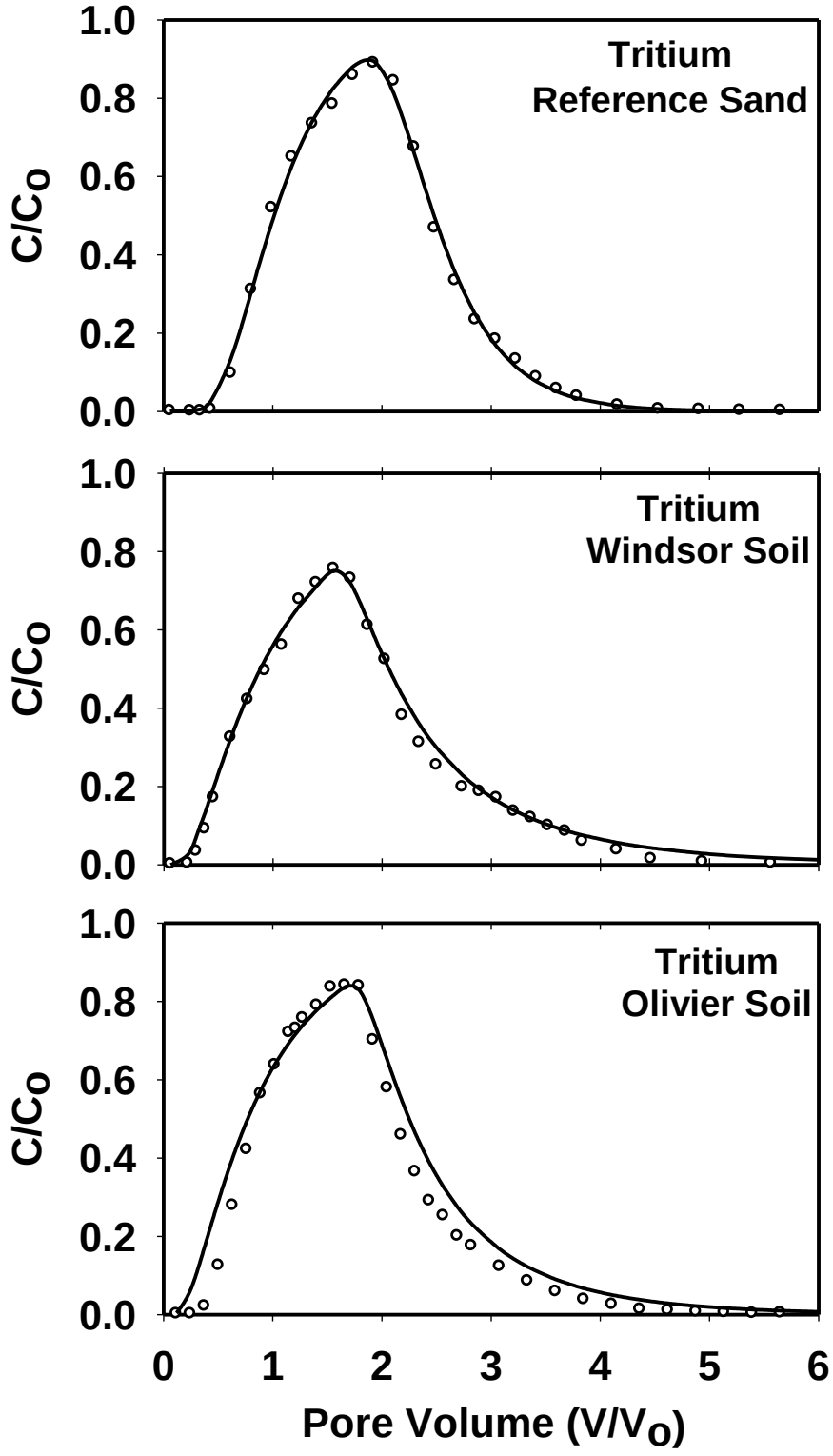

Fig.7.3. Tritium breakthrough curves (BTCs) from the reference sand, Windsor soil, and Olivier soil columns. Circles represent experimental data. Solid curves are simulations using the CXTFIT model.

For the Windsor and Olivier soils, some degree of tailing was observed. Such tailing is evidence of limited physical nonequilibrium, which was probably due to intraparticle diffusion and the presence of immobile water regions (Brusseau et al., 1992). All tritium BTCs for Olivier and Windsor soils as well as for the reference sand were successfully simulated with $r^2 > 0.98$. The estimated D values for Windsor and Olivier soils were found to be 1.541 $cm^2\ h^{-1}$ and 1.1$cm^2\ h^{-1}$, respectively and were significantly larger than D values for the reference sand of 0.515 $cm^2\ h^{-1}$. The values of D were subsequently used in the SOTS model to predict Pb and Sn mobility.

7.3.3 Tin and Pb Transport in Reference Sand

Tin BTC from the reference sand column is shown in Fig. 7.4. Here a Sn pulse of 19 pore volumes was applied to the column, then leached with 27 pore volumes of Sn-free solution. The BTC indicated that Sn was observed in the effluent solution after 5 pore volumes with a peak concentration C/C_o of 0.501. Sn exhibited late arrival and higher retention in the reference sand when compared to earlier studies for Cd and Cu using the same matrix (Elbana and Selim, 2010 and 2011). Based on the area under the BTC, the total mass recovered in the effluent solution of Sn was 32.4% of that applied. Such a finding is a strong indication of Sn mobility in such sand soil, where no clay or OM were present, relative to Windsor or Olivier soils.

Three versions of the SOTS model were utilized to simulate Sn mobility in the reference sand column. The first version (V1) accounted for S_e and S_k ; the second vesion (V2) accounted for S_k and S_s and the third version (V3) accounted for S_k and S_{irr} (see Table 7.4 and Fig 7.1). Based on the goodness of model simulations given by r^2 and RMSE, V2 provided the best simulation for Sn BTC in the reference sand with $k_1 = 0.0062 \pm 0.0009$ mL $\mu g^{-1}\ h^{-1}$, $k_2 = 0.0154 \pm 0.0028\ h^{-1}$, $k_3 = 0.0155 \pm 0.0005\ h^{-1}$, and $S_{max} = 256.06 \pm 6.0\ \mu g\ g^{-1}$ (see Fig. 7.4 and Table 7.4). The experimental results in Fig. 7.4 show a strong retardation of Sn breakthrough in the effluent; this justifies the use of models that accounts for reversible and irreversible processes.

Table 7.4. Second-order two-site (SOTS) model parameter estimates for Sn and Pb transport in Reference sand, Windsor, Olivier soil columns: Estimates of adsorption maximum (S_{max}) and reaction rates for root mean square error (*RMSE*), coefficient of determination (r^2) values and (standard error in parentheses).

	Model Version¶	*RMSE*	r^2	S_{max}† μg g^{-1}	K_e mL μg^{-1}	k_1 mL μg^{-1} h^{-1}	k_2	k_3 h^{-1}	k_{irr}
Reference Sand (Sn only)	V1	0.0698	0.8983	601.02±15.4	0.0019±0.0005	0.0005±0.00003	0.00004±0.0002	---	---
	V2	0.0393	0.9670	256.06±6.0	---	0.0062±0.0009	0.0154±0.0028	0.0155±0.0005	---
	V3	0.0555	0.933	717.33±15.2	---	0.0118±0.0006	2.6011±0.2452	---	0.0004±0.00002
Reference Sand (Pb only)	V1	0.0608	0.9795	102.3±8.9	0.0111±0.0018	0.0007±0.0001	0.0160±0.0022	---	---
	V2	0.0875	0.9640	111.9±11.0	---	0.0036±0.0008	0.1080±0.0277	0.0045±0.009	---
	V3	0.0581	0.9801	172.4±11.8	---	0.0034±0.0006	0.2903±0.0544	---	0.0002±0.00003
Windsor Pb-->Sn	V1	0.1141	0.8407	4617.6	0.0131±0.0009	0.000016±0.000005	0.000001±0.0000	---	---
	V2	0.1217	0.7774	4617.6	---	0.00184±0.000006	0.0752±0.0003	0.00051±0.000002	---
	V3	0.1182	0.7939	4617.6	---	0.001945±0.00008	0.0643±0.0014	---	0.000023±0.000003
Windsor Sn --> Pb	V1	0.0258	0.9783	4617.6	0.0057±0.00015	0.00005±0.000001	0.00028±0.00009	---	---
	V2	0.0356	0.9639	4617.6	---	0.00060±0.00018	0.0703±0.0247	0.00421±0.00028	---
	V3	0.0150	0.9928	4617.6	---	0.00053±0.00005	0.0680±0.0072	---	0.000059±0.000001
Windsor Sn & Pb (Mix)	V1	0.0669	0.9711	1728.3±24.2	0.0092±0.00001	0.00057±0.00004	0.0039±0.0004	---	---
	V2	0.0778	0.9596	2007.0±30.7	---	0.0047±0.0014	0.0397±0.0119	0.00080±0.00006	---
	V3	0.0615	0.9720	2403.8±23.0	---	0.0033±0.0001	0.0902±0.0056	---	0.00015±0.00001
Olivier Pb --> Sn	V1	0.1441	0.8545	4197.9	0.0245±0.0002	0.00238±0.00001	0.0042±0.00004	---	---
	V2	0.3693	0.6366	4197.9	---	0.002042±0.000279	0.0158±0.0005	0.000007±0.000001	---
	V3	0.3665	0.5898	4197.9	---	0.002095±0.00012	0.0194±0.0012	---	0.000029±0.000003
Olivier Sn --> Pb	V1	0.0408	0.9686	4197.9	0.0035±0.00016	0.00004±0.000002	0.0023±0.0002	---	---
	V2	0.0144	0.9957	4197.9	---	0.00019±0.000007	0.0261±0.0011	0.002828±0.000093	---
	V3	0.0261	0.9867	4197.9	---	0.000134±0.000006	0.0196±0.0012	---	0.000023±0.000001
Olivier Sn & Pb (Mix)	V1	0.1554	0.8851	2129.5±58.2	0.0137±0.0001	0.00005±0.00001	0.0031±0.0007	---	---
	V2	0.1546	0.9547	2287.3±36.7	---	0.0046±0.0001	0.0795±0.0042	0.000087±0.000003	---
	V3	0.1509	0.9467	2405.3±23.6	---	0.0048±0.0001	0.0962±0.0012	---	0.00001±0.00000

¶: V1 = S_e and S_k (K_e, k_1, and k_2,); V2 = S_k, and S_s (k_1,k_2, and k_3); V3 = S_k and S_{irr} (k_1,k_2, and k_{irr});

†: S_{max} was estimated by SOTS model for the reference sand and the case of mixed Pb and Sn pulse for Windsor and Oliver soils only and otherwise, maximum sorption based on the Langmuir model from the batch experiment was used.

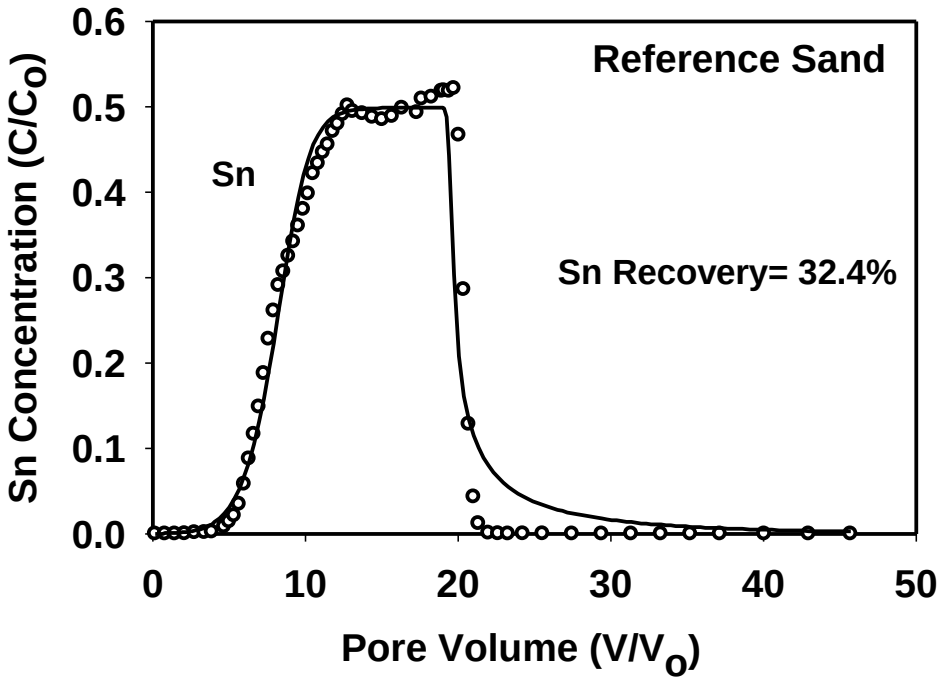

Fig.7.4. Breakthrough results of Sn from the reference sand. Solid curve is the SOTS model simulation.

Lead mobility in the reference sand column is illustrated by the BTC shown in Fig. 7.5 and indicated earlier arrival with a peak concentration (C/C_o) of 1.0. Specifically, Pb was observed in the effluent after only one pore volume and the amount of Pb recovery in the effluent solution was 81.4% of that applied. Therefore, much higher mobility in the sandy soil was observed when compared to Sn. Sheppard and Sheppard (1991) reported 33% of added Pb was flushed through more than 50 cm of a sandy soil depth. Also, in sandy soil irrigated with wastewater Lamy et al. (2006) reported Pb leaching into the subsurface soil. A decrease in Pb concentration in response to flow interruption was observed. Such decrease is indicative of continued Pb sorption due to physical and/or chemical nonequilibrium in this soil. This justifies the use of the SOTS model that accounts for kinetic reactions to simulate Pb mobility in soils. The best simulation of Pb BTC is shown in Fig. 7.5. Visually, all versions provided satisfactory simulations of Pb BTC for the reference sand column. However, V2 and V3 which account for irreversible reactions provided better simulations for tailing of Pb BTC compared to V1 (figure is not shown).

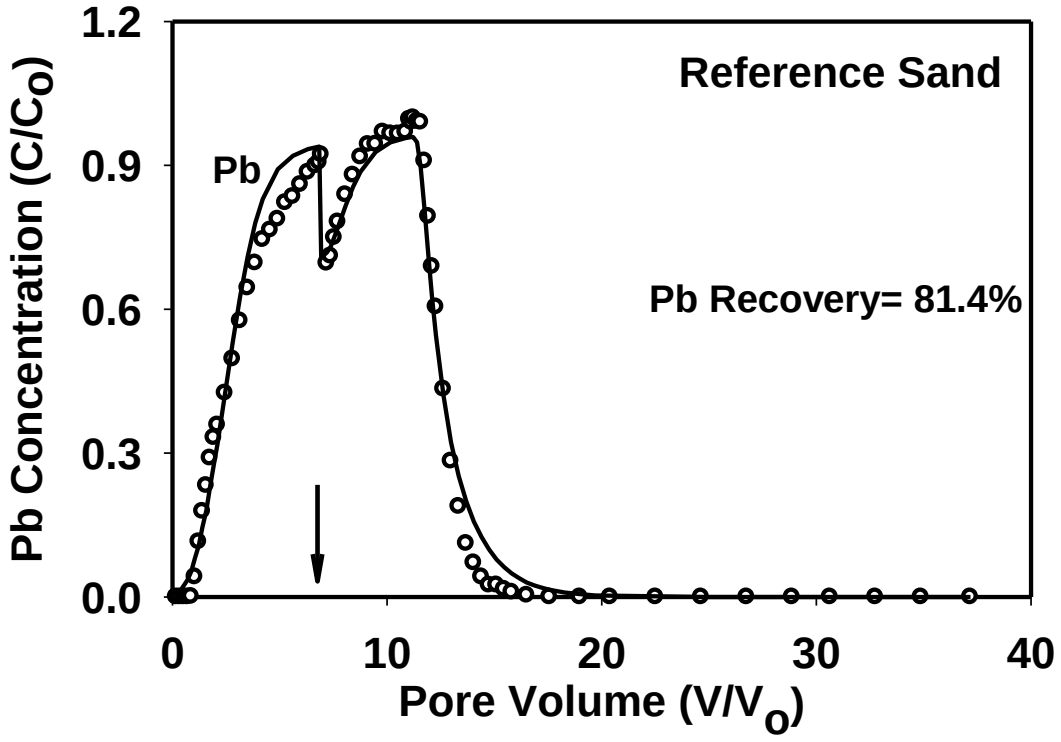

Fig. 7.5. Breakthrough results of Pb from the reference sand; the arrow indicates when flow interruption occurred. The solid curve is the SOTS model simulation.

The release of K, Mg, Al, and Fe as a result of application of Pb or Sn pulses into the reference sand column are shown in Fig. 7.6. Results indicated that Sn and Pb immediately discharged K ions into the effluent solution. Tin exhibited strong effects on the release of Fe and Al ions with maximum concentrations of 6.84 mg L^{-1} and 10.80 mg L^{-1}, respectively. Whereas, Pb showed a little effect on Fe release with maximum concentrations < 0.1 mg L^{-1} while no Al ions were detected in solution. Moreover, changes in K, Mg, and Fe release in response to flow interruption during application of Pb pulse were indicative of continued Pb sorption due to physical and/or chemical nonequilibrium in this soil. Measurements of Mn in effluent indicated that no Mn was detected in response to the Pb pulse whereas, very low released Mn was observed in response to the Sn pulse (< 0.05 mg L^{-1}).

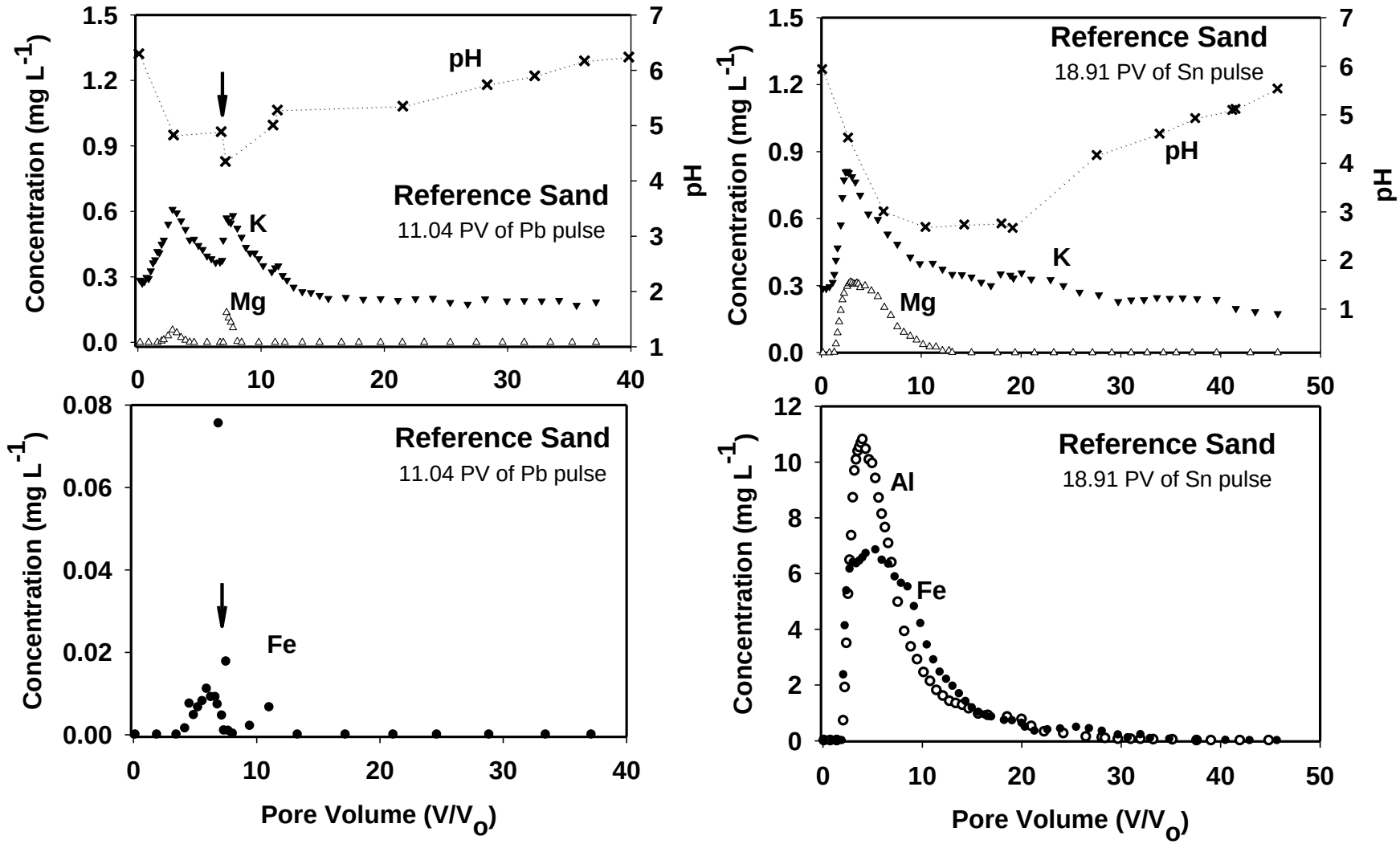

Fig. 7.6. Release of different elements (K, Mg, Fe, and Al) from reference sand and pH change due to application of 11.04 pore volumes of Pb pulse (right) and 18.91 pore volumes of Sn pulse (left); the arrow indicates when flow interruption occurred.

Also, monitoring of pH change during the experiment is shown in Fig. 7.6. A slight pH decrease in the effluent solution was observed during Pb pulse. In response to flow interruption, the pH decreased from 4.9 to 4.4 which was followed by a gradual increase during the leaching of Pb solution. For the reference sand, when a Sn pulse was introduced, the pH of the effluent solution was gradually decreased until reach 2.7, which is equal to the pH of the input solution, followed by a gradual increase during the leaching. Such results indicate the low buffering capacity of the reference sand (See Fig. 7.6).

7.3.4 Tin and Pb Transport in Windsor Soil

Four different miscible displacement experiments were carried out to quantify Pb and Sn mobility in the Windsor soil (see Table 7.2). Tin was not detected in the effluent solution except for the case when a long pulse of Sn was applied (170 pore volumes). Measured Sn concentrations in the effluent indicated limited mobility of Sn where > 99% of applied Sn was retained in the Windsor soil column (Fig. 7.7). Tin was observed in the effluent solution after more than 70 pore volumes with a peak concentration of 1.480 mg L^{-1}. Figure 7.7 shows the pH measurements in effluent during this long pulse. These measurements indicated a gradual decrease in pH during Sn pulse. Also, the releases of K, Mg, Fe, Al, and Mn from Windsor soil as a result of Sn pulse are shown in Fig. 7.7. Results indicated that Sn immediately discharged K and Mg ions into the effluent solution. Tin exhibited clear effects on the release of Mn, Fe and Al ions with maximum concentrations of 6.45 mg L^{-1}, 19.29 mg L^{-1} and 18.56 mg L^{-1}, respectively. Results indicated that the release of Al and Fe ions observed after 15 pore volumes whereas, Mn concentration increased to reach its maximum after 1.5 pore volumes followed by gradual decrease. In soil column experiments, Hou et al. (2005) found that Sn was not leached at all and most of the added Sn was held in the 0-2 cm layer of soil.

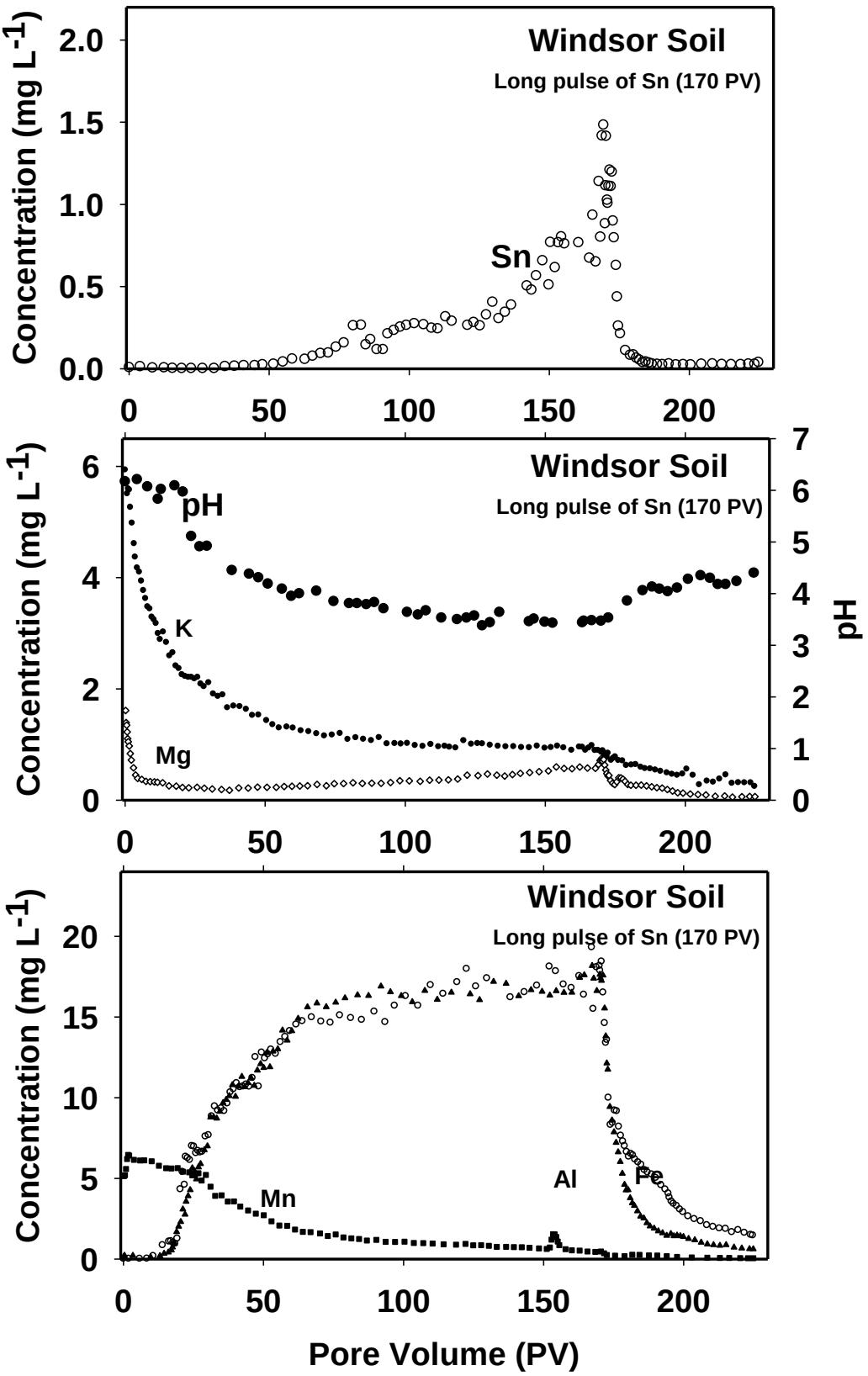

Fig. 7.7. Tin breackthrough curve (top) and release of different elements (K, Mg, Fe, Al, and Mn) from Windsor soil and pH change due to application of 170 pore volumes of Sn pulse.

Lead exhibited different transport behavior than Sn in the Windsor soil receiving a pulse sequence of Pb-Sn and Sn-Pb (see Fig. 7.8). For the Pb-Sn pulse sequence, 37.9 pore volumes of Pb pulse followed by 38.9 pore volumes of Sn pulse were applied. The BTC indicates that Pb was observed in the effluent solution after 20 pore volumes with a peak concentration (C/C_o) of 0.820. Lead concentration gradually increased in the effluent solution until the end of Pb pulse at 37.9 pore volumes with a maximum concentration (C/C_o) of 0.382. Then, Pb concentration continued increasing sharply in the effluent solution to reach a maximum concentration within 7 pore volumes, after introduction of a Sn pulse followed by extensive tailing of the BTC depicting slow release during leaching. Based on the area under the BTC, the total mass recovered in the effluent solution of Pb was 52.0% of that applied.

On the other hand, Pb exhibited less sorption when 42.3 pore volumes of Sn pulse followed by 41.6 pore volumes of Pb pulse were applied for Sn-Pb pulse sequence of Windsor column (Fig. 7.8). Here Pb was observed in the effluent solution after one pore volume from pulse introduction with a peak concentration (C/C_o) of 0.475. Such results indicated that the presence of Sn enhanced the Pb mobility in Windsor soil. The total mass recovered in the effluent solution of Pb was 37.4% of that applied. Different attempts were carried out to simulate Pb mobility in Windsor soil (see Table 7.4). These results suggest early arrival of Pb but continued slow sorption of the irreversible type.

For Windsor soil when Pb-Sn pulse sequence was applied, the SOTS model with kinetic-type (S_k) and equilibrium-type (S_e) sites of version1, V1, provided the best simulation of Pb BTC shown in Fig. 7.8 -top with an r^2 of 0.8407 and a root mean square error (RMSE) of 0.1141. Whereas, successful simulation was obtained for the Sn-Pb pulse sequence with vesion3, V3 of SOTS model (r^2 = 0.9928 and RMSE = 0.0150) as shown in Fig. 7.8-bottom. Chotpantarat et al.

(2012) found that the two site model described Pb BTC was better than the equilibrium convection-dispersion model on the best fit parameters.

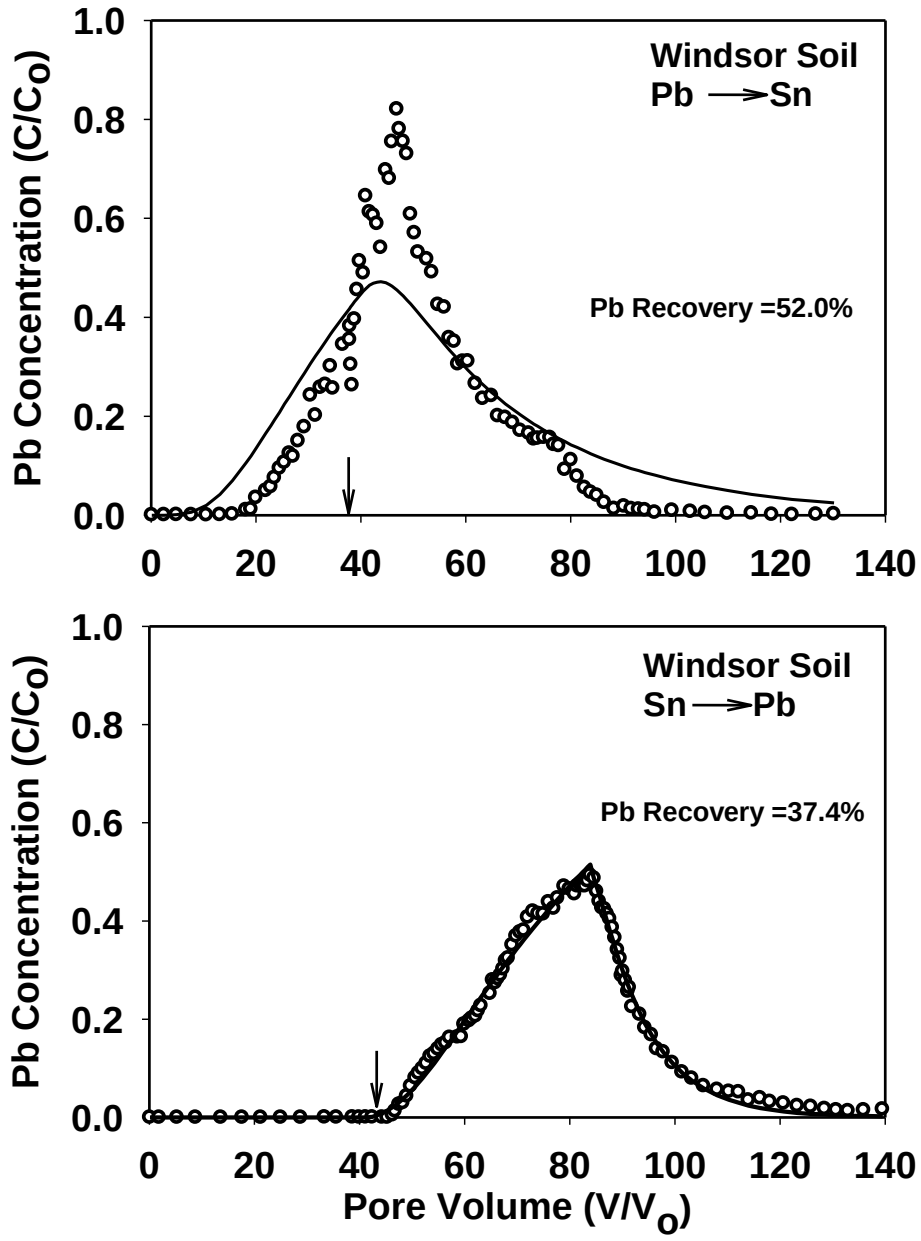

Fig. 7.8. Breakthrough results of Pb from Windsor soil where Pb - Sn (top) and Sn - Pb (bottom) pulses sequence were applied. The solid curve is the SOTS model simulation; the arrow indicates the introduction of the second pulse.

For Windsor soil when 41.75 pore volumes of mixed Pb+Sn pulse was applied, Pb exhibited earlier arrival (after 16 pore volumes) when compared to the BTC for the Pb-Sn pulse sequence (see Fig 7.8 and Fig. 7.9). The peak concentration (C/C_o) of 0.993 was observed at the

end of the mixed pulse and the total mass recovered in the effluent solution of Pb was 58.1% of that applied based on the area under the BTC (Fig. 7.9). A decrease in Pb concentration in response to flow interruption was observed. Such a decrease is indicative of continued Pb sorption due to physical and/or chemical nonequilibrium in this soil. Several attempts were made to describe the observed BTC using a different model version of SOTS. As shown in Table 7.4, accounting for kinetic-type (S_k) and - irreversibly-concurrent reaction (S_{irr}) sites in vesion3, V3 of SOTS model (r^2 = 0.9720 and RMSE = 0.0615) provided the best simulation for the Pb-BTC. Moreover, the simulation of Pb mobility in the Windsor soil using version1, V1, shown in Table 7.4 produced equally good results when compared with version3, V3 except that V1 overestimated Pb for the leaching part, tailing of the BTC (figure is not shown). Recently, Chotpantarat et al. (2012) obtained good simulation for the binary system of Pb and Ni, Zn, or Mn using a chemical nonequilibrium two site model.

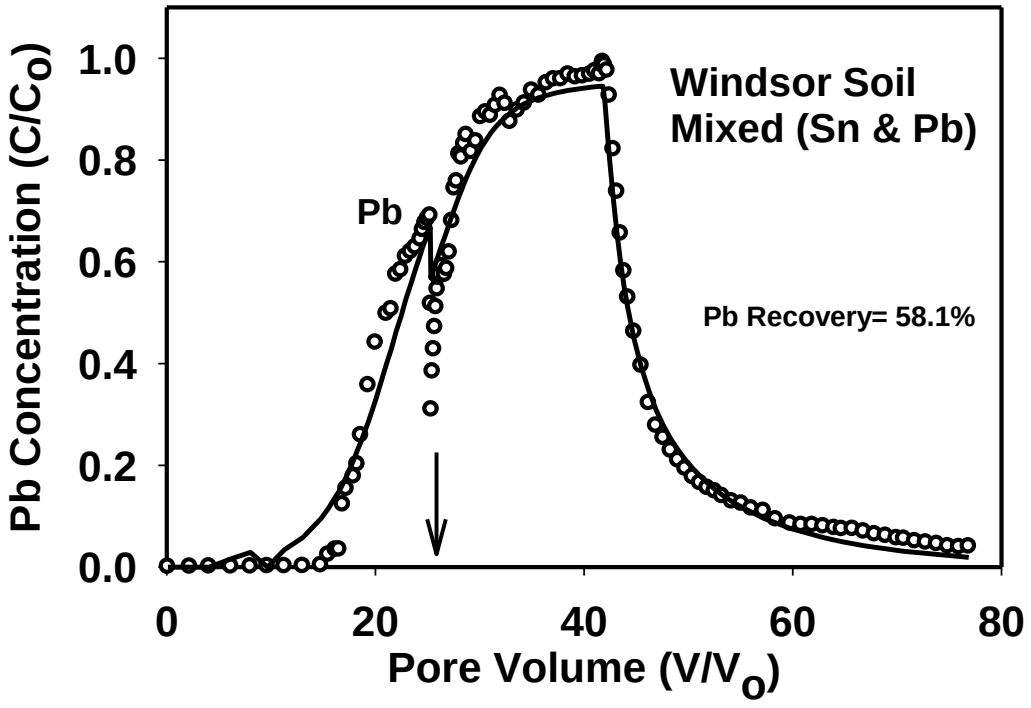

Fig. 7.9. Breakthrough results of Pb from Windsor soil where mixed Sn and Pb pulses were applied. The solid curve is the SOTS model simulation; the arrow indicates when flow interruption occurred.

Figure 7.10 shows the variation in the effluent pH during Sn and Pb pulses application into the Windsor soil. For the Pb-Sn pulse sequence, the average pH-value during the Pb pulse was 6.15 which decreased from 5.90 to 3.74 during the Sn pulse and then was followed by a pH increase during the leaching phase. For the Sn-Pb pulse sequence, the pH decreased from 5.93 to 4.34 during Sn pulse, followed by a steady a pH-level during the Pb pulse with average of 4.651, the pH increased gradually to 5.3 at the end of the leaching phase. After 17 pore volumes of introducing the mixed pulse, the pH decreased from 5.82 to 4.68. Also, the effluent pH changed after flow interruption from 4.64 to 5.83. Such a change in pH in response to the flow interruption is a strong indication of chemical nonequilibrium for Sn and Pb sorption in Windsor soil.

In addition, Fig. 7.10 shows the releases of K, Mg, Fe, Al, and Mn from Windsor soil verses pore volumes. Results indicated that Sn or Pb immediately discharged K and Mg ions into the effluent solution. Tin exhibited a strong influence on the release of Mn, Fe and Al ions as depicted by the BTCs shown in Fig. 7.10. For the Sn-Pb pulse sequence, Al and Fe released to effluent solution after 20 pore volumes whereas, Mn ions released earlier with maximum concentrations of 8.12 mg L^{-1}after 14 pore volumes followed by a gradual concentration decrease. However, introducing a Pb-Sn pulse revealed that Sn released Mn, Fe and Al ions immediately after 1 to 2 pore volumes. On the other hand, the released Mn decreased during the introduction of the Pb pulse, which could attributed to the sorption of Pb by Mn oxides. McKenzie (1980) found that Pb sorption by Mn oxides was up to 40 times greater than that by Fe oxides. The releases of K, Mg, Fe, and Mn were increased due to the flow interruption but, released Al was decreased as direct results of chemical nonequilibrium in soil.

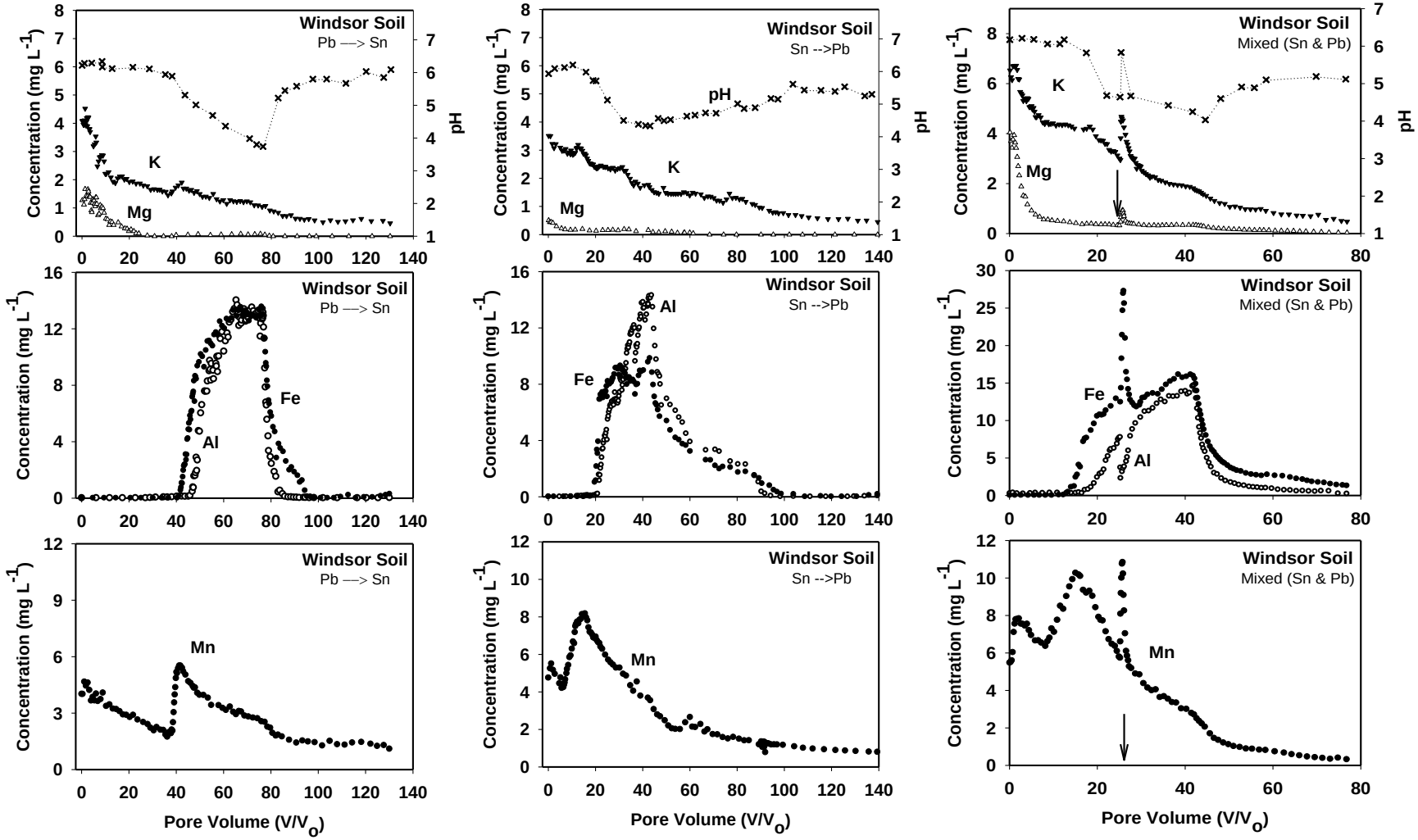

Fig. 7.10. Release of different elements (K, Mg, Fe, Al, and Mn) from Windsor soil and pH change due to application of Pb-Sn, Sn-Pb, and mixed Pb & Sn pulses from right to left, respectively; the arrow indicates when flow interruption occurred.

7.3.5 Tin and Pb Transport in Olivier Soil

Four different displacement experiments were carried out to quantify Pb and Sn mobility in the Olivier soil (see Table 7.2). Tin was not detected in the effluent solution from all Oliver displacement column experiments regardless of the size of the applied pulse (up to 176 pore volumes). For such a long Sn pulse in the Olivier soil, the pH in the effluent during pulse application decreased gradually from 6.2 at 29 pore volumes to 2.8 by the end of the pulse (Fig. 7.11). Also, the release of K, Mg, Fe, Al, and Mn from the Olivier soil as a result of a Sn pulse is shown in Fig. 7.11.

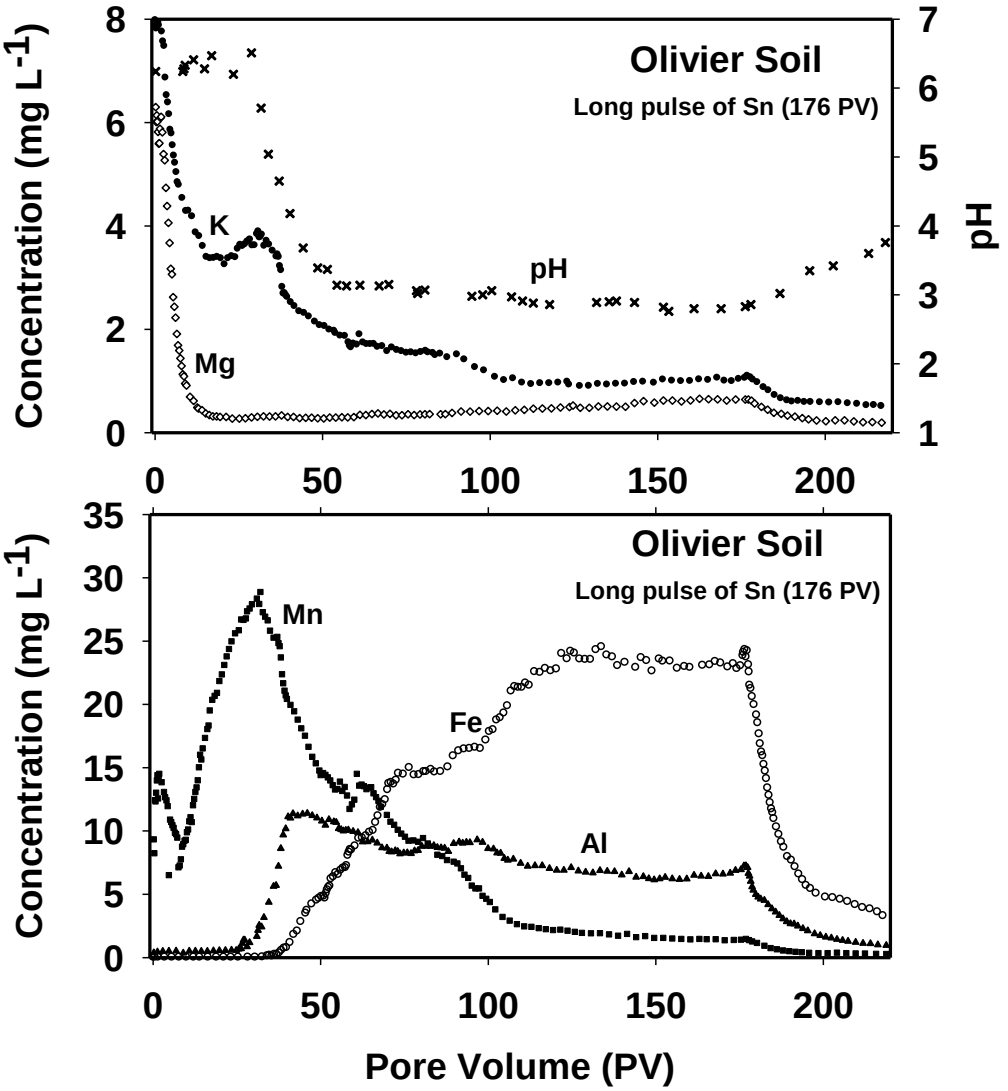

Fig. 7.11. Release of different elements (K, Mg, Fe, Al, and Mn) from Olivier soil and pH change due to application of 176 pore volumes of Sn pulse.

Results indicated that Sn discharged K and Mg ions into the effluent solution. Tin exhibited clear effects on the release of Mn, Fe and Al ions with maximum concentrations of 28.88 mg L^{-1}, 25.06 mg L^{-1} and 12.27 mg L^{-1}, respectively. Results indicated that release of Al and Fe ions after 25 and 37 pore volumes, respectively. Whereas, Mn released earlier after one pore volume and Mn concentration increased to reach its maximum after 32 pore volumes followed by a gradual decrease (See Fig. 7.11)

Lead exhibited different transport behavior in Olivier soil based on the pulse sequence (Pb-Sn or Sn-Pb). Lead BTCs from Olivier soil columns for Pb-Sn and Sn-Pb sequences are shown in Fig. 7.12. For the Pb-Sn pulse sequence, 44.1 pore volumes of Pb pulse were followed by 44.4 pore volumes of Sn applied pulse. The BTC indicates that Pb was observed in the effluent solution after 38 pore volumes with a peak concentration (C/C_o) of 0.978. Then, Pb concentration increased in the effluent solution sharply and reached a maximum concentration after 20 pore volumes following introduction of a Sn pulse. This was followed by extensive tailing of the BTC depicting a slow release during leaching. Based on the area under the BTC, the total mass recovered in the effluent solution of Pb was 96.4% of that applied.

Lead exhibited less retention by the Oliver soil based on the arrival time when 41.8 pore volumes of Sn pulse were followed by 41.9 pore volumes of Pb pulse applied for the Sn-Pb pulse sequence (Fig. 7.12). Here, Pb was observed in the effluent solution after one pore volume of pulse introduction with a peak concentration (C/C_o) of 0.622. Such results indicated that the presence of Sn enhanced Pb mobility in the Oliver soil. Based on the area under the BTC, the total mass recovered in the effluent solution of Pb was 57.6% of that applied. Different attempts were carried out to simulate Pb mobility in the Olivier soil (see Table 7.4). When the Pb-Sn pulse sequence was applied to the Oliver soil, the SOTS model with kinetic-type (S_k) and equilibrium-type (S_e) sites of version1, V1, provided the best simulation of Pb BTC shown in Fig. 7.12-top

with an r^2 of 0.8528 and a root mean square error (RMSE) of 0.1400. Whereas, successful simulation was obtained for Sn-Pb pulse sequence with version2, V2 of the SOTS model (r^2 = 0.9957 and RMSE = 0.0144) as shown in Fig. 7.12-bottom.

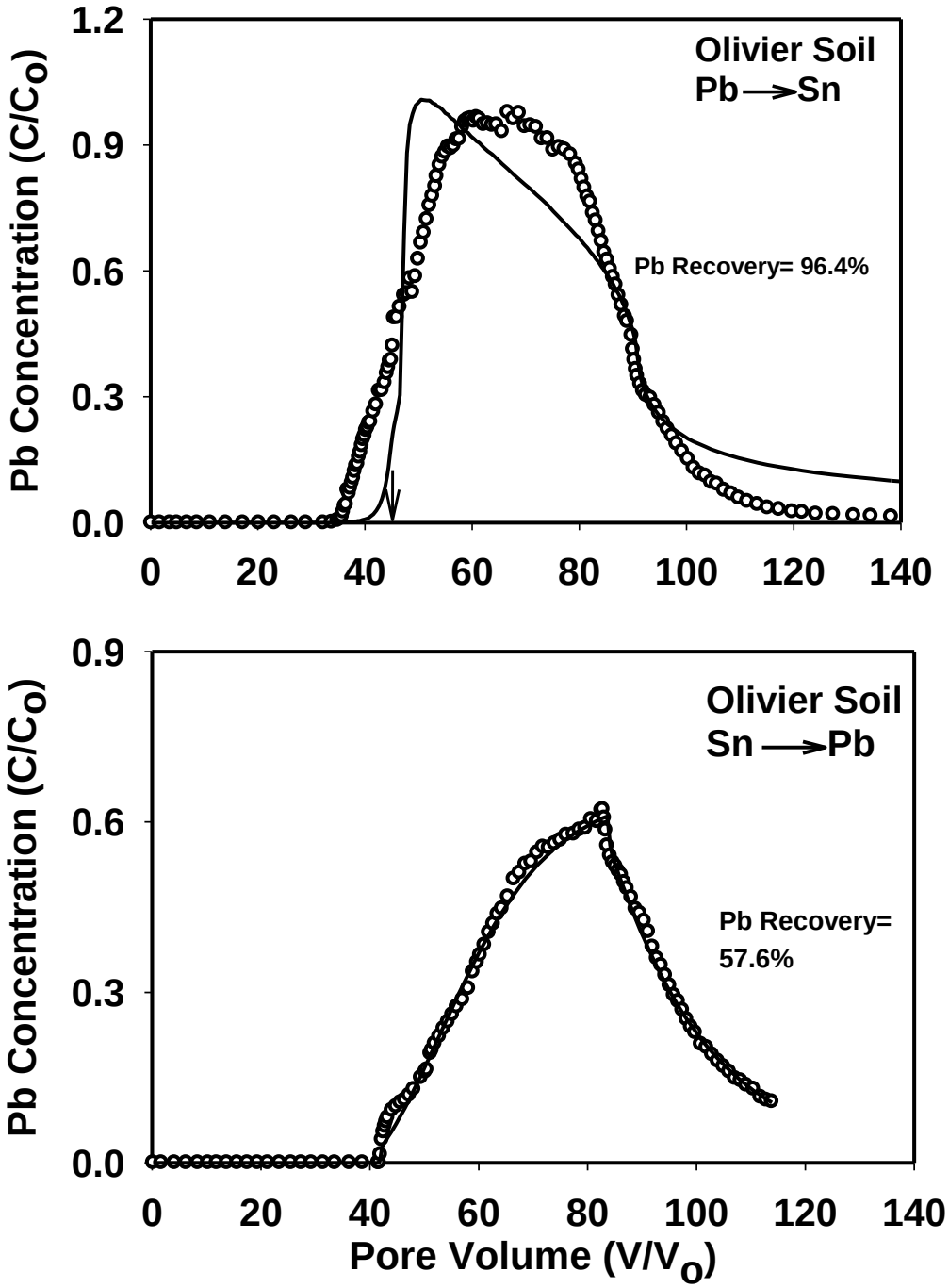

Fig. 7.12. Breakthrough results of Pb from Olivier soil where Pb-Sn (top) and Sn - Pb (bottom) pulses sequence were applied. The solid curve is the SOTS model simulation; the arrow indicates the introduction of the second pulse.

For the Oliver soil, when 41.9 pore volumes of mixed Pb&Sn pulse was applied, Pb exhibited arrival after 20 pore volumes compared to one when the Pb-Sn pulse sequence was applied. The peak concentration (C/C_o) was 1.24 and the total mass recovery in the effluent solution of Pb was 76.6% of that applied (Fig. 7.13). A decrease in Pb concentration in response to flow interruption was observed which indicated physical and/or chemical nonequilibrium in this soil for Pb sorption. As shown in Table 7.4, accounting for kinetic-type (S_k) and -irreversibly-consecutive reaction (S_s) sites in version2, V2 of the the SOTS model (r^2 = 0.9547 and RMSE = 0.1546), this provided the best simulation for the Pb-BTC.

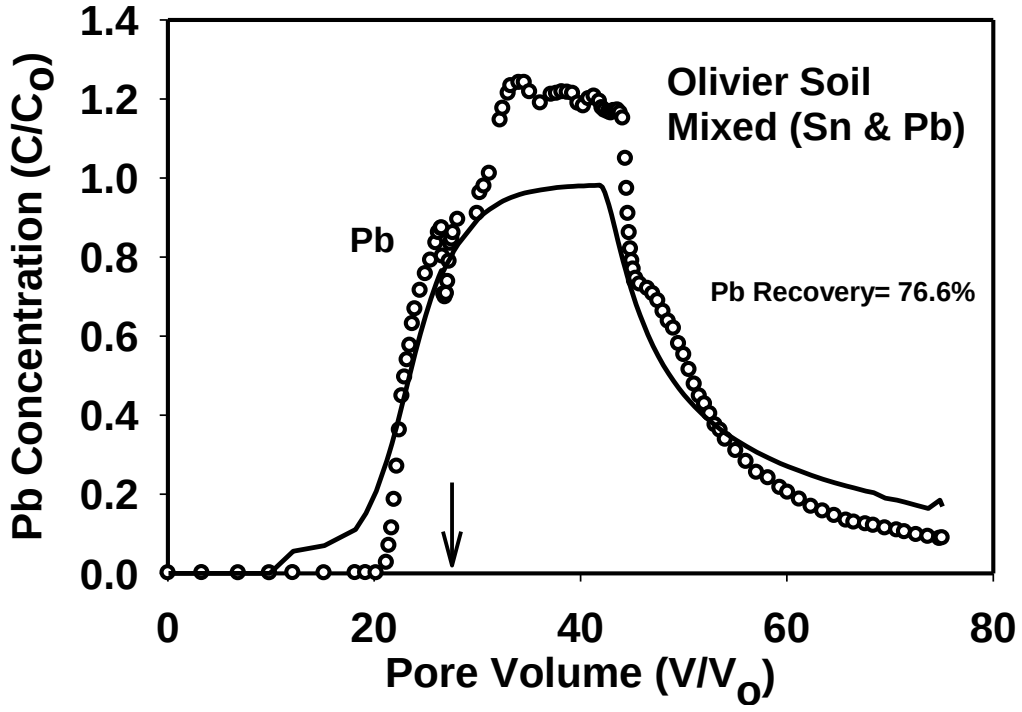

Fig. 7.13. Breakthrough results of Pb from Olivier soil where mixed Sn and Pb pulses were applied. The solid curve is the SOTS model simulation; the arrow indicates when flow interruption occurred.

Figure 7.14 shows the variation in effluent pH values during the introduction of Sn and Pb pulses into Olivier soil. For the Pb-Sn pulse sequence, the average pH-value during the Pb pulse was 6.12±0.45 that decreased from 5.13 to 3.47 during the Sn pulse, followed by pH increasing during the leaching phase. For the Sn-Pb pulse sequence, pH decreased from 6.62 to

2.98 during the Sn pulse, followed by a steady pH-level during the Pb pulse with an average of 3.49. The pH increased gradually to 4.48 by the end of the leaching phase. For the Sn+Pb mixed pulse, the pH decreased from 6.67 to 5.44. The effluent pH changed from 5.44 to 6.65 in response to flow interruption. Such an increase in pH during the flow interruption is indicative of chemical nonequilibrium for Sn and Pb sorption on the Olivier soil.

Moreover, Fig. 7.14 shows the release of K, Mg, Fe, Al, and Mn during the introduction of different Sn and Pb pulses into the Olivier soil. Results indicated that both Sn and Pb immediately discharged K and Mg ions into the effluent solution. Tin exhibited a clear effect on the release of Mn, Fe and Al ions as depicted by the BTCs shown in Fig. 7.14. For the Sn-Pb pulse sequence, Al and Fe were released to the effluent solution after 20 and 37 pore volumes during the Sn pulse, respectively. The release of Mn ions was observed with a maximum concentration of 24.65 mg L^{-1} after 23 pore volumes followed by a gradual concentration decrease. Whereas, introducing Pb-Sn pulse revealed that Sn released Mn and Al ions immediately after one pore volume however, no Fe was detected in the effluent solutions (see Fig. 7.14). Flow interruption resulted in somewhat higher K, Mg, and Mn and a decrease of Al release into effluent.

7.3.6 Tin and Lead Distribution with Depth

The distributions of sorbed Pb and Sn vs. depth in the Windsor and Olivier soils columns are shown in Fig 7.15 and 7.16, respectively. The sorbed Sn was primarily found in the top two centimeters. For Windsor soil, 58, 66, 76, and 83% of total sorbed Sn were retained in the surface (0 to 1cm) for the long-Sn pulse, mixed (Sn+Pb), Pb-Sn, and Sn-Pb columns, respectively. The respective values for Olivier soil were 59, 90, 97, and 71%, respectively. The non-uniformity and the decrease with depth of sorbed Sn indicated limited mobility and strong sorption in both soils

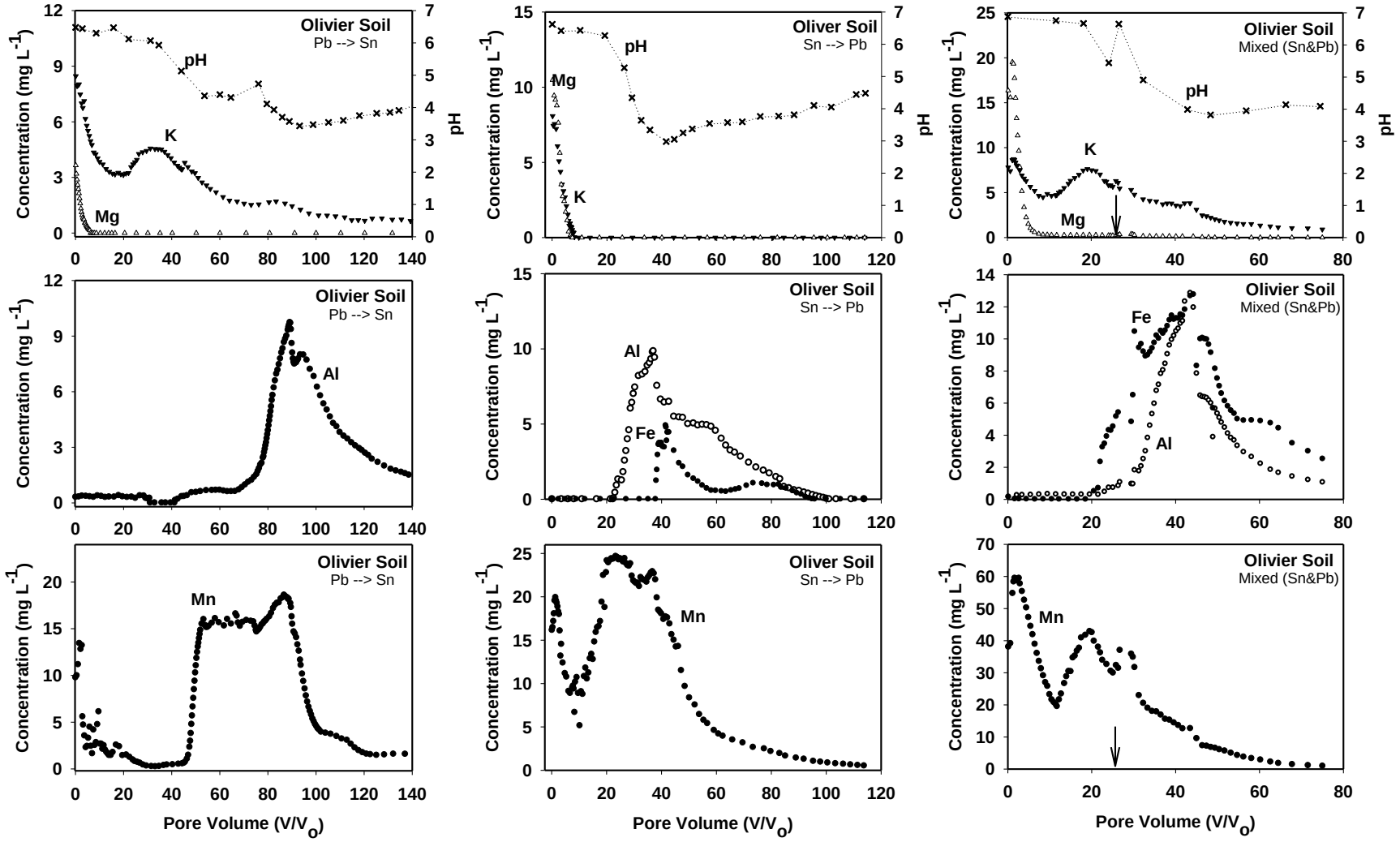

Fig. 7.14. Release of different elements (K, Mg, Fe, Al, and Mn) from Olivier soil and pH change due to application of Pb-Sn, Sn-Pb, and mixed Pb&Sn pulses from right to left, respectively; the arrow indicates when flow interruption occurred.

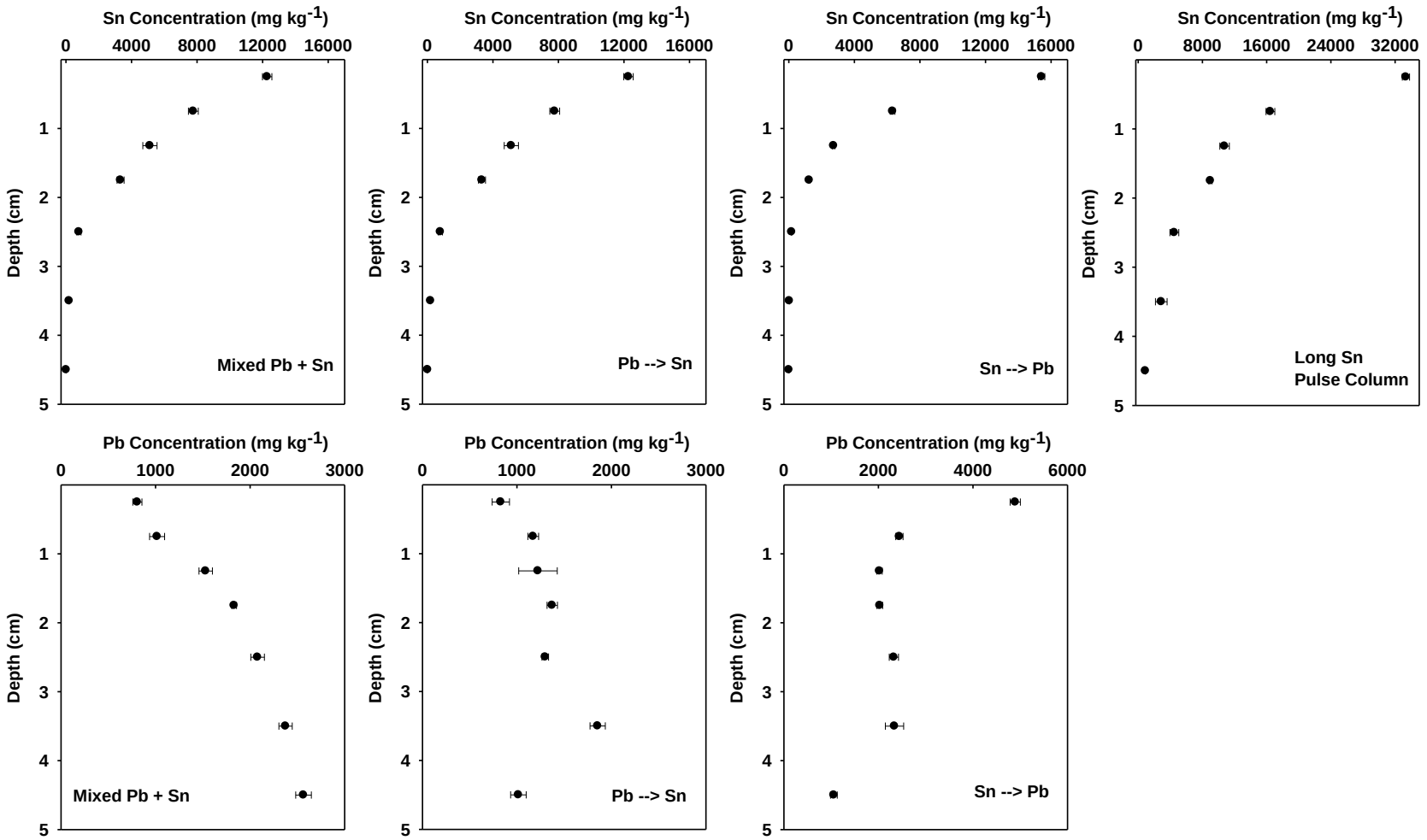

Fig. 7.15 . Tin (top) and lead (bottom) sorbed vs. column depth based on XRF measurements for Windsor soil columns (mixed Sn+Pb; sequential Pb-Sn; sequential Sn-Pb; long Sn pulse, respectively from right to left).

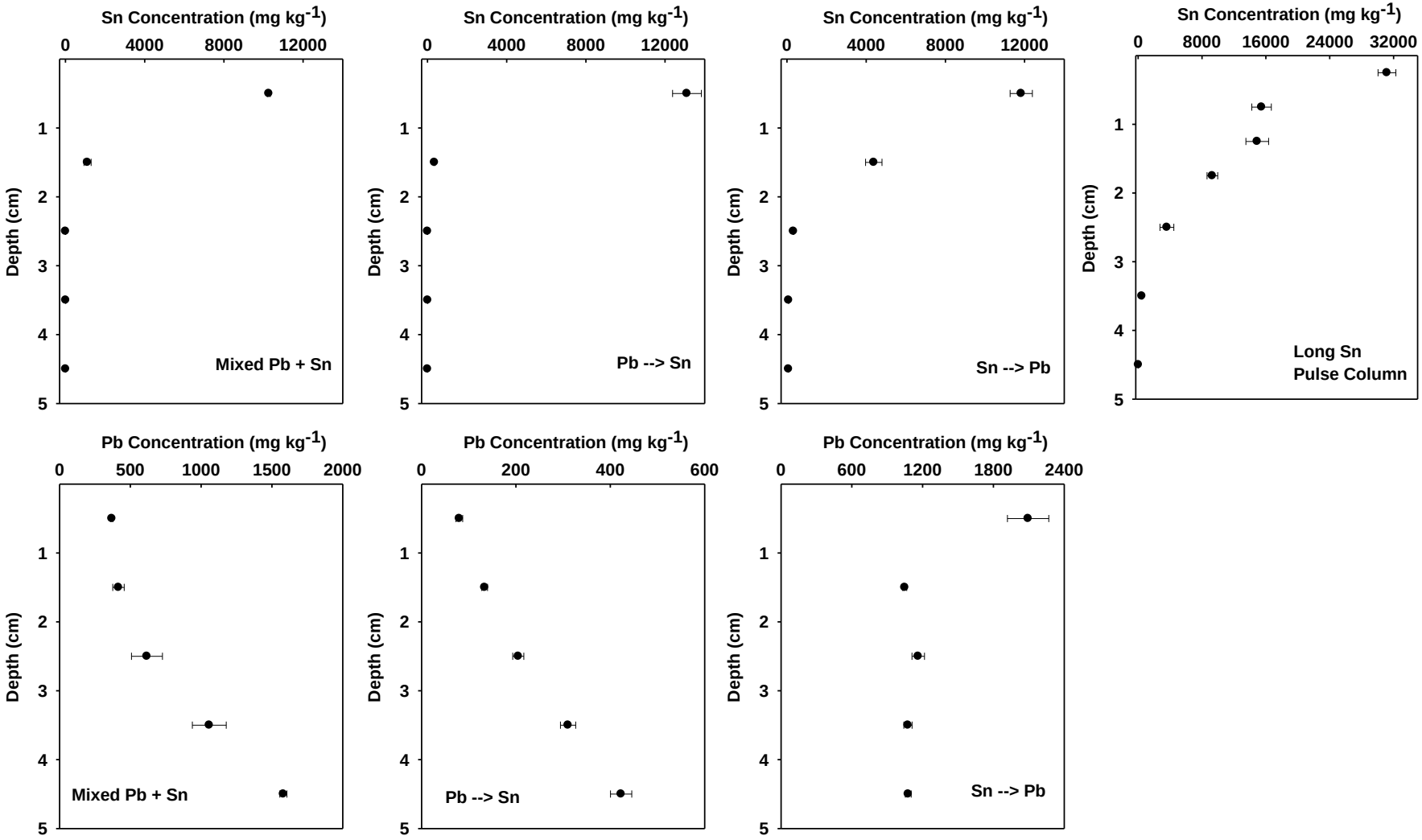

Fig. 7.16 . Tin (top) and lead (bottom) sorbed vs. column depth based on XRF measurements for Olivier soil columns (mixed Sn+Pb; sequential Pb-Sn; sequential Sn-Pb; long Sn pulse, respectively from right to left).

The distributions of sorbed Pb vs. depth in the Windsor and Olivier soils columns indicated less sorption and higher mobility compared to Sn. The increase of sorbed Pb with depth was observed in both soils when mixed Sn+Pb and Pb-Sn sequence pulses were applied (see Figs. 7.15 and 7.16). However, Pb exhibited less mobility when Sn-Pb sequence was applied for both soils. Specifically, 27, 36, and 50% of total sorbed Pb were retained in surface section (0 to 2cm) for mixed (Sn+Pb), Pb-Sn, and Sn-Pb Windsor columns, respectively. The respective values for Olivier soil were 19, 19, and 49%, respectively. Furthermore, the distributions of sorbed Pb and Sn vs. depth in the reference sand column are shown in Fig 7.17. Consistent with the breakthrough results, Sn exhibited less mobility and higher sorption compared to Pb in this sandy soil. Homogenous distribution of sorbed Sn and Pb were observed.

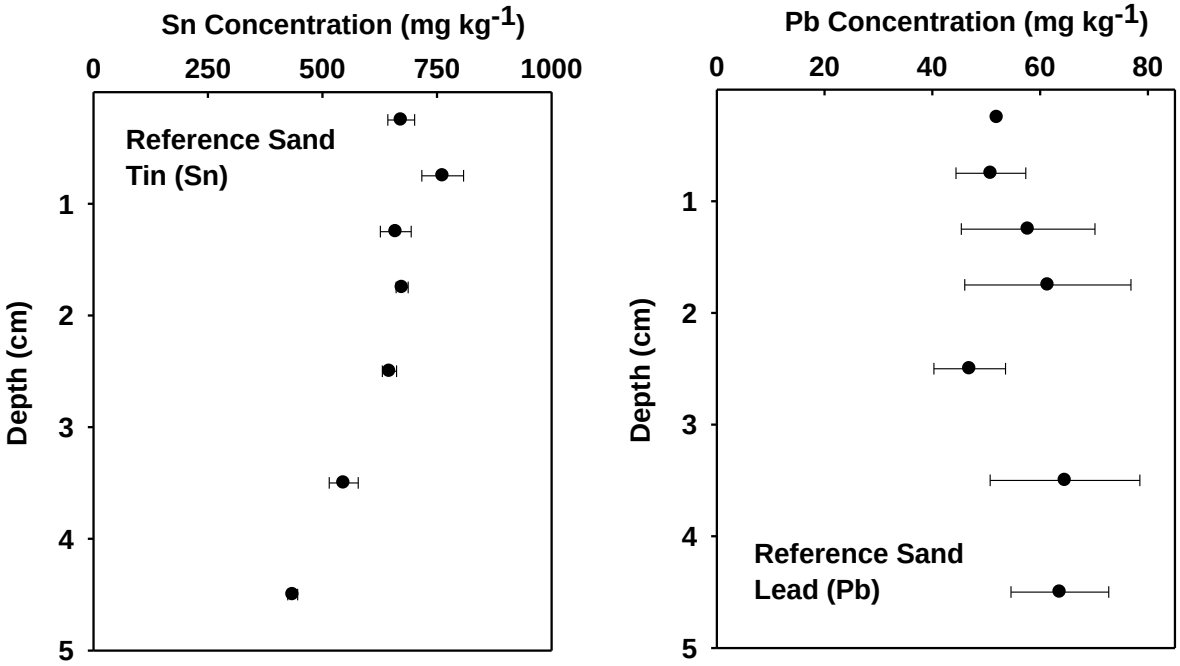

Fig. 7.17. Tin (left) and Lead (right) sorbed vs. column depth based on XRF measurements for reference sand columns.

7.4 Conclusions

Miscible displacement column techniques were used to assess the effect of Sn on Pb mobility in two soils (Windsor and Olivier). The presence of Sn in the soil solution reduced the

sorption capacity of Pb by the studied soil by 12-25%. Breakthrough results indicated incomplete recovery of Pb (81.4%) and Sn (32.4%) in the reference sand columns. Sn exhibited very limited mobility in Windsor and Olivier soils whereas Pb mobility was observed. The presence of Sn resulted in enhanced mobility of Pb for both soils as evidenced by early arrival of Pb in the effluent. Based on the area under the curve, the total mass recovery of Pb in the effluent solution was 52, 37, and 58% for Pb-Sn, Sn-Pb, and mixed Sn&Pb pulses, respectively in the Windsor soil. The respective values for the Olivier soil were 96, 85, and 77%. The second-order two-site model (SOTS) successfully described Pb mobility in both soils as well as Pb and Sn in the reference columns.

7.5 References

Amacher, M.C. 1996. Nickel, Cadmium, and lead. P. 739-768. In: Sparks (ed.) Methods of soil analysis: chemical methods. Part 3. SSSA No.5. ASA-CSSA-SSSA, Madison, WI.

Barkouch, Y., A. Sedki, and A. Pineau. 2007. A new approach for understanding lead transfer in agricultural soil. Water Air Soil Pollut. 186:3–13.

Brusseau, M.L., R.E. Jessup, and P.S.C. Rao. 1992. Modeling solute transport influenced by multiprocess nonequilibrium and transformation reactions. Water Resour. Res. 28:175–182.

Bryan, G. W, and W.J. Langston. 1992. Bioavailability, accumulation and effects of heavy metals in sediments with special reference to United Kingdom estuaries: a review. *Environ. Pollut.* 76, 89-131.

Chotpantarat S., S.K. Ong, C. Sutthirat, K. Osathaphan. 2012. Competitive modeling of sorption and transport of Pb^{2+}, Ni^{2+}, Mn^{2+} and Zn^{2+} under binary and multi-metal systems in lateritic soil columns. Geoderma.189-190: 278-287.

Dong, D., X. Zhao, X. Hua, J. Liu, and M. Gao. 2009. Investigation of the potential mobility of Pb, Cd and Cr(VI) from moderately contaminated farmland soil to groundwater in Northeast. China. Journal of Hazardous Materials 162:1261–1268.

Elbana, T. A. and H M. Selim. 2010. Cadmium transport in alkaline and acidic soils: miscible displacement experiments. Soil Sci. Soc. Am. J. 74: 1956–1966.

Elbana, T. A. and H M. Selim. 2011. Copper mobility in acidic and alkaline soils: miscible displacement experiments. Soil Sci. Soc. Am. J. 75:2101–2110.

Fonseca, B., H. Figueiredo, J. Rodrigues, A. Queiroz, and T. Tavares. 2011. Mobility of Cr, Pb, Cd, Cu and Zn in a loamy soil: a comparative study. Geoderma 164:232–237.

Garrido, F., V. Illera, C.G. Campbell, and M.T. Carcía-González. 2006. Regulating the mobility of Cd, Cu and Pb in an acid soil with amendments of phosphogypsum, sugar foam, and phosphoric rock, Eur. J. Soil Sci. 57:95-105.

Hanna K, L. Lassabatere, B. Bechet. 2009. Zinc and lead transfer in a contaminated roadside soil: experimental study and modeling. J Hazard Mater 161:1499–1505.

Hooda, P.S. and B.J. Alloway. 1998. Cadmium and lead sorption behaviour of selected English and Indian soils. Geoderma, 84:121-134.

Hou, H., T. Takamatsu, M.K. Koshikawa, and M. Hosomi. 2005. Migration of silver, indium, tin, antimony, and bismuth amd variations in their chemical fractions on addition to uncontaminated soils. Soil Science 170:624-639.

Kabata-Pendias A, and A.B. Mukherjee. 2007. Trace elements from soil to human. Springer. 556 pp.

Kabata-Pendias, A., and H. Pendias. 2001. Trace elements in soils and plants. 3rd ed. CRC Press, Boca Raton, FL.

Karathanasis A.D, D.M.C. Johnson, and C.J. Matocha. 2005. Biosolid colloid mediated transport of copper, zinc and lead in waste-amended soils. J Environ Qual. 34:1153– 1164.

Lamy, I., F. Van Oort, C. Dere and D. Baize, 2006. Use of major and trace element correlations to assess metal migration in sandy Luvisols irrigated with wastewater. European J. Soil Sci., 57: 731–740.

Li L.Y. 2006. Retention capacity and environmental mobility of pb in soils along highway corridor. Water, Air, Soil Pollut. 170: 211–227.

Liao, L., H.M. Selim, and R.D. DeLaune. 2009. Mercury adsorption–desorption and transport in soils. J. Environ. Qual. 38:1608–1616.

Lu, S.G. and Q.F Xu. 2009. Competitive adsorption of Cd, Cu, Pb and Zn by different soils of Eastern China. Environmental Geology. 57:685-693.

Martínez-Villegas, N., L.Ma. Flores-Vélez, and O. Domínguez, 2004. Sorption of lead in soil as a function of pH: a study case in México. Chemosphere 57, 1537–1542.

McKenzie R.M. 1980.The adsorption of lead and other heavy metals on oxides of manganese and iron, Aust. J. Soil Res. 18:61-73.

Melamed, R., X. Cao, M. Chen, and L.Q. Ma. 2003. Field assessment of lead immobilization in a contaminated soil after phosphate application. The Sci. Total Environ. 305:117–127.

Ostrakhovitch, E.A., and M.G. Cherian. 2007. Tin. In: Nordberg, G.F., B.A. Fowler, M. Nordberg, L.T. Friberg. (Eds.), Handbook on the Toxicology of Metals. Third edition. Academic Press, pp. 839–859.

Press, W.H., S.A. Teukolsky, W.T. Vetterling, and B.P. Flannery. 1992. Numerical recipes in FORTRAN (2nd ed.). Cambridge Univ. Press, New York.

SAS 9.3. 2011. Foundation for Microsoft® Windows® SAS Institute Inc., Cary, NC, USA.

Schafer S. G, and U. Fermfert. 1984. Tin – a toxic heavy metal? A review of the literature. Regul Toxicol Pharmacol 4:57–69.

Schmitt H, H. Sticher. 1986. Prediction of heavy metal contents and displacement in soils. Z. Pflanzenernaehr. Bodenk. 149: 157-171.

Selim, H. M. and M. C. Amacher. 1988. A second order kinetic approach for modeling solute retention transport in soils. Water Resources Research 24: 2061-2075.

Selim, H.M., and M.C. Amacher. 1997. Reactivity and transport of heavy metals in soils. CRC Press, Boca Raton, FL.

Sheppard, S.C., and M. I. Sheppard. 1991. Lead in boreal soils and food plants. Water Air Soil Pollut 57–58:79–91.

Steinnes, E. 2013. Lead. P. 395-409. *In*: Alloway B. Heavy Metals in Soils: Trace Metals and Metalloids in Soils and their Bioavailability.3rd. Dordrecht, Springer.

Strawn, D.G. and Sparks, D.L., 2000. Effects of soil organic matter on the kinetics and mechanisms of Pb(II) sorption and desorption in soils. Soil Sci. Soc. Am. J. 64:144-156.

Toride, N., F.J. Leij, and M. Th. van Genuchten. 1999.The CXTFIT code for estimating transport parameters from laboratory or field tracer experiments, version 2.1. Research Report No. 137, U.S. Salinity Laboratory, USDA, ARS, Riverside, CA.

USEPA (U.S. Environmental Protection Agency). 2005. Ecological Soil Screening Levels for Lead, Interim Final. Office of Solid Waste and Emergency Response. OWSER Directive 9285.7-70. 1200 Pennsylvania Ave. N.W. Washington, D.C. 20460.

USEPA (U.S. Environmental Protection Agency). 2007. Method 6200: Field Portable X-Ray Fluorescence Spectrometry for the Determination of Elemental Concentrations in Soil and Sediment. P 6200-1:6200-32 *In*: Test Methods for Evaluating Solid Waste, Physical/Chemical Methods (SW-846). http://www.epa.gov/epawaste/hazard/testmethods/sw846/online/index.htm

Vile, M.A., R.K. Wieder, and M. Novák. 1999. Mobility of Pb in Sphagnum-derived peat. Biogeochemistry 45: 35–52.

CHAPTER 8. HEAVY METALS ACCUMULATION AND SPATIAL DISTRIBUTION IN LONG TERM WASTEWATER IRRIGATED SOILS

8.1 Introduction

Use of municipal and industrial wastewater for irrigation is a widespread practice worldwide (USEPA, 2004; Bixio et al., 2006; Rutkowski et al., 2007). Due to the scarcity of freshwater resources, wastewater from urban areas has been commonly used for irrigation in arid and semi-arid regions (Pescod, 1992; van der Hoek, 2004; Carr et al., 2011). Moreover, the reuse of wastewater has grown rapidly in humid regions, particularly for urban irrigation (O'Connor et al., 2008). Qadir et al. (2010) indicated that irrigation with raw or diluted wastewater continued to increase in several regions of developing countries as long as wastewater treatment does not keep pace with urban growth and urban food demands. The use of wastewater for irrigation fulfills certain socioeconomic and environmental goals such as increasing production or profits and diminishing of wastewater discharge to the environment. On the other hand, wastewater is considered a source of harmful pathogenic diseases and the contamination of surface and ground water (Singh et al., 2004; Chen et al., 2005; Hamilton 2007).

Wastewater contains a variety of pollutants including pathogens and heavy metals which can potentially harm the environment as well as human and animal health (Qadir et al., 2007). Irrigation with wastewater contributes significantly to the build up of heavy metals in soils (Mapanda et al., 2005; Singh et al., 2004). The negative impact of heavy metal accumulation in soils affect the yield and quality of crops, and the quality of atmospheric and aquatic environments (Kabata-Pendias and Mukherjee, 2007; Srinivasan and Reddy, 2009). Soil contamination by heavy metals is of serious concern due to their toxicity and persistence in the environment (Facchinelli et al., 2001; Mico et al., 2006). Generally, irrigation with wastewater elevates the total and available heavy metals concentrations in soils. Liu et al. (2005) found that

application of sewage irrigation for 40 years in Beijing, China resulted in increased accumulation of Cd, Cr, Cu, Zn, and Pb. Rattan et al. (2005) showed that irrigation of soil with sewage water for 20 years led to an increases of extractable DTPA-Zn, -Cu, -Fe, -Ni, and -Pb by 208, 170, 170, 63, and 29%, respectively, when compared to adjacent water-irrigated soils.

Despite the fact that wastewater commonly contain various heavy metals and pathogens, nonconventional use of wastewater is practiced in regions with scarce water resources (Abu-Zeid, 1998). For example, in Egypt, according to the USEPA (2004), there were about 42,000 ha of land irrigated with treated, undiluted, or diluted wastewater. The reuse of municipal wastewater was implemented in Egypt's *Elgabal Elasfar* sewage farm since its establishment in 1911. During the first 20 years, the volume of sewage received by the treatment plant doubled in capacity. After 1990, the treatment plant was expanded and the standards for wastewater reuse were legislated (Abu-Zeid, 1998).

This long term and continued wastewater use at the *Elgabal Elasfar* farm resulted in accumulation of several heavy metals and a decrease in the pH of surface soils (El-Nennah et al., 1982; El-Hassanin et al., 1993; Badawy and Helal, 2002). In this study, surface and subsurface soil samples were collected throughout the landscape in order to assess the bioavailability of heavy metals as a result of their long term accumulation. This is significant in order to achieve sustainable wastewater irrigation goals and to minimize the impact of heavy metals on the environment (Hamilton et al., 2007; O'Connor et al., 2008). Long term accumulation of bioavailable forms of heavy metals in soils remain as particularly significant gaps in the science of sustainable wastewater irrigation (Hamilton et al., 2007). The behavior of these chemicals in the environment and the resulting risk to human health is largely unknown (O'Connor et al., 2008).

The objectives of the study were to: (i) assess the effects of long-term irrigation with sewage effluents on soil properties and accumulation of total and available forms of Cd, Cu, Ni, and Pb in soil, (ii) create spatial distribution maps of those heavy metals using remote sensing (RS) date and geographic information system (GIS) tools, and (iii) delineate areas of heavy metal contamination of surface and subsurface soils across the landscape.

8.2 Materials and Methods

8.2.1 Study Area

The *Elgabal Elasfar* farm is a government-owned farm established in 1911 in *Qalyubia* Governorate at the eastern desert 25 km northeast of Cairo, Egypt. This area has been irrigated with untreated sewage effluent for several decades (Abdel-Shafy and Abdel-Sabour, 2006). The area is partitioned into three sections (Fig. 8.1).The north (*Fondi*) section was irrigated with untreated domestic wastewater. After 1995, this section was irrigated with mixed water (secondary treated and untreated). This north section is the newest cultivated area in the region which was established in 1960.

The middle and south sections, which were cultivated since 1911, were irrigated with untreated wastewater until 1995. According to Abu-zeid (1998) and Elgala et al (2003) the two old (middle and south) sections received entirely raw sewage irrigation for some forty years which was the normal practice. The south section almost always received more frequent raw sewage applications than the middle section. In fact, Elgala et al (2003) reported that the total organic and inorganic suspended matter was found to be of ten times more in sewage water when compared to Nile water. After 1995, the south section received secondary treated wastewater. In contrast, the middle section received mixed water (secondary treated and untreated).

The study area is characterized by Mediterranean climate, and can be considered as a semi-arid zone. The average climatic data (over 30 years) collected from Bilbeis meteorological

station (closest to the study area) indicated that the annual rainfall is around 20.0 mm year^{-1}, the maximum temperature approximately 34.6°C during the summer months, while the minimum temperature about 8.0°C during winter season, and the humidity ranged from 50 to 67% during the year (FAO, 1993).

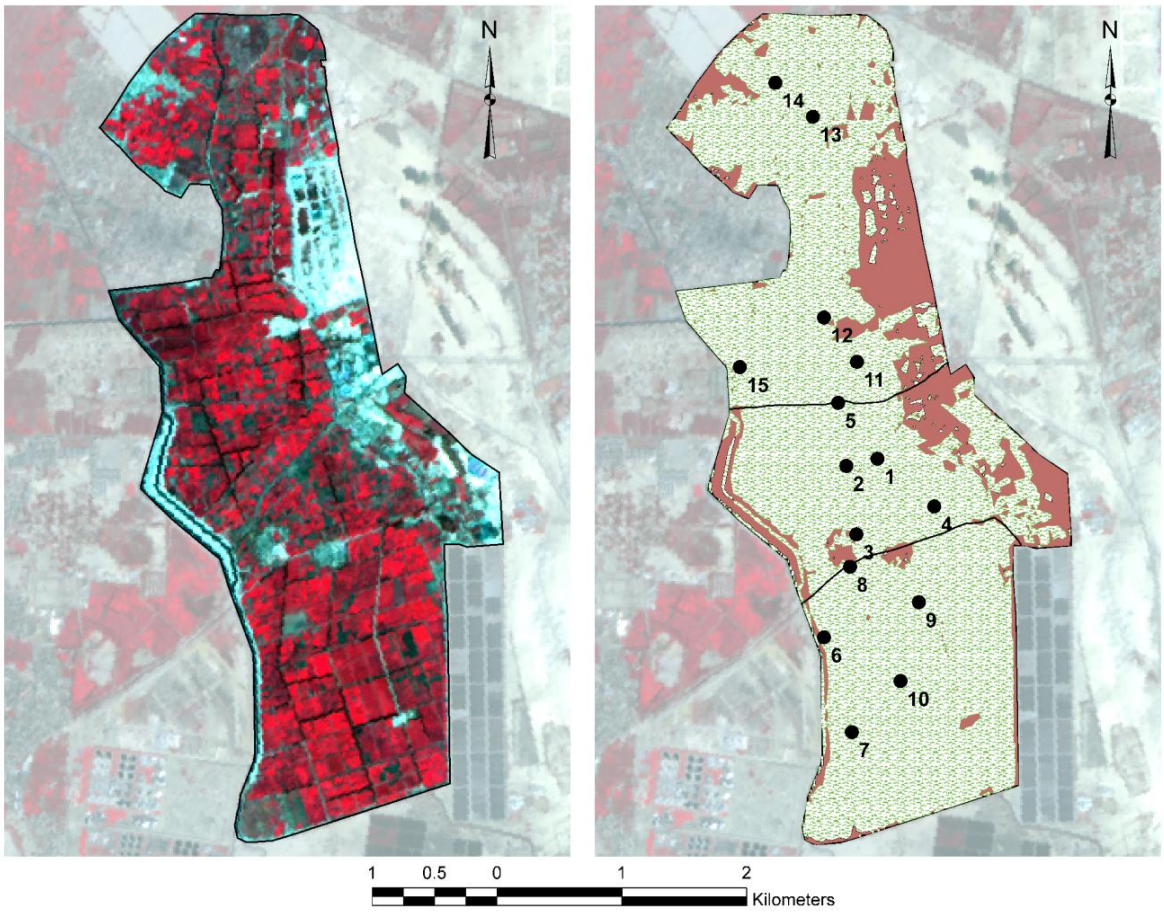

Fig. 8.1. Geo-spatial distribution of soil profiles in the study area; a) spaceborne thermal emission and reflection radiometer (ASTER) image for the study area, and b) unsupervised classified image with sampling locations among *Fondi*, *Bahari*, and *Kabli* sections.

8.2.2 Sampling and Laboratory Analyses

Based on the unsupervised classification for Advanced Spaceborne Thermal Emission and Reflection Radiometer (ASTER) image (Fig. 8.1), surface and subsurface soil samples were collected from fifteen locations. Each soil Sample location was geo-referenced using global positioning system (GPS). The geo-spatial distribution of the collected soil profiles is shown in

Fig. 8.1. In addition, water samples from the wastewater applied to each section was carried out. The soil samples were air-dried, grounded, and passed through a 2 mm sieve then stored for further analysis. Chemical properties were measured (Soil Survey Staff, 2004; Pansu and Gautheyrou, 2006). In addition, total carbonates equivalent was determined by Collin's calcimeterand (Loeppert and Suarez, 1996). Available trace elements (Cu, Cd, Pb, and Ni) were determined by ammonium bicarbonate-diethylene triamine pentaacetic acid (AB-DTPA) method according to Soltanpour and Workman (1979). Total trace elements (Cu, Cd, Pb, and Ni) were determined by digestion in a mixture of HNO_3 and $HClO_4$ acids (Jones, 2001). Heavy metals were measured by atomic absorption spectrometry using Varian flame atomic absorption. Classification of soil salinity, organic matter (OM) content, and cation exchange capacity (CEC) were achieved according to the International Center for Agricultural Research in the Dry Area – ICARDA (Ryan et al., 2001).

Wastewater samples were filtered and analyzed according to Standard Methods for the Examination of Water and Wastewater (Clesceri et al., 1998). The pH was measured by pH-meter (Jenway, pH-meter model 3305); and the water salinity (dS m^{-1}) was measured by Jenway conductivity meter model 4310. Complex-metric EDTA titration was employed for determining the concentration of soluble calcium (Ca) and magnesium (Mg). Soluble sodium (Na) and potassium (K) were determined using flame photometer (Corning 400). Soluble carbonate (CO_3^{-2}) and bicarbonate (HCO_3^-) were determined by titration with sulfuric acid, while silver nitrate was used to determine soluble chloride. Varian flame atomic absorption was used for measuring Pb, Cd, Cu, and Ni.

8.2.3 Spatial Analyses

The ASTER image, which was acquired in 2005, was used in order to distinguish between the urban and cultivated regions in the study area. The spatial resolution of this image

was 15×15 m^2. The image preprocessing included: geometric correction, subset the area of interest, and image classification using both unsupervised and supervised techniques. Spatial analyst extension under ArcGIS 9.2 software (ESRI, 2001) was used to produce the final classified image.

Attribute data were maintained in database management system represented by attribute tables in ArcMap. Maps were layered into a group of features each of them comprises a homogenous dataset. This step yields a digital vector database for the study area. Interpolation is used to convert data from point observations to continuous fields. Inverse distance weighting (IDW) module (Burrough and McDonnell, 1998) was used to interpolate the different soil attributes (soil chemical properties and heavy metals analyses) to produce the geo-spatial distribution maps. Spatial analyst extension was used to reclassify the interpolated maps in order to group the continuous data into contiguous units, and then calculate the areas of each polygon.

8.3 Results and Discussion

Image classification analysis of the region is shown in Fig. 8.1. Some 83 % of the entire region is cultivated lands of some 1100 hectares, the remaining represents urban land use. The geo-spatial distribution of soil properties and heavy metal concentrations are based on the cultivated area only. Figure 8.1 represents the geographical location of the three secotions with their physical boundaries.

8.3.1 Irrigation Water Characteristics

Chemical analysis of the irrigation wastewaters samples for the three sections are given in Table 8.1. These concentrations are compared to the permissible levels of heavy metals for irrigation as reported by Ayers and Westcot (1985), ECP 501 (2005); EEAA (1995); USEPA (2004), and the World Health Organization (2006).

Table 8.1. The mean characteristics of irrigation water sources in *Elgabal Elasfar* farm for north (*Fondi*), middle (*Bahari*), and south (*Kablia*) sections.

Location	EC ($dS\ m^{-1}$)	pH	Ca^{2}	Mg^{2+}	Na^{+}	K^{+}	Cl^{-}	CO_3^{-2}	HCO_3^{-}	Pb^{2+}	Cd^{2+}	Cu^{2+}	Ni^{2+}
			---------- (meq L^{-1})----------							---------- (mg L^{-1})----------			
Fondi	0.79	7.07	1.4	1.8	1.87	0.41	2.0	0.0	4.6	Nd	Nd	0.005	0.004
Bahari	0.78	6.83	1.2	2.0	1.82	0.39	2.0	0.0	4.9	0.02	Nd	0.022	0.015
Kablia	0.68	7.23	1.2	1.8	2.02	0.34	1.9	0.0	2.9	0.01	Nd	0.010	0.009
Recommended maximum concentrations of trace elements in irrigation water (Ayers and Westcot, 1985)										5.0	0.01	0.20	0.20
EEAA, 1995., Executive Regulation of Egyptian law 4/1994										0.5	0.05	1.50	0.10
Egyptian code of practice for the reuse of treated wastewater for agricultural purposes (ECP 501, 2005)										5.0	0.01	0.20	0.20
WHO Guidelines for the Safe Use of Wastewater, Excreta and Greywater (WHO,2006)										5.0	0.01	0.20	0.20

Nd: Not detected

All irrigation waters were slightly acidic to slightly alkaline with lowest pH values in the middle section that received a mix of treated and untreated wastewater. In the meantime, minmum salinity levels were observed for south section which receive treated wastewater. For all wasterwaters, the concentrations of Pb, Cd, Cu, and Ni were less than the permissible level for irrigation (see Table 8.1). Moreover, the highest heavy metals concentrations were observed for the middle section and the lowest for the north section. The decrease of the heavy metals concentration for the north section may be attributed to natural attenuation processes through movement from the middle section where mixing of treated and untreated waters take place.

8.3.2 Spatial Variability of Soil Properties

The geo-spatial distribution of surface soil pH, EC, OM, and CEC is shown in Fig. 8.2. The variability of soil properties, because of the different wastewater treatments, is demonstrated in the geo-spatial maps for the entire region. The pH of the surface soil did not exceed 7.7 in the entire region. Lowest pH levels (6.58 to 7.0) were found in the middle section. The results in Fig. 8.2 also indicated the acreage of none saline soils (salinity < 1.2 dS m^{-1}) represented 73.2% of the study area whereas 23.0% of the area may be considered slightly saline soils (1.2-2.4 dS m^{-1}). This salinity was observed by Friedel et al. (2000) who reported that continued wastewater irrigation for 80 years resulted in increased soil salinity. Moreover, Xu et al. (2010) reported that long term (20-years) wastewater irrigation significantly lowered soil pH in the soil to a depth of 140 cm. The subsurface soils exhibited pH of 7.53 and salinity of 0.9 dS m^{-1} in average whereas the respective value for the surface soils were 7.03 and 1.17 dS m^{-1}, respectively (see Table 8.2). Moreover, Elgala et al. (2003) found that the impact in of continued sewage water irrigation for 80 years in *Elgabal Elasfar* resulted in lower pH and higher salinity in surface soils when compared to subsurface soils.

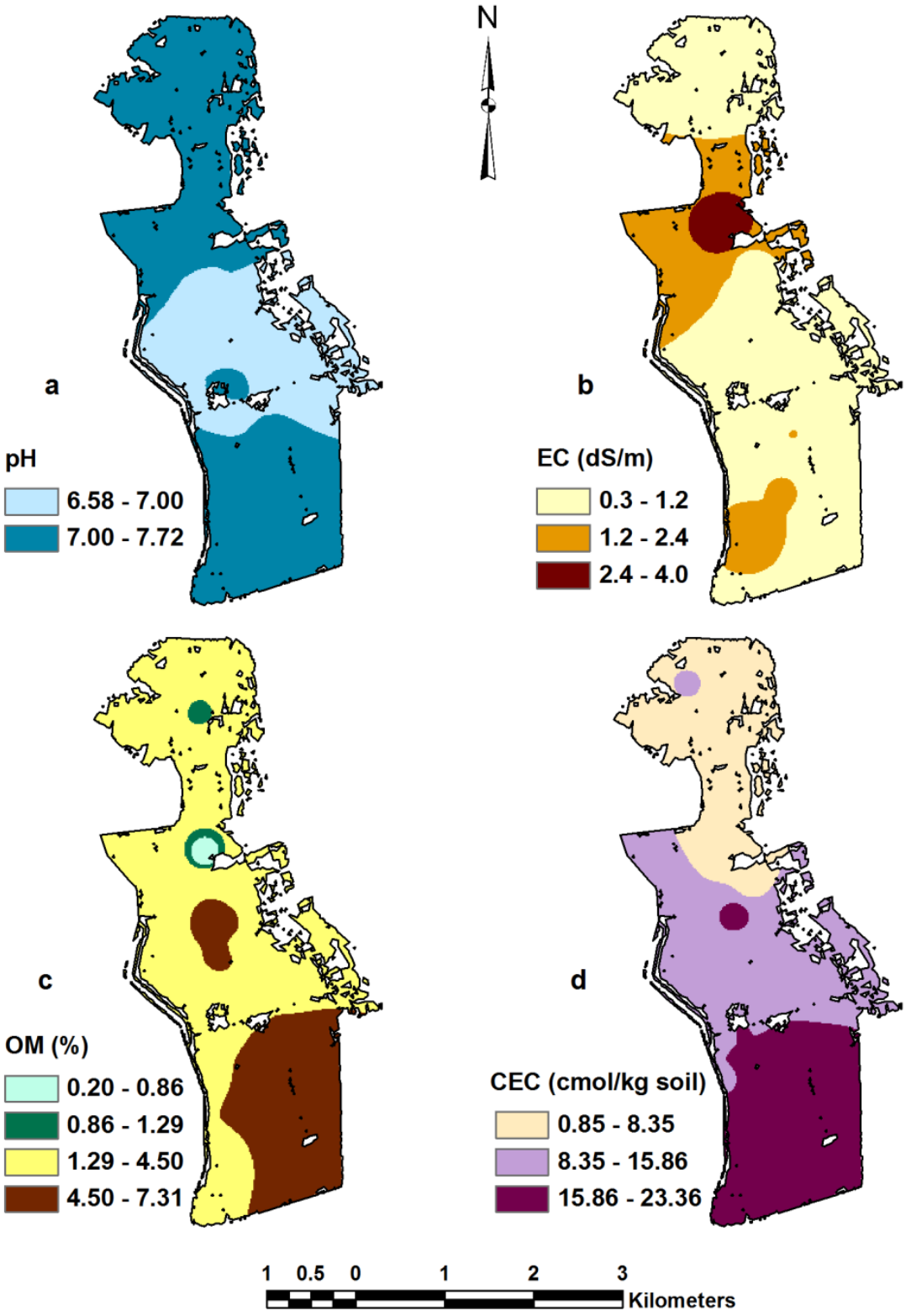

Fig. 8.2. Geo-spatial distribution of soil properties; a) calinity classes, b) pH, c) organic matter (OM), and d) cation exchange capacity (CEC).

Table 8.2. The main statistical parameters for physiochemical characteristics of surface and subsurface soil samples for 15 sampling locations.

		pH	ECe	CEC	OM	Pb		Cd		Ni		Cu	
						Available	Total	Available	Total	Available	Total	Available	Total
		1:2.5	dS m^{-1}	$cmol_c/kg$	%	(mg kg^{-1})							
Surface	Minimum	6.58	0.39	0.84	0.20	0.34	7.00	0.00	0.50	0.00	0.20	0.93	1.60
	Maximum	7.72	3.98	23.36	7.31	35.00	237.00	0.29	3.50	4.15	31.30	42.30	120.50
	Standard deviation	0.28	0.89	6.73	1.98	12.44	57.57	0.09	0.96	1.23	9.52	14.12	38.89
	Average	7.03	1.17	12.75	3.66	14.57	88.73	0.12	2.09	1.49	11.91	22.24	55.14
Subsurface	Minimum	6.67	0.33	0.51	0.00	0.20	1.00	0.00	0.60	0.00	0.30	0.51	1.20
	Maximum	8.97	4.41	16.10	1.64	7.32	39.00	0.07	2.80	3.95	13.50	18.60	40.50
	Standard deviation	0.66	1.00	4.99	0.49	1.92	10.19	0.03	0.69	0.95	5.14	5.80	12.30
	Average	7.53	0.90	5.30	0.57	2.07	10.27	0.02	1.63	0.63	4.73	6.77	14.59

The results in Fig. 8.2 indicated that 98% of the study area contained adequate contents of OM in the surface soil layer. Elevated OM is considered a positive consequence of long term wastewater irrigation that enhance soil physical and chemical soil properties, e.g. increased soil-moisture retention and CEC. The south section which received treated wastewater exhibited highest OM of 4.5 to 7.3% (Adequate II class). The middle and north sections which received a mix of untreated and treated wastewater exhibited OM level of 1.29 to 4.5% (Adequate I class). A consequence of such high OM in the surface layer, values for the CEC ranged from 15.86 to 23.36 $cmol_c\ kg^{-1}$ in the south section and lower values for the middle and north sections (see Fig. 8.2). These OM and CEC values are considerably higher than expected of sandy soils in arid and semi-arid regions. Therefore one attributes the long term utilization of municipal wastes increased the OM and CEC of surface soil. Elgala et al. (2003) showed that the upper layer of *Elgabal Elasfar* exhibited 30 fold increase relative to adjacent soils irrigated with Nile river water. Numerous studies reported increases OM and exchangeable cations as a result of wastewater application (Kiziloglu et al., 2008; Friedel et al., 2000; Xu et al., 2010).

8.3.3 Spatial Variability of Pb, Cd, Cu, and Ni Cationic Metals

Figures 8.3 – 8.6 demonstrate the geo-spatial distributions of Pb, Cd, Cu and Ni in surface soils of the entire region. In Figure 8.3, total Pb concentrations exhibited clear differences among the three sections and represent clear evidence of the influence of long-term use of wastewater on Pb accumulation in soils. The results indicated that soils contaminated with Pb in the soil surface are predominantly in the south section with total Pb concentration more than 100 mg kg^{-1}. In contrast, the recently cultivated north section exhibited lowest total Pb ranging from 7 to 50 mg kg^{-1}. According to Kabata-Pendias and Pendias (2001) soil Pb concentration ranging from 100 to 500 mg kg^{-1} is considered as excessive. Additionally, the spatial variability of available Pb (AB-DTPA extractable) indicated more than 80 % of the area

contained a concentration ranged from 0.5 to 20 mg kg^{-1} (see Fig. 8.3). Maiz et al. (2000) found that the available mobile (extracted using 0.01 mol L^{-1} $CaCl_2$) and mobilizeable (extracted using 5 mmol L^{-1} DTPA) fractions accounted for 14% of total Pb which is in agreement of the results presented here.

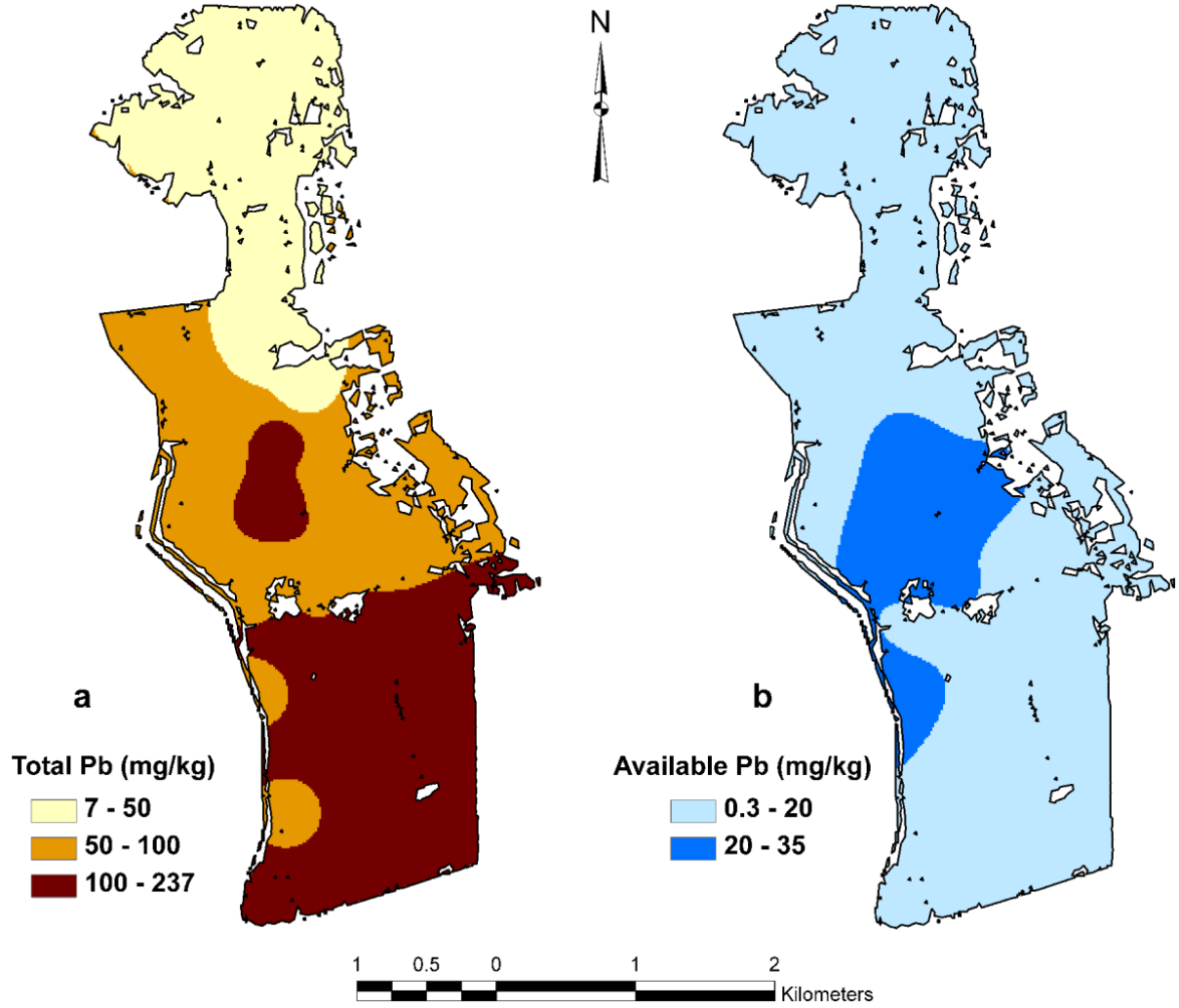

Fig.8.3. Geo-spatial distribution of (a) total and (b) available Pb (mg kg^{-1}).

Geo-spatial distribution for Cd in the soil surface is shown in Fig. 8.4 and indicated less spatial variability when compared to Pb of Fig. 8.3. In fact, total Cd concentration ranged from 0.8 to 3.0 mg kg^{-1} for 90% of the study area. In contrast, highest available Cd levels were found in the older middle and south sections. In the newest north section, which was cultivated since

1960, lowest available Cd levels were observed. We should also emphasize that these levels of total Cd in the soil surface presented in Fig. 8.4 were considerably higher than average values for uncontaminated soils (0.22 to 0.51 mg kg^{-1}) as reported by Kabata-Pendias and Mukherjee (2007). Mapanda et al. (2005) found that elevated Cd concentration (0.5 to 3.4 mg kg^{-1}) in soils irrigated with wastewater for more than10 years which are consistent with the range of Cd of Fig. 8.4.

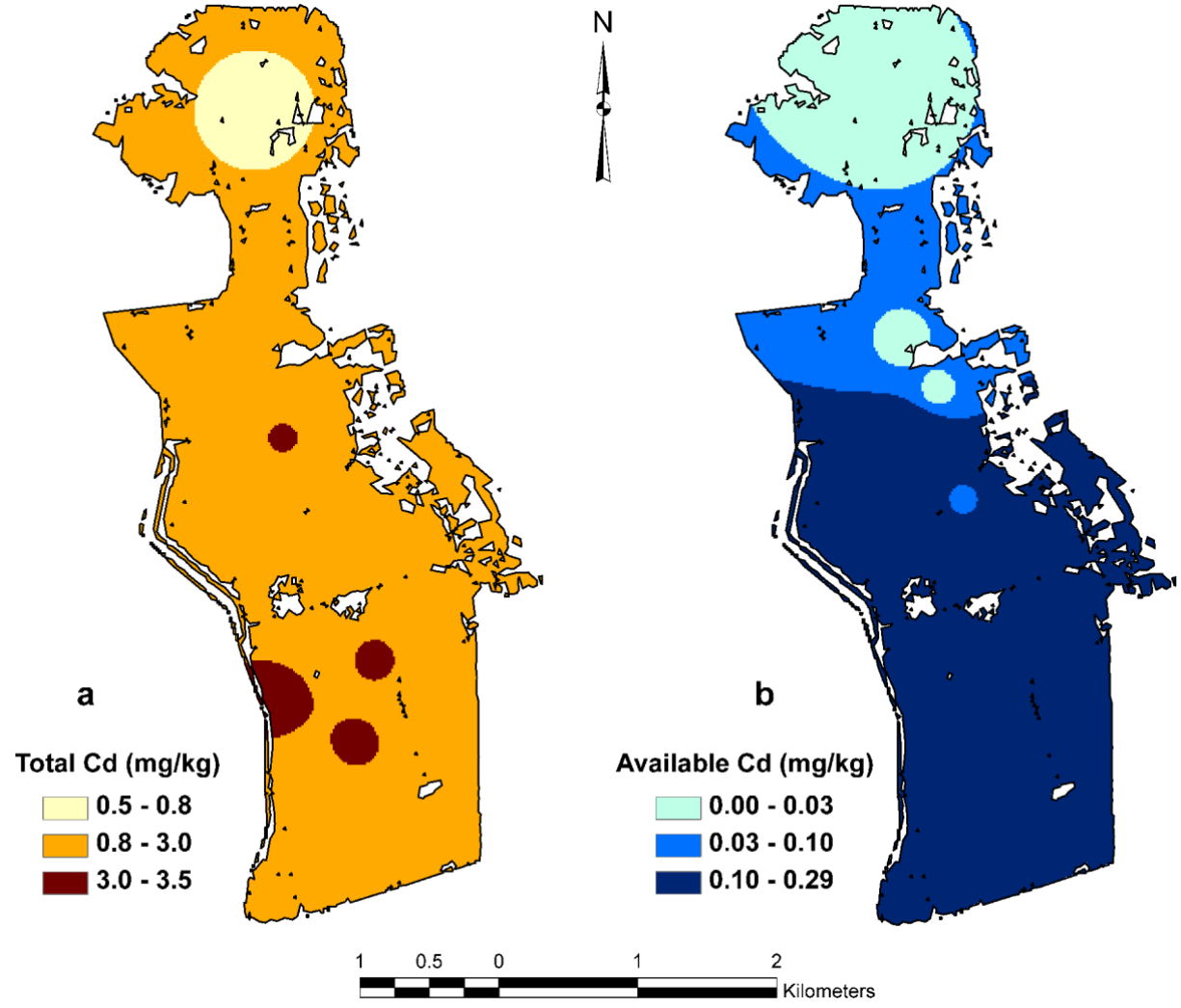

Fig. 8.4. Geo-spatial distribution of (a) total and (b) available Cd (mg kg^{-1}).

For Cu, the geo-spatial distribution shown in Fig. 8.5 indicated that highest levels in surface soils were observed in the middle and south sections. This is consistent with Pb and

somewhat Cd. Specifically, the results reveal that 64% of the area contained total Cu ranging from 50.0 to 120.5 mg/kg with lowest Cu levels in the north section. The geo-distribution map in Fig. 8.5 also indicated high concentrations of available Cu were predominantly in the soils of the middle and south sections. Moreover, the available Cu in these soils represented high percentage of the total Cu measured in these soils. Specifically, the available Cu represented 24 to 78% of total Cu with an average of 46.6%. This available fraction for Cu is substantial higher than that for Pb and Cd discussed previously. Moreover, these Cu concentrations were considerably higher than the average for uncontaminated soils of 20 to 30 mg Kg^{-1} as reported by Alloway (1995).

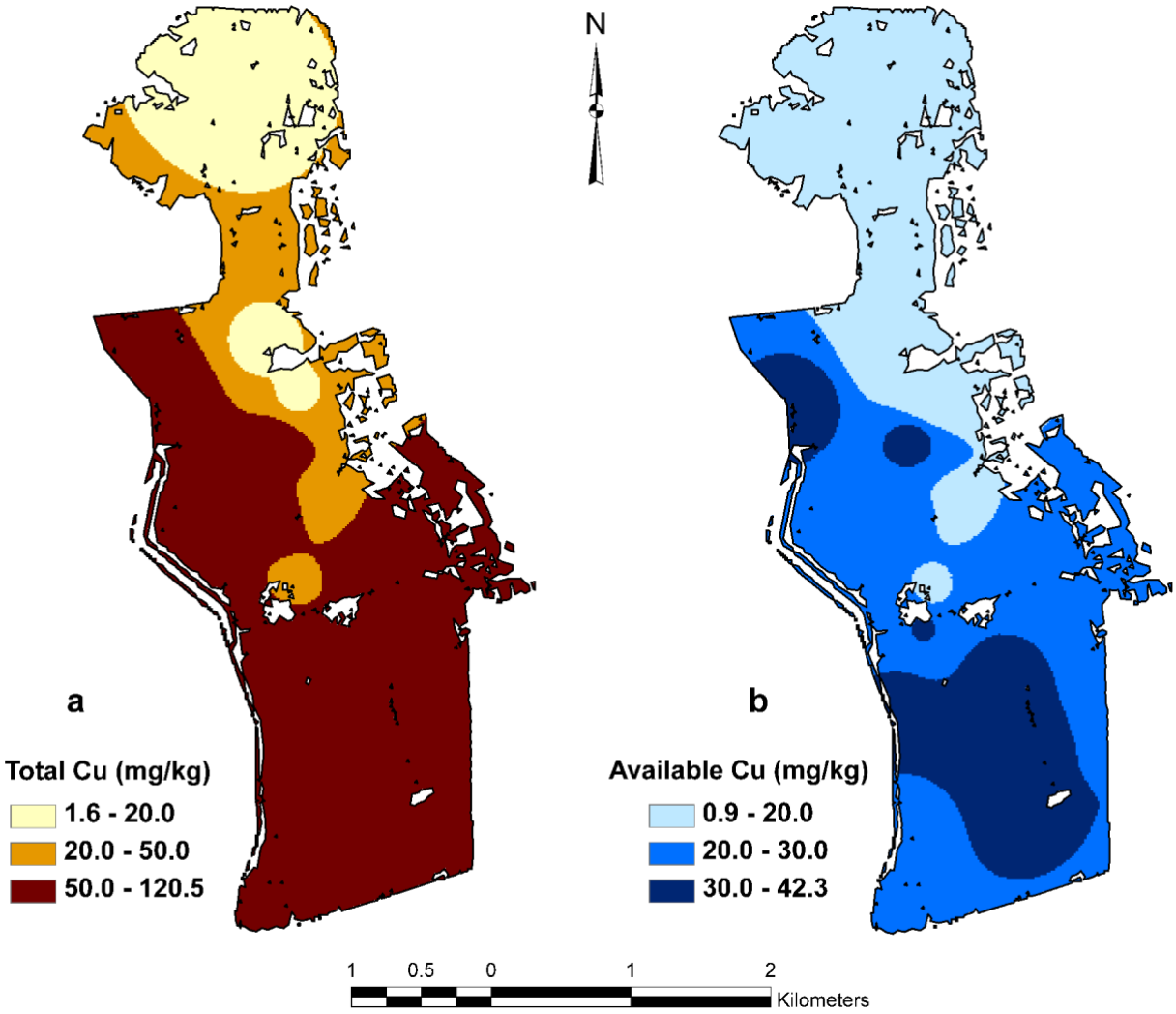

Fig. 8.5. Geo-spatial distribution of (a) total and (b) available Cu (mg kg^{-1}).

For Ni, the geo-spatial distribution of total Ni in surface soils shown in Fig. 8.6 followed similar patterns as that for the Pb and Cu. Results indicated that total Ni concentration in surface soils ranged from 0.2 mg kg^{-1} in the north section to 31.3 mg kg^{-1} in south section. Total Ni level was less than the maximum tolerable soil concentration, 107 mg kg^{-1}, reported by World Health Organization, WHO (2006). The spatial variability of AB-DTPA extractable Ni for the surface soils demonstrated that Ni concentration ranged from 1.38 to 2.70 mg kg^{-1} for 71% of the study area (Fig. 8.6). For the subsurface layer, the total concentration ranged from 0.3 to 13.5 mg kg^{-1} while the amounts of AB-DTPA extractable Ni were less than 3.95 mg kg^{-1} (see Table 8.2). Moreover, results revealed that the available Ni fraction represented 16.5% of the total in average.

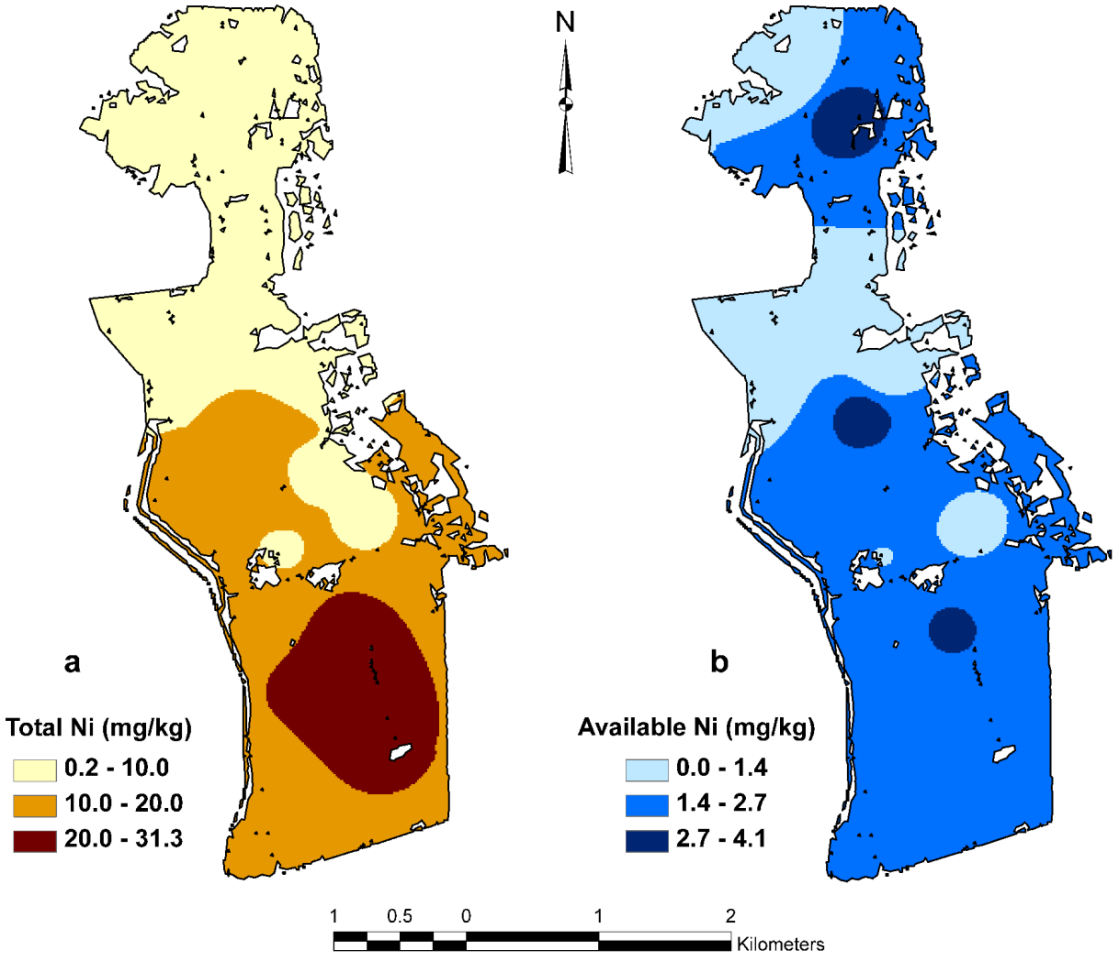

Fig. 8.6. Geo-spatial distribution of (a) total and (b) available Ni (mg kg^{-1}).

8.3.4 Distribution with Soil Depth

To assess the potential transfer or mobility of heavy metals to lower soil depths, soil samples were collected at 2-3 different depths (up to 85 cm) for all 15 locations. Results from sampling locations 2, 8, 10, and 13 of Fig. 8.1 representing the three different sections of the study region are given in Table 8.2. These results indicated that the surface and subsurface soil depths were neutral or acidic and low $CaCO_3$ content. However, high OM and CEC were observed for the surface soil. The results also illustrated the restricted mobility of Pb to lower soil depth whereas moderate mobility for Cu and Ni was observed. Cadmium exhibited highest potential mobility among all heavy metals. These differences in mobility and affinity of these heavy metals in soils are consistent with other studies (Adriano, 2001; Kabata-Pendias and Mukherjee, 2007). An example of the distribution of total and available heavy metals versus depth is given in Fig. 8.7. These results are for sampling location 5 in the middle section of the region (see Fig. 8.1). The concentrations versus depth illustrated the differences of the motilities of heavy metals in this soil. Cadmium results indicated extensive mobility to lower depth and potential hazard for soil contamination to great depths. In contrast, Pb exhibited high retention and limited mobility with soil depth.

Results of heavy metal distribution in the soil profile from sampling location 8 (in the south section) is presented in Fig. 8.8 and represents a special case of a buried soil profile. This is due to the high concentrations observed for all heavy metals in the third layer (30-50cm depth). In fact high levels for all heavy metals, especially Cd, were observed for all depth up to 115 cm. It is likely that past human activities such as earth movement and leveling resulted in the addition of uncontaminated soil material on top of the soil surface. It is also likely that the new soil layer (≈ 30cm) was added perhaps 4-6 decades ago and not mixed with the existing surface soil.

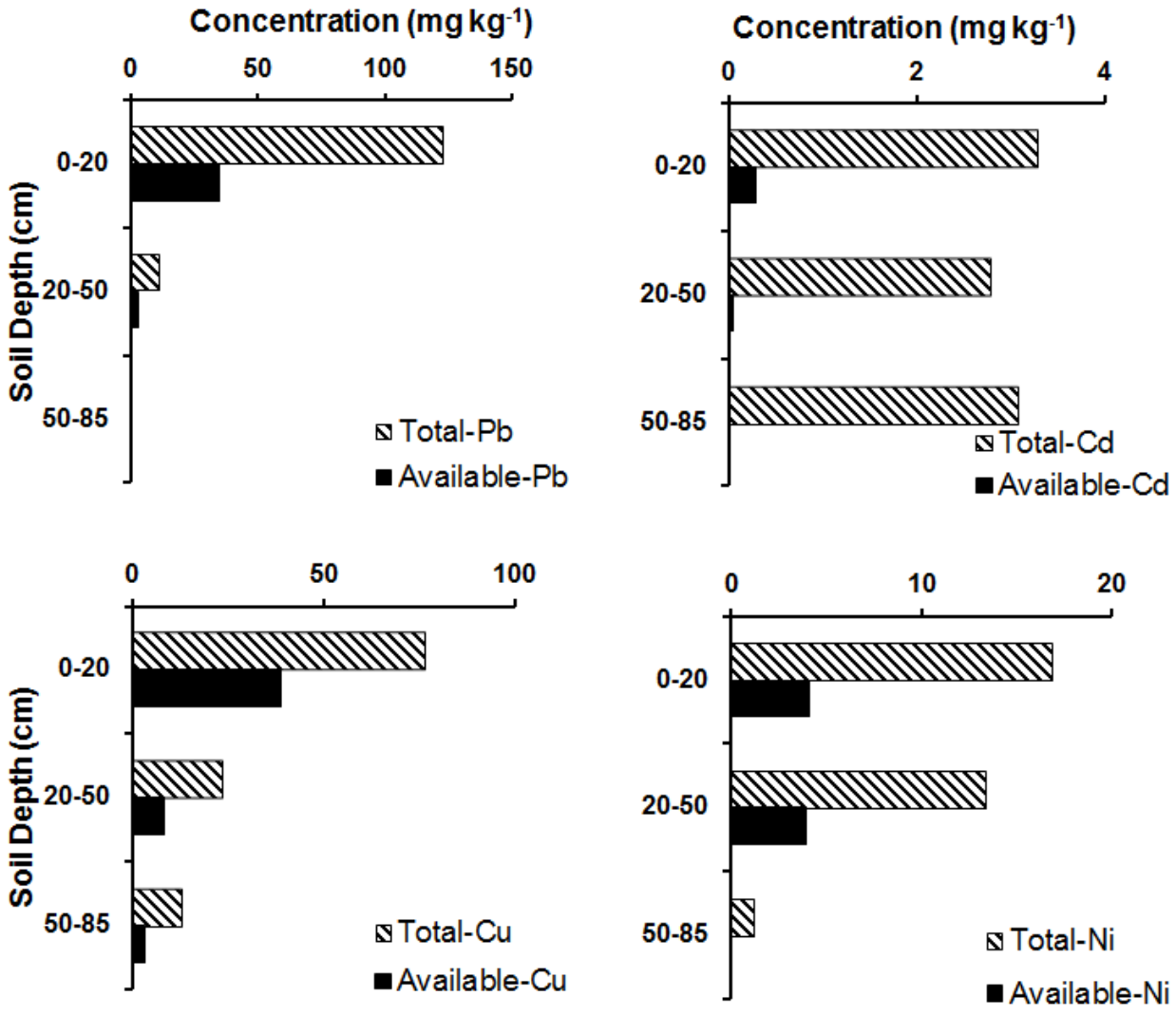

Fig. 8.7. Distribution of Pb, Cd, Cu, and Ni versus soil profiles depth (cm) for location 5.

This is evident by the high OM in the third layer (see Table 8.3). As outlined under Material and Methods, these high OM contents were anticipated due to the historical raw sewage sludge application in this study area (El-hassanin et al. 1993, Abdel-sabour et al, 1996). As shown in Fig. 8.8, concentrations of Pb, Ni, and Cu for the buried layer exceeded that of surface layer by 204%, 143%, and 253%, respectively. The only exception was Cd which illustrated its high mobility when compared to the other metals and is consistent with Cd results shown in Fig 8.7.

Table 8.3. Soil analyses of samples from sampling locations 2, 8, 10, and 13 in the study area shown in Fig. 8.1.

Location	Depth	pH	EC_e	CEC	OM	$CaCO_3$	Pb		Cd		Ni		Cu	
							Available	Total	Available	Total	Available	Total	Available	Total
		1:2.5	dS m^{-1}	$cmol_c/kg$	----- % -----		---------- (mg kg^{-1}) ----------							
North (13)	0-35	7.05	0.713	1.23	1.09	n.d¶	0.44	27.0	n.d	0.5	0.37	2.20	2.05	6.4
	35-60	7.27	0.51	1.36	0.14	0.09	0.42	2.0	n.d	0.7	0.66	2.20	1.52	2.8
Middle (2)	0-20	6.85	0.832	13.09	4.85	0.18	22.50	127.0	0.18	2.2	2.37	17.50	22.60	68.6
	20-45	7.29	0.672	8.35	1.09	0.30	3.02	5.0	0.06	1.7	0.50	1.30	6.74	11.6
South (10)	0-25	7.27	1.25	22.36	6.22	0.16	6.72	237.0	0.20	3.1	2.21	31.30	36.20	112.4
	25-50	7.56	0.575	10.93	0.82	0.23	0.92	12.0	0.07	1.8	0.68	11.70	18.32	40.5
South (8)	0-30	6.87	0.665	16.1	3.62	0.14	14.26	105.0	0.17	2.7	1.55	16.50	31.30	78.8
	30-40	6.7	0.49	4.64	1.23	0.14	4.32	13.0	0.04	1.8	0.40	1.10	6.46	12.7
	40-55	7.25	0.54	14.67	3.28	0.11	15.28	214.0	0.34	2.7	2.43	23.60	102.90	199.7
	55-75	7.47	0.51	3.57	0.07	0.09	1.00	2.0	n.d	1.4	0.03	5.50	12.62	23.8
	75-115	7.57	0.399	5.59	n.d	0.09	n.d	n.d	n.d	1.5	3.77	5.40	13.48	32.4

¶: Not detected.

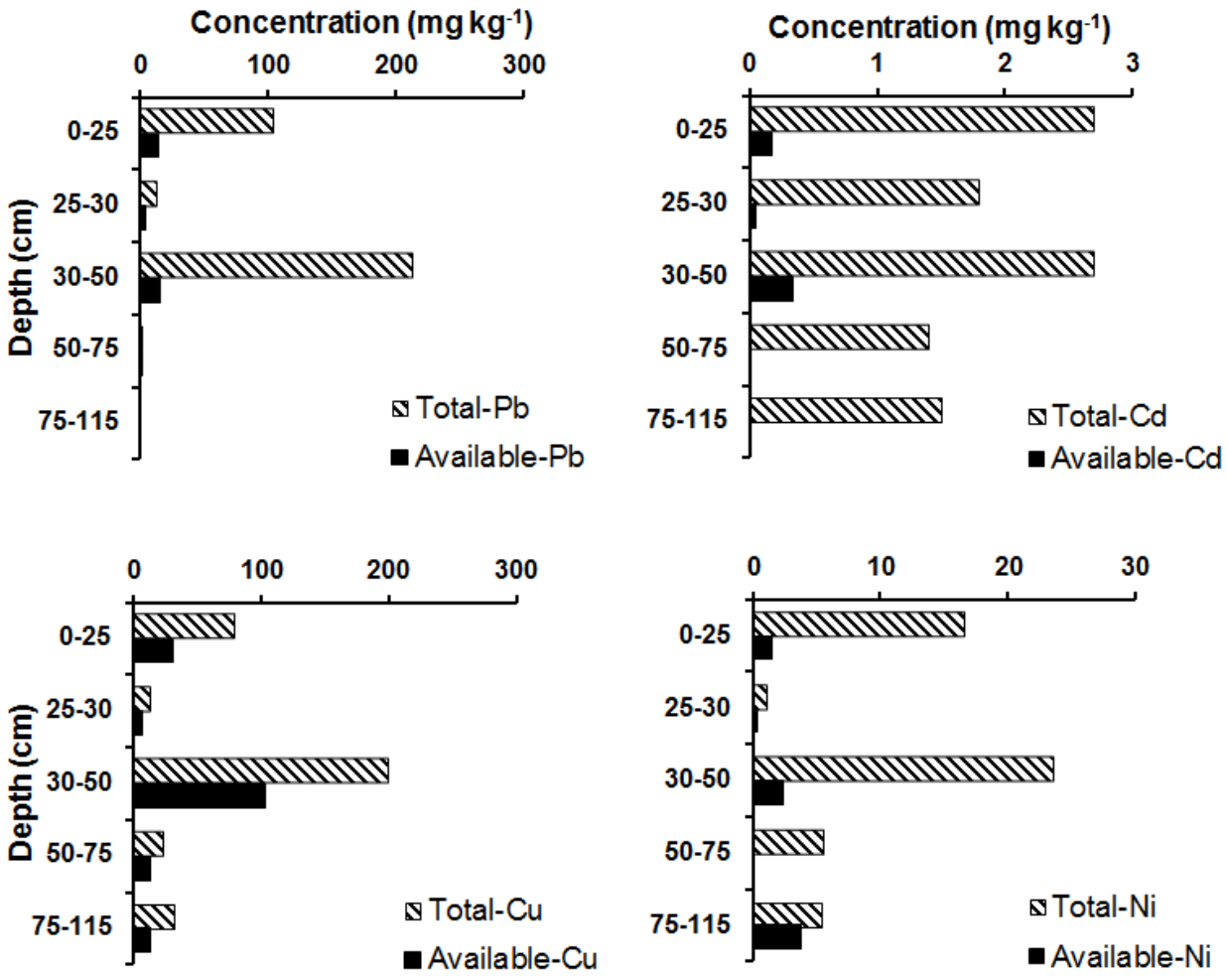

Fig. 8.8. Distribution of Pb, Cd, Cu, and Ni versus soil profiles depth (cm) for the buried profile, location 8.

8.4 Conclusions

Heavy metal analysis of irrigation water samples indicated that the water is considered safe to use for irrigation. Spatial variability analysis of heavy metals of the *Elgabal Elasfar* farm soil revealed that Pb, Cu, and Ni have a high affinity for the surface soil layers that had high OM content. Cadmium results showed a roughly homogeneous distribution with soil depth. The relative high mobility of Cd signified a risk on the ground water in this area. The accumulation of Pb and Cu in the surface layer was higher than the maximum tolerable soil concentrations based on human health protection in the southern part of the study area. On the other hand, total

Ni content was within the permissible level in most of the study area. The total Cd content in the surface layer represented a critical level for soil contamination. The impact of long term accumulation and spatial distribution illustrate the need for continued monitoring of the levels of heavy metals in the soil profile of the region for future management strategies.

8.5 References

Abdel-sabour, M.F., A.S. Ismail, and H. Abou Naga. 1996. Environmental impact of Cairo sewage effluent on El-gabal El-Asfar farm. Egypt. J. Soil Sci. 36: 329-342.

Abdel-Shafy, H.I. and M.F. Abdel-Sabour. (2006). Wastewater reuse for irrigation on the desert sandy soil of Egypt: long-term effect. *In*: Hlavinek et al., eds. Integrated Urban Water Resources Management. Springer Publisher, the Netherlands, pp. 301–312.

Abu-Zeid, K.M. 1998. Recent trends and developments: Reuse of wastewater in agriculture. Environ Manag Health. 2:79-89.

Adriano, D.C. 2001. Trace elements in terrestrial environments: biogeochemistry, bioavailability and risk of metals. Second edition. Springer, New York.

Alloway, B.J. 1995. The origins of heavy metals in soils. In: B.J. Alloway (Ed.), Heavy Metals in Soils. Blackie Academic and Professional Publ., New York.

Ayers, R.S., and Westcot. W.1985. Water Quality for Agriculture. Irrigation and Drainage Paper 29 (rev.1). FAO, Rome, Italy.

Badawy, S.H., and M.I.D. Helal, 2002. Chemical forms and movement of heavy metals in sandy soils irrigated with sewage effluent. Egypt. J. Soil Sci.42, No. 3, pp. 417-434.

Bixio, D., C. Thoeye, J. De Koning, D. Joksimovic, D. Savic, T. Wintgens, and T. Melin. 2006. Wastewater reuse in Europe. Desalination. 187: 89-101.

Burrough, P. A., and R. A. McDonnell. 1998. Principles of Geographical Information Systems. Spatial Information Systems and Geostatistics, Oxford University Press.

Carr, G., R.B. Potter, and S. Nortcliff. 2011. Water reuse for irrigation in Jordan: perceptions of water quality among farmers. Agric. Water Manage. 98:847-854.

Chen, Y., C. Wang, and Z. Wang. 2005. Residues and source identification of persistent organic pollutants in farmland soils irrigated by effluents from biological treatment plants. Environ. Int. 31:778–783.

Clesceri, L.S., A.E. Greenberg, and A.D. Eaton (ed.). 1998. Standard methods for the examination of water and wastewater, 20th ed. American Public Health Association (APHA), American Water Works Association, Water Environment Federation, Washington, DC.

ECP 501. 2005. Egyptian code of practice for the reuse of treated wastewater for agricultural purposes. The Ministry of Housing Utilities and Urban Communities. (*In Arabic*)

EEAA, 1995. Executive Regulation of law 4/1994: legislation-controlling disposal of wastewater. Egyptian Environmental Protection Agency.

Elgala A.M., M.A.O. Elsharawy, and M.M. Elbordiny, 2003. Impact of sewage water used for irrigation on soil characteristics and heavy metals composition of some grown crops. Egypt. J. Soil Sci.43, No. 3. pp 405-420.

El-Hassanin, A.S., T.M. Labib, and A.T. Dobal. 1993. Potential Pb, Cd, Zn and B contamination of sandy soils after different irrigation periods with sewage effluent. Water Air Soil Pollut. 66:239–249.

El-Nennah M., T. El-kobbia, A. Shehata, and I. EI-Gamal. 1982. Effect of irrigation of loamy sand soil by sewage effluents on its content of some nutrients and heavy metals. Plant Soil. 65:289-292.

ESRI. 2001. Arc-GIS 9.3 Spatial Analyst. Redlands, CA, USA.

Facchinelli, A., E. Sacchi, and L. Mallen. 2001. Multivariate statistical and GIS-based approach to identify heavy metal sources in soils. Environ. Pollut. 114:313–324.

FAO, 1993. CLIMWAT for CROPWAT: A climatic database for irrigation planning and management. FAO Irrigation and Drainage Paper 49. FAO, Rome, Italy.

Friedel, J.K., T. Langer, C. Siebe, and K. Stahr. 2000. Effects of long-term waste water irrigation on soil organic matter, soil microbial biomass and its activities in central Mexico. Biol. Fertil. Soils 31:414-421.

Hamilton, A.J., F. Stagnitti, X. Xiong, S.L. Kreidl, K.K. Benke, and P. Maher. 2007. Wastewater irrigation: The state of play. Vadose Zone J. 6:823–840.

Jones, J.B. Jr. 2001. Laboratory Guide for Conducting Soil Tests and Plant Analysis. CRC Press. Boca Raton, FL.

Kabata-Pendias A, A. B. Mukherjee. 2007. Trace elements from soil to human. Heidelberg, Germany: Springer Verlag; 550 pp.

Kabata-Pendias A, and H. Pendias. 2001. Trace elements in soils and plants, 3rd ed., CRC Press, Boca Raton, FL.

Kiziloglu, F.M., M. Turan, U. Sahin, Y. Kuslu, A. Dursun. 2008. Effects of untreated and treated wastewater irrigation on some chemical properties of cauliflower (Brassica olerecea L. var. botrytis) and red cabbage (Brassica olerecea L. var. rubra) grown on calcareous soil in Turkey. Agric. Water Manage. 95:716-724.

Liu W, J. Zhao, Z. Ouyang, L. Söderlund, and G. Liu. 2005. Impacts of sewage irrigation on heavy metal distribution and contamination in Beijing, China. Environ. Int. 31:805-812.

Loeppert, R.H. and D.L. Suarez. 1996. Carbonate and gypsum. p. 437–474. In D.L. Sparks et al. (ed.) Methods of soil analysis. Part 3. 3rd ed. SSSA Book Ser. 5. SSSA, Madison, WI.

Maiz, I., I. Arambarri, R. Garcia, and E. Millan. 2000. Evaluation of heavy metal availability in polluted soils by two sequential extraction procedures using factor analysis. Environ. Pollut.110:3-9.

Mapanda, F., E.N. Mangwayana, J. Nyamangara, and K.E. Giller. 2005. The effect of long-term irrigation using wastewater on heavy metal contents of soils under vegetables in Harare, Zimbabwe. Agric. Ecosyst. Environ. 107:151–165.

Mico, C., L. Recatala, M. Peris, and J. Sanchez. 2006. Assessing heavy metal sources in agricultural soils of an European Mediterranean area by multivariate analysis. Chemosphere 65:863–872.

O'Connor, G.A., H.A. Elliott, and R.K. Bastian. 2008. Degraded water reuse: An overview. J. Environ. Qual. 37:S-157–S-168.

Pansu M. and J. Gautheyrou. 2006. Handbook of Soil Analysis - Mineralogical, Organic and Inorganic Methods. Springer, 993 p., 183 illus.

Pescod, M.B. (1992) Wastewater treatment and use in agriculture. FAO Irrigation and Drainage Paper 47. Food and Agriculture Organization of the United Nations, Rome, Italy. 125 p.

Qadir, M., B.R. Sharma, A. Bruggeman, R. Choukr-Allah, and F. Karajeh. 2007. Non-conventional water resources and opportunities for water augmentation to achieve food security in water scarce countries. Agric. Water Manage. 87:2-22.

Qadir, M., D. Wichelns, L. Raschid-Sally, P.G. McCornick, P. Drechsel, A. Bahri, and P.S. Minhas. 2010. The challenges of wastewater irrigation in developing countries. Agric. Water Manage. 97:561-568.

Rattan, R.K., S.P. Datta, P.K. Chhonkar, K.Suribabu and A.K. Singh. 2005. Long term impact of irrigation with sewage effluents on heavy metal content in soils, crops and groundwater-a case study. Agric. Ecosys. Environ. 109:310-322.

Rutkowski, T., L. Raschid-Sally, and S. Buechler. 2007. Wastewater irrigation in the developing world-two case studies from the Kathmandu Valley in Nepal. Agric. Water Manage. 88: 83:91.

Ryan J, G Estefan, and A. Rashid. 2001.Soil and Plant Analysis Laboratory Manual. International Center for Agricultural Research in the Dry Areas (ICARDA), Aleppo, Syria. 172 pp.

Singh, K.P., D. Mohon, S. Sinha, and R. Dalwani. 2004. Impact assessment of treated/untreated wastewater toxicants discharge by sewage treatment plants on health, agricultural, and environmental quality in wastewater disposal area. Chemosphere 55:227–255.

Soil Survey Staff. 2004. Soil survey laboratory methods manual. Version No. 4.0. USDANRCS. Soil Survey Investigations Report No. 42. U.S. Govt. Print. Office, Washington, DC.

Soltanpour,P.N. and S. Workman.1979.Modification of the NH_4HCO_3-DTPA soil test to omit carbon black.Comm. Soil Sci. Plant Anal.10: 1411-1420.

Srinivasan, J. T. and V. R. Reddy. 2009. Impact of irrigation water quality on human health: a case study in India. Ecol. Econ. 68:2800-2807.

USEPA. 2004. Guidelines for Water Reuse. EPA /625/R-04/108, Washington, D.C.

van der Hoek, W., 2004. A framework for a global assessment of the extent of wastewater irrigation: the need for a common wastewater typology. In: Scott, C.A., Farunqui, N.I., Raschid-Sally, L. (Eds.), Wastewater Use in Irrigated Agriculture, Confronting the Livelihood and Environmental Realities. CAB International, International Water Management Institute, International Development Research Centre, Trowbridge, pp. 11–24.

WHO, World Health Organization. 2006. WHO Guidelines for the Safe Use of Wastewater, Excreta and Greywater. Vol. II, Wastewater Use in Agriculture, Geneva, world Health Organization.

Xu, J., L. Wu, A. C. Chang, Y. Zhang. 2010. Impact of long-term reclaimed wastewater irrigation on agricultural soils: a preliminary assessment. J. Hazard. Mater. 183:780–786.

CHAPTER 9. CONCLUSIONS

Modeling the reactivity and mobility of heavy metals in soils is necessary for managing and controlling contaminated sites. The mobility of Cd, Cu, Pb, and Sn in soils is affected by several rate-limiting processes including sorption and release reactions. For the Cd studies using alkaline, Bustan, and acidic, Windsor, soils, sorption and desorption isotherms exhibited strong nonlinearity. Breakthrough curves (BTCs) from column experiments indicated strong Cd retardation accompanied by slow release during leaching. The Cd was nearly immobile in the surface layer of a calcareous soil having 2.8% $CaCO_3$, whereas 20 and 30% of the applied Cd was mobile in the acidic soil and the subsurface alkaline soil with 1.2% $CaCO_3$. Sequential extractions of soils from the batch and column transport experiments indicated that Cd was associated mainly with carbonate in the alkaline soil and with exchangeable and oxide fractions in the acidic soil. A nonlinear multireaction and transport model (MRTM) successfully described adsorption with time as well as adsorption–desorption hysteresis. Also, the MRTM was capable of describing the Cd arrival time in the effluent and its concentration during leaching from the soil columns. Whereas, CXTFIT accounted for linear adsorption and provided adequate overall predictions of the BTCs, including the magnitude and time of peak arrival. However, effluent concentrations at advanced stages of leaching were underestimated.

For Cu studies, sorption isotherms were highly nonlinear with greater affinity for the alkaline soils compared to the acidic soil. Breakthrough results indicated that Cu mobility was strongly limited in the alkaline soil columns where <1% of applied Cu was recovered in the effluent solution. Such limited mobility was attributed to the presence of carbonates in the alkaline soils. Large Cu pulse inputs (≥50 pore volumes) resulted in higher mobility in the alkaline soils, with recoveries of 27 and 60% from the surface and subsurface soil columns, respectively. The respective recoveries from the acidic Windsor soil were 11.4 and 85.8%

associated with short and long pulse applications. The MRTM was successful in describing the BTCs for all soil columns except those from the surface alkaline soil. Based on model simulations, irreversible reactions were dominant for Cu in these alkaline soil columns. Improved predictions were obtained when a nonlinear kinetic irreversible reaction was incorporated into the MRTM model. Also, the use of a second-order two-site (SOTS) model provided a good description of the BTCs, with appearance of Cu in the effluent, concentration maxima, and the slow release during leaching were well predicted. The use of a SOTS model, which accounts for kinetic reversible and irreversible retention mechanisms, is recommended for predicting Cu transport in calcareous soils.

The study of Pb mobility in the calcareous soils revealed that more than 85 to 93% of the Pb applied was retained in the first 2 cm of the soil column although, Cd and Cu were introduced into the soil after Pb pulses. The studied soils exhibited a higher affinity for Pb>Cu>Cd. The results indicated that Cd posed a serious environmental problem attributed to the high mobility when Cd was applied into contaminated soils. The results indicated higher Cd mobility was observed when Pb contamination occurred prior to Cd introduction into the soil. Moreover, Cu in the Bustan surface soil depended not only on Cu loading but also the indigenous soil contamination with other heavy metals that occurred prior to Cu introduction.

Sorption batch and sequential extraction experiments were carried out using two acidic soils, Windsor and Olivier soils, to assess the retention and reactivity of Sn and Pb in the soils. Isotherm results exhibited highly nonlinear sorption for both heavy metals. Sn was almost completely sorbed; the contamination with Sn reduced sorption of Pb by both soils as evidenced by lowering the maximum sorption capacity. Moreover, Sn was nearly irreversible in the studied soils where more than 99% of the added Sn was retained by soil and did not desorb during the experimental time, whereas 3-15% and 13-28% of Pb was released for the Windsor and Olivier

soils, respectively. Tin was mainly associated with the oxide fraction while no exchangeable Sn was detected for both soils. Lead was associated with exchangeable, oxides and strongly bound fractions. The results revealed that the most susceptible Pb fraction for release from the studied soil was raised by increasing the input concentration of single Pb or by mixing it with Sn. This concentration-dependent release is consistent with the strong nonlinearity of Pb retention and implies that the mobility of Pb tends to increase as the inputs of Pb concentration increase. The use of a SOTS model that accounts for nonlinear equilibrium and kinetic reactions was capable of describing the kinetic behavior of Pb sorption and release in the Windsor and Olivier soils.

Miscible displacement experiments for Sn and Pb in Windsor and Olivier soils showed that Sn was not detected in the effluent solution except for a long pulse for the Windsor soil. Lead was detected in the solution after 20 and 38 pore volumes for the Windsor and Olivier soils, respectively. The presence of Sn in the soil solution reduced the sorption capacity of Pb by the soils and thus increased Pb mobility in the soils. Moreover, breakthrough results indicated incomplete recovery of Pb (81.4%) and Sn (32.4%) in reference sand columns.The second-order two-site model (SOTS) successfully described Pb mobility in both soils as well as Pb and Sn in the reference columns.

Based on a field study, spatial distributions and the accumulation among soil depth of lead (Pb), cadmium (Cd), copper (Cu), and nickels (Ni) as a consequence of irrigation with domestic wastewater were studied. Results revealed that 37.5% of the area had more than 100-Pb mg kg^{-1} and 63.9% of the area had a total amount of Cu ranging from 50.0 to 120.5 mg kg^{-1}. Total Cd represents the critical level content in the surface layer and ranged from 0.8 to 3.0 mg kg^{-1}. On the other hand the Ni content was within the permissible level in most of the study area. Moreover, Pb, Cu, and Ni had a high affinity to be retained in the surface soil layer whereas Cd results showed a homogeneous distribution with soil depth. The impact of time on accumulation

and spatial distribution of heavy metals indicated an urgent need for remediation and rational management.

APPENDIX. PERMISSION TO REPRINT

RightsLink

Copyright Clearance Center

Thank You For Your Order!

Dear Tamer Elbana,
Thank you for placing your order through Copyright Clearance Center's RightsLink service. ACSESS-Alliance of Crop, Soil, and Environmental Science Societies has partnered with RightsLink to license its content. This notice is a confirmation that your order was successful.
Your order details and publisher terms and conditions are available by clicking the link below:
http://s100.copyright.com/CustomerAdmin/PLF.jsp?ref=47b3398a-c14b-466b-8cc1-d719b1976257

Order Details
Licensee: Tamer A Elbana
License Date: Feb 11, 2013
License Number: 3085960434684
Publication: Soil Science Society of America Journal
Title: Cadmium Transport in Alkaline and Acidic Soils: Miscible Displacement Experiments
Type Of Use: Thesis/Dissertation
Total: 0.00 USD
To access your account, please visit https://myaccount.copyright.com.

Please note: Online payments are charged immediately after order confirmation; invoices are issued daily and are payable immediately upon receipt.
To ensure we are continuously improving our services, please take a moment to complete our customer satisfaction survey.
B.1:v4.2

+1-877-622-5543 / Tel: +1-978-646-2777
customercare@copyright.com
http://www.copyright.com

This email was sent to: tamerelbana@yahoo.com

Please visit Copyright Clearance Center for more information.

This email was sent by Copyright Clearance Center
222 Rosewood Drive Danvers, MA 01923 USA

To view the privacy policy, please go here.

ACSESS-Alliance of Crop, Soil, and Environmental Science Societies LICENSE TERMS AND CONDITIONS

Feb 11, 2013

This is a License Agreement between Tamer A Elbana ("You") and ACSESS-Alliance of Crop, Soil, and Environmental Science Societies ("ACSESS-Alliance of Crop, Soil, and Environmental Science Societies") provided by Copyright Clearance Center ("CCC"). The license consists of your order details, the terms and conditions provided by ACSESS-Alliance of Crop, Soil, and Environmental Science Societies, and the payment terms and conditions.

All payments must be made in full to CCC. For payment instructions, please see information listed at the bottom of this form.

License Number	3085960434684
License date	Feb 11, 2013
Licensed content publisher	ACSESS-Alliance of Crop, Soil, and Environmental Science Societies
Licensed content publication	Soil Science Society of America Journal
Licensed content title	Cadmium Transport in Alkaline and Acidic Soils: Miscible Displacement Experiments
Licensed copyright line	2010Soil Science Society of America
Licensed content author	Tamer A. Elbana and H. M. Selim
Licensed content date	Nov 1, 2010
Volume number	74
Issue number	6
Type of Use	Thesis/Dissertation
Requestor type	Author of requested content
Format	Print, Electronic
Portion	chapter/article
Rights for	Main product
Duration of use	0 - 5 years
Creation of copies for the disabled	no
With minor editing privileges	no
For distribution to	Worldwide
In the following language(s)	Original language of publication
With incidental promotional use	no
The lifetime unit quantity of new product	0 to 499
The requesting person/organization is:	Tamer A. Elbana
Order reference number	
Title of your thesis / dissertation	Transport and Adsorption-Desorption of Heavy Metals in Different Soils
Expected completion date	May 2013
Estimated size (number of pages)	250
Total	0.00 USD

RightsLink

Copyright Clearance Center

Thank You For Your Order!

Dear Tamer Elbana,
Thank you for placing your order through Copyright Clearance Center's RightsLink service. ACSESS-Alliance of Crop, Soil, and Environmental Science Societies has partnered with RightsLink to license its content. This notice is a confirmation that your order was successful.
Your order details and publisher terms and conditions are available by clicking the link below:
http://s100.copyright.com/CustomerAdmin/PLF.jsp?ref=b39d2d67-d507-43d1-9e1e-a5c5870fbd16

Order Details

Licensee: Tamer A Elbana
License Date: Feb 11, 2013
License Number: 3085961330997
Publication: Soil Science Society of America Journal
Title: Copper Mobility in Acidic and Alkaline Soils: Miscible Displacement Experiments
Type Of Use: Thesis/Dissertation
Total: 0.00 USD
To access your account, please visit https://myaccount.copyright.com.

Please note: Online payments are charged immediately after order confirmation; invoices are issued daily and are payable immediately upon receipt.
To ensure we are continuously improving our services, please take a moment to complete our customer satisfaction survey.
B.1:v4.2

+1-877-622-5543 / Tel: +1-978-646-2777
customercare@copyright.com
http://www.copyright.com

ACSESS-Alliance of Crop, Soil, and Environmental Science Societies LICENSE TERMS AND CONDITIONS

Feb 11, 2013

This is a License Agreement between Tamer A Elbana ("You") and ACSESS-Alliance of Crop, Soil, and Environmental Science Societies ("ACSESS-Alliance of Crop, Soil, and Environmental Science Societies") provided by Copyright Clearance Center ("CCC"). The license consists of your order details, the terms and conditions provided by ACSESS-Alliance of Crop, Soil, and Environmental Science Societies, and the payment terms and conditions.

All payments must be made in full to CCC. For payment instructions, please see information listed at the bottom of this form.

License Number	3085961330997
License date	Feb 11, 2013
Licensed content publisher	ACSESS-Alliance of Crop, Soil, and Environmental Science Societies
Licensed content publication	Soil Science Society of America Journal
Licensed content title	Copper Mobility in Acidic and Alkaline Soils: Miscible Displacement Experiments
Licensed copyright line	Copyright ©2011 by the Soil Science Society of America, Inc.
Licensed content author	Tamer A. Elbana and H. Magdi Selim
Licensed content date	Nov 1, 2011
Volume number	75
Issue number	6
Type of Use	Thesis/Dissertation
Requestor type	Author of requested content
Format	Print, Electronic
Portion	chapter/article
Rights for	Main product
Duration of use	0 - 5 years
Creation of copies for the disabled	no
With minor editing privileges	no
For distribution to	Worldwide
In the following language(s)	Original language of publication
With incidental promotional use	no
The lifetime unit quantity of new product	0 to 499
The requesting person/organization is:	Tamer A. Elbana
Order reference number	
Title of your thesis / dissertation	Transport and Adsorption-Desorption of Heavy Metals in Different Soils
Expected completion date	May 2013
Estimated size (number of pages)	250
Total	0.00 USD

RightsLink

Copyright Clearance Center

Thank You For Your Order!

Dear Tamer Elbana,
Thank you for placing your order through Copyright Clearance Center's RightsLink service. ACSESS-Alliance of Crop, Soil, and Environmental Science Societies has partnered with RightsLink to license its content. This notice is a confirmation that your order was successful.
Your order details and publisher terms and conditions are available by clicking the link below:
http://s100.copyright.com/CustomerAdmin/PLF.jsp?ref=ee7c5d83-34de-42af-853c-cd8a3a83a4d0

Order Details
Licensee: Tamer A Elbana
License Date: Feb 11, 2013
License Number: 3085970274247
Publication: Vadose Zone Journal
Title: Copper Transport in Calcareous Soils: Miscible Displacement Experiments and Second-Order Modeling
Type Of Use: Thesis/Dissertation
Total: 0.00 USD

To access your account, please visit https://myaccount.copyright.com.
Please note: Online payments are charged immediately after order confirmation; invoices are issued daily and are payable immediately upon receipt.
To ensure we are continuously improving our services, please take a moment to complete our customer satisfaction survey.
B.1:v4.2

+1-877-622-5543 / Tel: +1-978-646-2777
customercare@copyright.com
http://www.copyright.com

ACSESS-Alliance of Crop, Soil, and Environmental Science Societies LICENSE TERMS AND CONDITIONS

Feb 11, 2013

This is a License Agreement between Tamer A Elbana ("You") and ACSESS-Alliance of Crop, Soil, and Environmental Science Societies ("ACSESS-Alliance of Crop, Soil, and Environmental Science Societies") provided by Copyright Clearance Center ("CCC"). The license consists of your order details, the terms and conditions provided by ACSESS-Alliance of Crop, Soil, and Environmental Science Societies, and the payment terms and conditions.

All payments must be made in full to CCC. For payment instructions, please see information listed at the bottom of this form.

License Number	3085970274247
License date	Feb 11, 2013
Licensed content publisher	ACSESS-Alliance of Crop, Soil, and Environmental Science Societies
Licensed content publication	Vadose Zone Journal
Licensed content title	Copper Transport in Calcareous Soils: Miscible Displacement Experiments and Second-Order Modeling
Licensed copyright line	Copyright ©2012 by the Soil Science Society of America, Inc.
Licensed content author	Tamer A. Elbana and H. M. Selim
Licensed content date	May 1, 2012
Volume number	11
Issue number	2
Type of Use	Thesis/Dissertation
Requestor type	Author of requested content
Format	Print, Electronic
Portion	chapter/article
Rights for	Main product
Duration of use	0 - 5 years
Creation of copies for the disabled	no
With minor editing privileges	no
For distribution to	Worldwide
In the following language(s)	Original language of publication
With incidental promotional use	no
The lifetime unit quantity of new product	0 to 499
The requesting person/organization is:	Tamer A. Elbana
Order reference number	
Title of your thesis / dissertation	Transport and Adsorption-Desorption of Heavy Metals in Different Soils
Expected completion date	May 2013
Estimated size (number of pages)	250
Total	0.00 USD

well as any use of the materials beyond the scope of an unrevoked license, may constitute copyright infringement and publisher reserves the right to take any and all action to protect its copyright in the materials.

Copyright Notice: Disclaimer

You must include the following copyright and permission notice in connection with any reproduction of the licensed material: "Reprinted by Permission, ASA, CSSA, SSSA."

Warranties: None

Publisher makes no representations or warranties with respect to the licensed material.

Indemnity

You hereby indemnify and agree to hold harmless publisher and CCC, and their respective officers, directors, employees and agents, from and against any and all claims arising out of your use of the licensed material other than as specifically authorized pursuant to this license.

No Transfer of License

This license is personal to you and may not be sublicensed, assigned, or transferred by you to any other person without publisher's written permission.

No Amendment Except in Writing

This license may not be amended except in a writing signed by both parties (or, in the case of publisher, by CCC on publisher's behalf).

Objection to Contrary Terms

Publisher hereby objects to any terms contained in any purchase order, acknowledgment, check endorsement or other writing prepared by you, which terms are inconsistent with these terms and conditions or CCC's Billing and Payment terms and conditions. These terms and conditions, together with CCC's Billing and Payment terms and conditions (which are incorporated herein), comprise the entire agreement between you and publisher (and CCC) concerning this licensing transaction. In the event of any conflict between your obligations established by these terms and conditions and those established by CCC's Billing and Payment terms and conditions, these terms and conditions shall control.

Jurisdiction: Not Required*

This license transaction shall be governed by and construed in accordance with the laws of Wisconsin. You hereby agree to submit to the jurisdiction of the federal and state courts located in Wisconsin for purposes of resolving any disputes that may arise in connection with this licensing transaction.

Other Terms and Conditions

None

* If omitted, license will rely on New York law as stated in CCC terms and conditions agreed to by licensee during account creation.

V1.0

If you would like to pay for this license now, please remit this license along with your payment made payable to "COPYRIGHT CLEARANCE CENTER" otherwise you will be invoiced within 48 hours of the license date. Payment should be in the form of a check or money order referencing your account number and this invoice number RLNK500954270.
Once you receive your invoice for this order, you may pay your invoice by credit card. Please follow instructions provided at that time.

Make Payment To:
Copyright Clearance Center
Dept 001
P.O. Box 843006
Boston, MA 02284-3006

For suggestions or comments regarding this order, contact RightsLink Customer Support: customercare@copyright.com or +1-877-622-5543 (toll free in the US) or +1-978-646-2777.

Gratis licenses (referencing $0 in the Total field) are free. Please retain this printable license for your reference. No payment is required.

VITA

Tamer Elbana was born in May, 1978, Alexandria, Egypt, where he also grew up. He graduated from Faculty of Agriculture, Alexandria University in 1999, with a Bachelor of Soil and Water Sciences. He got his Master of Science in Soil and Water Sciences from the Faculty of Agriculture, Alexandria University in 2003. He worked as agricultural engineer in newly reclaimed farms in the western desert of Egypt from 2002 to 2004. He was employed as a research assistant in the National Research Center (NRC), Giza, Egypt in 2004 and re-enrolled at Alexandria University to pursue his doctoral degree in 2005. In 2008, he got the opportunity to be a visiting research associate in the School of Plant, Environmental, and Soil Sciences, Louisiana State University Agricultural Center, and was funded by the Egyptian government for two years. His major professor, Dr. H.M. Selim, offered him an assistantship to complete a full doctoral degree at Louisiana State University in 2010. He got married to Noura Bakr in 2004 and has two children, Yehia and Janna.